

**Incremental nonlinear control of hydraulic parallel robots
An application to the SIMONA research simulator**

Huang, Yingzhi

DOI

[10.4233/uuid:79ff3197-2134-4057-8e6c-c3239e2f2a7b](https://doi.org/10.4233/uuid:79ff3197-2134-4057-8e6c-c3239e2f2a7b)

Publication date

2019

Document Version

Final published version

Citation (APA)

Huang, Y. (2019). *Incremental nonlinear control of hydraulic parallel robots: An application to the SIMONA research simulator*. [Dissertation (TU Delft), Delft University of Technology].
<https://doi.org/10.4233/uuid:79ff3197-2134-4057-8e6c-c3239e2f2a7b>

Important note

To cite this publication, please use the final published version (if applicable).
Please check the document version above.

Copyright

Other than for strictly personal use, it is not permitted to download, forward or distribute the text or part of it, without the consent of the author(s) and/or copyright holder(s), unless the work is under an open content license such as Creative Commons.

Takedown policy

Please contact us and provide details if you believe this document breaches copyrights.
We will remove access to the work immediately and investigate your claim.

INCREMENTAL NONLINEAR CONTROL OF HYDRAULIC PARALLEL ROBOTS

AN APPLICATION TO THE SIMONA RESEARCH SIMULATOR

INCREMENTAL NONLINEAR CONTROL OF HYDRAULIC PARALLEL ROBOTS

AN APPLICATION TO THE SIMONA RESEARCH SIMULATOR

Proefschrift

ter verkrijging van de graad van doctor
aan de Technische Universiteit Delft,
op gezag van de Rector Magnificus prof. dr. ir. T.H.J.J Van der Hagen,
voorzitter van het College voor Promoties,
in het openbaar te verdedigen op maandag 18 maart 2019 om 15:00 uur

door

Yingzhi HUANG

ingenieur luchtvaart en ruimtevaart
geboren te Yueyang, Hunan, China.

Dit proefschrift is goedgekeurd door de promotoren:

prof. dr. ir. M. Mulder en dr. Q. P. Chu

Copromotor:

Dr. ir. Daan M. Pool

Samenstelling promotiecommissie:

Rector Magnificus,	voorzitter
prof. dr. ir. M. Mulder,	Technische Universiteit Delft, promotor
Dr. Q. P. Chu,	Technische Universiteit Delft, promotor
Dr. ir. Daan M. Pool,	Technische Universiteit Delft, copromotor

Onafhankelijke leden:

Dr. ir. F. Nieuwenhuizen,	Ampelmann Operations BV
Prof. dr. B. Yao,	Purdue University
Prof. dr. H. Nijmeijer,	Technische Universiteit Eindhoven
Prof. dr. ir. J. Hellendoorn,	Technische Universiteit Delft
Prof. dr. ir. J. M. Hoekstra,	Technische Universiteit Delft, reservelid



Keywords: Parallel Robots; Motion Control; Hydraulic Robots; Force Control; Nonlinear Systems; Model Uncertainty; Robustness; Incremental Non-linear Dynamic Inversion

Printed by: Ipskamp Printing

Front & Back: designed by Ye Zhang

Copyright © 2019 by Yingzhi HUANG

ISBN 978-94-028-1419-4

An electronic version of this dissertation is available at
<http://repository.tudelft.nl/>.

To my beloved wife and parents

SUMMARY

INCREMENTAL NONLINEAR CONTROL OF HYDRAULIC PARALLEL ROBOTS

AN APPLICATION TO THE SIMONA RESEARCH SIMULATOR

Yingzhi HUANG

In advanced robotic applications such as robotic locomotion, vehicle and flight simulators, and material test devices, there are higher requirements on stiffness, robustness and power ability for the mechanical structure and the actuator. Hence, it is common for such applications to use *parallel* manipulators and *hydraulic* actuators, due to their advantages in these aspects over their counterparts of serial manipulators and electrical actuators. When high-precision motion control is required for such systems, advanced model-based controllers, including feedback linearization and adaptive control, have been proposed in state-of-the-art studies for both hydraulic and parallel mechanical systems. However, the high complexity, nonlinearity and model uncertainty of these systems raise significant challenges for their motion control accuracy.

Parallel robots are kinematically different from the more commonly applied serial systems, as their end-effectors are connected to the base by multiple independent kinematic chains, which resemble the structure of a spider. Despite their advantages in stiffness and robustness, the dynamic modeling of parallel robots is inherently much more complicated due to their complex structure. For a general 6-DOF hexapod robot, a complete dynamic model that is linear with respect to its dynamic parameters (i.e., inertial and friction parameters) is difficult to obtain and almost no widely accepted systematic solutions exist in literature. This means that a complete model parameter identification for complex parallel robots is challenging. For this reason, in more practical parallel robot control studies significant model simplifications are often necessary by neglecting 'small' inertial terms. This will, however, inherently introduce model uncertainties.

The use of hydraulic actuators introduces even more serious model uncertainty problems to the complete system. On the one hand, hydraulic actuator dynamics are highly nonlinear, and subject to significant disturbances from nonlinear friction, oil leakage, additional dynamics and time-varying parameters, such as the oil bulk modulus that changes as the oil heats up. On the other hand, as hydraulic actuators are not force generators by nature, their usage in some advanced applications, such as force control, is not possible without an additional hydraulic force tracking controller. As a result, the hydraulic actuators not only complicate the overall control system, but also further deteriorate the model uncertainty problems of the complete system. As the precision of the uncertain system model is difficult to improve in practice, the control performance of advanced model-based controllers generally remains suboptimal.

This dissertation develops a novel control approach for hydraulic parallel robots, based on Incremental Nonlinear Dynamic Inversion (INDI), which is inherently insensitive to model uncertainties, while achieving better control performance than achievable with state-of-the-art model-based controllers, even with correct model information. A large-scale 6-DOF hydraulic parallel robot, the SIMONA research simulator (SRS) at TU Delft, will be used as an experimental testbed for control performance evaluation, as the high fidelity flight simulation requires high performance motion cueing for the pilots. The main research goal of this thesis can therefore be formulated as:

To develop high-precision, time-efficient motion control algorithms for parallel hydraulic robots, in the presence of considerable model uncertainties in both the hydraulic and mechanical subsystems.

In order to make the developed control system versatile, a cascaded control structure is adopted, which combines an inner-loop hydraulic force controller with an outer-loop motion controller. In this way, both control loops can be designed independently and more flexibly applied to more general applications. That is, the control system developed for the hydraulic actuator can also be used for serial manipulators or advanced force control tasks. Because the discussed model uncertainty problem exists for both the hydraulic and mechanical subsystems, the following research questions are raised:

1. How to achieve less model dependent nonlinear force/torque tracking control for the hydraulic actuators with high performance, when subjected to large hydraulic model uncertainties and disturbances?
2. How to achieve less model dependent and high precision motion control for general parallel manipulators with large dynamic model offsets and disturbances?

Before directly answering the research questions, a detailed research survey on the motion control of hydraulic parallel robots is given. The current state-of-the-art studies are still predominantly model-based control approaches, which rely on an accurate model of the plant, and their performance improvement is limited by the uncertainties of the studied systems. The more advanced adaptive approaches complicate the controller design procedure because of significantly increased computational load. Therefore, inspired by a less-model-dependent control approach emerging in flight control, namely, Incremental Nonlinear Dynamic Inversion (INDI), a novel control framework for both control loops is proposed in this thesis, to minimize the model dependency. As a novel modification of traditional feedback linearization, INDI replaces the use of full model information in the feedback linearization by state measurements of an incremental model, which becomes insensitive to model uncertainties, while still achieving an accurate linearization of the nonlinear plants. It is for this reason that INDI is also considered as a sensor-based control technique.

In order to establish a simulation testbed for controller design, to test and evaluate the effectiveness and performance improvement of the proposed controller over the state-of-the-art ones, a fully nonlinear high-fidelity model for a 6-DOF hydraulic hexapod robot is developed and implemented to match the SRS. The fully modelled nonlinear dynamics include the nonlinear hydraulic valve dynamics, actuator fluid dynam-

ics, parallel manipulator rigid body dynamics, and even oil transmission line dynamics, which are all modelled in full detail, based on physical principles. Those submodels are made modular, to be easily included or omitted from the complete model. The model is validated by comparing the simulation results with experiment data collected for the SRS. As a testbed for the proposed controller, the model provides important references for controller assumption validation, identification of practical issues, performance evaluations, and parameter tuning. The simulated performance indeed shows great agreement with the measured experiment results on the SRS .

To address the first research question, a hydraulic force-tracking controller based on INDI is developed theoretically and practically. In theory, the robustness of INDI is based on several assumptions, including sufficiently high sampling rate and fast actuator dynamics. In this thesis, the robustness of INDI to parameter uncertainties is rigorously proven in theory with a necessary condition for stability, based on which the maximum parameter mismatch level for stable performance can be determined. In practice, the implementation issues caused by unmodeled dynamics (for the controller) which may lead to serious stability problems, such as the valve dynamics, oil pipeline dynamics and sensor dynamics, are identified through simulations on the developed nonlinear model. Appropriate practical solutions with synchronized low-pass filters are proposed. The developed hydraulic force controller is combined with a model-based computed torque outer-loop motion controller to form the complete control system for the SRS.

To validate the effectiveness and robustness of the proposed inner-loop force tracking controller, motion tracking experiments under aggressive motion profiles are performed on the SRS, under both nominal and hydraulic parameter offset conditions. For the proposed inner-loop INDI controller, the hydraulic force tracking accuracy is improved by over 10 times as compared to the baseline model-based controller under nominal conditions. Under up to 50% hydraulic parameter mismatch, no visible performance decrease (less than 5%) is observed with the INDI controller, while the same mismatch quickly deteriorates performance by a factor of five for the baseline controller. As a result, the developed overall position controller achieves sub-millimeter tracking accuracy for a hydraulic parallel robot with an over 4000 kg cockpit under extreme levels of parameter offset. A calculation of standard performance indicators shows that even with a 50% model mismatch the control accuracy of the proposed control system is still three times better than the best according to a recent state-of-the-art survey of hydraulic robot control. This proves that the proposed controller is indeed not dependent on an accurate hydraulic system model and achieves much better performance than state-of-the-art model-based controllers.

To answer the second research question, an outer-loop parallel manipulator motion controller based on the INDI technique is developed and implemented on the SRS. As an extension of the INDI application from a single-input and single-output (SISO) system to a multiple-input and multiple-output (MIMO) system, the INDI control theory is also generalized. The robustness analysis for INDI control systems is extended to MIMO cases, with a more general stability condition for the model mismatch level. The controller is designed in the joint space, avoiding the cumbersome numerical forward kinematic calculation needed for controllers in the Cartesian space. The necessary actuator force feedback is achieved by hydraulic pressure measurements. The required actuator

acceleration measurements are obtained through numerical differentiation of the actuator position measurements.

The developed outer-loop INDI motion controller is combined with the developed inner-loop INDI force controller, completing the dual-INDI control system for hydraulic parallel robots. The resulting controlled system is not only robust to hydraulic parameter uncertainties, but also to parallel manipulator model mismatches, such as in its inertial and friction parameters. Together with a theoretical proof, the robustness is further verified and validated by simulation and experiment results. In the motion tracking experiments with nominal conditions, the dual-INDI controller shows slightly better position tracking performance than the previously developed inner-loop INDI plus outer-loop model-based controller, which already achieved a notable performance improvement over the state-of-the-art. In the robustness tests, extreme levels of model uncertainties are introduced, including up to 50% cockpit mass mismatches (around 2000 kg) and ± 0.5 meter center-of-gravity shifts along the longitudinal axis of the simulator body frame. The performance of the dual-INDI controller remains intact at sub-millimeter precision, while the performance of the reference model-based controller quickly degrades to over 5 mm, i.e., 10 times worse.

With the developed dual-INDI force/motion controller for hydraulic parallel robots, the research goal is achieved. On the one hand, the controller achieves world-class performance under extreme levels of model mismatches from both hydraulic and mechanical subsystems with supporting theory, validating the robustness and high performance. On the other hand, the controller design procedure is simple and computationally efficient, with the avoidance of the full model calculation and any explicit adaptive or robust control algorithms. The free combinations of the inner- and outer-loops also reflect the versatility of the developed control system.

In conclusion, this thesis presents a high-precision and time-efficient control system for hydraulic parallel robots, with inherent and proven robustness to typical model uncertainties, based on a less model-dependent control technique INDI. The high performance and robustness of the controller is proven in theory, verified with high-fidelity computer simulation and validated with real-world experiments. Overall, superior control performance is achieved compared with state-of-the-art related studies with at least three times better motion tracking accuracy.

In future work, the INDI control technique should be further refined. For instance, one key feature of the developed INDI controller is that it depends on system state measurements which may not be directly available, such as actuator accelerations. The current solution with numerical differentiation introduces noise or filter dynamics which may harm for the performance or stability. More advanced estimation methods are expected for future development. Besides, application wise, the proposed controllers for both loops should be applied to more general applications, such as force control for manipulators that interact with the environment, instead of only the motion in free space as is the case of the SRS.

SAMENVATTING

INCREMENTAL NONLINEAR CONTROL OF HYDRAULIC PARALLEL ROBOTS

AN APPLICATION TO THE SIMONA RESEARCH SIMULATOR

Yingzhi HUANG

Geavanceerde robotica-toepassingen zoals voortbeweging, voertuig- en vluchtsimulatoren en materiaaltestapparatuur stellen hogere eisen aan de mechanische structuur en de actuator in termen van stijfheid, robuustheid en vermogen. *Parallele* manipulatoren in combinatie met *hydraulische* actuatoren worden door hun superieure eigenschappen op deze gebieden daarom vaak verkozen boven hun tegenhangers van seriële manipulatoren en elektrische actuatoren. Wanneer voor dergelijke systemen zeer nauwkeurige bewegingsbesturing is vereist, zijn geavanceerde modelgebaseerde regelaars, inclusief terugkoppellingslinearisatie en adaptieve regelaars, voorgesteld in geavanceerde studies voor zowel hydraulische als parallele mechanische systemen. De hoge complexiteit, niet-lineariteit en modelonzekerheid van dit soort regelaars hebben echter een negatieve invloed op de bereikbare nauwkeurigheid van de bewegingsbesturing.

Parallele robots zijn kinematisch verschillend van de meer algemeen toegepaste seriële systemen, omdat hun eindeffectoren zijn verbonden met het onderstel door meerdere onafhankelijke kinematische ketens, die lijken op de structuur van een spin. Ondanks hun voordelen in stijfheid en robuustheid, maakt de complexe structuur de dynamische modellering van deze parallele robots inherent veel gecompliceerder. Voor een algemene robot met zes vrijheidsgraden ("hexapod") is een volledig dynamisch model dat lineair is met betrekking tot zijn dynamische parameters (d.w.z. traagheids- en wrijvingsparameters) moeilijk te verkrijgen en zijn bijna geen algemeen aanvaarde systematische oplossingen in de literatuur bekend. Dit betekent dat een complete modelparameteridentificatie voor complexe parallele robots een uitdaging is. Om deze reden zijn in meer praktische parallele robotbesturingsstudies aanzienlijke modelvereenvoudigingen vaak nodig door het negeren van 'kleine' traagheidsvoorwaarden. Dit zal echter inherent modelonzekerheden introduceren.

Het gebruik van hydraulische actuatoren introduceert nog meer serieuze onzekerheidsproblemen voor het complete systeem. Enerzijds zijn de hydraulische actuatordynamica hoogst niet-lineair en onderhevig aan significante verstoringen door niet-lineaire wrijving, olielekage, extra dynamica en in de tijd variërende parameters, zoals de compressiemodulus van de olie die verandert als de olie opwarmt. Aan de andere kant, omdat hydraulische actuatoren van nature geen krachtgeneratoren zijn, is het gebruik ervan in sommige geavanceerde toepassingen, zoals krachtregeling, niet mogelijk zonder een aanvullende hydraulische krachtregelaar. Dientengevolge compliceren de hydraulische actuatoren niet alleen het algehele regelsysteem, maar verslechtert verder

ook de modelonzekerheidsproblemen van het complete systeem. Omdat de precisie van het onzekere systeemmodel in de praktijk moeilijk te verbeteren is, blijven de besturingsprestaties van geavanceerde modelgebaseerde regelaars in het algemeen suboptimaal.

Dit proefschrift ontwikkelt een nieuwe besturingsaanpak voor hydraulische parallelle robots, gebaseerd op incrementele niet-lineaire dynamische inversie (INDI), die inherent ongevoelig is voor modelonzekerheden, terwijl betere regelprestaties worden bereikt dan met geavanceerde modelgebaseerde regelaars mogelijk is, zelfs als zij beschikken over de juiste modelinformatie. Een grootschalige hydraulische parallelle robot met zes vrijheidsgraden, de SIMONA vluchtsimulator (SRS) van de TU Delft, zal worden gebruikt voor de experimentele evaluatie van de regelprestaties. Deze vluchtsimulator stelt voor een realistische vluchtnabootsing hoge eisen aan de bewegingsnauwkeurigheid. Het belangrijkste onderzoeksdoel van dit proefschrift kan daarom worden geformuleerd als:

Ontwikkeling van uiterst nauwkeurige, tijdbesparende algoritmen voor bewegingsregeling voor parallelle hydraulische robots, in aanwezigheid van aanzienlijke modelonzekerheden in zowel de hydraulische als de mechanische subsystemen.

Om het ontwikkelde besturingssysteem veelzijdig te maken, wordt een trapsgewijze besturingsstructuur gebruikt, die een hydraulische krachtregelaar in de binnenste regelkring combineert met een bewegingsregelaar in de buitenste regelkring. Op deze manier kunnen beide regelkringen onafhankelijk worden ontworpen en makkelijker worden aangepast voor algemenere toepassingen. Dat wil zeggen dat het besturingssysteem dat is ontwikkeld voor de hydraulische actuator ook kan worden gebruikt voor seriële manipulators of geavanceerde krachtbesturingstaken. Omdat het besproken modelonzekerheidsprobleem geldt voor zowel de hydraulische als de mechanische subsystemen, zijn de volgende onderzoeksvragen aan de orde:

1. Hoe kan een hoge regelnauwkeurigheid behaald worden door een niet-lineaire kracht- of momentregelaar met een kleinere modelafhankelijkheid en werkend op een hydraulische actuator in de aanwezigheid van grote hydraulische modelonzekerheden en verstoringen?
2. Hoe kan een hoge bewegingsnauwkeurigheid behaald worden voor een algemene parallelle manipulator door een positierregelaar met een kleinere modelafhankelijkheid en in de aanwezigheid van grote veranderingen in dynamische eigenschappen en grote verstoringen?

Voordat de onderzoeksvragen direct worden beantwoord, wordt een gedetailleerd onderzoek naar de bewegingsregeling van hydraulische parallelle robots gegeven. De meest recente studies gebruiken nog steeds overwegend op modellen gebaseerde regelaars, die gebaseerd zijn op een nauwkeurig model van het te regelen systeem, en hun prestatieverbetering wordt beperkt door de onzekerheden van de betreffende systemen. De meer geavanceerde adaptieve benaderingen bemoeilijken de ontwerpprocedure van de regelaar vanwege aanzienlijk hogere rekenbelasting. Daarom, geïnspireerd door een minder modelafhankelijke besturingsaanpak die is ontwikkeld voor vliegtuigbesturingen, namelijk Incrementele niet-lineaire dynamische inversie (INDI), wordt in dit proef-

schrift een nieuw regelsysteem voor beide regelkringen voorgesteld om de afhankelijkheid van het model te minimaliseren. Als een nieuwe aanvulling op de traditionele terugkoppelingslinearisatie vervangt INDI het gebruik van volledige modelinformatie in de terugkoppelingslinearisatie door toestandsmetingen van een incrementeel model dat ongevoelig wordt voor modelonzekerheden, terwijl toch een nauwkeurige linearisering van de niet-lineaire systemen wordt bereikt. Het is om deze reden dat INDI ook wordt beschouwd als een op sensoren gebaseerde besturingstechniek.

Ter ondersteuning van het ontwerp van de regelaar en om de effectiviteit en prestatieverbeteringen van de voorgestelde regelaar te testen ten opzichte van bestaande systemen, is een gesimuleerde proefopstelling gemaakt die een volledig niet-lineair en realistisch model omvat van de hydraulische hexapod van de SRS. De volledig gemodelleerde niet-lineaire dynamica omvat de niet-lineaire hydraulische klepdynamica, actuatorvloeistofdynamica, starre lichaamsdynamica van de parallelle manipulator en zelfs de dynamica van de olietransportlijnen. Deze zijn allemaal in detail zijn gemodelleerd, gebaseerd op fysische principes. Deze submodellen zijn modulair gemaakt, zodat ze eenvoudig kunnen worden toegevoegd aan of weggelaten uit het complete model. Het model is gevalideerd door de simulatieresultaten te vergelijken met experimentgegevens die met de SRS zijn verzameld. Als een proefopstelling voor de voorgestelde regelaar, biedt het model belangrijke referentiewaarden voor de validatie van aannames voor het ontwerp van de regelaar, identificatie van praktische problemen, evaluaties van de prestaties en parameterafstemming. De gesimuleerde prestaties vertonen inderdaad grote overeenstemming met de gemeten experimentresultaten op de SRS.

Om de eerste onderzoeksvraag aan te pakken, is een hydraulische krachtvolgreelaar op basis van INDI theoretisch en praktisch ontwikkeld. In theorie is de robuustheid van INDI gebaseerd op verschillende aannames, waaronder een voldoende hoge bemonsteringsfrequentie en een snelle actuatordynamiek. In dit proefschrift is de robuustheid van INDI ten opzichte van parameteronzekerheden in theorie uitvoerig bewezen met een noodzakelijke voorwaarde voor stabiliteit, op basis waarvan het maximale verschilniveau in modelparameters voor stabiele prestaties kan worden bepaald. In de praktijk worden de implementatieproblemen veroorzaakt door ongemodelleerde dynamica (voor de regelaar) die kunnen leiden tot ernstige stabiliteitsproblemen, zoals de klepdynamiek, dynamiek van oliepijplijnen en sensordynamica. Deze problemen zijn geïdentificeerd door simulaties op het ontwikkelde niet-lineaire model. Passende praktische oplossingen met gesynchroniseerde laagdoorlaatfilters worden voorgesteld. Om het besturingssysteem van de SRS compleet te maken wordt de ontwikkelde hydraulische krachtregelaar gecombineerd met een modelgebaseerde bewegingsregelaar die in de buitenste regelkring de benodigde krachten genereert.

Om de effectiviteit en de robuustheid van de voorgestelde krachtregelaar te valideren, worden experimenten onder agressieve bewegingsprofielen uitgevoerd op de SRS, onder zowel nominale als condities waarin de hydraulische modelparameters afwijken van de werkelijkheid. Voor de voorgestelde INDI-regelaar in de binnenste regelkring wordt de nauwkeurigheid van de hydraulische krachtvolgving met meer dan 10 keer verbeterd vergeleken met de modelgebaseerde referentieregelaar onder nominale omstandigheden. Bij afwijkingen in de hydraulische parameters van 50% wordt geen zichtbare prestatieafname (minder dan 5%) waargenomen met de INDI-regelaar, terwijl de prestaties van

de referentieregelaar met een factor vijf afnemen. Als gevolg hiervan behaalt de ontwikkelde positieregelaar in de buitenste regelkring een nauwkeurigheid van minder dan een millimeter voor een hydraulische parallelle robot met een cockpit van meer dan 4000 kg onder extreme niveaus van fouten in modelparameters. Een berekening van standaardindicatoren voor regelprestaties toont aan dat zelfs met een 50% modelafwijking de regelnauwkeurigheid van het voorgestelde besturingssysteem nog steeds drie keer beter is dan het beste alternatief in een recent overzicht van hydraulische robotbesturingssystemen. Dit bewijst dat de voorgestelde regelaar inderdaad niet afhankelijk is van een nauwkeurig hydraulisch systeemmodel en veel betere prestaties behaalt dan de nieuwste modelgebaseerde regelaars.

Om de tweede onderzoeksvraag te beantwoorden is voor de buitenste regelkring van de parallelle manipulator een bewegingsregelaar ontwikkeld en op de SRS geïmplementeerd die is gebaseerd op de INDI-techniek. Als een uitbreiding van de INDI-applicatie van een SISO-systeem (Single-Input en Single-Output) naar een MIMO-systeem (Multiple-Input en Multiple-Output), wordt de INDI-besturingstheorie ook gegeneraliseerd. De robuustheidsanalyse voor INDI-regelsystemen wordt uitgebreid naar MIMO-gevallen, met een meer algemene stabiliteitsvoorwaarde voor het niveau van modelfouten. De regelaar is ontworpen in de ruimte van actuatorlengte en vermijdt daarmee de omslachtige numerieke kinematische transformatie die nodig is voor regelaars in de cartesische ruimte. De benodigde krachtterugkoppeling van de actuator wordt verkregen door metingen van de hydraulische druk. De vereiste versnellingsmetingen van de actuator worden verkregen door numerieke differentiatie van de positiemetingen van de actuator.

De ontwikkelde INDI-bewegingsregelaar in de buitenste regelkring wordt gecombineerd met de ontwikkelde INDI-krachtregelaar in de binnenste regelkring, waarmee het dubbel-INDI-regelsysteem voor hydraulische parallelle robots wordt voltooid. Het resulterende geregelde systeem is niet alleen robuust voor hydraulische parameteronzekerheden, maar ook voor aanpassingen in het model van de parallelle manipulator, zoals in zijn inertie- en wrijvingsparameters. Samen met een theoretisch bewijs wordt de robuustheid verder geverifieerd en gevalideerd door simulatie- en experimentresultaten. In de bewegingsexperimenten met nominale condities, vertoont de dubbel-INDI-regelaar een iets betere positiebepalingsprestatie dan de eerder ontwikkelde INDI krachtregelaar plus modelgebaseerde positieregelaar, die al een opmerkelijke prestatieverbetering behaalden ten opzichte van de laatste stand van de techniek. In de robuustheidstests worden extreme niveaus van modelonzekerheden geïntroduceerd, waaronder tot 50% fouten in de gemodelleerde cabinemassa (ongeveer 2000 kg) en $\pm 0,5$ meter zwaartepuntsverschuivingen langs de lengtes van het frame van de simulator. De prestaties van de dubbel-INDI-regelaar blijven intact met een nauwkeurigheid van minder dan een millimeter, terwijl de prestaties van de op een referentiemodel gebaseerde regelaar snel afnemen tot meer dan 5 mm, dat wil zeggen tien keer slechter.

Met de ontwikkelde dubbel-INDI kracht- en bewegingsregelaar voor hydraulische parallelle robots wordt het onderzoeksdoel bereikt. Aan de ene kant bereikt de regelaar prestaties van wereldklasse onder extreme niveaus van modelfouten van zowel de hydraulische als de mechanische subsystemen met ondersteunende theorie, waarbij de robuustheid en hoge prestaties worden gevalideerd. Anderzijds is de ontwerpprocedure van de regelaar eenvoudig en efficiënt in rekenkracht, door het vermijden van de

volledige modelberekening en eventuele expliciete adaptieve of robuuste besturingsalgoritmen. De vrije combinaties van de binnen- en buitenregelkringen weerspiegelen ook de veelzijdigheid van het ontwikkelde besturingssysteem.

Concluderend presenteert dit proefschrift een zeer nauwkeurig en tijdbesparend controlesysteem voor hydraulische parallelle robots, met inherente en bewezen robuustheid voor typische modelonzekerheden, gebaseerd op de minder modelafhankelijke besturingstechniek INDI. De hoge prestaties en robuustheid van de regelaar zijn in theorie bewezen, geverifieerd met realistische computersimulatie en gevalideerd met experimenten in de praktijk. Over het algemeen worden superieure regelprestaties bereikt waarbij de nauwkeurigheid van de beweging minstens een factor 3 beter is dan de nieuwste gepubliceerde onderzoeken.

In toekomstig werk moet de INDI-regeltechniek verder worden verfijnd. Een belangrijk kenmerk van de ontwikkelde INDI-regelaar is bijvoorbeeld dat deze afhankelijk is van signalen die mogelijk niet direct gemeten worden, zoals actuatorversnellingen. De huidige oplossing met numerieke differentiatie introduceert ruis of filterdynamiek die de prestaties of stabiliteit kan schaden. Voor toekomstige ontwikkeling worden meer geavanceerde schattingsmethoden verwacht. Bovendien moeten de voorgestelde regelaars voor beide regelkringen worden getoetst in meer algemene toepassingen, zoals krachtregeling voor manipulators die interactie hebben met de omgeving, in plaats van alleen de beweging in de vrije ruimte zoals het geval is bij de SRS.

CONTENTS

Summary	vii
Samenvatting	xi
1 Introduction	1
1.1 Hydraulic parallel manipulators	1
1.2 Hydraulic hexapod flight simulator	2
1.3 Motion control problems for hydraulic parallel robots	4
1.3.1 Hydraulic force control	5
1.3.2 Motion control for parallel manipulators	6
1.4 Research goal and research questions	7
1.5 Research approach and contributions	9
1.6 Scope and limitations	11
1.7 Outline of this thesis	11
References	13
2 Survey of Hydraulic Parallel Robot Control Systems	21
2.1 Introduction	22
2.2 Modeling	24
2.2.1 Manipulator dynamic modeling	24
2.2.2 Hydraulic actuator dynamic modeling	24
2.3 Control schemes	26
2.3.1 Stewart platform control schemes	26
2.3.2 Hydraulic actuator control schemes for integrated Stewart platform	31
2.4 Hydraulic Stewart platform control with INDI	34
2.4.1 Incremental Nonlinear Dynamic Inversion (INDI)	34
2.4.2 Preliminary INDI controller design for hydraulic actuator	36
2.4.3 Preliminary simulation results	36
2.4.4 Possible application in the outer-loop	37
2.5 Conclusion	39
References	39
3 Physical Modeling of the Hydraulic Parallel manipulator	45
3.1 Introduction	46
3.2 Modeling and control	48
3.2.1 Modeling hydraulic subsystem	48
3.2.2 Dynamic equations of hexapod mechanics	54
3.2.3 Control Strategy	56

3.3	Computer Modeling	57
3.3.1	Computer modeling in Simulink	57
3.3.2	Computer modeling with SimMechanics	58
3.4	Simulation results and validation	59
3.4.1	Results comparison of two modeling approaches	59
3.4.2	Model validation	60
3.5	Conclusion	62
	References	65
4	Sensor-Based Hydraulic Force Controller	69
4.1	Introduction	70
4.2	System Dynamic Model	72
4.3	Incremental Nonlinear Dynamic Inversion	74
4.3.1	Theory and Stability	74
4.3.2	Robustness to Parameter Uncertainty and Disturbance	77
4.4	Controller Design	80
4.4.1	Inner-loop INDI hydraulic force controller	80
4.4.2	Solving implementation issues	81
4.4.3	Inner-loop NDI based force controller	84
4.4.4	Outer-loop motion controller	85
4.5	Simulation Results	85
4.5.1	Performance under Nominal Conditions	86
4.5.2	INDI Assumption Validation	88
4.5.3	Robustness to Hydraulic Parameter Uncertainties	91
4.6	Experiment results	94
4.6.1	Hardware Setup	94
4.6.2	Motion Profile 1	94
4.6.3	Motion Profile 2	97
4.7	Conclusion	99
	References	99
5	Non-model-based Control of Hydraulic Parallel Robots	105
5.1	Introduction	106
5.2	System Dynamic Model	108
5.3	Sensor-Based Controller Design	109
5.3.1	INDI motion controller for parallel robot	110
5.3.2	robustness analysis	111
5.3.3	Practical implementation	114
5.3.4	Inner-loop INDI hydraulic force controller	116
5.4	Control system analysis	117
5.4.1	Resistance of pressure measurement errors	117
5.4.2	Easy calibration	118

5.5	Experimental results	118
5.5.1	Hardware setup	119
5.5.2	Motion controller setup and calibration	119
5.5.3	Nominal condition performance.	120
5.5.4	Robustness to model uncertainty	121
5.6	Conclusion	124
	References	125
6	Conclusion and Recommendations	129
6.1	Discussion	130
6.1.1	The philosophy of control approaches	130
6.1.2	The modular physical model: more than a test bed	130
6.1.3	The Inner-loop hydraulic force controller	131
6.1.4	Sensor based Outer-loop motion controller	133
6.2	Final conclusions	134
6.3	Recommendations and future work.	135
	References	136
A	Incremental Nonlinear Dynamic Inversion	139
	Acknowledgements	143
	Curriculum Vitæ	145
	List of Publications	147

1

INTRODUCTION

1.1. HYDRAULIC PARALLEL MANIPULATORS

The first programmable industrial robot, Unimate (Fig. 1.1 (a)), was invented by George Devol in 1959, only 38 years after the word "robot" was introduced in Karel Capek's play Rossum's Universal Robots [1]. Over half a century later, robotics technology has become increasingly important in industry and also our daily life, and is believed to be more important the coming decades with fast growing markets [2]. Despite the vast variety that the robots may have in forms, from micro air vehicles [3] to autonomous quadruped robots [4], the majority of robots can be characterized by a few technological aspects. Among them, actuation methods, kinematic/dynamic features and control algorithms are some of the most studied characteristics.

Acting as the drive of a system, the *actuator* is the basic element of robotic motion systems. Hydraulic and electric actuators are the most popular actuation techniques. Although electric actuators are becoming more and more popular nowadays for their advantages in size, energy efficiency and maintenance cost [5], hydraulic actuators are still attractive in performance-oriented or large-scale applications, as they provide significantly higher force and torque abilities and better robustness [6]. For instance, the Boston Dynamics Spot [7], an advanced four-legged hydraulic robot, provides twice higher payload capability than its electric driven little brother Spotmini with a barely larger size (See Fig. 1.1 (b), (c)). Thus, hydraulic actuation still sees frequent use in advanced industrial and academic applications, such as rough terrain locomotion of legged robots [8, 9], vehicle simulator motion systems [10] and offshore access systems [11].

The kinematic and dynamic features of a robot are largely defined by its mechanical structure. Currently, the most commonly applied robots are often built as serial manipulators with open kinematic chains, which strongly resemble human hands. The main characteristic of serial manipulators is the successive connected sequence of rigid bodies (links), each of which is connected to its predecessor by a one-degree-of-freedom joint [12]. A typical example of such serial manipulators is shown in Fig. 1.1 (d). Despite the advantages in straightforward kinematics and relatively simple dynamics, serial manipulators have inherent constraints in their accuracy, stiffness and payload capability.

Thus for applications where a heavy payload and high accuracy are important requirements, another type of configuration, the parallel robot, is often considered [13].

Parallel robots, which contain closed kinematic chains, generally consist of a moving end-effector and a fixed base, connected by multiple independent kinematic chains. The most typical parallel manipulator is a six degree-of-freedom (DOF) construction with six linear actuators which is known as the Stewart (or Gough-Stewart) platform [13], as shown in Fig. 1.2. This is the reason why these 6-DOF parallel manipulators are also often referred to as 'hexapods'. Even though this hexapod structure was first established by Gough in 1947 as a system allowing the positioning and orientation of a platform for tire wear and tear tests, it wasn't until the 1960's, when Stewart proposed a similar structure for flight simulator motion bases [14], that hexapods started to be widely used [12]. Compared with a serial structure, the advantages of parallel robots include much higher stiffness and load mass ratio, better robustness and higher accuracy [15]. Parallel manipulators are nowadays widely used in motion systems, machine tools, medical assistant systems and numerous other applications [12].

The combination of the hydraulic actuator and a parallel structure shares the advantages from both elements, and features significantly higher payload ability and robustness compared with their electrical serial robot counterparts. Hydraulic parallel manipulators are capable of handling heavy duty applications in rough environments, such as multiaxial material test devices [16] and offshore access systems [11] (see Fig. 1.1 (e) and (f)). Another typical application is the flight simulator motion system, for which the motion accuracy is a main criterion for performance evaluations, stemming from the requirement of high-fidelity motion cueing for the training of pilots. Despite the advantages provided by both the actuator and the manipulator, the high motion accuracy of such systems can not be guaranteed without a high performance control algorithm.

The high-precision motion control of hydraulic parallel robots, which often combine complicated actuators and less straightforward mechanical structures, is also one of the most challenging robotic control topics. As a hydraulic parallel flight simulator motion system is a typical representation of a broader class of hydraulic parallel robots with high accuracy control requirement, its performance provide validations for a variety of advanced robotic control techniques for general hydraulic parallel robots. The novel control of these parallel hydraulic robots forms the subject of this thesis.

1.2. HYDRAULIC HEXAPOD FLIGHT SIMULATOR

Hydraulic actuation has dominated the flight simulator industry for decades [18, 19]. Nowadays, however, the trend to use electrical drives is becoming more commonplace with the development of the electrical servomotor [5, 20, 21]. Electrical actuators offer several advantages over hydraulic ones, including higher energy efficiency, lower maintenance cost, and far less environment pollution possibility [18]. However, in applications where *performance* is the major requirement, such as in a research flight simulator, hydraulic actuators are still attractive due to their high power-to-weight ratio, extremely high power ability and less safety problems when facing a loss of power. Furthermore, hydraulic fluids inherently act as a lubrication, which guarantees a smoother motion while avoiding wear. Combined with a parallel robotic structure, the hexapod hydraulic motion system can provide an extremely smooth 6-DOF motion for a flight simulator.

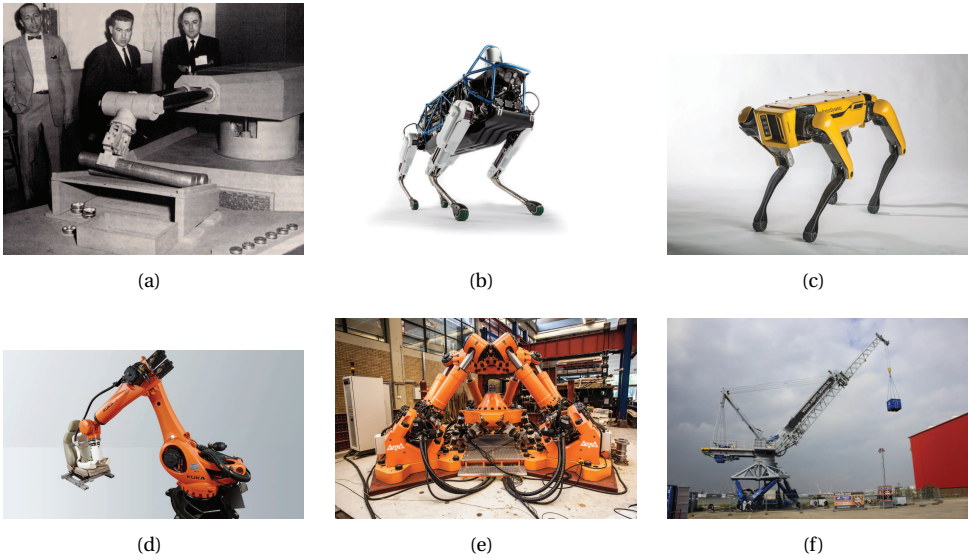


Figure 1.1: Examples of robotic systems with different actuators and structures: (a) Unimate invented by George Devol [1], (b) Boston Dynamics 'Spot' [7], (c) Boston Dynamics 'SpotMini' [7], (d) KUKA OccuBot [17], (e) TU Delft 'Hexapod' [16], (f) Ampelmann E8000 offshore motion compensation system [11]

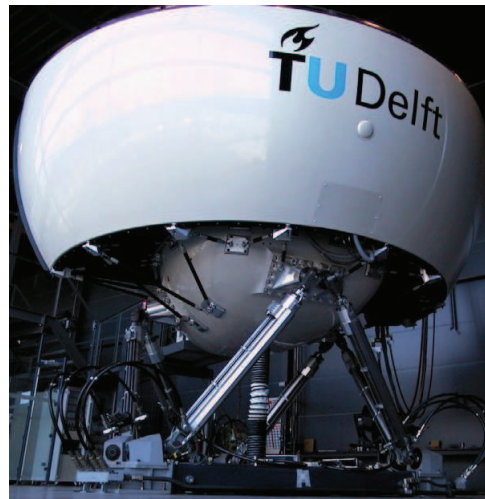


Figure 1.2: The SIMONA Research Simulator at TU Delft with its hydraulic hexapod motion system

The SIMONA Research Simulator (SRS) is a typical full scale hydraulic hexapod flight simulator developed by Delft University of Technology, and currently maintained by the Control and Operations department in the Faculty of Aerospace Engineering [22, 23]. One of the main purposes of the SRS is to provide the maximum possible motion simulation realism with new techniques. Integrated design of the cockpit and the use of light-weight materials helped minimizing the mass of the upper platform, an advanced visual display system was developed for providing realistic visual cueing, and a unique software architecture called the Delft University Environment for Communication and Activation, (DUECA) was developed for real-time simulation and hardware control [22]. One of the most important contributors to the fidelity of the flight simulation is how well the physical motions of the pilots resemble the reality of flight [22]. The ability to deliver high fidelity motion cueing is the main motivation for the high precision hydraulic parallel motion control system development.

The SRS motion system consists of six linear hydraulic actuators, each of which is controlled by a servo-valve. Currently, a nonlinear model-based motion control system is implemented on the SRS [19]. With an accurate model of the complete system, good motion tracking performance can be achieved. However, as will be discussed in more detail in this thesis, hydraulic parallel robots face inherent model uncertainty problems. As is well known, the performance of model-based nonlinear controllers degrades when these are subject to model and parameter uncertainties [24]. For instance, the motion tracking accuracy of the SRS is deteriorated 90% with only a 20% mismatch of the valve maximum flow parameter, one of the most important parameters of the hydraulic actuator model [25]. As the model accuracy of hydraulic systems is difficult to improve, as it contains time-varying parameters due to temperature changes, system wear and even system hardware modifications, the development of alternative motion control techniques that are less dependent (or even *independent*) of an accurate model of the systems will enable even higher control performance.

1.3. MOTION CONTROL PROBLEMS FOR HYDRAULIC PARALLEL ROBOTS

Motion control is a major topic for robotics. In order to achieve motion control, it is assumed that a desired motion trajectory of the robot/manipulator has been generated, to act as the ‘reference input’ for the control system to follow. The general task of motion control systems can therefore be formulated as follows: to determine the required actuation forces/torques to be generated by the actuators, such that the planned motion trajectory is executed by the manipulator, fulfilling the desired transient and steady-state requirements [26].

Specifically, for a flight simulator, a real-time computer program typically calculates the required motion of the simulated aircraft based on the aircraft model and the pilot (or autopilot) input. Due to the limited stroke of the simulator actuators, the simulated flight motion has to be transformed to a reference motion profile that the simulator motion system is capable of following. Once the resulting motion profile is generated, often using advanced ‘washout’ algorithms [27], the motion control problem of the hydraulic hexapod flight simulator becomes a general control problem for hydraulic parallel ma-

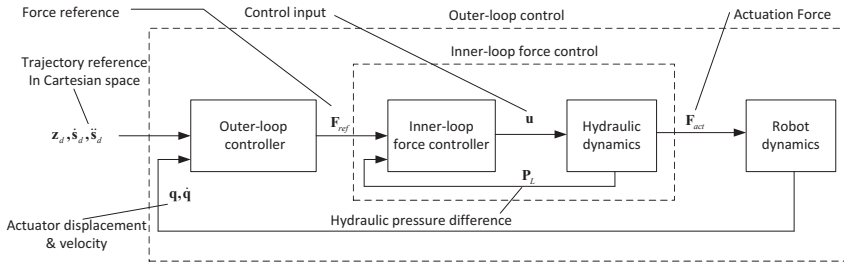


Figure 1.3: Cascaded control structure for hydraulic robots with inner- and outer-loop controllers

nipulators. In this regard, the developed control techniques developed in this thesis are not restricted to the simulator motion system. Instead, they can be implemented in a much broader class of hydraulic hexapod applications in free space.

Even though the motion control problem for general robots has been extensively studied during the past decades with a variety of advanced control techniques [28–31], fundamental problems still exist for hydraulic robots. As discussed, a typical motion controller calculates the required force/torque reference of the actuators, based on the assumption that the actuators are ‘force generators’. In more advanced control schemes such as impedance control and vibration isolation, this assumption is also often made [32, 33]. However, different from their electrical counterparts, hydraulic actuators are not force generators by nature. For hydraulic actuators, the control inputs are actually regarded as ‘velocity commands’ [10, 34]. This prevents the direct application of various well-studied motion control schemes.

One practical solution to this problem is to design the controller with a *cascaded* structure with multiple control loops [35–37]. Fig. 1.3 presents the basic structure of the cascaded control strategy. The control system consists of an outer-loop (high-level) controller, which is a typical robot motion controller that calculates the required reference actuation forces, and an inner-loop (lower-level) hydraulic force-tracking controller, guiding the hydraulic actuators to execute the reference forces. With this control structure, the control problem is decoupled into two sub-problems, i.e., the hydraulic actuator *force tracking* problem and the parallel manipulator *motion tracking* problem. However, as will be elaborated, both sub-problems have their own particular design and implementation issues, yet also face similar challenges.

1.3.1. HYDRAULIC FORCE CONTROL

The use of fluid power is a very old discipline, which dates back to the beginning of the last century, when hydraulic actuators were used in an open-loop manner [18]. From the middle of the last century, as the servo-control techniques improved, more accurate closed-loop control for hydraulic servo systems became possible. The hardware of a *hydraulic servo-system* generally consists of the following three subsystems: (1) The *power supply* unit, which provides hydraulic power in the form of a constant supply pressure, (2) the *servo-valve*, which controls the fluid flows into and out of the actuator chambers,

and (3) the *actuator* which generates the actuation force by the fluid pressure difference between its two chambers [38].

The hydraulic actuator dynamics are mainly determined by the pressure dynamics of the hydraulic oil in the actuator chambers, caused by the hydraulic fluid compressibility [19]. For the purpose of controller design, the pressure dynamics of the two chambers are generally combined into a single dynamic equation [39]. This requires a great simplification of the model (for the controller) with some small terms neglected, which introduces inherent model uncertainties. The dynamic equation itself turns out to be highly nonlinear. In addition, other nonlinear features such as nonlinear frictions, oil leakage and additional sensor and filter dynamics, all contribute to the nonlinearity and model uncertainty of the dynamics, as will be explored in Chapter 3.

The strongly nonlinear and complex hydraulic system dynamics explains why the hydraulic force/torque control is challenging. Traditional linear controllers designed for a particular operating point cannot guarantee sufficient performance for whole joint space [40], especially for long stroke actuators when used to simulate aggressive maneuvers. Thus, a variety of model-based nonlinear controllers have been proposed [39, 41–43]. However, as discussed, hydraulic actuators generally suffer from multiple model and parameter uncertainties, which come from model simplification, wear-out and dead-zones of the servo-valve, nonlinear frictions and leakages, and even time-varying parameters such as the oil bulk modulus which varies as actuators heat up. These factors all deteriorate the performance of traditional model-based nonlinear controllers. For instance, one of the most effective nonlinear control approaches, referred to as feedback linearization [8, 41, 44], strongly depends on an accurate model of the control plant. With an inaccurate model, the feedback linearization can be outperformed by simple fixed-gain linear controllers [45]. The same problem exists for its variants, including Nonlinear Dynamic Inversion (NDI) based controllers [46], Cascade ΔP controllers (CdP) [35] and flatness-based control [42]. Adaptive control approaches are proposed for a few hydraulic robot control problems [10, 47–49] in which the hydraulic parameter adaptation law is coupled to the payload dynamics. Despite the complex design procedure, these do not provide direct hydraulic force actuators for a generalized outer-loop control system. Very few publications can be found discussing the adaptive force controller that are decoupled from the payload dynamics [39].

In conclusion, due to the inherent nonlinear and model-uncertain features of hydraulic actuators, a high performance, less model-dependent and time efficient nonlinear force controller would benefit its robotic motion and force control applications.

1.3.2. MOTION CONTROL FOR PARALLEL MANIPULATORS

Even though the theoretical advantages of parallel manipulators over their serial counterparts in terms of robustness and load mass ratio are well known, the precise motion control of these systems faces unique challenges in practice [28]. Despite the difficult feedforward kinematic problem for hexapod systems, which has no analytical solution, the most challenging problem comes from the complex dynamic model, the accuracy of which is essential for advanced motion control [50].

The dynamic model of a parallel robot is nonlinear and generally more complicated than its serial counterparts. Specifically, the modelling of a typical 6-DOF hexapod ma-

nipulator is generally discussed as a 13-body rigid body dynamic problem with closed kinematic loops. As has been well studied in literature, the dynamic equations of parallel robots can be derived with different methods with their corresponding forms, such as the Lagrangian formulation [51–53], Newton–Euler formulation [54, 55] or solutions based on the virtual work principle [56, 57]. These models all allow for the calculation of the robot inverse dynamics, with different levels of efficiency. However, none of them are convenient for parameter identification, which poses a significant challenge to properly tune these models.

Advanced model-based control strategies generally require the identified parameters with a good match to their real values. For serial robots, this can be achieved by using the well-studied form of the rigid body dynamics, with a linear form with respect to the dynamic parameters characterizing the manipulator links. However, for parallel manipulators, very few publications address a systematic solution in the linear form [58, 59], and the resulting complete model dynamic equations are often ill-conditioned for identification, due to the parallel manipulator structure. As a result, simplified models are used in a number of more practical investigations [50, 60, 61]. Particularly, it is shown in [61] that even for a 3-DOF parallel manipulator, a simplified dynamic model provides better control performance than that of a more complex model with a complete set of parameters.

This means that for parallel manipulators, the intuitive effort to improve the completeness and details for the dynamic model might not contribute to an improved performance. Thus, the most popular model-based motion control strategy for parallel robots is still the feedforward computed torque control with PD feedback [8, 28, 62, 63], using a practical (often simplified) inverse dynamic model. More model-dependent nonlinear controllers, such as feedback linearization, are rarely applied in practice.

In addition, the dynamic model suffers from uncertainties and disturbances of the load carried by the robot. For instance, for the SIMONA flight simulator, the weight of two pilots could make a 5% mass difference for the moving platform (the cockpit) with a weight of about 4000 kg. It indicates that the inertia parameters of parallel manipulators with the load are actually time-varying. For more general applications, the contribution of the load can be even more significant. For serial robots, parameter adaptation is a feasible solution for this problem. However, for parallel manipulators, the aforementioned problems from ill-conditioned linear dynamic equations and heavy computation prevent its practical application. As concluded in [28], its practical applications are restricted to cases with simple mechanics or a strongly simplified model [64, 65].

As the studied case of this thesis, a full-size hexapod flight simulator, represents a typical 6-DOF parallel mechanism, the developed control architecture should fit for a general parallel manipulator. In this respect, a practical control strategy which is time efficient and not sensitive to the model uncertainties, while still providing high performance, is aimed to be developed for parallel robots.

1.4. RESEARCH GOAL AND RESEARCH QUESTIONS

With the aforementioned opportunities and challenges, it can be concluded that the effort to improve the parallel hydraulic robot control performance with a more accurate *model* may significantly complicate the problem, resulting in problems such as the ill-

conditioned models and impractical computational load. Thus, in this dissertation an opposite control philosophy is adopted, that is, to develop control algorithms that are inherently *model independent*, or *model-free*, without compromising the control performance. Currently, no systematic solution that relaxes the model dependency is directly available for the research gaps identified for both control loops of a parallel hydraulic robot motion control system. As the studied case, a 6-DOF hexapod hydraulic flight simulator SRS, represents a typical example of a broader family of its kind, its precision motion control requirement leads to the main research goal of this thesis.

Research Goal

To develop high-precision, time-efficient motion control algorithms for parallel hydraulic robots, in the presence of considerable model uncertainties in both the hydraulic and mechanical subsystems.

1

In this dissertation, the research goal is achieved in a cascaded formulation, i.e., two control loops are designed individually for the low-level hydraulic force/torque control problem and the high-level parallel manipulator motion control problem. These are combined to form the complete control system (see Fig.1.3).

With the insights of the discussed system elaborated in the previous sections, it is easy to explain the advantages of the cascaded control structure. By decoupling the complete system, the dimension of the studied system dynamics is split and thus reduced, which simplifies the controller design procedure. More importantly, the cascaded control structure has a great versatility. For instance, the controlled inner-loop hydraulic actuator can be directly applied to other mechanical structures, such as serial manipulators, and other control applications such as competence control for legged robots [8]. Meanwhile, the individually developed motion controller for hydraulic manipulators can be applied to systems with other drives, including the more popular electrical ones. From this respect, the choice of cascaded control structure increases the generality of the work discussed in this thesis.

The inner-loop (low-level) control task is to solve the hydraulic actuator force/torque tracking problem. Given the required reference actuation force/torque, the time history of the servo-valve input (generally a voltage) is calculated and given by the controller, such that the reference force/torque is executed with designed transient and steady-state requirements. When considering the inner-loop, its application is not restricted to the parallel motion control in this dissertation, thus no assumption is made with regard to the mechanical structure or high-level control mission for the outer-loop. As discussed in the previous sections, the accurate hydraulic force/torque control faces serious challenges from system nonlinearity and model uncertainty problems. This leads to the first research question of this thesis:

Research Question 1

How to achieve *less model dependent* nonlinear **force/torque tracking control** for the hydraulic actuators with high performance, even when subjected to large hydraulic model uncertainties and disturbances?

The outer-loop (high-level) control task is a typical motion control problem for the challenging parallel manipulator mechanics. Again for generality, when considering the outer-loop motion control, the actuators are assumed to be general ‘force generators’ with stable dynamics, and no assumptions related to the hydraulic actuators themselves are made. As elaborated in the previous section, the precision control of parallel manipulators faces challenges from the problems encountered when obtaining an accurate dynamic model, which can be even time-varying due to changes in payload (e.g., inertia). This brings us the second research question:

Research Question 2

How to achieve *less model dependent* and high precision **motion control** for general parallel manipulators with large dynamic model offsets and disturbances?

These two research questions are formulated based on the research gaps identified in the cascaded control system design for the hydraulic parallel robots. By answering and solving the two research questions, a direct combination of both gives the solution for the research goal in this dissertation.

1

1.5. RESEARCH APPROACH AND CONTRIBUTIONS

As elaborated in the previous sections, efforts to improve the accuracy of the system model, e.g., with more advanced identification or adaptation methods, face practical limitations for both research questions. A totally opposite approach would be to make the control system inherently less model dependent. A recently-developed ‘model-free control’ [66, 67] aimed at designing controllers based on an universal ‘ultra-local model’ method for any system dynamics has shown significant theoretical merit, even though the theory is still not mature (especially for MIMO systems) and the local model still needs to be identified.

The more practical approaches, *incremental* control methods, are novel control techniques developed for nonlinear systems with model uncertainty, without the identification of a global model. By replacing the global system model by a locally linearized system in an incremental form on every small sampling period, the dependency of the controller on model accuracy can be significantly reduced. Based on this concept, several nonlinear control strategies have been proposed, such as Incremental Nonlinear Dynamic Inversion (INDI) [68], Incremental Backstepping (IBS) [69] and Incremental Reinforcement Learning [70]. By applying the incremental control concept within the traditional input-output feedback linearization approach, INDI significantly reduces the feedback linearization’s sensitivity to model uncertainties. A number of theoretical and practical applications of INDI have been reported recently on flight attitude control [3, 71, 72], showing great robustness against model uncertainties. This gives the motivation to develop an INDI-based motion control system for hydraulic parallel manipulators, as an approach to overcome the inevitable model uncertainty problems.

However, with the application of INDI to hydraulic parallel robot motion system control, several theoretical and practical problems are encountered. On the one hand, the INDI technique is not yet mature in theory, as its stability, robustness and disturbance

rejection features currently lack rigorous mathematical proofs. On the other hand, all practical INDI implementations to date rely on a few major assumptions on the control system dynamics, such as fast actuator dynamics, and accurate state derivative measurements. As INDI has only been applied to flight control systems, it is not known whether the required assumptions also hold for the hydraulic and parallel mechanical systems, as they have totally different inherent and additional dynamics. As a result, before the theoretical controller is implemented to the real system, a detailed high-fidelity nonlinear numerical model for the hydraulic hexapod system will be developed in this thesis, to serve as a test bed. Developing the motion control system with the INDI control technique will help to identify all aforementioned problems, and come up with general solutions.

The main contributions of this thesis are listed as follows:

- The novel Incremental Nonlinear Dynamic Inversion (INDI) control technique is applied to the hydraulic actuator force/torque control, and is implemented in practice on a real-life hydraulic system (the SRS) for the first time. Acting as the inner-loop controller, it is tested with different outer-loop controllers to form the complete motion control system, which shows the versatility of the INDI method.
- The INDI control technique is applied to the motion control for a parallel manipulator and implemented on a typical 6-DOF hexapod motion system (the SRS) for the first time. Connected with an inner-loop INDI hydraulic force control, this results in a complete motion control system that is based on INDI.
- The developed full-INDI control system is shown to have great robustness to model uncertainties from both hydraulic and mechanic subsystems. The robustness is *experimentally validated* through the introduction of an offset in important parameters, for both the hydraulic actuators and the hexapod system, including the valve flow, the total mass and the mass distribution of the manipulator.
- The robustness of INDI against model uncertainties is properly *proven in theory* for the first time, for both SISO and MIMO cases. As a result, a complete analysis of the stability margin and disturbance rejection capability of INDI are performed for the first time.
- High precision motion control performance is achieved by the developed control system. For a 4000 kg hydraulic flight simulator with over one meter stroke, sub-millimeter position tracking errors in fast maneuvers are achieved. Besides, compared with the state-of-the-art related studies available in literature, significant performance improvements are experimentally demonstrated for the developed INDI control system, even at extreme levels of model uncertainty.
- Practical issues preventing the real-world application of INDI for the hydraulic parallel manipulators are identified through simulation and experiments. Especially for long-stroke hydraulic actuators, the valve dynamics and additional oil transmission line dynamics can cause stability problems. Effective practical solutions are proposed and integrated into the basic framework for INDI.

1.6. SCOPE AND LIMITATIONS

This thesis focuses on the most relevant problems stated for the research goal and research questions. Despite that generality is ensured for the developed approach, its implementation is achieved and tested on a single hardware system (i.e., the SRS at TU Delft) with unique physical characteristics. This leads to several limitations of the work performed:

- **Symmetrical hydraulic actuators:** Although there are no additional theoretical difficulties for the proposed approach for asymmetric hydraulic actuators, the control systems are only designed and implemented for symmetrical actuators. Every actuator is assumed to be controlled by a four-way servo-valve with a bandwidth that is significantly higher than the natural frequency of the actuator. The friction of the actuators is assumed to be negligible, because of good lubrication.
- **Parallel manipulator:** While the typical 6-DOF hexapod motion system of the SRS is used as the case study, all development is done without loss of generality, as a general dynamic model for a parallel manipulator (with uncertainties) is used for the controller design. The inverse kinematic model is assumed to be known accurately, which allows for the motion reference transformation from work space to joint space. Besides, although not required by the proposed controller, the forward kinematics are assumed to be solved in real-time by numerical iteration, for the purpose of performance evaluation in the work space.
- **Inner/outer-loop frequency separation:** Theoretically, the stability of multiple loop control systems is often difficult to prove. In this thesis, the dynamics of the inner-loop (hydraulic actuator) are assumed to be significantly faster than that of the outer-loop (parallel manipulator), such that the stability of both loops can be analyzed independently.
- **State measurements:** The INDI approach followed in this thesis relies on sensor data from both the hydraulic and mechanical systems. Followed by the symmetry assumption for the actuators, only pressure difference transducers, instead of absolute pressure transducers, are required to obtain load force feedback. Also, the actuator piston displacements are measured by widely applied high resolution position transducers. In addition, servo-valve spool displacements are assumed to be accessible, as in the SRS. All sensor data are available at a sampling rate, that is as fast (or faster) as the controller update rate.

1.7. OUTLINE OF THIS THESIS

The structure of this thesis follows the research approach of developing a hydraulic hexapod motion control system, that depends less on an accurate model. In total two parts and six chapters are included, as illustrated in Fig.1.4.

Part I provides the theoretical foundation for the hydraulic parallel robot control, including a comprehensive literature survey of current hydraulic parallel manipulator control systems in Chapter 2, and a detailed mathematical model of the discussed system in Chapter 3, developed for the purpose of numerical simulations and control ef-

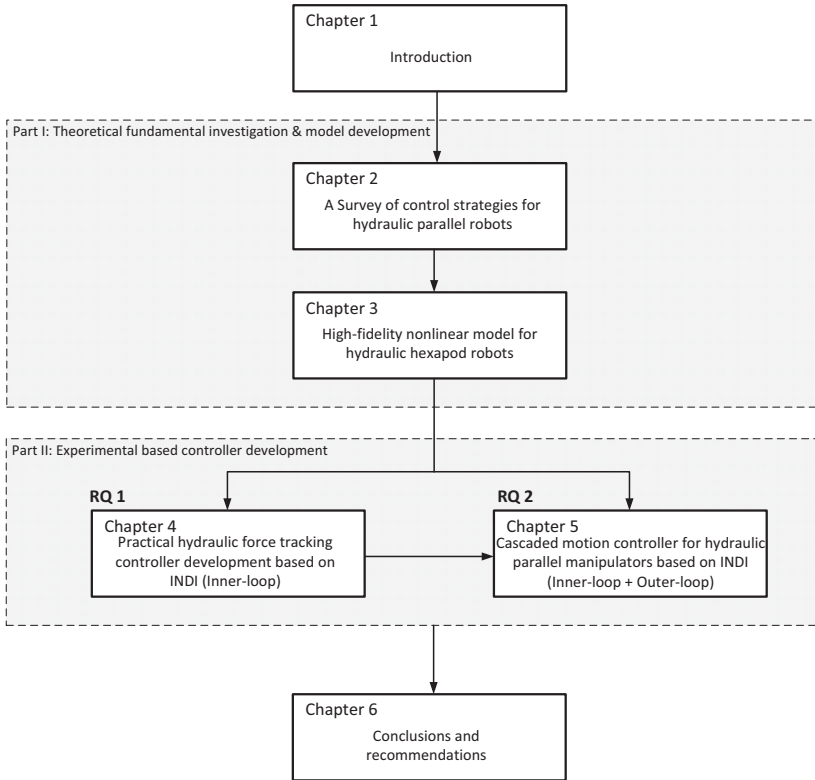


Figure 1.4: Outline of this thesis

efficiency tests. Part II discusses solutions for the research questions, elaborating on the INDI based control system development for the hydraulic subsystem in Chapter 4, and for the mechanical subsystem in Chapter 5.

Chapter 2: Hydraulic Parallel Control Survey. This chapter gives a comprehensive literature survey of control technologies that have been proposed or implemented for hydraulic parallel manipulators. Benefits and disadvantages of current state-of-the-art techniques are discussed, and theoretical and practical issues for the discussed control system are identified for a better insight in the characteristics of the proposed INDI control technique.

Chapter 3: High-fidelity nonlinear model for hydraulic hexapod robots. This chapter gives a comprehensive discussion on how the hydraulic system and parallel robotic system are modeled based on physical laws. The detailed model will not only be used as a test bed for high-fidelity numerical simulations, but will also help to identify and diagnose which parts of the system can form a potential problem for the proposed sensor-based INDI controller.

Chapter 4: Hydraulic force controller based on INDI. The proposed sensor-based

INDI control technique is introduced in detail with proofs of stability and robustness to model uncertainties. Based on the insights of the studied system obtained through the physical model discussed in Chapter 3, a practical controller design procedure for the hydraulic force controller is developed and tested. Practical problems such as valve dynamics and oil pipeline dynamics are discussed and solved. The effectiveness and performance of the proposed controller is compared with the state-of-the-art model-based controller reviewed in Chapter 2, based on numerical simulations of the model developed in Chapter 3 and experiment data collected with the SRS.

Chapter 5: Parallel Robotic Motion Controller based on INDI. The novel sensor-based INDI controller is applied to the outer-loop motion control problem for the parallel manipulator. Combined with the inner-loop force control system developed in the previous chapter, the complete motion control system is developed based on sensor-based INDI for the studied system. Simulation results on the model developed in Chapter 3 and experiment results obtained with the SRS are presented for verification and validation.

Chapter 6: Conclusions and recommendations. This chapter reviews the theoretical and experiment results. Conclusions are drawn with respect to the opportunities provided in this research, that is, the application of the sensor-based INDI controller for hydraulic hexapod flight simulator motion control and other similar systems. Recommendations for future work are provided.

REFERENCES

- [1] B. Malone, "George Devol: a life devoted to invention, and robots," <https://spectrum.ieee.org/automaton/robotics/industrial-robots/george-devol-a-life-devoted-to-invention-and-robots>, 2011, accessed: 2018-07-10.
- [2] EU Robotics, "Strategic research agenda for robotics in europe 2014–2020," https://www.eu-robotics.net/cms/upload/topic_groups/SRA2020_SPARC.pdf, 2014, accessed: 2018-07-10.
- [3] E. J. J. Smeur, Q. P. Chu, and Guido C. de Croon, "Adaptive incremental nonlinear dynamic inversion for attitude control of micro aerial vehicles," *Journal of Guidance, Control, and Dynamics*, vol. 39, no. 3, pp. 450–461, 2016.
- [4] M. Kalakrishnan, J. Buchli, P. Pastor, M. Mistry, and S. Schaal, "Learning, planning, and control for quadruped locomotion over challenging terrain," *The International Journal of Robotics Research*, vol. 30, no. 2, pp. 236–258, 2011.
- [5] S. Murthy, "Electric actuators replace hydraulics in full-flight simulators while still maintaining that aircraft "feel"," <http://www.moog.com/content/dam/moog/literature/ICD/Machine-Design-US-Jan-22-2009-Electrifying-the-Feel-of-Flight-E-print.pdf>, 2009, accessed: 2018-07-10.
- [6] H. E. Merritt, *Hydraulic control systems*. John Wiley & Sons, 1967.

- [7] Boston Dynamics, “Changing your idea of what robots can do,” <https://www.bostondynamics.com/robots>, accessed: 2018-07-10.
- [8] T. Boaventura, J. Buchli, C. Semini, and D. G. Caldwell, “Model-based hydraulic impedance control for dynamic robots,” *IEEE Transactions on Robotics*, vol. 31, no. 6, pp. 1324–1336, Dec 2015.
- [9] C. Semini, V. Barasuol, J. Goldsmith, M. Frigerio, M. Focchi, Y. Gao, and D. G. Caldwell, “Design of the hydraulically actuated, torque-controlled quadruped robot hyq2max,” *IEEE/ASME Transactions on Mechatronics*, vol. 22, no. 2, pp. 635–646, April 2017.
- [10] M. R. Siroospour and S. E. Salcudean, “Nonlinear control of hydraulic robots,” *IEEE Transactions on Robotics and Automation*, vol. 17, no. 2, pp. 173–182, 2001.
- [11] Ampelmann, “Safe and efficient people transfer,” <https://www.ampelmann.nl/systems/a-type>, accessed: 2018-07-10.
- [12] J.-P. Merlet, *Parallel robots*. Springer Science & Business Media, 2006.
- [13] B. Dasgupta and T. Mruthyunjaya, “The stewart platform manipulator: a review,” *Mechanism and Machine Theory*, vol. 35, no. 1, pp. 15 – 40, 2000.
- [14] D. Stewart, “A platform with six degrees of freedom,” *Proceedings of the Institution of Mechanical Engineers*, vol. 180, no. 1, pp. 371–386, 1965.
- [15] J.-P. Merlet and C. Gosselin, “Parallel mechanisms and robots,” in *Springer handbook of robotics*, B. Siciliano and O. Khatib, Eds. Springer, 2016, ch. 12, pp. 269–285.
- [16] TU Delft, “TU Delft ready to unleash the beast,” <https://www.tudelft.nl/en/3me/research/check-out-our-science/tu-delft-ready-to-unleash-the-beast/>, accessed: 2018-07-10.
- [17] KUKA, “Kuka occubot: the intelligent test system,” https://www.kuka.com/en-de/products/robot-systems/ready2_use/occubot, accessed: 2018-07-10.
- [18] G. van Schothorst, “Modelling of Long-Stroke Hydraulic Servo-Systems for Flight Simulator Motion Control and System Design,” Ph.D. dissertation, Delft University of Technology, 1997.
- [19] S. Koekebakker, “Model based control of a flight simulator motion system,” Ph.D. dissertation, Delft University of Technology, 2001.
- [20] M. Becerra-Vargas and E. M. Belo, “Robust control of flight simulator motion base,” *Journal of Guidance, Control, and Dynamics*, vol. 34, no. 5, pp. 1519–1528, 2011.
- [21] H. Duda, S. K. Advani, and M. Potter, “Design of the DLR AVES research flight simulator,” in *AIAA Modeling and Simulation Technologies (MST) Conference*, 2013.

- [22] S. K. Advani, "The development of SIMONA - A simulator facility for advanced research into simulation techniques, motion system control and navigation systems technologies," in *Flight Simulation and Technologies*. Monterey, CA, U.S.A., 1993, pp. 156–166.
- [23] O. Stroosma, M. M. van Paassen, and M. Mulder, "Using the SIMONA Research Simulator For Human-Machine Interaction Research," in *AIAA Modeling and Simulation Technologies Conference and Exhibit*, 2003.
- [24] J.-J. E. Slotine, W. Li *et al.*, *Applied nonlinear control*. Prentice hall Englewood Cliffs, NJ, 1991, vol. 199, no. 1.
- [25] Y. Huang, D. M. Pool, O. Stroosma, and Q. P. Chu, "Incremental nonlinear dynamic inversion control for hydraulic hexapod flight simulator motion systems," *IFAC-PapersOnLine*, vol. 50, no. 1, pp. 4294 – 4299, 2017, 20th IFAC World Congress.
- [26] B. Siciliano, L. Sciacivco, L. Villani, and G. Oriolo, *Robotics: modelling, planning and control*. Springer Science & Business Media, 2010.
- [27] O. Stroosma, M. M. van Paassen, M. Mulder, R. J. Hosman, and S. K. Advani, "Applying the objective motion cueing test to a classical washout algorithm," in *AIAA Modeling and Simulation Technologies (MST) Conference*, 2013.
- [28] H. Abdellatif and B. Heimann, "Advanced model-based control of a 6-DOF hexapod robot: A case study," *IEEE/ASME Transactions on Mechatronics*, vol. 15, no. 2, pp. 269–279, April 2010.
- [29] M. Díaz-Rodríguez, A. Valera, V. Mata, and M. Valles, "Model-based control of a 3-DOF parallel robot based on identified relevant parameters," *IEEE/ASME Transactions on Mechatronics*, vol. 18, no. 6, pp. 1737–1744, Dec 2013.
- [30] L. Ren, J. K. Mills, and D. Sun, "Experimental comparison of control approaches on trajectory tracking control of a 3-DOF parallel robot," *IEEE Transactions on Control Systems Technology*, vol. 15, no. 5, pp. 982–988, Sept 2007.
- [31] P. H. Chang and J. H. Jung, "A systematic method for gain selection of robust pid control for nonlinear plants of second-order controller canonical form," *IEEE Transactions on Control Systems Technology*, vol. 17, no. 2, pp. 473–483, March 2009.
- [32] A. Alleyne and R. Liu, "A simplified approach to force control for electro-hydraulic systems," *Control Engineering Practice*, vol. 8, no. 12, pp. 1347 – 1356, 2000.
- [33] T. Boaventura, M. Focchi, M. Frigerio, J. Buchli, C. Semini, G. A. Medrano-Cerda, and D. G. Caldwell, "On the role of load motion compensation in high-performance force control," in *2012 IEEE/RSJ International Conference on Intelligent Robots and Systems*, Oct 2012, pp. 4066–4071.
- [34] J. Koivumäki and J. Mattila, "High performance nonlinear motion/force controller design for redundant hydraulic construction crane automation," *Automation in Construction*, vol. 51, pp. 59 – 77, 2015. [Online]. Available: <http://www.sciencedirect.com/science/article/pii/S0926580514002581>

- [35] J. Heintze and A. van der Weiden, "Inner-loop design and analysis for hydraulic actuators, with an application to impedance control," *Control Engineering Practice*, vol. 3, no. 9, pp. 1323 – 1330, 1995.
- [36] H. Guo, Y. Liu, G. Liu, and H. Li, "Cascade control of a hydraulically driven 6-DOF parallel robot manipulator based on a sliding mode," *Control Engineering Practice*, vol. 16, no. 9, pp. 1055 – 1068, 2008.
- [37] T. A. Johansen and T. I. Fossen, "Control allocation—a survey," *Automatica*, vol. 49, no. 5, pp. 1087 – 1103, 2013. [Online]. Available: <http://www.sciencedirect.com/science/article/pii/S0005109813000368>
- [38] I. Davliakos and E. Papadopoulos, "Model-based control of a 6-DOF electrohydraulic Stewart–Gough platform," *Mechanism and Machine Theory*, vol. 43, no. 11, pp. 1385 – 1400, 2008.
- [39] M. Namvar and F. Aghili, "A combined scheme for identification and robust torque control of hydraulic actuators," *Journal of Dynamic Systems, Measurement, and Control*, vol. 125, no. 4, pp. 595–606, Jan 2004. [Online]. Available: <http://dx.doi.org/10.1115/1.1636777>
- [40] A. Alleyne, R. Liu, and H. Wright, "On the limitations of force tracking control for hydraulic active suspensions," in *Proceedings of the 1998 American Control Conference. ACC (IEEE Cat. No.98CH36207)*, vol. 1, Jun 1998, pp. 43–47 vol.1.
- [41] G. Vossoughi and M. Donath, "Dynamic feedback linearization for electrohydraulically actuated control systems," *ASME. J. Dyn. Sys., Meas., Control.*, vol. 117, no. 4, pp. 468–477, 1995.
- [42] F. Kock and C. Ferrari, "Flatness-based high frequency control of a hydraulic actuator," *Journal of Dynamic Systems, Measurement, and Control*, vol. 134, no. 2, p. 021003, 2012.
- [43] W. Kim, D. Won, and M. Tomizuka, "Flatness-based nonlinear control for position tracking of electrohydraulic systems," *IEEE/ASME Transactions on Mechatronics*, vol. 20, no. 1, pp. 197–206, Feb 2015.
- [44] G. A. Sohl and J. E. Bobrow, "Experiments and simulations on the nonlinear control of a hydraulic servosystem," *IEEE Transactions on Control Systems Technology*, vol. 7, no. 2, pp. 238–247, Mar 1999.
- [45] J. J. Craig, P. Hsu, and S. S. Sastry, "Adaptive control of mechanical manipulators," *The International Journal of Robotics Research*, vol. 6, no. 2, pp. 16–28, 1987.
- [46] A. Plummer, "Model-based motion control for multi-axis servohydraulic shaking tables," *Control Engineering Practice*, vol. 53, pp. 109 – 122, 2016.
- [47] B. Yao, F. Bu, J. Reedy, and G. T. C. Chiu, "Adaptive robust motion control of single-rod hydraulic actuators: theory and experiments," *IEEE/ASME Transactions on Mechatronics*, vol. 5, no. 1, pp. 79–91, Mar 2000.

- [48] S. Chen, Z. Chen, B. Yao, X. Zhu, S. Zhu, Q. Wang, and Y. Song, "Adaptive robust cascade force control of 1-DOF hydraulic exoskeleton for human performance augmentation," *IEEE/ASME Transactions on Mechatronics*, vol. 22, no. 2, pp. 589–600, April 2017.
- [49] J. Koivumäki and J. Mattila, "High performance non-linear motion/force controller design for redundant hydraulic construction crane automation," *Automation in construction*, vol. 51, pp. 59–77, 2015.
- [50] F. Caccavale, B. Siciliano, and L. Villani, "The tricept robot: dynamics and impedance control," *IEEE/ASME Transactions on Mechatronics*, vol. 8, no. 2, pp. 263–268, June 2003.
- [51] Z. Geng, L. S. Haynes, J. D. Lee, and R. L. Carroll, "On the dynamic model and kinematic analysis of a class of stewart platforms," *Robotics and Autonomous Systems*, vol. 9, no. 4, pp. 237 – 254, 1992.
- [52] C. C. Nguyen and F. J. Pooran, "Dynamic analysis of a 6 DOF CKCM robot end-effector for dual-arm telerobot systems," *Robotics and Autonomous Systems*, vol. 5, no. 4, pp. 377 – 394, 1989.
- [53] G. Lebret, K. Liu, and F. L. Lewis, "Dynamic analysis and control of a stewart platform manipulator," *Journal of Robotic Systems*, vol. 10, no. 5, pp. 629–655.
- [54] B. Dasgupta and T. Mruthyunjaya, "Closed-form dynamic equations of the general stewart platform through the newton–euler approach," *Mechanism and Machine Theory*, vol. 33, no. 7, pp. 993 – 1012, 1998.
- [55] —, "A Newton-Euler formulation for the inverse dynamics of the stewart platform manipulator," *Mechanism and Machine Theory*, vol. 33, no. 8, pp. 1135 – 1152, 1998.
- [56] C. Zhang and S. Song, "An efficient method for inverse dynamics of manipulators based on the virtual work principle," *Journal of Robotic Systems*, vol. 10, no. 5, pp. 605–627, 7 1993.
- [57] A. Codourey, "Dynamic modeling of parallel robots for computed-torque control implementation," *The International Journal of Robotics Research*, vol. 17, no. 12, pp. 1325–1336, 1998.
- [58] P. Renaud, A. Vivas, N. Andreff, P. Poignet, P. Martinet, F. Pierrot, and O. Company, "Kinematic and dynamic identification of parallel mechanisms," *Control Engineering Practice*, vol. 14, no. 9, pp. 1099 – 1109, 2006.
- [59] H. Abdellatif and B. Heimann, "Experimental identification of the dynamics model for 6-DOF parallel manipulators," *Robotica*, vol. 28, no. 3, p. 359–368, 2010.
- [60] Y. Li and Q. Xu, "Design and development of a medical parallel robot for cardiopulmonary resuscitation," *IEEE/ASME Transactions on Mechatronics*, vol. 12, no. 3, pp. 265–273, June 2007.

- [61] M. Díaz-Rodríguez, A. Valera, V. Mata, and M. Valles, “Model-based control of a 3-DOF parallel robot based on identified relevant parameters,” *IEEE/ASME Transactions on Mechatronics*, vol. 18, no. 6, pp. 1737–1744, Dec 2013.
- [62] H. Berghuis and H. Nijmeijer, “Robust control of robots via linear estimated state feedback,” *IEEE Transactions on Automatic Control*, vol. 39, no. 10, pp. 2159–2162, Oct 1994.
- [63] M. Honegger, R. Brega, and G. Schweiter, “Application of a nonlinear adaptive controller to a 6 DOF parallel manipulator,” in *Proceedings 2000 ICRA. Millennium Conference. IEEE International Conference on Robotics and Automation. Symposia Proceedings (Cat. No.00CH37065)*, vol. 2, 2000, pp. 1930–1935 vol.2.
- [64] M. Honegger, A. Codourey, and E. Burdet, “Adaptive control of the hexaglide, a 6 DOF parallel manipulator,” in *Proceedings of International Conference on Robotics and Automation*, vol. 1, April 1997, pp. 543–548 vol.1.
- [65] I. T. Pietsch, M. Krefft, O. T. Becker, C. C. Bier, and J. Hesselbach, “How to reach the dynamic limits of parallel robots? an autonomous control approach,” *IEEE Transactions on Automation Science and Engineering*, vol. 2, no. 4, pp. 369–380, Oct 2005.
- [66] M. Fliess and C. Join, “Model-free control and intelligent pid controllers: Towards a possible trivialization of nonlinear control?” *IFAC Proceedings Volumes*, vol. 42, no. 10, pp. 1531 – 1550, 2009, 15th IFAC Symposium on System Identification. [Online]. Available: <http://www.sciencedirect.com/science/article/pii/S147466701638870X>
- [67] —, “Model-free control,” *International Journal of Control*, vol. 86, no. 12, pp. 2228–2252, Dec. 2013. [Online]. Available: <https://hal-polytechnique.archives-ouvertes.fr/hal-00828135>
- [68] S. Sieberling, Q. P. Chu, and J. A. Mulder, “Robust Flight Control Using Incremental Nonlinear Dynamic Inversion and Angular Acceleration Prediction,” *Journal of Guidance, Control, and Dynamics*, vol. 33, no. 6, pp. 1732–1742, nov 2010.
- [69] P. Lu, E.-J. Van Kampen, and Q. P. Chu, “Robustness and tuning of incremental backstepping approach,” in *AIAA Guidance, Navigation, and Control Conference*, 2015, p. 1762.
- [70] Y. Zhou, E.-J. van Kampen, and Q. P. Chu, “Incremental model based online dual heuristic programming for nonlinear adaptive control,” *Control Engineering Practice*, vol. 73, pp. 13 – 25, 2018.
- [71] P. Simplício, M. D. Pavel, E. van Kampen, and Q. P. Chu, “An acceleration measurements-based approach for helicopter nonlinear flight control using incremental nonlinear dynamic inversion,” *Control Engineering Practice*, vol. 21, no. 8, pp. 1065 – 1077, 2013.

- [72] F. Grondman, G. Looye, R. O. Kuchar, Q. P. Chu, and E.-J. Van Kampen, ser. AIAA SciTech Forum. American Institute of Aeronautics and Astronautics, Jan 2018, ch. Design and Flight Testing of Incremental Nonlinear Dynamic Inversion-based Control Laws for a Passenger Aircraft.

2

SURVEY OF HYDRAULIC PARALLEL ROBOT CONTROL SYSTEMS

This chapter gives a literature review of proposed or implemented control systems for the hydraulic parallel motion systems. As relatively few works directly discuss the integrated hydraulic parallel robots, researches discussing both the hydraulic subsystem and the parallel mechanic subsystem are reviewed separately. Pros and cons of the reviewed control methods for both subsystems are discussed. The analysis of the current control methods gives us more insights on how the nonlinear dynamics of the hydraulic parallel robots prevent the traditional control methods from achieving better performance. Based on the drawbacks of the state-of-the-art researches and the remaining challenges, an innovative control framework for the studied system is proposed. In this chapter, after a brief introduction, a summary of the system model for hydraulic parallel robots for control purpose is given in Section 2.2. literature review of hydraulic control systems and parallel robotic control systems are given in Section 2.3. Motivated by the disadvantages of the current control systems, an innovative Incremental Nonlinear Dynamic Inversion (INDI) control method is introduced in Section 2.4, as a potential technique for an improvement of performance.

This chapter is based on the following chapter:

Y. Huang, D. M. Pool, O. Stroosma, Q. P. Chu, and M. Mulder, "A review of control schemes for hydraulic Stewart platform flight simulator motion systems," in AIAA Modeling and Simulation Technologies Conference, January 2016. [1]

This Chapter offers a brief review of hydraulic Stewart platform related control schemes, for purpose of obtaining a guideline for high performance flight simulator motion system control strategy design. The motion tracking control schemes for a pure Stewart platform for a outer-loop are discussed first, then applicable inner-loop hydraulic actuator control strategies are introduced. Inverse dynamics control, force feedforward control, adaptive and robust control schemes are discussed for the outer-loop mechanical system, while feedback linearization control, cascade pressure difference control as well as other simple and advanced control schemes are discussed for the inner-loop hydraulic system. Based on an analysis of system requirements of the control system after the the review, an novel sensor based Incremental Nonlinear Dynamic Inversion (INDI) controller is introduced to deal with the hydraulic actuator. The robustness of INDI is verified and compared with model-based controller by simulation. Finally the possible application of INDI to outer-loop Stewart platform control is discussed.

2.1. INTRODUCTION

For current high performance research and training flight simulator motion systems, Stewart platforms, also referred to as hexapod systems, are almost invariably used due to the advantages of high stiffness and accuracy, as well as their simplicity. The basic structure of such a manipulator is shown in Figure 2.1 As relatively large forces are applied with actuators of flight simulators, hydraulic actuators dominated high payload simulators for the past decades, owing to their rapid response, high loading capabilities and smoothness[2]. A representation of such simulator is the SIMONA Research Simulator (SRS) at TU Delft[3] (Figure 2.1). The control schemes on the motion system largely decide the motion performance of the simulators.

During the past decades, a number of papers have discussed different approaches to hexapod system control and hydraulic manipulator control, while fewer explicitly considered the combined hydraulic Stewart platform system[4, 5]. For most papers treating control of parallel mechanical systems the dynamics of actuators are considered as parasitic influences and accounted for with simplified models[6, 7]. On the other hand, for studies concerning hydraulic manipulator control, the actuator dynamics are often considered in detail while the driven mechanics are not considered in the kinematic framework of a Stewart platform[8, 9]. Considering the heavy interaction of actuators dynamics and kinematics, control strategies of both subsystems should be studied. However, there has been little cohesive discussion and comparative evaluation of different integrated control approaches.

The control of Stewart platform manipulators is a classic robot control problem, since hexapods are representative for a broader class of parallel robots[10]. Out of a growing demand of accuracy and performance of parallel robots, model-based control schemes like inverse dynamic control and feedforward force control have been applied to compensate for the highly nonlinear dynamics of such a robot. In order to overcome the problem that the inevitable dynamic and parameter uncertainties and disturbances significantly deteriorate the model based control performance, advanced control schemes like adaptive[11, 12] and robust[6, 13] control have been introduced. However, those control methods are difficult to apply to hydraulic manipulators directly, as hydraulic actuators resemble velocity sources rather than force/torque sources, as for

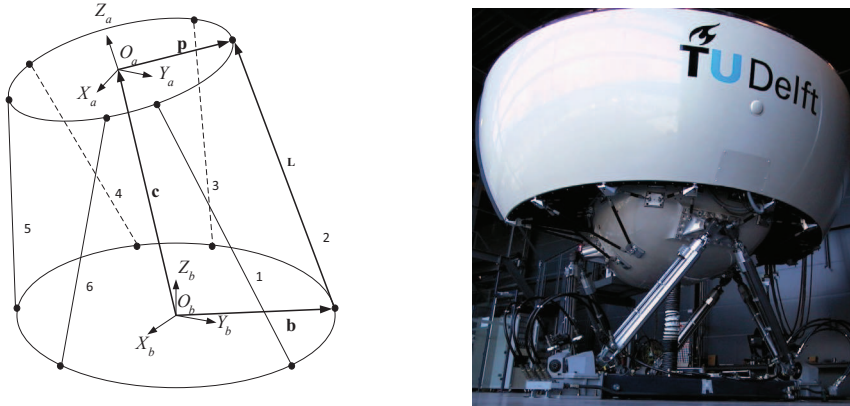


Figure 2.1: Basic structure of a Stewart platform (left) and a hexapod motion system SRS at TU Delft (right)

instance present in electrical actuators.[14] Thus a cascaded control configuration is generally designed to divide the whole system into an outer-loop manipulator motion tracking system and an inner-loop hydraulic force tracking system. Hydraulic actuator dynamics experience an even more severe problem of nonlinearity and model uncertainties compared with just the mechanism, due to phenomena like nonlinear servo-valve flow characteristics, valve opening overlaps, oil leakage and even time varying oil modulus[15]. For better performance, model-based control schemes need a careful identification of parameters. Meanwhile, control schemes which are more resistant to uncertainties like adaptive control[16, 17] robust control[18] and sliding mode control [19] approaches have been applied to hydraulic systems. However, most of the applications of these control techniques are restricted to single actuator situation, and are not directly available for parallel manipulators. Besides, practical problems such as chattering and high computational burden exist.

This study will present a review of papers on motion control of hydraulic parallel manipulators, which is the foundation of hydraulic hexapod flight simulator motion system. Papers on control schemes of both perspectives of discussed control object, parallel manipulators control and hydraulic driven manipulators control, will be summarized respectively. First, parallel manipulators control schemes are discussed and categorized as: Inverse dynamics scheme, feedforward force scheme, adaptive scheme and robust scheme. Motivation and disadvantages of each scheme will be discussed. Then, considering the integrated system with actuators, control schemes for hydraulic actuators to be integrated with outer-loop will be discussed. Feedback linearization controller, cascade pressure difference (CdP) controller and other simple and advanced control schemes will be discussed. At the end of the review, as this study aims to provide a guideline to advanced control strategy design of hydraulic hexapod flight simulator motion systems, a novel sensor based control strategy is introduced for hydraulic actuator force tracking, based on the analysis of drawbacks of current hydraulic control schemes covered in this review. Simulation results show much better performance of the introduced controller in

robustness compared with a currently implemented model-based CdP Controller. This literature review can also be of interest to other applications of hydraulic manipulator and parallel manipulator-based machines and robots.

2.2. MODELING

2.2.1. MANIPULATOR DYNAMIC MODELING

An appropriate model of a system plays a crucial role in controller design and stability analysis. As a representation of a bigger family of parallel manipulators, the well known dynamic equation of Stewart platform is given in a Lagrange formulation as[14, 20]:

$$\mathbf{M}(\mathbf{z}) \ddot{\mathbf{s}} + \mathbf{C}(\mathbf{z}, \dot{\mathbf{s}}) \dot{\mathbf{s}} + \mathbf{G}(\mathbf{z}) = \boldsymbol{\tau} = \mathbf{J}^T(\mathbf{z}) \mathbf{f}_a \quad (2.1)$$

where \mathbf{M} is the mass matrix, \mathbf{C} is the coriolis and centripetal terms, \mathbf{G} represents gravitation forces, \mathbf{J} is the Jacobian matrix, \mathbf{z} , $\dot{\mathbf{s}}$ and $\ddot{\mathbf{s}}$ represent the position, velocity and acceleration vectors of the moving platform, $\boldsymbol{\tau}$ and \mathbf{f}_a are the generalized and actuation forces.

Equation (2.1) is the most recognizable model for general robots. It is useful in a lot of applications, from controller design, system analysis to numerical simulation [21]. However, the Lagrange formulation is hard to solve and require a heavy computational effort for hexapods. Thus, a more computational efficient model is proposed in an New-Euler formulation as

$$\mathbf{J}_{q,s}^T \mathbf{f}_a = \mathbf{M}(\mathbf{z}) \ddot{\mathbf{s}} + \boldsymbol{\eta}(\dot{\mathbf{s}}, \mathbf{z}), \quad (2.2)$$

where the the coriolis terms, centripetal terms and gravitation forces are lumped in the term $\boldsymbol{\eta}$, without distinction. This formulation is particularly useful in numerical simulation and inverse dynamic computation.

The dynamic equation can also be written in the form that the dynamic model is linear with respect to dynamic parameters, written as[22]:

$$\mathbf{f}_a = \boldsymbol{\Psi}(\mathbf{z}, \dot{\mathbf{s}}, \ddot{\mathbf{s}}) \boldsymbol{\pi} \quad (2.3)$$

where $\boldsymbol{\pi}$ is a vector of constant dynamic parameters (mass, first moment and inertia tensor) and $\boldsymbol{\Psi}$ is a matrix called regressor which is a function of platform position, velocity and acceleration. The linear regressive form is almost invariably used for purposes of parameter identification and adaptive controller design. For typical serial robots (which strongly resemble human hands), this linear form is well-studied with various successful applications. However, for parallel robots represented by the discussed Stewart platform, very few publications give a systematic solution [23]. Due to the complex structure of the Stewart platform, the resulting model is complicated and often ill-conditioned [24]. Its real-life applications are often achieved by considering significant model simplification based on the features of the studied mechanism [21, 24–26].

2.2.2. HYDRAULIC ACTUATOR DYNAMIC MODELING

The basic structure of a linear hydraulic actuator driven by a servo valve can be observed on Figure 2.2. The dynamics of hydraulic actuators are the main obstacle of direct im-

plementation of general robotic manipulator control schemes. The highly nonlinear dynamics of hydraulic actuators which interacts with the motion of mechanical subsystem is mainly caused by the compressibility of the oil. With the signs defined in Figure 2.2, the pressure dynamics of each chamber are described as:

$$\begin{aligned}\dot{P}_{p1} &= \frac{E}{A_{p1}(q_{max} + q)} (\Phi_{p1} - \Phi_{lp} - \Phi_{l1} - A_{p1}\dot{q}) \\ \dot{P}_{p2} &= \frac{E}{A_{p2}(q_{max} - q)} (-\Phi_{p2} + \Phi_{lp} - \Phi_{l2} + A_{p2}\dot{q})\end{aligned}\quad (2.4)$$

where Φ_{p1} and Φ_{p2} are inlet and outlet oil flows from the valve, Φ_{l1} , Φ_{l2} and Φ_{lp} are the respective leakage flows, A_{p1} and A_{p2} are the respective piston areas, E is the oil modulus, q is the actuator displacement and q_{max} is the actuator stroke in the neutral position.

The valve flows Φ_{pi} are considered as turbulent through the respective valve restriction with constant discharge coefficient C_d [27, 28], written as:

$$\Phi = C_d A_m x_m \sqrt{2(P_{in} - P_{out})/\rho} \quad (2.5)$$

where A_m is the maximum area of the valve orifice, x_m is the valve displacement, ρ is the oil density, P_{in} and P_{out} are the oil pressures of the inlet and outlet side of the valve restriction. As the frequency in terms of the valve is much higher than that of the actuator, the dynamics of valve spool is neglected in most studies on hydraulic control, thus the spool displacement x_m is regarded as system input, i.e.:

$$x_m = u$$

The actuation force f_a can now described by:

$$f_a = P_{p1} A_{p1} - P_{p2} A_{p2} \quad (2.6)$$

By differentiating the above equation and substituting for the appropriate terms from equations (2.4-2.5), we get[29]:

$$\dot{f}_a = Q(P_{pi}, q) k_q u - T(A_{pi}, q) \dot{q} - L(q) P_L \quad (2.7)$$

where

$$Q = \begin{cases} E \left(\frac{\sqrt{P_s - P_{p1}}}{q_{max} + q} + \frac{\sqrt{P_{p2} - P_r}}{q_{max} - q} \right) & x_m \geq 0 \\ E \left(\frac{\sqrt{P_{p1} - P_r}}{q_{max} + q} + \frac{\sqrt{P_s - P_{p2}}}{q_{max} - q} \right) & x_m < 0 \end{cases} \quad (2.8)$$

$$T = E \left(\frac{A_{p1}}{q_{max} + q} + \frac{A_{p2}}{q_{max} - q} \right) \quad (2.9)$$

and where $P_L = P_{p1} - P_{p2}$ is the pressure difference between two chambers, $k_q = C_d A_m \sqrt{2/\rho}$ is the flow gain coefficient. It should be noted that the leakage related term L differs with different configurations of actuators.

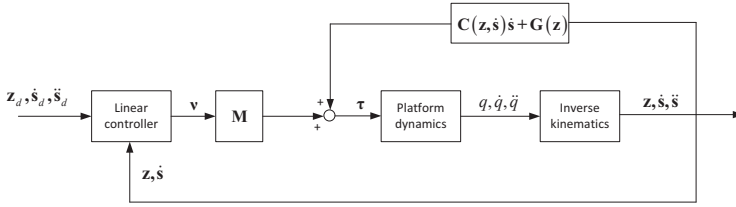


Figure 2.3: Block diagram of inverse dynamics controller for Stewart platform motion tracking

inverse dynamics control[20, 32]. The controller design is summarized as follows. Recall the dynamic model in Equation 2.1, the inverse dynamics control law is given by:

$$J^T(z) f_a = M(z) v + C(z, \dot{s}) \dot{s} + G(z) \quad (2.12)$$

Substituting Equation (2.12) into (2.1), exact linearization is achieved as $\ddot{s} = v$. By choosing:

$$v = \ddot{s}_d + K_d \dot{e} + K_p e \quad (2.13)$$

where $e = s_d - s$, the error dynamics of the closed-loop system is:

$$\ddot{e} + K_d \dot{e} + K_p e = 0 \quad (2.14)$$

where asymptotic stability is ensured by choosing appropriate K_d and K_p . The structure of inverse dynamics control is shown in Figure 2.3, the subscript d denotes the reference values.

The main disadvantage of the inverse dynamics controller is a lack of robustness: the exact linearization depends on the exact knowledge of the model. However, models never identically present the real physical systems. When the modeling is not accurate enough, the performance is generally significantly degraded. To this end, for parallel robots, inverse dynamics control is more often discussed in theoretical papers[33]. For the few practical-oriented studies on inverse dynamic control for parallel robots[30, 32], an accurate model parameter identification is often emphasized. As will be elaborated later, parameter identification for parallel robots, especially the 6-DOF Stewart platform, faces more challenges than their serial counterparts. Model simplification is often necessary for computational efficiency that often provide better control accuracy [32, 34]. From this respect, a more complicated model does not necessarily lead to better performance for parallel robots.

Figure 2.3 presents the inverse dynamic control in the Cartesian space instead of the joint space, which is more common in serial robot control studies. This is due to the fact that the dynamic equation for parallel manipulators is difficult to be fully expressed in joint space. In theory, the Cartesian space controller for parallel robots provides several advantages over the other one, including a more direct error feedback and the avoidance of kinematic model identification and singularity [30]. However, in practice, it is

less straight-forward because their forward kinematic problem does not have an analytic solution. A practical solution requires numerical iteration which is time consuming. Flavien [30] proposed a Cartesian space inverse dynamic control with direct measurements of the system end-effector pose, using exteroceptive sensors such as laser trackers and computer vision solutions. However, their applications are not given in the experiments. From this point of view, in terms of inverse dynamic control, parallel robots face more problems in both joint space and Cartesian space, compared with their serial counterparts.

In order to relax the robustness problem of the inverse dynamic control, a passivity-based control designed in joint space was proposed for a 3-DOF parallel robot in [34]. Since it does not rely on the exact cancellation of the system nonlinearity, it is in theory more robust than the typical inverse dynamic control. However, for performance in practical application, accurate parameter identification is still suggested in the study.

FEEDFORWARD FORCE WITH PD FEEDBACK

To further relax the accurate model dependency and computational load, a feedback controller plus a feedforward force compensation was used in a number of applications[21, 22, 35, 36], which is, to the best of the author's knowledge, the most popular control strategy applied to parallel manipulators. When the feedback loop is designed as a simple PD controller, the structure is similar in form to computed torque control discussed above, and in a number of literature it's called computed-force controller[37]. The basic structure of feedforward force control with PD feedback controller is shown in Figure 2.4, and the general control law is given by

$$\mathbf{f}_a = \mathbf{M}_q (\mathbf{K}_d \dot{\mathbf{e}}_q + \mathbf{K}_p \mathbf{e}_q) + \mathbf{F}_{ff}, \quad (2.15)$$

where $\mathbf{e}_q = \mathbf{q}_d - \mathbf{q}$ and \mathbf{F}_{ff} is the feedforward force computed by the system inverse dynamics and the reference motion profile. Compared with a single PD feedback controller, the performance is significantly improved with the introduction of model based feedforward. Compared with the inverse dynamics control approach, this technique is more robust since the uncertainties in the inverse dynamics model will not significantly affect the performance since they are corrected by the PD feedback loop. This makes it possible to use simplified dynamic model which will largely reduce the computational burden. In real-world applications, model parameters should be identified for better performance[2, 21, 34], by using dynamic equation (2.3). Indeed, the errors in the feedforward force have to be compensated by the feedback force, which is by definition linear to the tracking errors.

This control structure is particularly attractive for parallel manipulators also because of the avoidance of the forward kinematics. The feedforward force can be designed in Cartesian space and the feedback force directly designed in the joint space. The cumbersome numerical iteration for forward kinematic calculation is no longer required for the controller.

ADAPTIVE CONTROL

For model based inverse dynamics control, when the model and parameter uncertainties are significant, the application may lead to performance that is inferior to a much

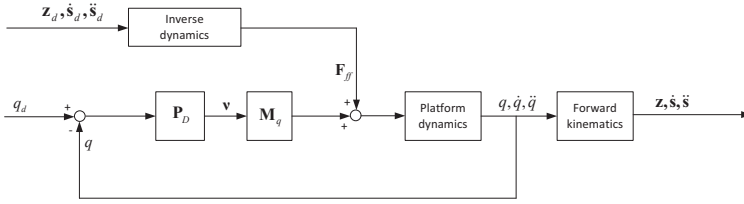


Figure 2.4: Feedforward force with PD controller for Stewart platform motion tracking

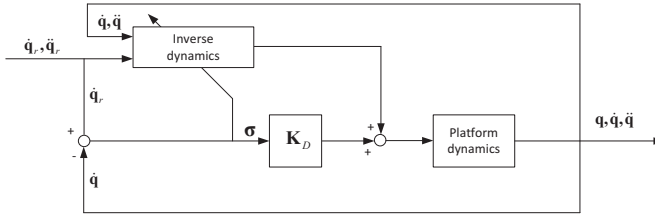


Figure 2.5: Adaptive controller for Stewart platform motion tracking

simpler fixed gain controller[38]. A certain degree of uncertainty always exist in a model due to imperfect knowledge of the system[20], meanwhile the computational burden asks for a simplified model with a certain degree of approximation. Thus from a practical application point of view, perfect linearization does not exist. An intuitive technique to deal with the imperfect compensation is to use an adaptive control scheme to ensure the limited tracking errors. To the best of the author's knowledge, all the current adaptive control studies for parallel robots use the linear regression form of the system dynamic model in joint space, which is identical in form to that of the serial manipulators, given as

$$\mathbf{M}(\mathbf{q})\ddot{\mathbf{q}} + \mathbf{C}(\mathbf{q}, \dot{\mathbf{q}})\dot{\mathbf{q}} + \mathbf{G}(\mathbf{q}) = \Psi(\mathbf{q}, \dot{\mathbf{q}}, \ddot{\mathbf{q}})\boldsymbol{\pi} \quad (2.16)$$

where $\boldsymbol{\pi}$ is a set of constant minimal dynamic parameter, $\Psi(\mathbf{q}, \dot{\mathbf{q}}, \ddot{\mathbf{q}})$ is called the regressor, which is a function of joint positions, velocities and accelerations.

Taking advantage of the linear form of the manipulator dynamics model (2.16) in joint space, typical adaptive control algorithm developed for serial manipulators[20] can be directly used, with control law:

$$\begin{aligned} \mathbf{u} &= \mathbf{f}_a = \hat{\mathbf{M}}_q(\mathbf{q})\ddot{\mathbf{q}}_r + \hat{\mathbf{C}}_q(\mathbf{q}, \dot{\mathbf{q}})\dot{\mathbf{q}}_r + \hat{\mathbf{G}}_q(\mathbf{q}) + \mathbf{K}_D(\dot{\mathbf{e}}_q + \boldsymbol{\Lambda}\mathbf{e}_q) \\ &= \Psi(\mathbf{q}, \dot{\mathbf{q}}, \ddot{\mathbf{q}}_r)\hat{\boldsymbol{\pi}} + \mathbf{K}_D(\dot{\mathbf{e}}_q + \boldsymbol{\Lambda}\mathbf{e}_q) \end{aligned} \quad (2.17)$$

Where $\Psi(\mathbf{z}, \dot{\mathbf{s}}, \ddot{\mathbf{q}}_r, \ddot{\mathbf{q}}_r)\hat{\boldsymbol{\pi}}$ is the regression matrix, $\dot{\mathbf{q}}_r = \dot{\mathbf{q}}_d + \boldsymbol{\Lambda}\mathbf{e}_q$ and the circumflex superscript denotes the estimated terms in the dynamic model, \mathbf{K}_D and $\boldsymbol{\Lambda}$ are positive definite matrix which provide a PD action of the last term. Using the adaptive law:

$$\dot{\hat{\pi}} = \mathbf{K}_\pi^{-1} \Psi^T(\mathbf{q}, \dot{\mathbf{q}}, \ddot{\mathbf{q}}_r, \ddot{\mathbf{q}}_r) (\dot{\mathbf{e}}_q + \Lambda \mathbf{e}_q) \quad (2.18)$$

where \mathbf{K}_π is a symmetric positive definite, the system globally asymptotically converges to $\mathbf{e}_q = 0$ and $\dot{\mathbf{e}}_q = 0$, and the boundedness of $\hat{\pi}$ is ensured [20]. The basic structure of such typical adaptive controller is illustrated in Figure 2.5.

Despite there being a number of different adaptive control algorithms for parallel manipulators, a common feature of them [8, 12, 14, 31, 39, 40] is that the control laws and adaptive law are proposed based on the linear dynamic equation $\mathbf{f}_a = \Psi(\mathbf{q}, \dot{\mathbf{q}}, \ddot{\mathbf{q}}) \boldsymbol{\pi}$. For serial manipulators, dynamic equation in this linear regression form is well studied and elaborated concluded in standard books [20]. However, for parallel robots, they are all derived with strongly simplified model or structure, and very few publications give a systematic solution [41]. For a general 6-DOF parallel manipulator without major model simplification, the resulting linear model can be very complicated and often ill-conditioned [24]. It is concluded in [41] that 88 base inertial parameters need to be identified for a typical 6-DOF parallel manipulator, even with necessary parameter number reduction. Thus in practice the model simplification is achieved by neglecting small inertial terms based on the characteristic of the studied system, such the mass of the legs [23] or the end-effector [21]. However, for a typical Stewart platform that both legs and upper-platform contribute significantly to the nonlinear dynamics, those simplifications are not technologically sound.

Another disadvantage of an adaptive controller is that the computational burden is even heavier than inverse dynamics controller, as the system dynamic model is calculated on-line in both the control law and the adaptive procedure. Their real-time application is limited to either simple mechanisms or special cases of geometry with high-end hardware [21].

ROBUST CONTROL

Apart from adaptive control, robust control is another way to deal with model uncertainties. However, for a parallel manipulators, few papers discussing the application of robust control can be found and many on them give computed-torque-like strategies. For instance, Lee [32] proposed an inverse dynamic controller based on significantly simplified dynamic model, the modeling errors introduced by which are compensated by an outer-loop H_∞ controller. However, it is assumed that the manipulator work in a small working space, such that the dynamic matrices are simplified as constants. This does not necessarily hold for parallel manipulators designed to exploit a large working space, such as a flight simulator. Mauricio [13] introduced a robust control strategy for Stewart platforms that counteracts the uncertainties by computing the inverse dynamics in working space, inspired by a joint space approach proposed in Ref. [20]. The basic idea is that the boundary of uncertainty which is introduced by inaccurate dynamics inversion could be approximated and counteracted with the proper design of the controller, while the stability could be guaranteed. Recall Equation (2.1), the model can be written in the form:

$$\mathbf{M}(\mathbf{z}) \ddot{\mathbf{s}} + \mathbf{N}(\mathbf{z}, \dot{\mathbf{s}}) = \boldsymbol{\tau} \quad (2.19)$$

Considering uncertainties in the model, following an inverse dynamics controller leads to:

$$\boldsymbol{\tau} = \hat{\mathbf{M}}(\mathbf{z}) \mathbf{v} + \hat{\mathbf{N}}(\mathbf{z}, \dot{\mathbf{s}}) \quad (2.20)$$

Then the closed-system dynamic is written as:

$$\ddot{\mathbf{s}} = \mathbf{v} + (\mathbf{M}^{-1} \hat{\mathbf{M}} - \mathbf{I}) \mathbf{v} + \mathbf{M}^{-1} (\mathbf{N} - \hat{\mathbf{N}}) = \mathbf{v} - \mathbf{n} \quad (2.21)$$

Now choose the virtual control input as:

$$\mathbf{v} = \ddot{\mathbf{s}}_d + \mathbf{K}_d \dot{\mathbf{e}} + \mathbf{K}_p \mathbf{e} + \mathbf{u} \quad (2.22)$$

where \mathbf{u} is a term introduced to overcome the uncertainty term \mathbf{n} . Now the error dynamics is given by:

$$\ddot{\mathbf{e}} + \mathbf{K}_d \dot{\mathbf{e}} + \mathbf{K}_p \mathbf{e} = \mathbf{n} - \mathbf{u} \quad (2.23)$$

By defining $\boldsymbol{\xi} = [\mathbf{e}^T, \dot{\mathbf{e}}^T]^T$, the above equation is described in state-space form:

$$\dot{\boldsymbol{\xi}} = \mathbf{A}\boldsymbol{\xi} + \mathbf{B}(\mathbf{n} - \mathbf{u}) \quad (2.24)$$

Based on the above nonlinear time-varying error system, the robust control law is designed as:

$$\mathbf{u} = \frac{\rho}{\|\mathbf{B}^T \mathbf{P} \mathbf{s}\|} \mathbf{B}^T \mathbf{P} \mathbf{s} \quad (2.25)$$

where \mathbf{P} is the unique solution of Lyapunov equation $\mathbf{A}^T \mathbf{P} + \mathbf{P} \mathbf{A} = -\mathbf{T}$ with \mathbf{T} a symmetric positive definite matrix, and ρ is chosen based on the boundary of \mathbf{n} . With the above control law, the system described in Equation (2.24) converges to zero, which is proven by Lyapunov second method[20].

Similar robust control laws for Stewart platform are derived by other researchers[6, 42]. The common disadvantage of these techniques is that the control law leads to a chattering problem. A boundary layer containing the sliding surface $\mathbf{B}^T \mathbf{P} \mathbf{s} = 0$ can be designed to release the problem, however, the control accuracy will be affected.

2.3.2. HYDRAULIC ACTUATOR CONTROL SCHEMES FOR INTEGRATED STEWART PLATFORM

SIMPLE CONTROLLERS

The control inputs of the aforementioned outer-loop manipulators are the forces acting on every actuators, thus the basic function of an inner-loop hydraulic actuator controller is to generate the required forces. PID controller are still used in most industrial hydraulic robots[16], and a typical PID controller for actuation force tracking is given by[8]:

$$x_m = \left(k_p + \frac{k_i}{s} + k_d s \right) \cdot \left(\frac{\omega_0}{s + \omega_0} \right)^3 \cdot (f_{des} - f_{act}) \quad (2.26)$$

which is described in frequency domain with a 3rd order low-pass filter.

The gain tuning of these linear controllers generally requires a local model linearization of the hydraulic actuator dynamics about an operating point [43]. However, as the actuator dynamics are highly nonlinear, the control performance can not be guaranteed when the system states are far away from the nominal operating point. In order to solve this problem, Thiago etc. [43] proposed a gain scheduling control structure, making the PID controller gains adaptive according to the actuator position. However, only three gain scheduling workspaces are designed in the study due to the relatively small actuator stroke. For long-stroke hydraulic actuators exploiting a large working space, the gain scheduling algorithm may be complicated. Besides, the control performance can still not be guaranteed in presence of model uncertainties.

In some cases, the dynamic equation of a hydraulic actuator can be given in a simplified form compared with a general one described in Equation (2.7), such that the controller can be designed directly. For instance, by neglecting the leakage term [8, 14], the valve opening (input) can be explicitly described by actuation force derivative and velocity:

$$x_m = h \cdot \dot{f}_a + g \cdot \dot{q} \quad (2.27)$$

where h and g are nonlinear functions of the system states.

When oil compressibility is neglected [4, 33, 44], the spool displacement can be explicitly described by actuation force and velocity:

$$x_m = h_1 \cdot f_a + g_1 \cdot \dot{q} \quad (2.28)$$

In both cases, the spool position x_m could be directly calculated by feedforward force and feedback velocity, or by feedforward force with PID controller. Obviously, for such a highly nonlinear system, those controllers without or with an over-simplified model are hardly competent of high performance trajectory tracking.

FEEDBACK LINEARIZATION

With a good knowledge of the hydraulic actuator model, model-based feedback linearization can once again be designed to cope with the nonlinearity [9, 29, 45–47]. If we consider the general pressure dynamics model (2.7), the control law is given by:

$$u = \frac{v + T(A_{pi}, q) \dot{q} + L(q) P_L}{Q(P_{pi}, q) k_q} \quad (2.29)$$

which leads to first a order integrator $\dot{f}_a = v$ which is easily controlled by a linear controller.

A direct theoretical advantage of the feedback linearization approach is that the force control loop is totally decoupled from the outer-loop load dynamics, with an accurate velocity feedback. However, the hydraulic actuator system suffers from even more serious model uncertainty than outer-loop Stewart platform. The dynamics of the valve spool, simply modeled leakage and even time-varying oil compressibility modulus (which changes with temperature) contribute to the uncertainties of the model. Thus in real-world implementation, feedback linearization faces challenges.

Several approaches have been proposed to deal with the robustness problem of a typical feedback linearization. For instance, Namvar [48] proposed a combination of parameter identification and outer-loop H_∞ linear controller to improve the baseline controller performance. Besides, similar to the feedforward plus PD feedback controller for the parallel robot, flatness-based control [49, 50] have been introduced for hydraulic force control. With the flatness of hydraulic dynamics being proved, their inversion are used to calculate the feedforward control input based on the motion reference. A linear feedback controller is designed parallelly to compensate for the force tracking error. Similarly, despite the improved robustness with respect to feedback linearization, the control performance is still influenced when the inverse dynamic model is subject to model uncertainties, since the error in the feedforward loop has to be compensated by the increased error in the feedback loop.

CASCADE PRESSURE DIFFERENCE CONTROLLER (CDP)

Cascade pressure difference control is proposed by Heintze[51, 52] and Sepehri [53] for force tracking of hydraulic actuators. Considering the model given in (2.10), the control law is given as:

$$u = \frac{K_v \dot{q} + K_c (F_c / A_p P_s - P_L / P_s) + K_L P_L}{\sqrt{1 \pm P_L / P_s}} \quad (2.30)$$

where F_c is the reference force of the actuator. With gains K_v and K_L chosen as $K_v = A_p / \Phi_n$ and $K_L = L_{lm} / \Phi_n$, the equation for the close inner-loop is then written as:

$$\dot{P}_L = 2C_m K_c \Phi_n (F_c / A_p - P_L) / P_s \quad (2.31)$$

From the above expression we can see that the controlled system is turned into a nonlinear gain varying force generator instead of a full linearized system. This means less model information is used in this controller. In fact, the oil stiffness C_m contains the temperature-varying oil modulus E which largely contributes to parameter uncertainty. Such a feature makes CdP controller a practical technique with recent application[15, 54] and is currently implemented in the SRS motion system.

ADAPTIVE CONTROL

Aiming at overcoming the model uncertainties of hydraulic actuators, several control schemes with parameter adaptation have been proposed [9, 14, 45, 48], in some cases combined with other advance control methods such as sliding mode control[19] and robust control[55–57]. Generally the stability of the complete controlled hydraulic motion system is given. However, for most of the cases, only selected few hydraulic parameters are adapted, thus the unmodeled dynamics still contribute to the decreased performance. More importantly, in order to prove the stability of the complete system, the hydraulic force control is generally coupled with the outer-loop load (mechanical) dynamics. This makes the adaptive hydraulic control difficult, if not impossible, to be directly applied to a more general outer-loop mechanism, such as a 6-DOF Stewart platform. To the best of the author's knowledge, very few publications provide an adaptive hydraulic controller which is decoupled with the load dynamics [48]. Besides, for the sliding mode approaches, the chattering problem or computational burden problem in those advanced control algorithms makes it even more difficult to be applied to a Stewart

platform with six actuators. At this point, a practical control scheme with implementable computational effort and model uncertainty resistant ability is sought after for the inner-loop actuator control of hydraulic hexapod platform.

2.4. HYDRAULIC STEWART PLATFORM CONTROL WITH INDI

From the above review it can be concluded that the control problem for outer-loop manipulator is studied relatively comprehensively, as it is a sub-field of robot control. The feasible hydraulic actuator controller design for Stewart system, however, still poses a performance challenge. On one hand, the model used for actuator controller design is highly simplified with some parameters and dynamics neglected, while the parameters in the already simplified model are not accurate or even time varying, which dramatically degrade the model-based controller performance; On the other hand, problems like chattering or computation burden in robust or adaptive control schemes as well as the complex mechanical structure prevent those advanced controller to be applied in such systems. To meet the high fidelity requirement of flight simulator motion system, a time efficient and less model dependent controller is required to be applied to hydraulic systems.

To this end, in this chapter, an Incremental Nonlinear Dynamic Inversion (INDI) control approach developed by Control and Simulation (C&S) section in TU Delft which has been successfully implemented in some flight control applications[58, 59], is introduced to deal with the hydraulic actuator control problem. The INDI approach uses sensor information to achieve model linearization and it will be shown in the section below that this approach is resistant to model uncertainties and time efficient.

2.4.1. INCREMENTAL NONLINEAR DYNAMIC INVERSION (INDI)

To exemplify the principle of INDI, consider an n^{th} nonlinear control affined system:

$$\dot{\mathbf{x}} = \mathbf{f}(\mathbf{x}) + \mathbf{G}(\mathbf{x}) \mathbf{u} \quad (2.32)$$

where \mathbf{f} is vector field in \mathbb{R}^n , $\mathbf{u} \in \mathbb{R}^m$ is the input and $\mathbf{G} \in \mathbb{R}^{n \times m}$ is the control effectiveness matrix.

To demonstrate the core idea of INDI, a special case for the system in Eq. (2.32) when $n = m$ is considered in this section. For more general systems when $n \neq m$, a comprehensive discussion of INDI is given in Appendix A of this thesis for reference. The motivation of INDI is not to compute the complete control inputs as feedback linearization dose, but rather to compute only changes of the control inputs with respect to its current value[59], thus only a small part of the model is still needed and the impact of model mismatch is reduced. To this end, consider a first-order Taylor series expansion of Equation (2.32) at any time instant[58]:

$$\dot{\mathbf{x}} \approx \dot{\mathbf{x}}_0 + \frac{\partial}{\partial \mathbf{x}} [\mathbf{f}(\mathbf{x}) + \mathbf{G}(\mathbf{x}) \mathbf{u}]_{\mathbf{x}_0, \mathbf{u}_0} (\mathbf{x} - \mathbf{x}_0) + \mathbf{G}(\mathbf{x}_0) (\mathbf{u} - \mathbf{u}_0) \quad (2.33)$$

where subscript 0 denotes the states at the instant.

The above equation can be further simplified using the time scale separation principle. The idea is for a very small time increment which require high sampling rate of

controller, the dynamics of \mathbf{u} is significantly faster than that of \mathbf{x} , since \mathbf{x} is the integration of $\dot{\mathbf{x}}$ which is at the same level of dynamic of \mathbf{u} . Thus compared with the term $\mathbf{u} - \mathbf{u}_0$ the increment of states $\mathbf{x} - \mathbf{x}_0$ can be assumed to be negligible. Thus:

$$\dot{\mathbf{x}} \approx \dot{\mathbf{x}}_0 + \mathbf{G}(\mathbf{x}_0)(\mathbf{u} - \mathbf{u}_0) \quad (2.34)$$

Now based on equation (2.34), if the matrix \mathbf{G} is nonsingular, the typical feedback linearization control technique can be used by choosing:

$$\mathbf{u} - \mathbf{u}_0 = \mathbf{G}^{-1}(\mathbf{x}_0)(\mathbf{v} - \dot{\mathbf{x}}_0) \quad (2.35)$$

where \mathbf{v} is the virtual control input and $\dot{\mathbf{x}}_0$ is the measured state derivative. With the above relation selected, The linearization of simplified model is achieved by:

$$\dot{\mathbf{x}} = \mathbf{v} \quad (2.36)$$

Now the obtained linear system can be stabilized using typical linear control techniques. Recalling equation (2.35), the INDI control law is given in an incremental form as follows:

$$\mathbf{u} = \mathbf{G}^{-1}(\mathbf{x}_0)(\mathbf{v} - \dot{\mathbf{x}}_0) + \mathbf{u}_0 \quad (2.37)$$

From the above control law, the model independent feature of INDI can be shown. The control law is independent of non-input-dependent dynamics \mathbf{f} in equation 2.32, thus the model uncertainty in this part will not affect the linearization result. However, it cannot be concluded that INDI doesn't consider \mathbf{f} of the model, instead, it should be noted that online measurement of state derivative $\dot{\mathbf{x}}_0$ appears in equation (2.37), which means the full dynamic information is already contained in this term. A more detailed discussion on this topic is give in Appendix A of this thesis.

From the analysis above it is clear that when evaluating the robustness of this control strategy, only the uncertainty in control effectiveness matrix \mathbf{G} needs to be considered. In various numerical and practical INDI control applications [58–61], it is verified that INDI is also not sensitive to the model uncertainties in \mathbf{G} . For example, in [59] it is validated that even with 50% model mismatch in \mathbf{G} , the control performance of the INDI is not influenced.

Several theoretical proofs have been provided, regarding to the robustness of INDI to model uncertainties in the control effectiveness matrix \mathbf{G} . However, all of them require the assumption that state derivatives between the small time increment are identical [58, 59]. This assumption is not reasonable, since it implies that the control input increment $\mathbf{u} - \mathbf{u}_0$ is zero according to Equation 2.34, which is not true. This means that a proper theoretical proof for the robustness of INDI is still to be developed. In addition to the robustness, the stability analysis of the INDI and the stability margin in the presence of model uncertainties are still to be further discussed in the rest of this thesis. These topics will be addressed in detail in Chapter 4 and Chapter 5 of this thesis.

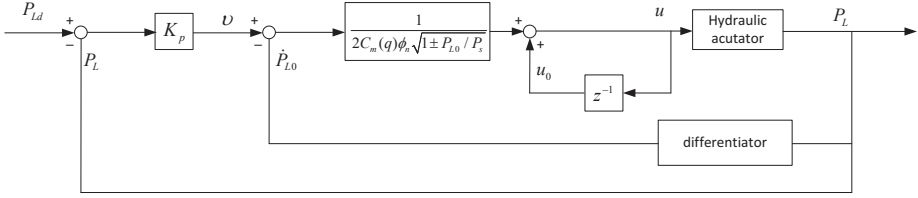


Figure 2.6: INDI controller for hydraulic actuator force tracking

2.4.2. PRELIMINARY INDI CONTROLLER DESIGN FOR HYDRAULIC ACTUATOR

Similar to the CdP control technique, the INDI control strategy aims to solve the inner-loop hydraulic force (pressure difference) tracking problem. Consider the hydraulic actuator model described by Equation (2.10), in order to obtain the INDI control law in an incremental form, the model is simplified following the procedure given in Equations (2.32-2.35) as:

$$\dot{P}_L = \dot{P}_{L0} + 2C_m(q)\Phi_n\sqrt{1 \pm P_{L0}/P_s}(u - u_0) \quad (2.38)$$

It is clear from the above equation that this form of the model is independent of leakage term $L_{lm}dP$ and hydraulic-mechanic interaction term $A_p\dot{q}$ in (2.10), as the most of their information are already included in the measurement $d\dot{P}_0$. Based on this model, the INDI control law is designed in the form of equation (2.37) as:

$$u = u_0 + \frac{v - \dot{P}_{L0}}{2C_m(q)\Phi_n\sqrt{1 \pm P_{L0}/P_s}} \quad (2.39)$$

Substituting the above control law in Equation (2.38), the linearization is achieved as $\dot{P}_L = v$. By simply choosing the virtual control input a proportional controller $v = K_p(P_{Ld} - dP)$, where $P_{Ld} = F_c/A_p$ is the desired pressure difference, the hydraulic actuator is turned into a linear first-order force generator following the desired outer-loop force input:

$$\dot{P}_L = K_p(P_{Ld} - P_L) \quad (2.40)$$

The block diagram of an INDI controller for hydraulic actuator is given in Figure (2.6).

It should be noted that the INDI control law (2.39) requires accurate measurements of the derivative of the pressure difference P_L . The pressure sensors inside the hydraulic valve only provide pressure information, which means the derivative should be estimated.

2.4.3. PRELIMINARY SIMULATION RESULTS

In order to evaluate the robustness of the introduced control strategy, the performance of both the CdP and INDI controllers in hydraulic actuator force (pressure difference)

tracking are compared in simulations using Matlab/Simulink. In Ref. [62], a full computer model of hydraulic Stewart platform motion system is built considering sufficient detail. A single hydraulic actuator model with the main driving spool is taken from that model to drive a constant mass load $M = 1500\text{kg}$ (without gravity) to be used as test case. All physical parameters of the actuator and valve spool used in the model can be found in Ref. [62]. Simple square waves were used as reference with an amplitude of $P_L/P_s = 0.15$ and a frequency of 2Hz. The outer-loop gain in CdP is set to $K_c = 0.5$, and in case of INDI $K_p = 120$. In both cases the measurement of P_L is accurate without delay, while in INDI controller the derivative \dot{P}_L is estimated by an approximated differentiator with a transfer function of $s/(1000s + 1)$. The sample time is set to 0.2ms (unless otherwise noticed) and the ode4 solver is used for simulation.

The performance of both controllers with nominal model parameters are given in Figure 2.7. Obvious tracking errors of the CdP controller can be observed while INDI controller provides more accurate tracking performance. It should be noted that the mismatch of CdP controller tracking result comes from the model uncertainty. The model used for controller design in Equation (2.10) is simplified from the one used for simulation, without consideration of nonlinear features such as orifice underlap in valve and with neglecting of small terms [2]. Thus even nominal parameters are used, the model uncertainty still exist. It should also be noted that when decreasing the update frequency of INDI, the performance degraded. A small stationary error exists for the INDI controller at a frequency of 1000Hz. This result verified the conclusion that the validity of linearization of INDI depends on the high sampling frequency assumption.

The performance of both controllers with an 10% offset of Φ_n is shown in Figure 2.8. In this case, the performance of CdP controller is significantly deteriorates while INDI still provides accurate tracking. As the maximum valve flow Φ_n is a parameter in control effectiveness \mathbf{G} , the offset significantly affects the compensation of CdP but has almost no influence on the INDI. This result illustrates the robustness of INDI in this application.

2.4.4. POSSIBLE APPLICATION IN THE OUTER-LOOP

Inspired by the robustness of the INDI and the dynamic equation form of the Stewart platform, it will be argued that INDI is also suitable for the outer-loop motion control. Recall Equation (2.1), by denoting $\mathbf{v} = \dot{\mathbf{x}}$, the dynamic equation is written as:

$$\dot{\mathbf{v}} = \mathbf{M}^{-1}(\mathbf{z}) \mathbf{J}^T(\mathbf{z}) \mathbf{f}_a - \mathbf{M}^{-1}(\mathbf{z}) \mathbf{C}(\mathbf{z}, \mathbf{v}) \mathbf{v} - \mathbf{M}^{-1}(\mathbf{z}) \mathbf{G}(\mathbf{z}) \quad (2.41)$$

Similar to the INDI control law design for the hydraulic actuator, the model simplification procedure described by Equations (2.32-2.35) will be followed. Once again, time scale separation principle is used as \mathbf{v} and \mathbf{z} are first and second integration of $\dot{\mathbf{v}}$, so that their increments are negligible leading to:

$$\dot{\mathbf{v}} = \dot{\mathbf{v}}_0 + \mathbf{M}^{-1}(\mathbf{z}) \mathbf{J}^T(\mathbf{z}) (\mathbf{f}_a - \mathbf{f}_{a0}) \quad (2.42)$$

The INDI control law is then given by:

$$\mathbf{f}_a = \mathbf{f}_{a0} + \mathbf{J}^{-T}(\mathbf{z}) \mathbf{M}(\mathbf{z}) (\mathbf{v} - \dot{\mathbf{v}}_0) \quad (2.43)$$

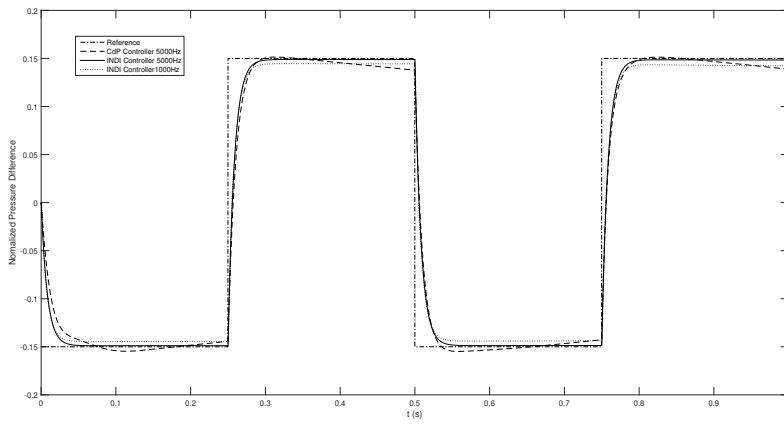


Figure 2.7: Performance of CdP and INDI controllers in force tracking test

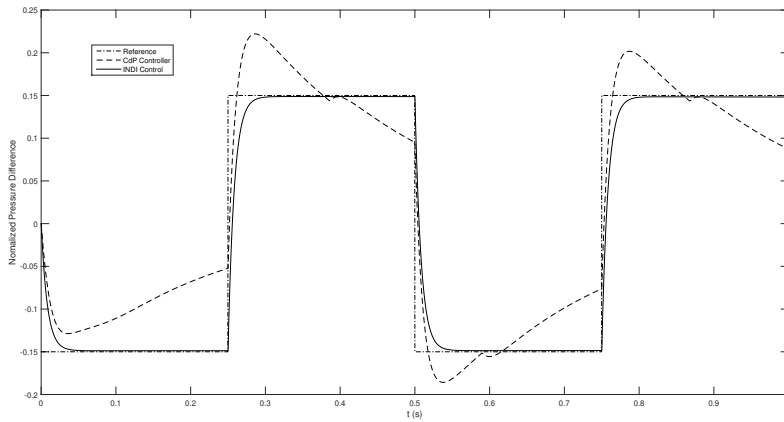


Figure 2.8: Performance of two controllers in force tracking with model parameter uncertainty

Taking advantage of the fact that Inertial Measurement Unit (IMU) is available in the SRS, the acceleration information $\dot{\mathbf{v}}_0$ in the above control law is directly measurable.

Substituting the control law into the incremental model, the linearization is achieved as:

$$\ddot{\mathbf{x}} = \dot{\mathbf{v}} = \mathbf{v} \quad (2.44)$$

By choosing an appropriate linear controller of virtual control input \mathbf{v} , $\mathbf{v} = \ddot{\mathbf{x}}_d - \mathbf{k}_0 \mathbf{e} - \mathbf{k}_1 \dot{\mathbf{e}}$ for instance, the reference motion can be tracked. As discussed in the above subsection, the linearization of outer loop dynamics is robust to model and parameter uncertainties.

2.5. CONCLUSION

A review of control strategies for the hydraulic Stewart platform manipulator, acting as a flight simulator motion system, is presented. The control problem is usually cascaded into an outer-loop robotic motion control problem and an inner-loop hydraulic force tracking problem. Control schemes for both subsystem are divided into a few important categories and advantages and disadvantages have been discussed. Facing the model uncertainty problem and disadvantages of current hydraulic actuator controller, a time efficient sensor-based INDI controller is introduced to overcome the existing problems. Simulation result demonstrated the robustness of the new controller which is almost model-free. Possible implementation of INDI to outer-loop manipulator control is also discussed.

REFERENCES

- [1] Y. Huang, D. M. Pool, O. Stroosma, Q. P. Chu, and M. Mulder, "A Review of Control Schemes for Hydraulic Stewart Platform Flight Simulator Motion Systems," in *AIAA Modeling and Simulation Technologies Conference*, January 2016.
- [2] S. Koekebakker, "Model based control of a flight simulator motion system," Ph.D. dissertation, Delft University of Technology, 2001.
- [3] O. Stroosma, M. M. van Paassen, and M. Mulder, "Using the SIMONA Research Simulator For Human-Machine Interaction Research," in *AIAA Modeling and Simulation Technologies Conference and Exhibit*, 2003.
- [4] J. H. Chin, Y. H. Sun, and Y. M. Cheng, "Force computation and continuous path tracking for hydraulic parallel manipulators," *Control Engineering Practice*, vol. 16, no. 6, pp. 697–709, 2008.
- [5] I. Davliakos and E. Papadopoulos, "Impedance model-based control for an electro-hydraulic stewart platform," *European Journal of Control*, vol. 15, no. 5, pp. 560 – 577, 2009.
- [6] H. S. Kim, Y. M. Cho, and K.-I. Lee, "Robust nonlinear task space control for 6 DOF parallel manipulator," *Automatica*, vol. 41, no. 9, pp. 1591 – 1600, 2005. [Online]. Available: <http://www.sciencedirect.com/science/article/pii/S0005109805001342>

- [7] S. Chen and L. Fu, "Output feedback sliding mode control for a stewart platform with a nonlinear observer-based forward kinematics solution," *IEEE Transactions on Control Systems Technology*, vol. 21, no. 1, pp. 176–185, Jan 2013.
- [8] M. Honegger and P. Corke, "Model-based control of hydraulically actuated manipulators," in *Proceedings 2001 ICRA. IEEE International Conference on Robotics and Automation (Cat. No.01CH37164)*, vol. 3, May 2001, pp. 2553–2559 vol.3.
- [9] G. A. Sohl and J. E. Bobrow, "Experiments and simulations on the nonlinear control of a hydraulic servosystem," *IEEE Transactions on Control Systems Technology*, vol. 7, no. 2, pp. 238–247, Mar 1999.
- [10] Q. Meng, T. Zhang, X. Gao, and J. Y. Song, "Adaptive sliding mode fault-tolerant control of the uncertain stewart platform based on offline multibody dynamics," *IEEE/ASME Transactions on Mechatronics*, vol. 19, no. 3, pp. 882–894, June 2014.
- [11] C. C. Nguyen, S. S. Antrazi, Z.-L. Zhou, and C. E. Campbell, "Adaptive control of a stewart platform-based manipulator," *Journal of Robotic Systems*, vol. 10, no. 5, pp. 657–687.
- [12] M. Honegger, A. Codourey, and E. Burdet, "Adaptive control of the hexaglide, a 6 DOF parallel manipulator," in *Proceedings of International Conference on Robotics and Automation*, vol. 1, April 1997, pp. 543–548 vol.1.
- [13] M. Becerra-Vargas and E. M. Belo, "Robust control of flight simulator motion base," *Journal of Guidance, Control, and Dynamics*, vol. 34, no. 5, pp. 1519–1528, 2011.
- [14] M. R. Sirouspour and S. E. Salcudean, "Nonlinear control of hydraulic robots," *IEEE Transactions on Robotics and Automation*, vol. 17, no. 2, pp. 173–182, 2001.
- [15] Y. Pi and X. Wang, "Observer-based cascade control of a 6-DOF parallel hydraulic manipulator in joint space coordinate," *Mechatronics*, vol. 20, no. 6, pp. 648 – 655, 2010.
- [16] W.-H. Zhu and J.-C. Piedboeuf, "Adaptive output force tracking control of hydraulic cylinders with applications to robot manipulators," *Journal of Dynamic Systems, Measurement, and Control*, vol. 127, no. 2, pp. 206–217, Jun 2004.
- [17] T. Knohl and H. Unbehauen, "Adaptive position control of electrohydraulic servo systems using ann," *Mechatronics*, vol. 10, no. 1, pp. 127 – 143, 2000.
- [18] F. Bu and B. Yao, "Observer based coordinated adaptive robust control of robot manipulators driven by single-rod hydraulic actuators," in *Proceedings 2000 ICRA. Millennium Conference. IEEE International Conference on Robotics and Automation. Symposia Proceedings (Cat. No.00CH37065)*, vol. 3, 2000, pp. 3034–3039 vol.3.
- [19] C. Guan and S. Pan, "Adaptive sliding mode control of electro-hydraulic system with nonlinear unknown parameters," *Control Engineering Practice*, vol. 16, no. 11, pp. 1275 – 1284, 2008.

- [20] B. Siciliano, L. Sciacivco, L. Villani, and G. Oriolo, *Robotics: modelling, planning and control*. Springer Science & Business Media, 2010.
- [21] H. Abdellatif and B. Heimann, “Advanced model-based control of a 6-DOF hexapod robot: A case study,” *IEEE/ASME Transactions on Mechatronics*, vol. 15, no. 2, pp. 269–279, April 2010.
- [22] M. Honegger, R. Brega, and G. Schweiter, “Application of a nonlinear adaptive controller to a 6 DOF parallel manipulator,” in *Proceedings 2000 ICRA. Millennium Conference. IEEE International Conference on Robotics and Automation. Symposia Proceedings (Cat. No.00CH37065)*, vol. 2, 2000, pp. 1930–1935 vol.2.
- [23] P. Renaud, A. Vivas, N. Andreff, P. Poignet, P. Martinet, F. Pierrot, and O. Company, “Kinematic and dynamic identification of parallel mechanisms,” *Control Engineering Practice*, vol. 14, no. 9, pp. 1099 – 1109, 2006.
- [24] M. Díaz-Rodríguez, A. Valera, V. Mata, and M. Valles, “Model-based control of a 3-DOF parallel robot based on identified relevant parameters,” *IEEE/ASME Transactions on Mechatronics*, vol. 18, no. 6, pp. 1737–1744, Dec 2013.
- [25] Y. Li and Q. Xu, “Design and development of a medical parallel robot for cardiopulmonary resuscitation,” *IEEE/ASME Transactions on Mechatronics*, vol. 12, no. 3, pp. 265–273, June 2007.
- [26] F. Caccavale, B. Siciliano, and L. Villani, “The tricept robot: dynamics and impedance control,” *IEEE/ASME Transactions on Mechatronics*, vol. 8, no. 2, pp. 263–268, June 2003.
- [27] H. E. Merritt, *Hydraulic Control Systems*. John Wiley & Sons, 1967.
- [28] G. van Schothorst, “Modelling of Long-Stroke Hydraulic Servo-Systems for Flight Simulator Motion Control and System Design,” Ph.D. dissertation, Delft University of Technology, 1997.
- [29] G. Vossoughi and M. Donath, “Dynamic feedback linearization for electrohydraulically actuated control systems,” *ASME. J. Dyn. Sys., Meas., Control.*, vol. 117, no. 4, pp. 468–477, 1995.
- [30] F. Paccot, N. Andreff, and P. Martinet, “A review on the dynamic control of parallel kinematic machines: Theory and experiments,” *The International Journal of Robotics Research*, vol. 28, no. 3, pp. 395–416, 2009.
- [31] W.-W. Shang, S. Cong, and Y. Ge, “Adaptive computed torque control for a parallel manipulator with redundant actuation,” *Robotica*, vol. 30, no. 3, p. 457–466, 2012.
- [32] S.-H. Lee, J.-B. Song, W.-C. Choi, and D. Hong, “Position control of a stewart platform using inverse dynamics control with approximate dynamics,” *Mechatronics*, vol. 13, no. 6, pp. 605 – 619, 2003.

- [33] I. Davliakos and E. Papadopoulos, "Model-based control of a 6-DOF electrohydraulic stewart–gough platform," *Mechanism and Machine Theory*, vol. 43, no. 11, pp. 1385 – 1400, 2008.
- [34] M. Díaz-Rodríguez, A. Valera, V. Mata, and M. Valles, "Model-based control of a 3-DOF parallel robot based on identified relevant parameters," *IEEE/ASME Transactions on Mechatronics*, vol. 18, no. 6, pp. 1737–1744, 2013.
- [35] J. Wang, J. Wu, L. Wang, and Z. You, "Dynamic feed-forward control of a parallel kinematic machine," *Mechatronics*, vol. 19, no. 3, pp. 313 – 324, 2009.
- [36] M. Grotjahn and B. Heimann, "Model-based feedforward control in industrial robotics," *The International Journal of Robotics Research*, vol. 21, no. 1, pp. 45–60, 2002.
- [37] B. Denkena, B. Heimann, H. Abdellatif, and C. Holz, "Design, modeling and advanced control of the innovative parallel manipulator palida," in *Proceedings, 2005 IEEE/ASME International Conference on Advanced Intelligent Mechatronics.*, July 2005, pp. 632–637.
- [38] J. J. Craig, P. Hsu, and S. S. Sastry, "Adaptive control of mechanical manipulators," *The International Journal of Robotics Research*, vol. 6, no. 2, pp. 16–28, 1987.
- [39] L. Ren, J. K. Mills, and D. Sun, "Experimental comparison of control approaches on trajectory tracking control of a 3-DOF parallel robot," *IEEE Transactions on Control Systems Technology*, vol. 15, no. 5, pp. 982–988, Sept 2007.
- [40] I. T. Pietsch, M. Krefft, O. T. Becker, C. C. Bier, and J. Hesselbach, "How to reach the dynamic limits of parallel robots? an autonomous control approach," *IEEE Transactions on Automation Science and Engineering*, vol. 2, no. 4, pp. 369–380, Oct 2005.
- [41] W. Khalil and S. Guegan, "Inverse and direct dynamic modeling of gough-stewart robots," *IEEE Transactions on Robotics*, vol. 20, no. 4, pp. 754–761, Aug 2004.
- [42] D. H. Kim, J.-Y. Kang, and K.-I. Lee, "Robust tracking control design for a 6 DOF parallel manipulator," *Journal of Robotic Systems*, vol. 17, no. 10, pp. 527–547.
- [43] T. B. Cunha, C. Semini, E. Guglielmino, V. J. D. Negri, and Y. Yang, "Gain scheduling control for the hydraulic actuation of the hyq robot leg," 2009.
- [44] C. Yang, Q. Huang, and J. Han, "Computed force and velocity control for spatial multi-DOF electro-hydraulic parallel manipulator," *Mechatronics*, vol. 22, no. 6, pp. 715 – 722, 2012, special Issue on Intelligent Mechatronics.
- [45] D. Garagic and K. Srinivasan, "Application of nonlinear adaptive control techniques to an electrohydraulic velocity servomechanism," *IEEE Transactions on Control Systems Technology*, vol. 12, no. 2, pp. 303–314, March 2004.
- [46] T. Boaventura, J. Buchli, C. Semini, and D. G. Caldwell, "Model-based hydraulic impedance control for dynamic robots," *IEEE Transactions on Robotics*, vol. 31, no. 6, pp. 1324–1336, Dec 2015.

- [47] L. D. Re and A. Isidori, "Performance enhancement of nonlinear drives by feedback linearization of linear-bilinear cascade models," *IEEE Transactions on Control Systems Technology*, vol. 3, no. 3, pp. 299–308, Sept 1995.
- [48] M. Namvar and F. Aghili, "A combined scheme for identification and robust torque control of hydraulic actuators," *Journal of Dynamic Systems, Measurement, and Control*, vol. 125, no. 4, pp. 595–606, Jan 2004. [Online]. Available: <http://dx.doi.org/10.1115/1.1636777>
- [49] F. Kock and C. Ferrari, "Flatness-based high frequency control of a hydraulic actuator," *Journal of Dynamic Systems, Measurement, and Control*, vol. 134, no. 2, p. 021003, 2012.
- [50] W. Kim, D. Won, and M. Tomizuka, "Flatness-based nonlinear control for position tracking of electrohydraulic systems," *IEEE/ASME Transactions on Mechatronics*, vol. 20, no. 1, pp. 197–206, Feb 2015.
- [51] J. Heintze and A. van der Weiden, "Inner-loop design and analysis for hydraulic actuators, with an application to impedance control," *Control Engineering Practice*, vol. 3, no. 9, pp. 1323 – 1330, 1995.
- [52] J. Heintze, P. Teerhuis, and A. van der Weiden, "Controlled hydraulics for a direct drive brick laying robot," *Automation in Construction*, vol. 5, no. 1, pp. 23 – 29, 1996.
- [53] N. Sepehri, G. Dumont, P. D. Lawrence, and F. Sassani, "Cascade Control of Hydraulically Actuated Manipulators," *Robotica*, vol. 8, no. 03, pp. 207–216, mar 1990.
- [54] H. Guo, Y. Liu, G. Liu, and H. Li, "Cascade control of a hydraulically driven 6-DOF parallel robot manipulator based on a sliding mode," *Control Engineering Practice*, vol. 16, no. 9, pp. 1055 – 1068, 2008.
- [55] D. Hiseine, "Robust tracking control for a hydraulic actuation system," in *Proceedings of 2005 IEEE Conference on Control Applications, 2005. CCA 2005.*, Aug 2005, pp. 422–427.
- [56] B. Yao, F. Bu, J. Reedy, and G. T. C. Chiu, "Adaptive robust motion control of single-rod hydraulic actuators: theory and experiments," *IEEE/ASME Transactions on Mechatronics*, vol. 5, no. 1, pp. 79–91, Mar 2000.
- [57] J. Koivumäki and J. Mattila, "High performance non-linear motion/force controller design for redundant hydraulic construction crane automation," *Automation in construction*, vol. 51, pp. 59–77, 2015.
- [58] P. Simplício, M. D. Pavel, E. van Kampen, and Q. P. Chu, "An acceleration measurements-based approach for helicopter nonlinear flight control using incremental nonlinear dynamic inversion," *Control Engineering Practice*, vol. 21, no. 8, pp. 1065 – 1077, 2013.

- [59] S. Sieberling, Q. P. Chu, and J. A. Mulder, “Robust Flight Control Using Incremental Nonlinear Dynamic Inversion and Angular Acceleration Prediction,” *Journal of Guidance, Control, and Dynamics*, vol. 33, no. 6, pp. 1732–1742, nov 2010.
- [60] E. J. J. Smeur, Q. P. Chu, and Guido C. de Croon, “Adaptive incremental nonlinear dynamic inversion for attitude control of micro aerial vehicles,” *Journal of Guidance, Control, and Dynamics*, vol. 39, no. 3, pp. 450–461, 2016.
- [61] F. Grondman, G. Looye, R. O. Kuchar, Q. P. Chu, and E.-J. Van Kampen, ser. AIAA SciTech Forum. American Institute of Aeronautics and Astronautics, Jan 2018, ch. Design and Flight Testing of Incremental Nonlinear Dynamic Inversion-based Control Laws for a Passenger Aircraft.
- [62] Y. Huang, D. M. Pool, O. Stroosma, Q. P. Chu, and M. Mulder, “Modeling and Simulation of Hydraulic Hexapod Flight Simulator Motion Systems,” in *AIAA Modeling and Simulation Technologies Conference*, January 2016.

3

PHYSICAL MODELING OF THE HYDRAULIC PARALLEL MANIPULATOR

The previous chapter discussed how the nonlinear and uncertain dynamics of the hydraulic parallel robots make their precision control a challenging work. In this chapter, a high fidelity modular simulation model of a hydraulic parallel robot is developed, based on the physical laws. Physical phenomena causing the nonlinearity and model uncertainties can thus be replicated in computer simulation. With the model, the effectiveness of various control methods can be verified and validated. Furthermore, as a test platform, the performance of the INDI based nonlinear control system for hydraulic parallel robots can be predicted by computer simulation before the real-life experiments. In this chapter, the modeling of hydraulic actuation system and parallel robotic system are discussed modularly in Section 3.2. The implementation of the theoretical model on computer is discussed in Section 3.3. The fidelity of the integrated system model is verified by comparing the simulation results with the experiment data, as discussed in Section 3.4. A brief conclusion is then given in Section 3.5.

This chapter is based on the following article:

Y. Huang, D. M. Pool, O. Stroosma, Q. P. Chu, and M. Mulder, "Modeling and Simulation of Hydraulic Hexapod Flight Simulator Motion Systems," in AIAA Modeling and Simulation Technologies Conference, January 2016.

[1]

The purpose of this chapter is to develop a complete model of a six-DOF hydraulic hexapod flight simulator motion system for computer simulation. Hydraulic servo-valves and actuators are modeled in detail based on physical laws of flows and parts, the dynamic equations of the hexapod motion base are derived with Newton-Euler approach and an inner-loop cascaded pressure difference controller and a outer-loop computed force controller are included in the model. The model is implemented in Simulink software, and the multibody dynamic modeling approach SimMechanics is also used in the model to verify the motion base dynamics. The established model is validated by comparing the simulation performance with real-world experiment data of SIMONA research simulator.

3.1. INTRODUCTION

Stewart platforms, also referred to as hexapod systems in industry, are six-DOF parallel robots which are widely used in industry applications and almost invariably used in motion(flight) simulator owing to their higher rigidity and accuracy[2, 3]. The basic structure consists of a moving platform linked to a fixed base with six linear actuators. Compared with electrical motors, hydraulic actuators offer distinct advantages like high power-to-size ratios, rapid response and high stiffness[4–7]. Even more importantly, hydraulic actuators allow for smoothly running on long stroke which is necessary in simulation requiring unnoticeable change of sign in the direction of motion. Therefore, a hydraulic 6-DOF parallel flight simulator shares a twofold advantage. a representation of such simulator is SIMONA Research Simulator (SRS) at TU Delft[8] (Figure 3.1). Out of an increasing demand of performance and accuracy on flight simulators, high performance control schemes are required to improve the trajectory tracking performance. Therefore, detailed models of hydraulic hexapod systems are essential for configuration design and high performance controller evaluation.

The most distinctive feature of this kind of system is the heavy interaction of the nonlinear Stewart platform mechanics with the highly nonlinear hydraulic actuator dynamics. For the latter, the dynamics of multistage electro servo-valve and hydraulic actuator are the main contributors to the nonlinearity of the system. In most research on the modeling and control of hydraulic Stewart platforms[9–11], the dynamics of the servo-valve are neglected, the dynamics of hydraulic actuators are highly simplified, while the motion base mechanics are modeled in detail. The absence of intrinsic nonlinearity of electro-hydraulic subsystem in model may leads to deflection of trajectory tracking performance between simulation and experiment under designed control scheme.

Generally the servo-valve dynamics is described by first or second (or even higher) order transfer function[12] parameterized by time constants, natural frequencies and damping ratios calculated from frequency characteristics determined by experiments. However, such model could just give limited insight of the system in a restricted operating range, due to the nonlinearity of servo-valve systems. In addition, such a modeling approach is not suitable for a computer model acting as simulation platform which requires enough detailed insight into the system. Therefore, a comprehensive mathematical model considering physical phenomena of every part of the valve should be established.

To model the complicated dynamics of a Stewart platform, several methods have

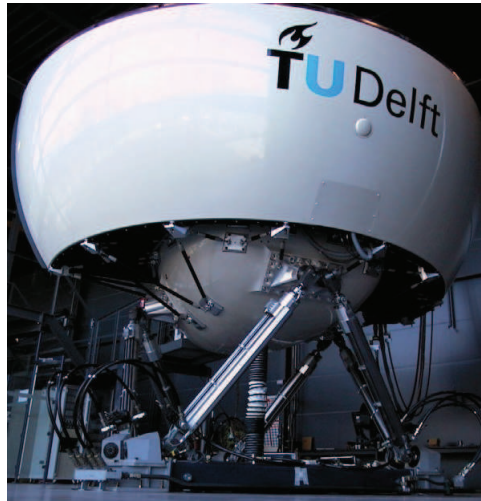


Figure 3.1: The SRS at TU Delft

been proposed such as Newton-Euler approach[13, 14], lagrangian equations of motion approach[15, 16] and Kane's method[2]. The Newton-Euler approach is the most intuitive and direct method, with the advantage to avoid large amount of symbolic computation while calculating partial derivatives of Lagrangian. The disadvantage of Newton-Euler approach is that internal constraint forces and moments should be calculated. However, for a purpose to build computer model that is easily accessible to states and constraint forces on every joints, this feature is actually a positive factor. For most cases, Newton-Euler approach is restricted to the inverse dynamics. However in case of a parallel structure as Stewart platform, closed-form equations could be derived that are suitable for both inverse and forward dynamics[17].

The aim of this chapter is to establish a full model of a 6-DOF electro-hydraulic parallel flight simulator motion system. Comprehensive mathematical model of hydraulic system is discussed considering physical phenomena of flapper-nozzle dynamics, three stage servo-valve, double concentric hydraulic actuator dynamics as well as the long oil supply line dynamics. The hydraulic modeling largely follows the previous work of Schothorst[18] and more recent advances in servovalve and hydraulic actuator modeling[19–21]. Meanwhile, closed-form dynamic equations of Stewart platform are introduced with a Neton-Euler approach, which is capable of dealing with both inverse and forward dynamics. The complete computer is build in Simulink environment with hydraulic subsystem and mechanics subsystem integrated by inner- and outer-loop controllers which is currently implemented in the SRS. In order to verify the newton-Euler dynamic equations, Simmechanics[22, 23], a multibody modeling toolbox integrated in Simulink environment which provides a 'physical' approach for mechanic modeling, is also used to establish a second model. The results of two computer models are compared and thus bilaterally verified. Finally, the complete computer model is validated by comparing simulation results with real-world experiment data of the SRS.

3.2. MODELING AND CONTROL

In this section, a hydraulic hexapod motion system is modeled in detail based on basic physical laws which are capable of providing enough physical insight into behaviour and phenomena of the whole system, out of a requirement of computer model for controller design and performance validation. First, modeling of hydraulic actuator of one leg with servo-valve taken into consideration is discussed, since all six legs are assumed to be identical. Next, closed-form dynamic equations of the whole mechanical Stewart platform will be discussed with Newton-Euler approach. Finally, control strategies for both hydraulic and mechanic subsystems are introduced, with which a complete motion tracking system is build, and close loop simulation can be implemented.

3.2.1. MODELING HYDRAULIC SUBSYSTEM

The electro-hydraulic servo system consists of hydraulic actuator with a piston moving in a cylinder, the servo-valve which supplies the oil, the power supply system, the sensors as well as the controller[10]. The power supply system is simply modeled as a constant oil supply pump which provides constant supply pressure P_s and return pressure P_t .

MODELING HYDRAULIC ACTUATOR

Hydraulic actuators transfer hydraulic energy into mechanical motion or force. The basic structure of a linear hydraulic actuator driven by a servo valve can be observed on Figure 3.2. A movable piston is driven by oil pressure difference, i.e. $P_{1p}-P_{2p}$, of the two compartments encompassed by a cylinder, due to the inlet oil flow Φ_{p1} to one compartment and the outlet oil flow Φ_{p2} from the other. The fact that oil flow and pressure difference compensate for each other causes the coupling of velocity and force generated by the actuator. The actuator model consists of the equation of motion which will be discussed in the next subsection, and the pressure dynamic equations regarding oil mass balance and oil compressibility under the oil bulk modulus E , of respective actuator compartments[18]:

$$\begin{aligned}\dot{P}_{p1} &= \frac{E}{A_{p1}(q_{max} + q) + V_{l1}} (\Phi_{p1} - \Phi_{lp} - \Phi_{l1} - A_{p1}\dot{q}) \\ \dot{P}_{p2} &= \frac{E}{A_{p2}(q_{max} - q) + V_{l2}} (-\Phi_{p2} + \Phi_{lp} - \Phi_{l2} + A_{p2}\dot{q})\end{aligned}\quad (3.1)$$

where Φ_{l1} , Φ_{l2} and Φ_{lp} are respective leakage flow defined in Figure 3.2, A_{p1} and A_{p2} are respective piston areas, q is the actuator displacement and q_{max} is the actuator stroke in the neutral position. Hereby, the volumes of each actuator out of designed stroke, i.e. V_{l1} and V_{l2} , are considered. For a double concentric actuator as used in SIMNOA simulator, the term Φ_{lp} dose not exist and A_{p1} and A_{p2} are identical[18].

The leakage flows are generally considered as laminar flows through a narrow gap, which are linear to the relative pressure differences across. In the actually used actuators, hydraulic bearing are used to minimize Coulomb friction by maintaining small oil film between the moving parts. Schothorst[18] derived the equation of leakage flow through a single hydrostatic bearing based on the assumption that the cylinder is centered in the bearing, according to analysis of Viersma[24]. The leakage terms in Eq. (3.1) which exist in a double concentric actuator are therefore described as:

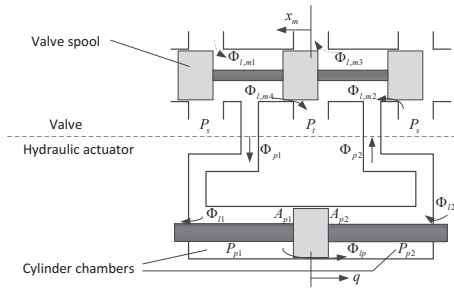


Figure 3.2: Schematic of hydraulic actuator with the third stage valve

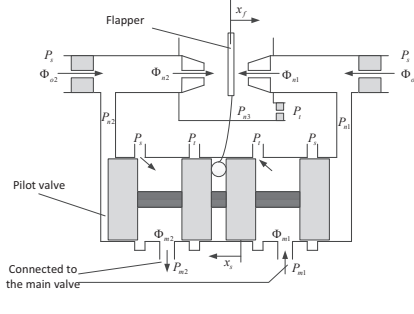


Figure 3.3: Schematic drawing of the two stage pilot valve [2]

$$\begin{aligned} \Phi_{l1} &= \Phi_{l,b4} = LP_{b4} (P_{p1} - P_t) - A_{p,b4} \dot{q} \\ \Phi_{l2} &= \Phi_{l,b3} - \Phi_{l,b2} = LP_{b3} (P_{p2} - P_t) + A_{p,b3} \dot{q} - LP_{b2} (P_s - P_{p2}) + A_{p,b2} \dot{q} \end{aligned} \quad (3.2)$$

where $\Phi_{l,bi}$ are leakage flows of bearing i , $i = 1, 2, 3, 4$, LP_{bi} and $A_{p,bi}$ are leakage parameter and displacement flow parameter of bearing i which are determined by geometry parameters of respective bearings. The detailed expression of these parameters can be found in [18].

The inlet and outlet oil flows Φ_{p1} and Φ_{p2} in Equation (3.1) are directly controlled by the last stage main spool of the servo valve, as depicted in Figure 3.2. The spool displacement determines the opening areas of a number of orifices cut in the cylinder sleeve with supply and return pressure acted on, thus determines the oil flows outputted to the actuator. The flows through its respective restrictions are generally modeled as turbulent with constant discharge coefficient C_d [18, 25] with assumptions of symmetrical orifices and no leakage. A more accurate model considers the leakages through overlaps, which dominant near the neutral position in existence of overlaps of ports. Based on the valve configuration in Figure 3.2, the output flows are written as:

$$\begin{aligned} \Phi_{p1} &= C_d h_m x_{m1} \sqrt{\frac{2}{\rho} \Delta p_{m1}} - C_d h_m x_{m4} \sqrt{\frac{2}{\rho} \Delta p_{m4}} + \Phi_{l,m1} - \Phi_{l,m4} \\ \Phi_{p2} &= C_d h_m x_{m3} \sqrt{\frac{2}{\rho} \Delta p_{m3}} - C_d h_m x_{m2} \sqrt{\frac{2}{\rho} \Delta p_{m2}} + \Phi_{l,m3} - \Phi_{l,m2} \end{aligned} \quad (3.3)$$

with h_m the width of the orifices, and ρ the density of oil. From Figure 3.2 the pressure drops are:

$$\Delta p_{mi} = \begin{cases} P_s - P_{p1}, & i = 1 \\ P_s - P_{p2}, & i = 2 \\ P_{p2} - P_t, & i = 3 \\ P_{p1} - P_t, & i = 4 \end{cases} \quad (3.4)$$

The valve opening values x_{mi} , $i = 1, 2, 3, 4$ are:

$$x_{mi} = \begin{cases} \sqrt{(x_m(-1)^{i+1} + d_{mi})^2 + c_{cm}^2}, & x_m(-1)^{i+1} \geq -d_{mi} \\ 0, & x_m(-1)^{i+1} < -d_{mi} \end{cases} \quad (3.5)$$

where x_m is the spool displacement, d_{mi} , $i = 1, 2, 3, 4$ are the underlaps of each orifices and c_{cm} is the clearance between the spool stand and its bushing. For the leakage flows $\Phi_{l,mi}$ inside the valve, several models exist. Gordic [21] modeled different pressure-flow relations for different overlap ranges, a more convenient way is to consider the leakage flow as combination of laminar part that is linear to laminar resistance and turbulent part that is related to flow along the edge of the spool, which leads to a set of quadratic equations that can be explicitly solved [18]:

$$\begin{cases} \frac{\rho}{2C_d h_m^2 c_{cm}^2} \Phi_{l,mi}^2 - \frac{12\eta(x_m(-1)^{i+1} + d_{mi})}{h_m c_{rm}^3} \Phi_{l,mi} = \Delta p_{mi}, & x_m(-1)^{i+1} < -d_{mi} \\ \Phi_{l,mi} = 0, & x_m(-1)^{i+1} \geq -d_{mi} \end{cases} \quad (3.6)$$

With the above equations, the hydraulic actuator dynamic model is build and is ready to be combined with motion equations of parallel manipulators to form a whole motion system.

MODELING THE TRANSMISSION LINE

In the hydraulic valve-actuator model given by Equations (3.1-3.3), the oil transmission line dynamics have been neglected. With the assumption that the oil pressure and flow are identical everywhere along each of the two oil pipelines, no distinction is made between the oil flows connected to the valve and the actuator chambers. For most hydraulic actuated systems, this assumption is valid as the effective frequency range of the pipeline dynamics is generally much higher than the rest of the hydraulic system. However, for applications that the relatively large workspace requires long stroke actuators, such as a flight simulator, the relatively long transmission lines tend to have lower eigenfrequency, which may cause stability problems for the hydraulic control systems [2]. For practical hydraulic pressure feedback, the transmission line dynamics exist between the actual pressure in the chambers and the available one in the valve. Schothorst [26] showed that the hydraulic control system stability margin may be violated by the these dynamics. It will be illustrated in the next chapter that without consideration of these dynamics, unstable self-sustaining vibration can be excited with the proposed controller. Thus in this section, the transmission line dynamics for the long-stroke hydraulic actuators are modeled.

The transmission lines generally show a lightly damped resonating behaviour at a number of eigenfrequencies [2]. The analytical solutions of the rigid circular fluid transmission lines have been discussed since the middle of the last century [26], and have been studied extensively since. However, as concluded in [27], a complete theoretical model of transmission lines results in an infinite order form which do not allow proper analysis in both time domain and frequency domain. In this section, a more practical model approximation approach introduced in [27] and [26] will be adopted, in which the transmission dynamics are decoupled by an infinite product series of second order

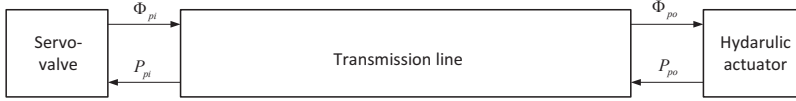


Figure 3.4: Flows and pressures at inlet and outlet ports of a single transmission line

models, each of which gives rise to a resonance mode. By choosing the (few) most relevant modes, the linear model can be easily included between the valve and actuator models in time domain, with physical parameters preserved.

Consider the representation of the transmission line given in Fig. 3.4, the flow (and pressure) on the valve side and the actuator side are denoted by Φ_{pi} (P_{pi}) and Φ_{po} (P_{po}), respectively. The added subscripts i and o are used to indicate the inlet and outlet sides of the transmission line. with the inputs and outputs defined in Fig. 3.4, the one dimensional distributed parameter model of a uniform rigid fluid transmission line with laminar is given in the Laplace domain by Yang [27] as

$$\begin{bmatrix} P_{pi} \\ \Phi_{po} \end{bmatrix} = \begin{bmatrix} \frac{1}{\cosh\Gamma(s)} & -\frac{Z_c(s)\sinh\Gamma(s)}{\cosh\Gamma(s)} \\ \frac{\sinh\Gamma(s)}{Z_c(s)\cosh\Gamma(s)} & \frac{1}{\cosh\Gamma(s)} \end{bmatrix} \begin{bmatrix} P_{po} \\ \Phi_{pi} \end{bmatrix}, \quad (3.7)$$

where $\Gamma(s)$ is the propagation operator and $Z_c(s)$ is the characteristic impedance.

The theoretical model is approximated by the sum of a set of linear second order systems [27], each of which defines a resonance frequency. The i th second order system can be written in a state space form, described by

$$\begin{bmatrix} \dot{P}_{pi,i} \\ \dot{\Phi}_{po,i} \end{bmatrix} = \begin{bmatrix} 0 & -(-1)^{i+1} Z_0 \lambda_{ci} \\ -\frac{(-1)^{i+1} \lambda_{ci}}{Z_0 \alpha^2} & -\frac{8\beta}{\alpha} \end{bmatrix} \begin{bmatrix} P_{pi,i} \\ \Phi_{po,i} \end{bmatrix} + \begin{bmatrix} 0 & -\frac{2Z_0}{D_n} \\ \frac{2}{Z_0 D_n \alpha^2} & 0 \end{bmatrix} \begin{bmatrix} P_{po} \\ \Phi_{pi} \end{bmatrix}. \quad (3.8)$$

The parameters in Equation (3.8) keep a physical interpretation. The dissipation number D_n and the line impedance constant Z_0 are defined by

$$D_n = \frac{Lv}{c_0 r_h^2}, \quad Z_0 = \frac{\rho_0 c_0}{A_0} \quad (3.9)$$

where L , r_h and A_0 are the line length, cross section radius and area, v is the kinematic viscosity, ρ_0 is the oil density and c_0 is the sound velocity in the oil.

In Equation (3.8), the factors α and β are frequency dependent modification factors for liquid, which can be determined by the graphs given in [27]. λ_{ci} is the undamped natural frequency of the i th mode, defined by

$$\lambda_{ci} = \frac{\pi(i-0.5)}{D_n} \quad (3.10)$$

For the actuators of the SRS with 1.25 m stroke, the transmission lines are around one meter long with a cross section radius of around 10 mm. An preliminary estimation of the model found the resonance frequencies of the first few modes at about 200, 600 and

1000 Hz and the rest higher [26]. Consider the bandwidth of the servo-valves at about 150 Hz, only the first mode is included in the model developed in this research, i.e. $i = 1$ is used for Equation (3.8). Thus the two transmission lines are actually modelled as two second order systems given by Equation (3.8) with according parameters, with the inlet flows from the valve and outlet pressures at the actuator as the input, and the opposites as the output. In this way the transmission line models are made modular, such that they can be easily included or omitted from the complete model, as will be illustrated in Fig. 3.7.

MODELING THREE STAGE SERVO-VALVE

The electro-hydraulic servo-valve acts as a high gain transducer controlling the high power oil flow output with low power current or voltage input. In case of hydraulic actuators working with large oil flows, multistage servo-valve are often used for multiple power amplification. In the hydraulic system of SIMONA simulator, three-stage servo-valves are used as depicted in Figure 3.2 and 3.3. The main spool positioning itself is controlled by a typical two-stage flapper-nozzle valve which consists of a flapper-nozzle system and a pilot spool. The flapper motion driven by electrical torque motor controls pressure difference that drives the motion of pilot spool, then the small displacement of pilot spool controls large oil flows driving the third stage main spool. The main phenomena considered when modeling servo-valve are the flapper dynamics, the spool dynamics and the pressure dynamics connecting each stage.

The equation of motion of the flapper is written as[18, 28]:

$$T_t = \frac{J_a}{l_f} \ddot{x}_f + \frac{B_a}{l_f} \dot{x}_f + \frac{K_a}{l_f} x_f + T_{fbs} - l_f (F_{f1} - F_{f2}) \quad (3.11)$$

with l_f the flapper length, J_a, B_a and K_a respectively the inertia, viscous friction coefficient and spring constant of the flapper, and F_{fi} the flow forces acting on the flapper. The term T_{fbs} is the mechanical feedback spring torque of the pilot spool position. The driving torque T_t generated by the torque motor are generally considered to be linear to the torque motor current i_{ca} (linear to input voltage u) and rotational displacement of the flapper-armature[21, 25]:

$$T_t = K_t i_{ca} + K_b x_f = K_t K_{ca} u + K_b x_f \quad (3.12)$$

and the nozzle flow forces F_{fi} acting on the flapper can be expressed as[25]:

$$F_{fi} = \left[P_{ni} + \frac{16C_d^2 (x_{f0} + x_f (-1)^{i+1})^2 (P_{ni} - P_{n3})}{d_n^2} \right] A_n, \quad i = 1, 2 \quad (3.13)$$

where A_n is the area of the nozzle orifice, d_n is the nozzle diameter and P_{ni} the pressure in respective chambers as shown in Figure 3.3.

The dynamics of the pilot spool come with the pressure difference, inertial, friction, spring feedback force and flow force, which is written as[18, 29]:

$$A_s (P_{n2} - P_{n1}) = M_s \ddot{x}_s + \omega_s \dot{x}_s + T_{fbs} / (l_f + l_{fbs}) + F_{ax} \quad (3.14)$$

where l_{fbs} is the length of feedback spring and x_s is the displacement of pilot spool, the expression spring feedback T_{fbs} and flow force F_{ax} can be found in literature like [18, 21, 25].

The pressure dynamics interacting with flapper-nozzle and pilot spool considers mass balances and compressibility of oil flows for the valve chambers, with signs defined in Figure 3.3 following equations hold [18, 29]:

$$\dot{P}_{n1} = \frac{E}{V_{n1}} (\Phi_{01} - \Phi_{n1} + A_s \dot{x}_s) \quad \dot{P}_{n2} = \frac{E}{V_{n2}} (\Phi_{02} - \Phi_{n2} - A_s \dot{x}_s) \quad (3.15)$$

where V_{ni} , $i = 1, 2$ are the valve chamber volumes and A_s the spool area. The nozzle flows Φ_{ni} and the inlet flows Φ_{0i} are considered as turbulent determined by curtain area and inlet restriction, written as:

$$\Phi_{01} = C_d A_0 \sqrt{\frac{2}{\rho} (P_s - P_{n1})} \quad \Phi_{02} = C_d A_0 \sqrt{\frac{2}{\rho} (P_s - P_{n2})} \quad (3.16)$$

and

$$\Phi_{n1} = C_d \pi d_n (x_{f0} + x_f) \sqrt{\frac{2}{\rho} (P_{n1} - P_{n3})} \quad \Phi_{n2} = C_d \pi d_n (x_{f0} - x_f) \sqrt{\frac{2}{\rho} (P_{n2} - P_{n3})} \quad (3.17)$$

Hereby, A_0 is the area of inlet restrictions, and the nozzle output pressure P_{n3} holds:

$$\dot{P}_{n3} = \frac{E}{V_{n3}} \left(\Phi_{n1} + \Phi_{n2} - C_d A_{n3} \sqrt{\frac{2}{\rho} (P_{n3} - P_t)} \right) \quad (3.18)$$

with V_{n3} and A_{n3} the respective volume and outlet orifice area.

With equations (3.11) to (3.18), the theoretical model of two-stage flapper-nozzle valve is completed and the behavior of pilot spool can be determined. The flows through pilot spool ports that drive the main spool can now be written, exactly the same with Equation 3.3 with different parameters, as follows:

$$\begin{aligned} \Phi_{m1} &= C_d h_s x_{s1} \sqrt{\frac{2}{\rho} (P_s - P_{m1})} - C_d h_s x_{s4} \sqrt{\frac{2}{\rho} (P_{m1} - P_t)} + \Phi_{l,s1} - \Phi_{l,s4} \\ \Phi_{m2} &= C_d h_s x_{s3} \sqrt{\frac{2}{\rho} (P_{m2} - P_t)} - C_d h_s x_{s2} \sqrt{\frac{2}{\rho} (P_s - P_{m2})} + \Phi_{l,s3} - \Phi_{l,s2} \end{aligned} \quad (3.19)$$

where the valve opening values x_{si} and leakage flows $\Phi_{l,si}$ are computed with the same form of equations (3.5) and (3.6) with parameters substituted with that of pilot spool.

As analysed by Schothorst [18], the natural frequency related to the main spool considering the oil compressibility is much larger than the frequency of interest due to the relative large spool side areas with respect to the chamber volumes and relative small acceleration and friction forces compared with hydraulic driving force. Thus the pressure

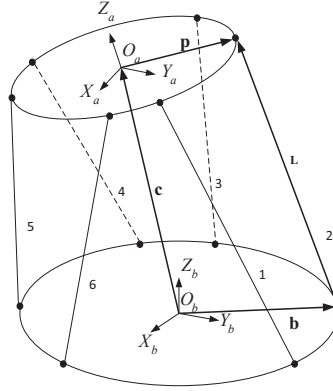


Figure 3.5: The schematic drawing of a Stewart platform (the SRS)

dynamic of the main spool can be neglected and in static state the oil mass balance and force balance equations is given as:

$$\Phi_{m1} = \Phi_{m2} = A_m \dot{x}_m \quad (3.20)$$

$$P_{m1} = P_{m2} \quad (3.21)$$

The above balance equations together with equation (3.19) determine the open-loop behavior of main spool movement, in order to make the main spool position follow the reference input voltage signal u_r , x_m is measured and fed back to the input by a Proportional controller, written as [18]:

$$u = K_{pm} (u_r - K_{ms} x_m) \quad (3.22)$$

with K_{pm} the feedback gain and K_{ms} the main spool position sensor gain.

With the above equations, the complete non-linear model of a close-loop three stage servo-valve is available. Together with the dynamics of hydraulic actuators and pipelines, the model of hydraulic subsystem is completed.

3.2.2. DYNAMIC EQUATIONS OF HEXAPOD MECHANICS

The Stewart platform is modeled as a moving platform supported by six linear actuators, each of which consists of a cylinder and a piston, as depicted in Figure 3.5. Two important reference frames are defined as E_a , the body frame attached to the moving platform, and E_b the inertial frame attached to the static base. The translation vector of the upper platform is \mathbf{c} described in E_b , and the rotational relationship between two frames is described by rotation matrix T_{ba} defined by Euler angles Φ . The platform position is defined as $\mathbf{z} = [\mathbf{c}^T, \Phi^T]^T$, and the platform speed is defined as $\dot{\mathbf{s}} = [\dot{\mathbf{c}}^T, \omega_p^T]^T$, where ω_p is the angular velocity of the moving platform.

When considering one actuator, the leg vector \mathbf{L} from lower gimble point to upper gimble is:

$$\begin{aligned} \mathbf{L} &= \mathbf{L}\mathbf{l} = \mathbf{c} + T_{ba}\mathbf{p} - \mathbf{b} \\ &= \mathbf{c} + \mathbf{q} - \mathbf{b} \end{aligned} \quad (3.23)$$

where L and \mathbf{l} are the length and unit vector of leg vector \mathbf{L} , \mathbf{b} the lower gimble position in base frame and \mathbf{p} and \mathbf{q} the upper gimble position relative to body frame origin in two different frames.

Considering the dynamics of one whole leg, under the constraint force acting on the upper gimble point \mathbf{F}_s and gravity forces on leg cylinder and piston, the Euler's equation can be expressed as:

$$\mathbf{L}\mathbf{l} \times \mathbf{F}_s = -(m_1\mathbf{r}_1 + m_2\mathbf{r}_2) \times \mathbf{g} + m_1\mathbf{r}_1 \times \mathbf{a}_1 + m_2\mathbf{r}_2 \times \mathbf{a}_2 + (\mathbf{I}_1 + \mathbf{I}_2)\dot{\mathbf{W}} + \mathbf{W} \times (\mathbf{I}_1 + \mathbf{I}_2)\mathbf{W} \quad (3.24)$$

where m_i , \mathbf{r}_i , \mathbf{I}_i and \mathbf{a}_i are the mass, center of gravity, moments of inertia and gravity center acceleration of the two parts of one leg, with subscript 1 denoting the lower cylinder and 2 the upper piston, \mathbf{g} is the gravity acceleration vector, and \mathbf{W} is the angular velocity of the leg.

Taking cross products of both sides of equation (3.24) with \mathbf{l} results in[17]:

$$\mathbf{F}_s = (\mathbf{l} \cdot \mathbf{F}_s)\mathbf{l} + \mathbf{D} \times \mathbf{l}/L \quad (3.25)$$

where \mathbf{D} is the right side terms of equation (3.24).

considering the dynamics of the upper rod, Newton's equation in the direction of the leg axis is written as:

$$F + \mathbf{l} \cdot \mathbf{F}_s + m_2\mathbf{l} \cdot \mathbf{g} = m_2\mathbf{l} \cdot \mathbf{a}_2 \quad (3.26)$$

where F is the actuator driving force acting on the joint connecting the leg cylinder and piston, which is viewed as the input of the hexapod mechanical subsystem.

Combining equations (3.25) and (3.26), the constraint force \mathbf{F}_s given as:

$$\mathbf{F}_s = (m_2\mathbf{l} \cdot \mathbf{a}_2 - m_2\mathbf{l} \cdot \mathbf{g}) + \mathbf{D} \times \mathbf{l}/L - F\mathbf{l} = \mathbf{K} - F\mathbf{l} \quad (3.27)$$

Defining a vector $\mathbf{A} = \ddot{\mathbf{c}} + \dot{\boldsymbol{\omega}}_p \times \mathbf{q}$, Dasgupta discussed in[17] that the complex term \mathbf{K} in equation (3.27) can be expressed as:

$$\mathbf{K} = \mathbf{Q}(\mathbf{z})\mathbf{A} + \mathbf{V}(\mathbf{z}, \dot{\mathbf{s}}) \quad (3.28)$$

Substituting equation (3.28) into (3.27) results in:

$$\begin{aligned} \mathbf{F}_s &= \mathbf{Q}(\ddot{\mathbf{c}} + \dot{\boldsymbol{\omega}}_p \times \mathbf{q}) + \mathbf{V} - F\mathbf{l} \\ &= \mathbf{Q}\ddot{\mathbf{c}} - \mathbf{Q}\tilde{\mathbf{q}}\dot{\boldsymbol{\omega}}_p + \mathbf{V} - F\mathbf{l} \end{aligned} \quad (3.29)$$

where $\tilde{\mathbf{q}}$ is the skew-symmetric matrix form of vector \mathbf{q} . With this equation, the force acting on one upper gimble point is explicitly described by platform input, actuator force F and platform states, which should be individually computed for each leg.

Consider the dynamics of the moving upper platform, Newton's equation of motion and Euler's equation of the moving platform are written as:

$$-\sum_{n=1}^6 (\mathbf{F}_s)_i + M_p\mathbf{g} = M_p\mathbf{a}_p \quad (3.30)$$

and

$$-\sum_{n=1}^6 (\mathbf{q}_i \times \mathbf{F}_s)_i + M_p \mathbf{R} \times \mathbf{g} = M_p \mathbf{R} \times \mathbf{a}_p + \mathbf{I}_p \dot{\boldsymbol{\omega}}_p + \boldsymbol{\omega}_p \times \mathbf{I}_p \boldsymbol{\omega}_p \quad (3.31)$$

where M_p and \mathbf{I}_p are the mass and moment of inertia of the upper platform, \mathbf{R} is the position vector of center of gravity relative to the body frame origin in base frame of reference, and \mathbf{a}_p is the acceleration of the center of gravity, given as:

$$\mathbf{a}_p = \dot{\boldsymbol{\omega}}_p \times \mathbf{R} + \boldsymbol{\omega}_p \times (\boldsymbol{\omega}_p \times \mathbf{R}) + \ddot{\mathbf{c}} \quad (3.32)$$

Combining equations (3.29) to (3.32), the complete dynamic equations of the Stewart platform are derived as[17]:

$$\mathbf{M}(\mathbf{z}) \ddot{\mathbf{s}} + \boldsymbol{\eta}(\dot{\mathbf{s}}, \mathbf{z}) = \mathbf{H}\mathbf{F} \quad (3.33)$$

where

$$\mathbf{M} = \begin{bmatrix} ME_3 & -M\tilde{\mathbf{R}} \\ M\tilde{\mathbf{R}} & \mathbf{I}_p + M(R^2 E_3 - \mathbf{R}\mathbf{R}^T) \end{bmatrix} + \sum_{n=1}^6 \begin{bmatrix} \mathbf{Q}_i & -\mathbf{Q}_i \tilde{\mathbf{q}}_i \\ \tilde{\mathbf{q}}_i \mathbf{Q}_i & -\tilde{\mathbf{q}}_i \mathbf{Q}_i \tilde{\mathbf{q}}_i \end{bmatrix}$$

$$\boldsymbol{\eta} = \begin{bmatrix} M\{\boldsymbol{\omega}_p \times (\boldsymbol{\omega}_p \times \mathbf{R}) - \mathbf{g}\} \\ \boldsymbol{\omega}_p \times \mathbf{I}_p + M\mathbf{R} \times \{(\boldsymbol{\omega}_p \cdot \mathbf{R})\boldsymbol{\omega}_p - \mathbf{g}\} \end{bmatrix} + \sum_{n=1}^6 \begin{bmatrix} \mathbf{V}_i \\ \mathbf{q}_i \times \mathbf{V}_i \end{bmatrix}$$

\mathbf{F} is the stacked input actuator forces of each leg

$$\mathbf{F} = [F_1 \quad F_2 \quad F_3 \quad F_4 \quad F_5 \quad F_6]$$

and \mathbf{H} the stacked column input-output force transformation vectors

$$\mathbf{H}_i = \left[\mathbf{l}_i^T, (\mathbf{q}_i \times \mathbf{l}_i)^T \right]^T$$

With equation (3.33), the closed form equations of motion of a Stewart platform is build that can be used for both inverse problem in controller design and forward problem in computer modeling and simulation.

3.2.3. CONTROL STRATEGY

In order to achieve full simulation of the simulator motion system, the controller used in the motion tracking tasks should also be included in the model. Hereby the control strategy currently used in SIMONA simulator will be briefly introduced.

The so called model based cascaded pressure difference (CdP) controller is used in the inner-loop hydraulic subsystem to turn the velocity source resembling hydraulic manipulators into force generators, thus common controllers for outer-loop mechanical subsystem can be applied to the motion system. When designing the CdP controller, the dynamics of the servo-valve are neglected, such that the displacement of main spool x_m is equal to the input voltage u . The actuator dynamic equations (3.1) can be simplified into one dynamic equation describing the pressure difference of two actuator compartments[2]:

$$\dot{P}_L = 2C_m(q) \left(\Phi_n \sqrt{1 \pm P_L/P_s} u - L_{lm} P_L - A_p \dot{q} \right) \quad (3.34)$$

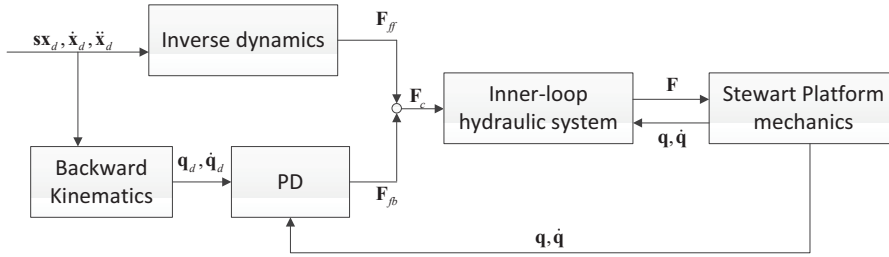


Figure 3.6: Structure of outer-loop controller of Stewart platform manipulator

where P_L is the pressure difference, C_m is the position dependent oil stiffness, Φ_n is the maximum valve flow and L_{lm} is the main leakage parameter. The CdP control law is given by:

$$u = \frac{K_v \dot{q} + K_c (F_c / A_p P_s - P_L / P_s) + K_L P_L}{\sqrt{1 \pm P_L / P_s}} \quad (3.35)$$

where F_c is the reference force of the actuator. With gains K_v and K_L chosen as $K_v = A_p / \Phi_n$ and $K_L = L_{lm} / \Phi_n$, the equation for the close inner-loop is then written as:

$$\dot{P}_L = 2C_m K_c \Phi_n (F_c / A_p - P_L) / P_s \quad (3.36)$$

which shows that the actuator is turned into a first-order force generator with a variable gain.

The structure of the outer-loop controller is shown in Figure 3.6. The model-based feedforward term, i.e. F_{ff} , calculates the forces needed for each leg using inverse dynamics of Stewart platform mechanism, given reference signals of platform motion trajectories. The outer-loop PD controller is a typical PD controller designed in joint space, which is introduced to stabilize the system. Similar outer-loop control structure can be found in a number of recent literature [9, 30].

3.3. COMPUTER MODELING

3.3.1. COMPUTER MODELING IN SIMULINK

The complete model of a hydraulic hexapod motion system is built in Matlab/Simulink environment with dynamics of actuators and servo-valves, dynamics of Stewart platform mechanics as well as the inner-loop and outer-loop controllers. The complete model for computer simulation with controllers in the loop is illustrated in Fig. 3.7. The model is designed to be modular. The dynamics of each sub-system are connected to their neighbouring modules, such that the outputs of each module act as inputs of the adjacent ones, and vice versa. In this way each module can be included or omitted from the complete model, or replaced by a simplified model (such as a linear second-order system), based on the requirement of the simulation. For instance, when only the parallel manipulator rigid-body dynamics is of interest, for instance for cases for inertial parameter

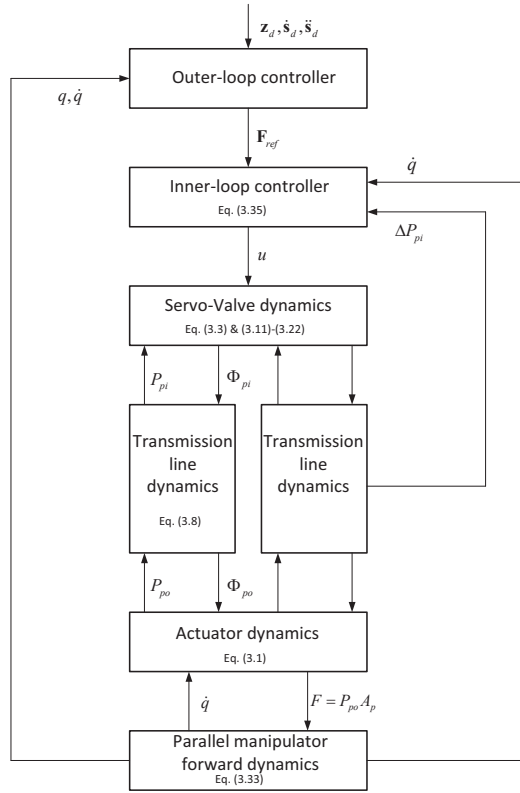


Figure 3.7: Logic structure of the complete model for computer simulation with feedback controllers

identification, the complete hydraulic system controlled by the inner-loop controller can be neglected and replaced by a unit gain or first or second-order systems. When the influence of a particular nonlinear physical disturbance to the system is to be investigated, such as the over-laps or under-laps of the servo-valve openings, the proposed detailed model based on physical laws should be used.

The modular structure of the model helps to identify which part of the system dynamics makes significant contribution to the closed-loop system behaviour. For instance, it will be shown in Chapter 4 that an inclusion of the transmission line dynamics helps to replicate the unstable vibration at around 200 Hz in computer simulation, which was observed in the experiments with the proposed controller without the consideration of the transmission line. This brings a conclusion that the transmission line dynamics are the cause of the unstable vibration. The corresponding solution verified by the computer model is proven to be effective for the later experiments.

3.3.2. COMPUTER MODELING WITH SIMMECHANICS

SimMechanics is a multibody modeling toolbox integrated in Matlab/Simulink environment as a 'physical' approach for mechanic modeling, which will formulate and solve

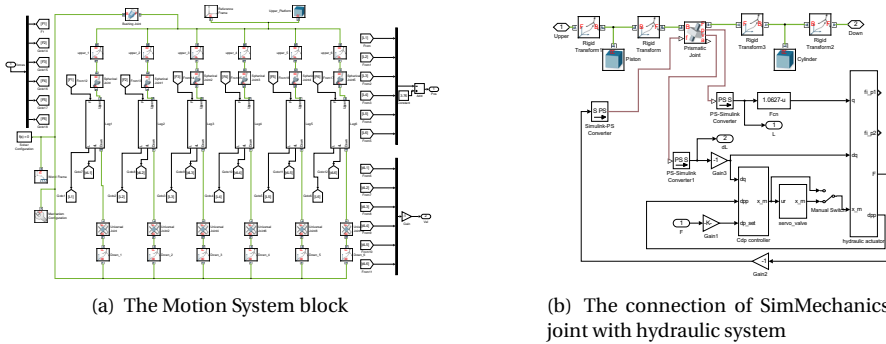


Figure 3.8: Computer model of SRS with SimMechanics

the equations of motion after users have assembled the system by blocks representing bodies, joints, constraints and force elements. In this modeling approach, basic structure of computer model is kept the same as previous subsection while the inverse dynamics based force computation block and forward dynamics of 6-DOF Stewart platform mechanics are built with SimMechanics rather than Newton-Euler dynamic equations. The complete motion platform is depicted in Figure 3.8(a). The hydraulic subsystem is connected to SimMechanics prismatic joint block as a source of force and displacement, as shown in Figure 3.8(b).

3.4. SIMULATION RESULTS AND VALIDATION

3.4.1. RESULTS COMPARISON OF TWO MODELING APPROACHES

Two complete computer models of flight simulator with different model of mechanics, i.e. Newton-Euler dynamic equations and SimMechanics, are implemented in Matlab/Simulation Environment, as a bilateral verification. The geometry of Stewart platform used is that of the Simona which is depicted in Figure 3.1 and Figure 3.9, the top view of which looks like two uneven hexagons in its neutral position. The geometric and inertial parameters of the platform are given in Table 1. The parameters of hydraulic servo-valve and actuator use that of literature[18] in its appendix F. In both simulations, the sample time is set to 1ms and ODE45 solver is used in Simulink environment.

As the purpose of this section is to verify the dynamics of mechanics, the servo-valve dynamics is neglected to alleviate the computation load. Reference trajectories of the moving platform are generated and tracked by the complete motion system under control of the inner- and outer-loop controllers. For simulation, straight line paths designed by Dasgupta[14] is used as reference trajectory, with each coordinate of \mathbf{z} linear with parabolic blends at the beginning and the end thus change in three steps with constant acceleration, constant velocity and constant deceleration. The initial and final position is set as $\mathbf{c}_0 = [0, 0, 3.0]^T$, $\Phi_0 = [-0.2, 0, 0]^T$, $\mathbf{c}_f = [0, 0, 3.5]^T$, $\Phi_f = [0.2, 0, 0]^T$, the total time τ_f , maximum linear velocity V and maximum angular velocity ω are set to 6, 0.14 and 0.08, with SI units used for all quantities. The control gains K_p and K_d are tuned to $6e4$ and $1e4$. The feedforward forces computed by the inverse dynamics in two modeling ap-

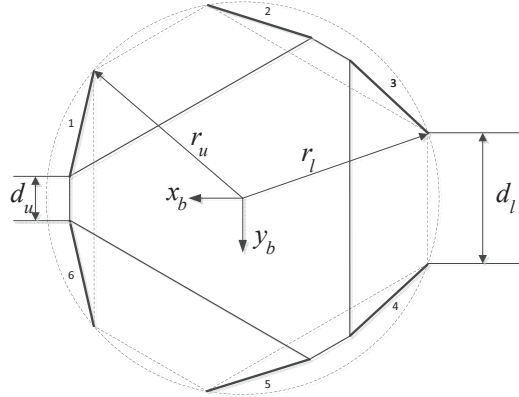


Figure 3.9: SRS top view

Table 3.1: Geometric and inertial parameters

Parameters	Value
Upper/lower gimbal radius, r_a r_b	1.6, 1.65 m
Upper/lower radius spacing, d_u d_l	0.2, 0.6 m
Piston/cylinder masses, m_2 m_1	120, 150 kg
Piston/cylinder inertia wrt cog, i_2 i_1	20, 36 $kg\ m^2$
Piston/cylinder cog wrt to gimbal, r_2 r_1	0.7, 0.5 m
Platform mass M_p	4000 kg
Platform nonzero inertial I_{xx} I_{yy} I_{zz} I_{xz}	7, 7, 8, $0.5 \times 10^3\ kg\ m^2$

proaches are shown in Figure 3.10. The leg length history tracking the reference motion for both models are shown in Figure 3.11.

As shown in Figure 3.10, the feedforward forces computed by both models are consistent, given the same reference motion. The inverse dynamics of both Newton-Euler and SimMechanics approaches are verified with this result. As the Newton-Euler dynamic equation are given in closed form, the forward dynamics of it can also be validated. Figure 3.11 shows the consistence of dynamic responses of both models including inverse and forward dynamics, which further verifies the correctness of both modeling approaches.

3.4.2. MODEL VALIDATION

In order to validate the complete model, simulation results are compared to real world performance of the SRS. Open loop simulation results of each subsystem (input output response of servo-valve for instance) are hard to be compared to experiment data due to two reasons: first, parameters used in computer model are not exactly the same with that of the real simulator. secondly, the time accumulating error can make the simulation result explode during integration of dynamic functions even with precise parameters.

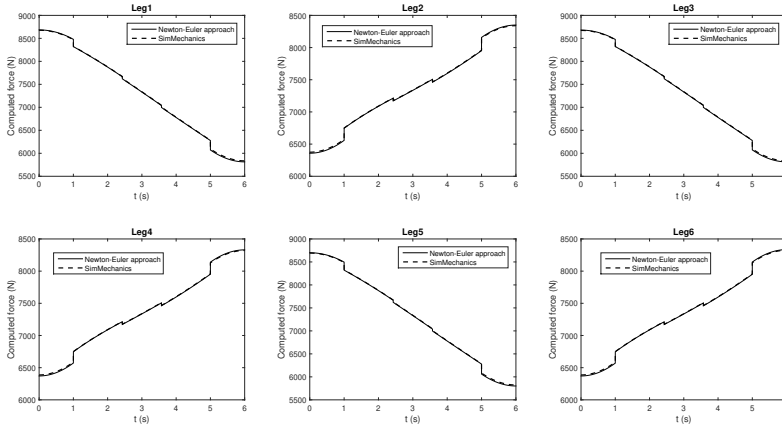


Figure 3.10: Feedforward forces of 6 actuators calculated by inverse dynamics of two approaches

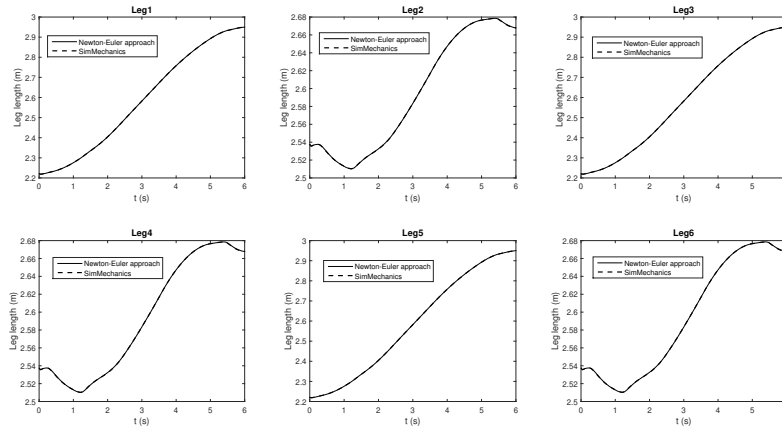


Figure 3.11: Leg lengths of two computer model simulations given the same reference trajectory

Thus in this section, close loop simulation of the complete model with controllers is implemented and reference trajectories used in real-world experiment are used as input (see Figure 3.6). The model is validated by comparing the computed history of states of the motion system like spool displacement of each valve or pressure difference of each actuator with that of the experiment measurements.

The motion profile from a state reconstruction experiment of SRS[31] is used, in which the origin of body frame periodically moves in a horizontal circular path with a radius of 0.5 meters, with a period of five seconds, the joint space conversion of which is given in Figure 3.12. The motion profile exploits most of the DOFs of the platform with relatively large amplitude and thus sufficiently exploits the stroke of hydraulic actuators and nonlinear dynamics of the platform[31]. The control gain K_p is set to $8e5$ as the same with SRS, and K_d is tuned to $1e5$. Figure 3.12 shows the joint space trajectory tracking results of experiment and simulation. The history of three states of the system, i.e. the feedforward forces, the actuator pressure differences and the spool displacements, are shown in Figures 3.13, 3.14 and 3.15.

Figure 3.12 shows consistent tracking performance of real SRS system and the established computer model. However, the conclusion of model correctness can not be drawn without validation of inner states, as closed-loop experiment and simulation are conducted. Figures 3.14 and 3.15 indicate that the simulated pressure differences in hydraulic actuators and spool displacement in valves fit well with the measurements of experiment, as the responses to particular motion commands match well. The performances are not completely consistent due to the fact that hydraulic and mechanical parameters used in computer model are different from the real SRS, since some of them (like mass) are modified during the simulator construction and some are even not accessible. It can be further explained with figure 3.13 that the computed feedforward forces in real system differs a little from simulation. Designed mass and inertia parameters are used in computer model while identified parameters are used in real system. This parameter mismatch dose not prevent the computer model from showing enough features of the real system in general. It can be concluded that the computer model is feasible of simulating hydraulic hexapod motion systems, with correct physical phenomena reflected.

3.5. CONCLUSION

The complete computer model of a hydraulic hexapod flight simulator motion system is build, with hydraulic servo-valve, hydraulic actuator and Stewart platform mechanics integrated. The dynamics of hydraulic servo-valve and actuator are derived based on physical laws describing the performance of every part like spools and flapper, as well as the oil flows and pressure. The dynamic equations of the Stewart platform are derived using Newton-Euler approach. The currently implemented inner-loop CdP controller and outer-loop controller of the SRS are used in the model.

The complete model is established and executed with Matlab/Simulink software. A second modeling approach with Stewart platform mechanics established by SimMechanics is also implemented in Simulink. Simulation results of these two models verifies the validity of both mechanics modeling approaches. Furthermore, closed loop simulation results fit well with real-world experiment measurements of SRS, which validates

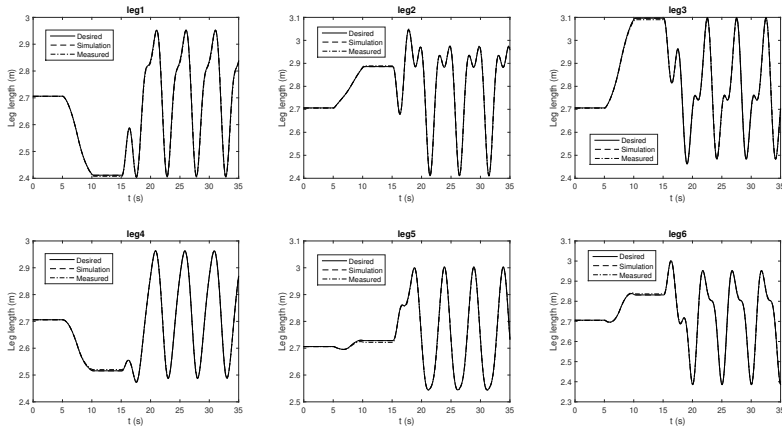


Figure 3.12: Reference motion tracking result of experiment and simulation

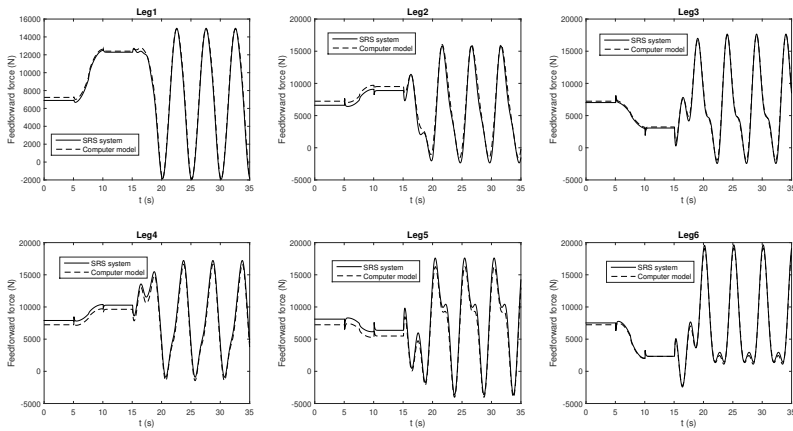


Figure 3.13: Feedforward forces calculated by controllers in SRS and computer model

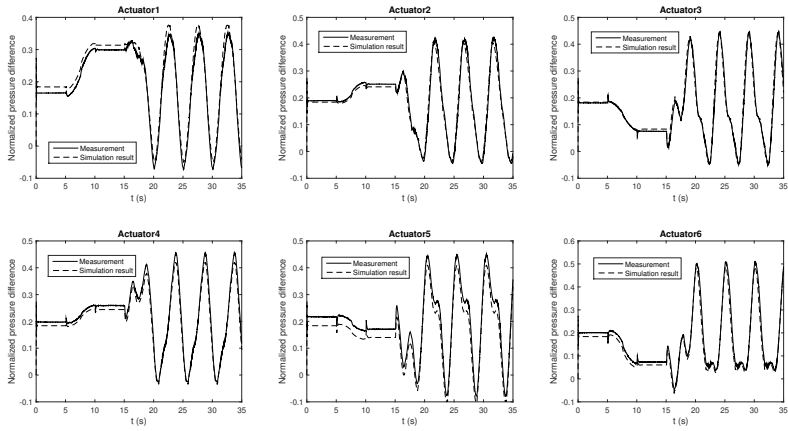


Figure 3.14: Pressure differences of 6 actuators in experiment and simulation

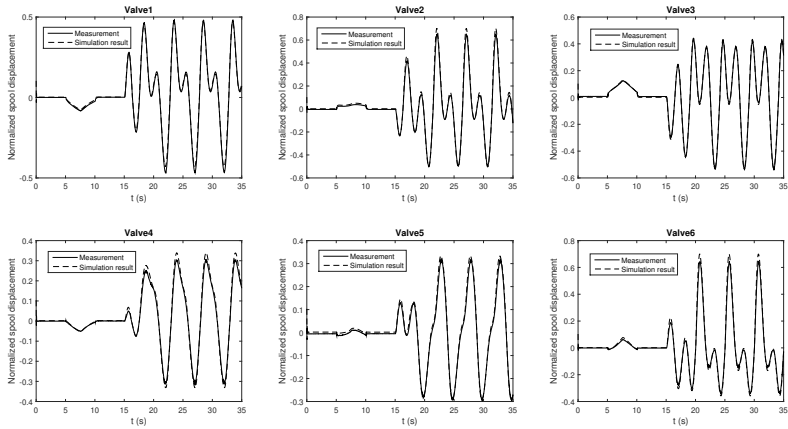


Figure 3.15: Spool displacements of 6 valves in experiment and simulation

that the computer model can be used as simulation platform for flight simulator motion system controller design and performance evaluation.

REFERENCES

- [1] Y. Huang, D. M. Pool, O. Stroosma, Q. P. Chu, and M. Mulder, "Modeling and Simulation of Hydraulic Hexapod Flight Simulator Motion Systems," in *AIAA Modeling and Simulation Technologies Conference*, January 2016.
- [2] S. Koekebakker, "Model based control of a flight simulator motion system," Ph.D. dissertation, Delft University of Technology, 2001.
- [3] B. Dasgupta and T. Mruthyunjaya, "The stewart platform manipulator: a review," *Mechanism and Machine Theory*, vol. 35, no. 1, pp. 15 – 40, 2000.
- [4] M. R. Siroospour and S. E. Salcudean, "Nonlinear control of hydraulic robots," *IEEE Transactions on Robotics and Automation*, vol. 17, no. 2, pp. 173–182, 2001.
- [5] Y. Pi and X. Wang, "Trajectory tracking control of a 6-DOF hydraulic parallel robot manipulator with uncertain load disturbances," *Control Engineering Practice*, vol. 19, no. 2, pp. 185 – 193, 2011. [Online]. Available: <http://www.sciencedirect.com/science/article/pii/S0967066110002534>
- [6] F. Bu and B. Yao, "Observer based coordinated adaptive robust control of robot manipulators driven by single-rod hydraulic actuators," in *Proceedings 2000 ICRA. Millennium Conference. IEEE International Conference on Robotics and Automation. Symposia Proceedings (Cat. No.00CH37065)*, vol. 3, 2000, pp. 3034–3039 vol.3.
- [7] M. Becerra-Vargas and E. M. Belo, "Robust control of flight simulator motion base," *Journal of Guidance, Control, and Dynamics*, vol. 34, no. 5, pp. 1519–1528, 2011.
- [8] O. Stroosma, M. M. van Paassen, and M. Mulder, "Using the SIMONA Research Simulator For Human-Machine Interaction Research," in *AIAA Modeling and Simulation Technologies Conference and Exhibit*, 2003.
- [9] C. Yang, Q. Huang, and J. Han, "Computed force and velocity control for spatial multi-DOF electro-hydraulic parallel manipulator," *Mechatronics*, vol. 22, no. 6, pp. 715 – 722, 2012, special Issue on Intelligent Mechatronics.
- [10] I. Davliakos and E. Papadopoulos, "Model-based control of a 6-DOF electrohydraulic stewart–gough platform," *Mechanism and Machine Theory*, vol. 43, no. 11, pp. 1385 – 1400, 2008.
- [11] —, "Impedance model-based control for an electrohydraulic stewart platform," *European Journal of Control*, vol. 15, no. 5, pp. 560 – 577, 2009.
- [12] D. Li and S. E. Salcudean, "Modeling, simulation, and control of a hydraulic stewart platform," in *Proceedings of International Conference on Robotics and Automation*, vol. 4, April 1997, pp. 3360–3366 vol.4.

- [13] W. Q. D. Do and D. C. H. Yang, "Inverse dynamic analysis and simulation of a platform type of robot," *Journal of Robotic Systems*, vol. 5, no. 3, pp. 209–227. [Online]. Available: <https://onlinelibrary.wiley.com/doi/abs/10.1002/rob.4620050304>
- [14] B. Dasgupta and T. Mruthyunjaya, "A Newton-Euler formulation for the inverse dynamics of the Stewart platform manipulator," *Mechanism and Machine Theory*, vol. 33, no. 8, pp. 1135 – 1152, 1998.
- [15] Z. Geng, L. S. Haynes, J. D. Lee, and R. L. Carroll, "On the dynamic model and kinematic analysis of a class of Stewart platforms," *Robotics and Autonomous Systems*, vol. 9, no. 4, pp. 237 – 254, 1992.
- [16] J. Lee and Z. Geng, "A dynamic model of a flexible Stewart platform," *Computers & Structures*, vol. 48, no. 3, pp. 367 – 374, 1993. [Online]. Available: <http://www.sciencedirect.com/science/article/pii/0045794993903133>
- [17] B. Dasgupta and T. Mruthyunjaya, "Closed-form dynamic equations of the general Stewart platform through the Newton–Euler approach," *Mechanism and Machine Theory*, vol. 33, no. 7, pp. 993 – 1012, 1998.
- [18] G. van Schothorst, "Modelling of Long-Stroke Hydraulic Servo-Systems for Flight Simulator Motion Control and System Design," Ph.D. dissertation, Delft University of Technology, 1997.
- [19] K. Dasgupta and H. Murrenhoff, "Modelling and dynamics of a servo-valve controlled hydraulic motor by bondgraph," *Mechanism and Machine Theory*, vol. 46, no. 7, pp. 1016 – 1035, 2011. [Online]. Available: <http://www.sciencedirect.com/science/article/pii/S0094114X1000203X>
- [20] M. El-Araby, A. El-Kafrawy, and A. Fahmy, "Dynamic performance of a nonlinear non-dimensional two stage electrohydraulic servovalve model," *International Journal of Mechanics and Materials in Design*, vol. 7, no. 2, pp. 99–110, 2011.
- [21] D. Gordić, M. Babić, and N. Jovičić, "Modelling of spool position feedback servovalves," *International Journal of Fluid Power*, vol. 5, no. 1, pp. 37–51, 2004. [Online]. Available: <https://doi.org/10.1080/14399776.2004.10781182>
- [22] D. Hroncova and M. Pastor, "Mechanical system and SimMechanics simulation," *American Journal of Mechanical Engineering*, vol. 1, no. 7, pp. 251–255, 2013.
- [23] G. D. Wood and D. C. Kennedy, "Simulating mechanical systems in Simulink with SimMechanics," 01 2003.
- [24] T. J. Viersma, "Analysis, synthesis, and design of hydraulic servosystems and pipelines(book)," *Amsterdam, Elsevier Scientific Publishing Co.(Studies in Mechanical Engineering.*, vol. 1, 1980.
- [25] H. E. Merritt, *Hydraulic Control Systems*. John Wiley & Sons, 1967.

- [26] G. van Schothorst, P. Teerhuis, and A. van der Weiden, “Stability analysis of a hydraulic servo-system including transmission line effects,” in *Proceedings of the Third International conference on Automation, Robotics and Computer Vision, Singapore*, 1994, pp. 1919–1923.
- [27] W. C. Yang and W. E. Tobler, “Dissipative Modal Approximation of Fluid Transmission Lines Using Linear Friction Model,” *Journal of Dynamic Systems, Measurement, and Control*, vol. 113, no. 1, pp. 152–162, 1991.
- [28] S. J. Lin and A. Akers, “A dynamic model of the flapper-nozzle component of an electrohydraulic servovalve,” *Journal of Dynamic Systems, Measurement, and Control*, vol. 111, no. 1, pp. 105–109, Mar 1989. [Online]. Available: <http://dx.doi.org/10.1115/1.3153006>
- [29] —, “Dynamic analysis of a flapper-nozzle valve,” *Journal of Dynamic Systems, Measurement, and Control*, vol. 113, no. 1, pp. 163–167, Mar 1991. [Online]. Available: <http://dx.doi.org/10.1115/1.2896343>
- [30] J. Wang, J. Wu, L. Wang, and Z. You, “Dynamic feed-forward control of a parallel kinematic machine,” *Mechatronics*, vol. 19, no. 3, pp. 313 – 324, 2009.
- [31] I. Miletovic, “Optimal Reconstruction of Flight Simulator Motion Cues,” MSc. thesis, Delft University of Technology, 2014.

4

SENSOR-BASED HYDRAULIC FORCE CONTROLLER

Chapter 2 discussed the challenges for achieving high precision motion control of hydraulic parallel robots in a perspective of nonlinear uncertain system design. A novel INDI control technique is proposed to overcome the disadvantages of the current state-of-the-art hydraulic control systems. However, the controller design procedure based on the INDI is not given in detail, nor is its effectiveness verified by the simulation model developed in Chapter 3. In this chapter, a detailed hydraulic force controller is designed based on the proposed INDI control technique. The effectiveness and performance of the developed control system are verified and validated by computer simulation and real-world experiments on the SIMONA hydraulic parallel flight simulator. This chapter is organized as follows. After a brief introduction in Section 4.1, Section 4.2 gives a brief review of the system dynamics for controller design. Section 4.3 gives a detailed discussion on the INDI control theory, including the stability and robustness analysis. The detailed hydraulic force controller design is given in Section 4.4. Section 4.5 and 4.6 present the simulation results and experiment results for the developed control system, validating the effectiveness and the robustness. A conclusion is given in Section 4.7.

This chapter is based on the following articles:

Y. Huang, D. Pool, O. Stroosma, and Q. Chu, "Incremental nonlinear dynamic inversion control for hydraulic hexapod flight simulator motion systems," IFAC-PapersOnLine, vol. 50, no. 1, pp. 4294 – 4299, 2017, 20th IFAC World Congress. [1]

Y. Huang, D. Pool, O. Stroosma, and Q. Chu, "Long-stroke hydraulic robot motion control with incremental nonlinear dynamic inversion," IEEE/ASME Transactions on Mechatronics, vol.24, no. 1, pp. 304-314, Feb 2019. [2]

High precision motion control of hydraulic manipulators is challenging due to the highly nonlinear dynamics and model uncertainties typical for hydraulic actuators. This chapter addresses the implementation of a novel sensor-based Incremental Nonlinear Dynamic Inversion control technique for a high-precision hydraulic force controller in existence of parameter uncertainties. Combined with a widely used force computation outer-loop controller, the proposed motion control structure is implemented on a 6-DOF hexapod hydraulic robot, the SIMONA (Simulation, Motion and Navigation) Research Simulator at TU Delft. The proposed control technique is inherently robust to hydraulic parameter uncertainties. As an important contribution, the robustness against parameter uncertainty is rigorously proven. Stability of the proposed controller is also analysed. Techniques for solving characteristic implementation issues, such as higher-order valve dynamics and oil transmission effects, are discussed in detail. Motion tracking experiment results on the SIMONA simulator validate the effectiveness of the proposed method in terms of performance and the robustness against parameter uncertainties. Significant control accuracy improvement is demonstrated by comparing with the state-of-the-art motion control implementations.

4.1. INTRODUCTION

Hydraulic robotic systems are widely used in heavy-duty machines, legged robots, and vehicle simulator motion systems. They still have higher power-to-weight ratios and inherently higher stiffness and rigidity compared with electrical motors. For applications where high precision control performance is required, such as legged robots control [3, 4], manipulator impedance control [5, 6] and flight simulator motion control [7], high performance controller development is receiving increasing attention in the academia.

One challenge of the hydraulic robot control problem is that hydraulic actuators regard the input as a velocity command, instead of a force command as their electrical counterparts do. This fact prevents the extensively studied general robot control techniques [8–11] from direct application, which generally work with force inputs. A few studies successfully implemented model-based control methods based on the integrated mechanics and hydraulic dynamics. Nevertheless, the highly nonlinear hydraulic dynamics have to be significantly simplified by linearization or neglecting leakage or oil compressibility [12, 13]. More importantly, a lack of hydraulic pressure/force controllers largely limits their applications in robot impedance control, vibration isolation and active suspension, where ideal force actuators are generally assumed [14]. One systematic solution for hydraulic systems is cascading the controller into a multi-loop structure, as shown in Fig. 4.1. An inner-loop hydraulic force controller decouples the hydraulic dynamics from the mechanics, while guiding it to generate the required actuation forces given by the outer-loop motion controller. With a decoupled inner-loop force controller, various advanced (outer-loop) control schemes developed for electrical manipulators become possible to be directly applied to hydraulic robotic systems.

Force control of a hydraulic actuator is challenging due to the highly nonlinear dynamic behavior, and the model uncertainties resulting from model simplification and parameter uncertainty. Furthermore, fundamental limits exist in simple controllers (e.g. PID) for hydraulic force tracking problems, as shown in [15]. This makes more advanced model-based control schemes necessary, such as feedback linearization [5, 16] and its

variants, including Nonlinear Dynamic Inversion (NDI) based control [17], Cascade ΔP controller (CdP) [18] and flatness-based control [19]. However, the performance of the feedback linearization based controllers relies on an accurate model and is significantly degraded in existence of parameter mismatches. For linear dynamic inversion, general techniques such as additive-state-decomposition (ASD) have been proposed to deal with model uncertainty and disturbance [20, 21]. When considering the nonlinear hydraulic model uncertainty problem, nonlinear adaptive control is one extensively studied approach [22–25]. Among them, as concluded in [26], the most advanced works in terms of motion control accuracy are [24] for hydraulic serial manipulators and [25] for hydraulic parallel robots, each of which provides a stability-guaranteed controller with adaptation of hydraulic parameters. However, in all the mentioned adaptive approaches, the design of the hydraulic parameter adaptation law is coupled with the complete control system design in order to guarantee the stability. It is difficult to directly combine the hydraulic adaptive methods with a different outer-loop controller. Therefore, a high performance, fully decoupled and less model-dependent hydraulic force controller is still to be developed.

Incremental Nonlinear Dynamic Inversion (INDI) [27] is a novel sensor-based nonlinear control technique based on the feedback linearization of the nominal incremental part of the system dynamics. INDI solves the inherent problem of model dependency of traditional feedback linearization. A number of state-of-the-art nonlinear control applications with INDI have been reported [28, 29], validating the achievable control performance and robustness of INDI towards model uncertainties under the assumption of a high sampling rate. INDI is particularly attractive to high precision force control of hydraulic robots with the following features:

1. Inherently robust to parameter uncertainty and continuous external disturbances, without an explicitly adaptive or robust control algorithm.
2. High control precision with low computation load and straightforward controller design procedures.
3. Achieving precise feedback linearization of highly nonlinear systems without precise knowledge of their dynamics.

In previous reports of this research project, the preliminary theoretical application of INDI was recently discussed for a single hydraulic actuator model [30] and a hydraulic flight simulator model [1]. However, these simulation studies did not provide any experimental validation. Also, practical issues such as oil pipeline dynamics of long-stroke hydraulic actuators were neglected in the simulation models. Furthermore, none of aforementioned works gave a rigorous proof of the parameter uncertainty resistance features and the stability of INDI.

In this chapter, the novel INDI technique is improved in theory, and implemented in real-world for the inner-loop force controller of the long-stroke hydraulic hexapod motion system of the SIMONA Research Simulator (SRS) at TU Delft. The key practical issues for INDI, such as additional dynamics between controller output and actuator sensor (including the valve dynamics and oil pipeline dynamics), are considered and solved. Directly combined with a typical model-based feedforward outer-loop controller with

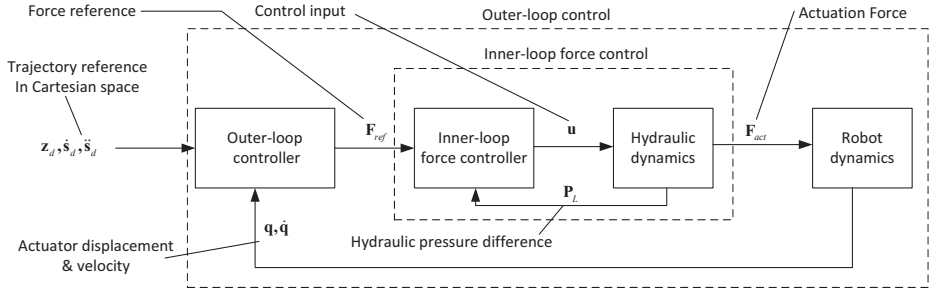


Figure 4.1: Cascade-control architecture for hydraulic robots with inner and outer control loops

PD feedback in the actuator space, the overall motion control system is designed. Two motion profiles are used for experiments in this chapter: a symmetric motion for control performance evaluation and benchmarking and an asymmetrical profile to validate the effectiveness of the proposed controller with more system nonlinearities excited.

The main contributions of this chapter are:

1. The robustness of the INDI against parameter uncertainty is rigorously proved for the first time, based on which a necessary stability condition for the INDI with parameter uncertainty is provided. A rigorous stability proof of the INDI is also given.
2. The novel INDI method is applied in a real-life hydraulic parallel robot for the first time.
3. The experiment results demonstrate improved control performance compared with the state-of-the-art methods discussed in a recent survey paper [26], even in existence of large model parameter mismatches.

This chapter is organized as follows. Section 4.2 summarizes the model of the hydraulic robots for purpose of controller design. Section 4.3 introduces the novel INDI methodology, including the stability and robustness proofs. Section 4.4 discusses the application details and practical issues in designing the INDI hydraulic control system. The simulation and experiment results on the SRS are described in Section 4.5 and Section 4.6, and the main conclusions are given in Section 4.7.

4.2. SYSTEM DYNAMIC MODEL

The rigid-body dynamic equations of an n -link robot are generally given by a second-order nonlinear differential equation [25]. Particularly, for parallel robots such as hexapod robotic systems considered in this research as an example, Newton-Euler approach [31] is typically used to obtain the dynamic equations in Cartesian space:

$$M(z)\ddot{s} + \eta(\dot{s}, z) = J^T F, \quad (4.1)$$

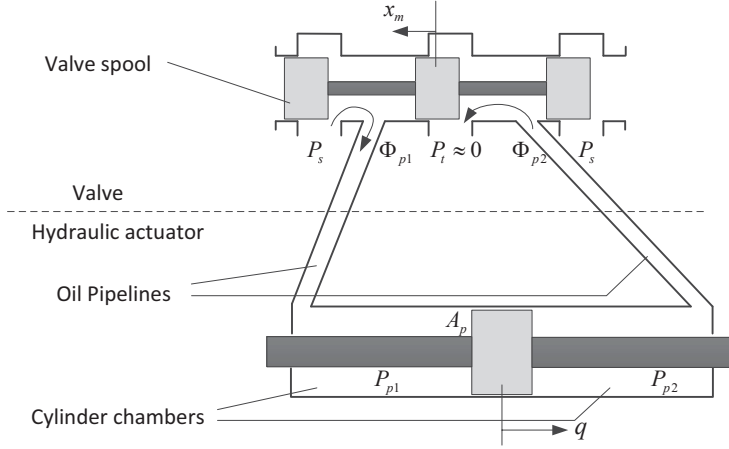


Figure 4.2: A valve controlled symmetry hydraulic actuator

where $\mathbf{z} \in \mathbb{R}^6$ and $\dot{\mathbf{s}} \in \mathbb{R}^6$ are the end effector pose and velocity vectors defined in the Cartesian space, $\mathbf{F} \in \mathbb{R}^6$ is the vector of actuation forces, $\mathbf{M} \in \mathbb{R}^{6 \times 6}$ is the mass matrix and $\boldsymbol{\eta} \in \mathbb{R}^6$ contains the centrifugal and Coriolis terms. $\mathbf{J} \in \mathbb{R}^{6 \times 6}$ is the Jacobian matrix of the system, defined by $\mathbf{J} = \partial \dot{\mathbf{q}} / \partial \dot{\mathbf{s}}$, where \mathbf{q} is the vector of the actuator displacements. A detailed discussion of the model can be found in [32].

A single symmetrical hydraulic actuator controlled by a typical valve is illustrated schematically in Fig. 4.2. Φ_{p1} and Φ_{p2} are the oil flows into and out of the cylinder chambers through the oil transmission lines. The oil supply and return pressures are denoted by P_s and P_t , respectively. The hydraulic force dynamics are generally described by writing the dynamic equation of the cylinder pressure difference, $P_L = P_{p1} - P_{p2}$, based on the oil compressibility effect, given by [1]:

$$\dot{P}_L = 2C_m(q) (\Phi_m - C_l P_L - A_p \dot{q}), \quad (4.2)$$

where q denotes the actuator cylinder displacement, A_p is the cylinder area, C_l is the leakage coefficient, $\Phi_m = (\Phi_{p1} + \Phi_{p2}) / 2$ is the controlled oil flow. The piston dependent oil stiffness C_m is

$$C_m = \frac{1}{2} \left(\frac{E}{V_1(q)} + \frac{E}{V_2(q)} \right), \quad (4.3)$$

where E is the oil bulk modulus and V_1 and V_2 are the volumes of the cylinder chambers.

For an ideal critical center valve with matched and symmetrical orifices, the oil flow is given by [33]

$$\Phi_m = C_d w x_m \sqrt{\frac{P_s}{\rho} \left(1 - \frac{x_m}{|x_m|} \frac{P_L}{P_s} \right)}. \quad (4.4)$$

where x_m is the valve displacement, C_d is the discharge coefficient and w is the orifice width.

By defining the maximum flow at the maximum valve stroke $x_{m,max}$ and zero load pressure as $\Phi_n = C_d w x_{m,max} \sqrt{P_s / \rho}$, and the system input as the normalized valve displacement $u = x_m / x_{m,max}$, (4.4) is substituted in (4.2) and gives:

$$\begin{aligned} \dot{P}_L &= 2C_m(q) \left(\Phi_n \sqrt{1 - \frac{x_m}{|x_m|} \frac{P_L}{P_s}} u - C_l P_L - A_p \dot{q} \right) \\ &= G_A(P_L, x_m, q) u + f_A(P_L, q, \dot{q}). \end{aligned} \quad (4.5)$$

The servo-valve dynamics are generally modeled as a second-order linear system with a bandwidth much higher than the rest of the system [5]. It will be shown in Section 4.4 that with a valve displacement feedback in the proposed control scheme, the explicit use of the valve dynamic model can be avoided. The influence of the oil transmission line dynamics is also discussed in Section 4.4.

Combining (4.1) and (4.5) through the relation $F = A_p P_L$, the overall dynamic model of a hydraulic robot is given. Note that good lubrication is assumed for the hydraulic actuator and that frictions are considered as small continuous disturbances. Hence, friction is neglected for controller design, due to their smallness and the fact that the proposed INDI controller is inherently resistant to continuous disturbances, which will be discussed in Section 4.3.

4.3. INCREMENTAL NONLINEAR DYNAMIC INVERSION

Traditional Nonlinear Dynamic Inversion (NDI) control is a variant of the feedback linearization [34] approach, which is widely used in flight control problems [35]. Similar approaches using inverse dynamics, such as computed torque [36] or flatness-based control [19], are also developed for other applications. However, a common disadvantage of feedback linearization based approaches is the dependency on a precise model and hence an inherent sensitivity to model uncertainties. The INDI technique implements the NDI method based on an incremental form of the system dynamics, in which the contribution of most model parameter dependent terms is minimized to a small perturbation. As a consequence, the INDI approach does not explicitly depend on precise model and is thus not sensitive to uncertainties.

4.3.1. THEORY AND STABILITY

The system of interest is a general n^{th} order nonlinear control inputs affine system given by

$$\begin{aligned} \dot{\mathbf{x}} &= \mathbf{f}(\mathbf{x}) + \mathbf{G}(\mathbf{x}) \mathbf{u} + \mathbf{d} \\ \mathbf{y} &= \mathbf{h}(\mathbf{x}), \end{aligned} \quad (4.6)$$

where \mathbf{f} is a vector field in \mathbb{R}^n , $\mathbf{u} \in \mathbb{R}^m$ is the input, $\mathbf{d} \in \mathbb{R}^n$ is a continuous external disturbance and $\mathbf{G} \in \mathbb{R}^{n \times m}$ is the control effectiveness matrix. \mathbf{x} , \mathbf{d} and \mathbf{h} are assumed continuous, $\mathbf{f}(\mathbf{x})$ and $\mathbf{G}(\mathbf{x})$ are assumed to be \mathcal{C}^∞ functions of \mathbf{x} and all degrees of differentiation are bounded.

Assuming that $\mathbf{h}(\mathbf{x}) = \mathbf{x}$, the relative degree of the system is $(1, \dots, 1)_{1 \times n}$, and the first-order time derivative of the output is

$$\dot{\mathbf{y}} = \dot{\mathbf{x}} = \mathbf{f}(\mathbf{x}) + \mathbf{G}(\mathbf{x}) \mathbf{u} + \mathbf{d}, \quad (4.7)$$

where the control input \mathbf{u} appears explicitly in the above equation. For a fully actuated system for which $m = n$, the traditional NDI, or a general feedback linearization approach, can be directly implemented if $\mathbf{G}(\mathbf{x})$ is invertible. For general case when $m \neq n$, a diffeomorphism of system states need to be designed for the system, subject to the accompanying conditions for feedback linearizability. For simplicity, only the case when $m = n$ will be discussed in this section, and the INDI technique for general cases is given in Appendix A of this thesis.

Different from the NDI approach, in order to obtain the incremental form of the studied system, the system dynamics in (4.7) are rewritten by applying the Taylor series expansion at the beginning instant of each sampling interval (denoted by subscript 0):

$$\begin{aligned} \dot{\mathbf{x}} = & \dot{\mathbf{x}}_0 + \mathbf{G}(\mathbf{x}_0)(\mathbf{u} - \mathbf{u}_0) + \left. \frac{\partial [\mathbf{f}(\mathbf{x}) + \mathbf{G}(\mathbf{x})\mathbf{u}]}{\partial \mathbf{x}} \right|_0 (\mathbf{x} - \mathbf{x}_0) \\ & + (\mathbf{d} - \mathbf{d}_0) + \mathbf{O}((\mathbf{x} - \mathbf{x}_0)^2). \end{aligned} \quad (4.8)$$

Defining the last three terms of (4.8) as

$$\boldsymbol{\delta}(\Delta \mathbf{x}, \Delta \mathbf{d}) = \left. \frac{\partial [\mathbf{f}(\mathbf{x}) + \mathbf{G}(\mathbf{x})\mathbf{u}]}{\partial \mathbf{x}} \right|_0 \Delta \mathbf{x} + \Delta \mathbf{d} + \mathbf{O}(\Delta \mathbf{x}^2), \quad (4.9)$$

in which the increments of the variables with respect to their current values are denoted by Δ , (4.8) is then written as

$$\dot{\mathbf{x}} = \underbrace{\dot{\mathbf{x}}_0 + \mathbf{G}(\mathbf{x}_0)(\mathbf{u} - \mathbf{u}_0)}_{\text{nominal part}} + \underbrace{\boldsymbol{\delta}(\Delta \mathbf{x}, \Delta \mathbf{d})}_{\text{perturbation}}, \quad (4.10)$$

In (4.10) the system dynamics are divided into an incremental nominal part, which contains the first two terms, and a perturbation term.

Using the continuity of \mathbf{x} and \mathbf{d} and the boundedness of the differentiation of $\mathbf{f}(\mathbf{x})$ and $\mathbf{G}(\mathbf{x})$, the limits of (4.9) as the time increment T_s goes to 0 is calculated as

$$\lim_{T_s \rightarrow 0} \boldsymbol{\delta}(\Delta \mathbf{x}, \Delta \mathbf{d}) = 0. \quad (4.11)$$

(4.11) suggests that with a fast sampling rate, the contribution of the perturbation $\boldsymbol{\delta}$ to the system dynamics in (4.10) approaches zero. Note that the continuity is not assumed for the system input \mathbf{u} in (4.10). Thus the INDI control law is designed by using the NDI based on the nominal part of (4.10) *in every sampling interval*, given by

$$\mathbf{u} = \mathbf{u}_0 + \mathbf{G}^{-1}(\mathbf{x}_0)(\mathbf{v} - \dot{\mathbf{x}}_0), \quad (4.12)$$

where \mathbf{v} is the pseudo control input to be determined and the system state derivatives $\dot{\mathbf{x}}_0$ are assumed to be measured. Note that the subscript 0 means the beginning of every sampling interval, instead of a fixed reference point. For every sampling interval, the control increment $\Delta \mathbf{u} = \mathbf{G}^{-1}(\mathbf{x}_0)(\mathbf{v} - \dot{\mathbf{x}}_0)$ is calculated and recursively added to \mathbf{u}_0 , the integrated or measured control input of the previous sample, as illustrated in the block diagram presented in Fig. 4.3. Thus the control law (4.12) can also be written in a recursive discrete form as:

$$\begin{aligned} \mathbf{u}_k &= \mathbf{u}_{k-1} + \Delta \mathbf{u} \\ \Delta \mathbf{u} &= \mathbf{G}^{-1}(\mathbf{x}_{k-1})(\mathbf{v} - \dot{\mathbf{x}}_{k-1}), \end{aligned} \quad (4.13)$$

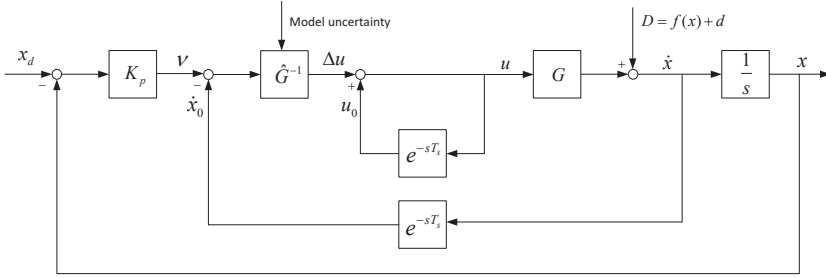


Figure 4.3: Block diagram of a general INDI controller

Substituting (4.12) into (4.10), the closed-loop system dynamics are given by

$$\dot{\mathbf{x}} = \mathbf{v} + \boldsymbol{\delta}(\Delta \mathbf{x}, \Delta \mathbf{d}). \quad (4.14)$$

Combining (4.11) and (4.14), it is clear that under an infinitesimal sampling time, the system is fully linearized. By simply choosing the linear control law $\mathbf{v} = \dot{\mathbf{x}}_d + K_p(\mathbf{x}_d - \mathbf{x})$, where $-K_p$ is Hurwitz and the subscript d denotes the desired trajectory, the system error dynamics are written as

$$\dot{\mathbf{e}} = -K_p \mathbf{e} + \boldsymbol{\delta}(\Delta \mathbf{x}, \Delta \mathbf{d}), \quad (4.15)$$

where $\mathbf{e} = \mathbf{x} - \mathbf{x}_d$. With an infinitesimal T_s , the origin of (4.15) is globally exponentially stable. This is the reason that the INDI is based on the assumption of a high sampling rate. However, in practice, the small sample time T_s is a finite value. (4.11) suggests that $\forall \varepsilon > 0, \exists T_s > 0$, s.t. $\|\boldsymbol{\delta}(\Delta \mathbf{x}, \Delta \mathbf{d})\|_2 \leq \varepsilon$. Thus the stability of INDI is given by the lemma below.

Lemma 1: Consider the closed-loop system in (4.15), where $-K_p$ is Hurwitz, if $\|\boldsymbol{\delta}(\Delta \mathbf{x}, \Delta \mathbf{d})\|_2 \leq \varepsilon$, the error \mathbf{e} will be globally ultimately bounded by εc for some $c > 0$.

Proof: applying Lemma 13.4 in [37]. \square

Lemma 1 shows that the tracking error of the proposed INDI controlled system is globally ultimately bounded and that the ultimate bound can be decreased by reducing the magnitude of the perturbation term $\boldsymbol{\delta}(\Delta \mathbf{x}, \Delta \mathbf{d})$ in a single time increment, with a higher controller sampling frequency. In practice, the perturbation term is sufficiently small with a sufficiently high sampling frequency such that it can be neglected from (4.14). Besides, a simple proportional controller is generally chosen for the pseudo control \mathbf{v} , as the system is linearized as a single integrator. Fig. 4.3 gives the general structure of the INDI controller, where e^{-sT_s} denotes the transport delay in a single sample time T_s . When model uncertainties exist for \mathbf{G} , the estimated value $\hat{\mathbf{G}}$ is used for the controller.

Note that in the INDI control law (4.12), the information of $\dot{\mathbf{x}}_0$ is assumed to be obtained by reliable sensor measurements and updated in every sampling period. Consider the system dynamics in (4.10), by reducing the sampling time, the contribution of the perturbation term to the system dynamics is reduced to be significantly less than the rest nominal part that contains $\dot{\mathbf{x}}_0$. This does imply that INDI is dependent on an accurate measurement.

4.3.2. ROBUSTNESS TO PARAMETER UNCERTAINTY AND DISTURBANCE

Considering the general system given by (4.6), INDI is inherently insensitive to parameter uncertainty in $\mathbf{f}(\mathbf{x})$ and continuous disturbances \mathbf{d} . This is because information of these quantities is not explicitly used in the INDI control law in (4.12), and the contribution of these two terms to the system dynamics only appear in the perturbation term which, will only influence the ultimate bound of the error dynamics and can be reduced to be negligible by increasing the sampling rate.

It is observed in various applications that INDI is also insensitive to parameter uncertainty in the matrix $\mathbf{G}(\mathbf{x})$ in (4.6), with according proofs[27, 28]. However, all these proofs are based on the assumption that $\dot{\mathbf{x}} = \dot{\mathbf{x}}_0$ with small time increment. This assumption requires the continuity of $\dot{\mathbf{x}}$, which conflicts with the basic assumption of the INDI that the system input \mathbf{u} , and consequently the state derivative $\dot{\mathbf{x}}$, are not necessarily continuous. In this section, it is rigorously proven that INDI is insensitive to parameter uncertainty in $\mathbf{G}(\mathbf{x})$ without requiring the continuity of $\dot{\mathbf{x}}$.

First consider a SISO system for which \mathbf{G} is a scalar. In Fig. 4.3, with the assumption of high sampling rate, the system dynamics of \mathbf{G} is regarded as a slowly varying gain of a input-linear system. $\mathbf{f}(\mathbf{x}) + \mathbf{d}$ is regarded as a lumped disturbance term, i.e., $\mathbf{D} = \mathbf{f}(\mathbf{x}) + \mathbf{d}$, the increment of which in one sampling period is δ in (4.11). When the estimated $\hat{\mathbf{G}}$ is used for the controller, the transfer function from $\mathbf{v}(s)$ to $\dot{\mathbf{x}}(s)$ can be easily calculated as

$$\begin{aligned} H(s) &= \frac{\dot{\mathbf{x}}(s)}{\mathbf{v}(s)} = \frac{\mathbf{G}\hat{\mathbf{G}}^{-1}}{1 + (\mathbf{G}\hat{\mathbf{G}}^{-1} - 1)e^{-sT_s}} \\ &= \frac{1}{\alpha + (1 - \alpha)e^{-sT_s}}, \end{aligned} \quad (4.16)$$

where $\alpha = \hat{\mathbf{G}}\mathbf{G}^{-1}$ indicates the level of model mismatch.

Replacing e^{-sT_s} in (4.16) by z^{-1} , the stability condition of the equivalent z domain transfer function is that the poles are located inside the unit circle, which requires that $\alpha > 0.5$. Consider the frequency response of $H(j\omega)$, it can be proved that if $\alpha > 0.5$, the real part of $H(j\omega)$ is always positive for any ω , thus the phase angle of $H(j\omega)$ satisfy

$$-0.5\pi < \angle H(s) < 0.5\pi, \text{ if } \alpha > 0.5. \quad (4.17)$$

According to the final value theorem, the step response of $H(s)$ is $\lim_{s \rightarrow \infty} H(s) = 1$. This means that if only the estimated $\hat{\mathbf{G}}$ is bigger than half of the real \mathbf{G} ($\alpha > 0.5$), $\dot{\mathbf{x}}$ will converge to \mathbf{v} . Thus the model uncertainty in $\hat{\mathbf{G}}$ introduces dynamics, instead of a disturbance, to the linearized single integrator $\mathbf{v} = \dot{\mathbf{x}}$. The speed of the dynamics would increase when the sample time T_s decreases. In fact, (4.16) shows that $H(s)$ is equal to 1 when T_s approaches zero. This proves why the INDI controller is robust to model uncertainty in \mathbf{G} .

The robustness of INDI against uncertainty in $\mathbf{f}(\mathbf{x})$ and \mathbf{d} has been explained in the time domain, but can be further verified by calculating the closed-loop transfer function from the lumped disturbance $\mathbf{D} = \mathbf{f}(\mathbf{x}) + \mathbf{d}$ to $\dot{\mathbf{x}}$, which is

$$\frac{\dot{\mathbf{x}}(s)}{\mathbf{D}(s)} = \frac{1 - e^{-sT_s}}{1 - e^{-sT_s} + \mathbf{G}\hat{\mathbf{G}}^{-1}e^{-sT_s}}. \quad (4.18)$$

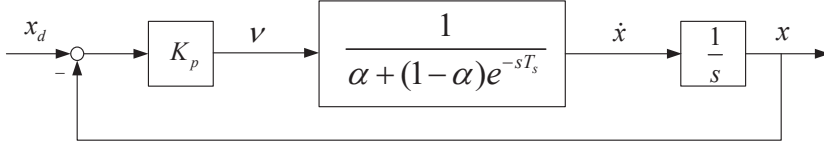


Figure 4.4: The transfer function of the controlled system

When the controller sampling rate is sufficiently high, the magnitude of (4.18) approaches 0 as T_s approaches 0. This is consistent with the fact that δ becomes negligible when T_s is small. Besides, even without this assumption, according to the final value theorem, the step response of (4.18) converges to 0. This means that the lumped disturbance term $\mathbf{D} = \mathbf{f}(\mathbf{x}) + \mathbf{d}$ is inherently rejected over time, and its influence is further attenuated with a small sampling period.

The transfer function of the controlled system is thus given in Fig. 4.4. The open-loop transfer function is

$$P(s) = \frac{K_p}{s(\alpha + (1-\alpha)e^{-sT_s})}. \quad (4.19)$$

According to (4.16) and (4.17), if $\alpha > 0.5$, $P(s)$ is stable and its phase angle satisfy $-\pi < \angle P(j\omega) < 0$ because $\angle P(j\omega) = -0.5\pi + \angle H(j\omega)$. This means the Nyquist plot of $\angle P(j\omega)$ will stay below (and never intersect with) the real axis. This first means that the open-loop Nyquist plot will never encircle the $-1+i0$ point (which guarantees the stability of the closed-loop system). Second, as the Nyquist plot of $\angle P(j\omega)$ will always intersect with the unit circle below the real axis, the controlled system always has positive phase margin and infinite gain margin in the presence of model uncertainty. Note that the validity of (4.16) to (4.19) relies on the linearization of the system within a single sampling period in (4.10), which requires a fast sampling rate.

This proves the robustness of INDI for SISO systems with a single necessary condition $\widehat{\mathbf{G}}\mathbf{G}^{-1} > 0.5$, which will be validated with experiments in Section 4.6. It can be extend to MIMO systems with the following lemma.

Lemma 2: If the square matrix $\widehat{\mathbf{G}}\mathbf{G}^{-1}$ is diagonalizable and all its eigenvalues are real and bigger than 0.5, then the nominal part of (4.10) can still be exactly linearised to be $\dot{\mathbf{x}} = \mathbf{v}$, given the control law in (4.12) with estimated control effectiveness matrix $\widehat{\mathbf{G}}$, with an infinitesimal sample time T_s .

Proof: The INDI control law with parameter uncertainty in $\widehat{\mathbf{G}}(\mathbf{x})$ is given by

$$\mathbf{u} = \mathbf{u}_0 + \widehat{\mathbf{G}}^{-1}(\mathbf{x}_0)(\mathbf{v} - \dot{\mathbf{x}}_0), \quad (4.20)$$

thus the nominal dynamics of (4.10) become

$$\dot{\mathbf{x}} = \dot{\mathbf{x}}_0 + \mathbf{G}\widehat{\mathbf{G}}^{-1}(\mathbf{v} - \dot{\mathbf{x}}_0). \quad (4.21)$$

Considering (4.21) as a linear system with slowly changing gain $\mathbf{G}\widehat{\mathbf{G}}^{-1}$ (as the sampling rate is high), and describing it in terms of samples instead of signals, we obtain

$$\dot{\mathbf{x}}_{(k)} = \dot{\mathbf{x}}_{(k-1)} + \mathbf{G}\widehat{\mathbf{G}}^{-1}(\mathbf{v}_{(k)} - \dot{\mathbf{x}}_{(k-1)}), \quad (4.22)$$

which is identical to

$$\widehat{\mathbf{G}}\mathbf{G}^{-1}\dot{\mathbf{x}}_{(k)} = (\widehat{\mathbf{G}}\mathbf{G}^{-1} - \mathbf{I})\dot{\mathbf{x}}_{(k-1)} + \mathbf{v}_{(k)}. \quad (4.23)$$

Consider the eigenvalue decomposition of the matrix $\widehat{\mathbf{G}}\mathbf{G}^{-1}$

$$\widehat{\mathbf{G}}\mathbf{G}^{-1} = \mathbf{M}\mathbf{\Lambda}\mathbf{M}^{-1}, \quad (4.24)$$

and the state variable transformation

$$\dot{\boldsymbol{\chi}} = \mathbf{M}^{-1}\dot{\mathbf{x}}, \mathbf{v} = \mathbf{M}^{-1}\mathbf{v}, \quad (4.25)$$

then (4.23) is transformed to diagonal form:

$$\mathbf{\Lambda}\dot{\boldsymbol{\chi}}_{(k)} = (\mathbf{\Lambda} - \mathbf{I})\dot{\boldsymbol{\chi}}_{(k-1)} + \mathbf{v}_{(k)}, \quad (4.26)$$

the system is transformed into n decoupled scalar equations:

$$\lambda_i \dot{\chi}_{i(k)} = (\lambda_i - 1) \dot{\chi}_{i(k-1)} + v_{i(k)}. \quad (4.27)$$

Taking the z -transform to the above equations, the transfer function between the transformed pseudo control inputs and system state derivatives is calculated as:

$$H_i(z) = \frac{\dot{\chi}_i(z)}{\mathbf{v}_i(z)} = \frac{1}{\lambda_i + (1 - \lambda_i)z^{-1}}, \quad (4.28)$$

which turns out to be a discrete filter that has a stable pole inside the unit circle when $\lambda_i > 0.5$. When the sample time T_s is infinitesimal, the normalized frequency $\omega = fT_s$ approaches zero, thus the frequency response of $H_i(z)$ is

$$\lim_{T_s \rightarrow 0} H_i(e^{jfT_s}) = \frac{1}{\lambda_i + (1 - \lambda_i)} = 1, \quad (4.29)$$

Combining this result with (4.25), we obtain $\dot{\mathbf{x}} = \mathbf{v}$. □

Lemma 2 shows that (4.14) still holds with parameter uncertainty in $\mathbf{G}(\mathbf{x})$ for a high sampling rate. The uncertainty adds dynamics in the form of a stable discrete filter in (4.28) for the linearized nominal system, instead of disabling it as in the case of traditional feedback linearization.

In practice the controller sampling rate for INDI is chosen to be sufficiently higher than that of the trajectory signal, which validates the assumption of an infinitesimal normalized frequency. Lemma 2 also gives the tolerance of the INDI to the model mismatch of $\mathbf{G}(\mathbf{x})$, as a condition for (4.28) to be stable.

In conclusion, INDI is a practical nonlinear control technique for overcoming the sensitivity to parameter uncertainties and continuous disturbances of traditional feedback linearization methods.

The proposed INDI controller is similar in form to the well-known Time-Delay-Control (TDC) technique [38], which also introduced an incremental form of the control law. However, both have totally different theoretical bases. Consequently, different approaches are used to prove stability and robustness. Besides these differences, the application of this incremental form of control law on hydraulic force control problems has so far not been reported.

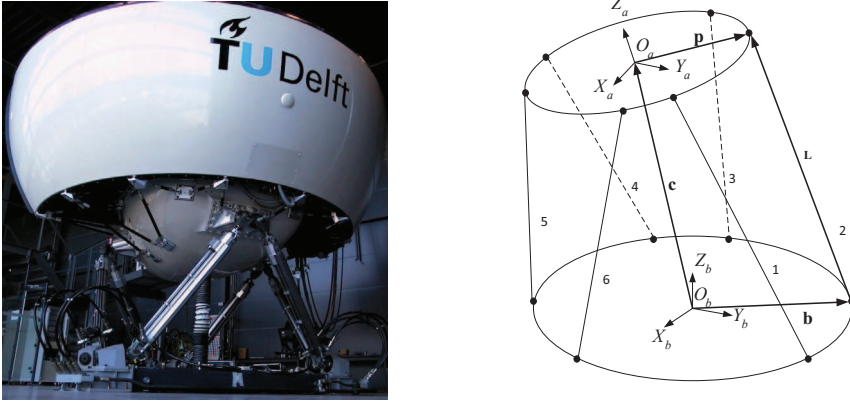


Figure 4.5: A hexapod motion system SRS at TU Delft (left), and its schematic drawing (right) [1]

4.4. CONTROLLER DESIGN

This section addresses the design of the INDI-based hydraulic actuator force controller for the SRS, a 6-DOF hydraulic parallel robot, which is illustrated in Fig. 4.5. Implementation issues such as valve dynamics and oil pipeline dynamics are discussed. As a baseline controller to be compared with, a traditional NDI-based force controller is briefly introduced. A force computation outer-loop motion controller is combined with the proposed inner-loop controller to close the loop of the complete motion control system, as proposed in Fig. 4.1. Note that the proposed approach can be applied to more general outer-loop controllers.

4

4.4.1. INNER-LOOP INDI HYDRAULIC FORCE CONTROLLER

The hydraulic actuator dynamics given by (4.5) are a first-order system with a relative degree of 1 if we choose the state P_L as the output. The control effectiveness matrix \mathbf{G} is G_A in this case, which is a scalar and it is not equal to zero except in the case of load saturation. In practice, a small constant is chosen for G_A in the controller when it is smaller than a particular value, in order to avoid singularity. By choosing a high-bandwidth servo-valve, the valve dynamics bandwidth is well above that of the rest of the system (the bandwidth of the servo-valve is around 150Hz for the SRS) [39]. As pressure sensors are commonly used in the hydraulic actuators, the state measurement is generally available. Thus, all assumptions and conditions for INDI are fulfilled for the studied hydraulic system.

Consider the hydraulic pressure dynamics in (4.5), the actuator velocity term $2C_m A_p \dot{q}$ exists as an interaction from the platform dynamics. It is considered as a continuous disturbance to the local pressure dynamics. Following the procedure of the INDI methodology from (4.8) to (4.14), the incremental form pressure dynamics are written as

$$\dot{P}_L = \dot{P}_{L0} + G_A (u - u_0) + \delta(\Delta \dot{q}, \Delta P_s), \quad (4.30)$$

where

$$G_A = 2C_m(q_0)\Phi_n\sqrt{1 - \text{sgn}(x_{m0})\frac{P_{L0}}{P_s}}. \quad (4.31)$$

Linearizing the nominal part of (4.30), the INDI control law is given by [1]

$$u = u_0 + G_A^{-1}(v - \dot{P}_{L0}), \quad (4.32)$$

and the linear relation between v and \dot{P}_L is achieved in existence of the perturbation term:

$$\dot{P}_L = v + \delta(\Delta\dot{q}, \Delta P_s). \quad (4.33)$$

By choosing a sufficiently high controller sampling rate, the magnitude of the perturbation is reduced to be negligible. A simple linear controller can be chosen for v , turning the hydraulic system into a force generator:

$$\dot{P}_L = v = K_p(F_{ref}/A_p - P_L), \quad (4.34)$$

where F_{ref} is the desired actuation force.

From a controller design perspective, the INDI approach is straightforwardly implementable for control applications in industry, and the stability and robustness against uncertainties are guaranteed by Lemma 1 and Lemma 2. The effectiveness of the proposed controller is verified in simulation work in [1]. However, some implementation issues are met in real-world application for the SRS. It will be shown below that they can be solved with simple techniques integrated in the framework of the INDI method.

4.4.2. SOLVING IMPLEMENTATION ISSUES

NUMERICAL DIFFERENTIATION

The derivative of the current actuator pressure difference \dot{P}_{L0} is required by the INDI control law in (4.32), which is typically not directly available as measurement. In practice it is obtained by numerical differentiation of the measurement of the pressure sensor available on most hydraulic actuators. The noises amplified by numerical differentiation are attenuated by a typical low-pass filter [29]. As will be discussed later in this section, the filter has a second function to attenuate the oil pipeline dynamics, thus the corresponding solution for the common issue of the introduced phase lag will be discussed in detail there.

In addition to the practical low-pass filter, more advanced differentiation methods such as Kalman filters or Savitzky–Golay filters [40] can be considered to deal with the noise. Note, however, that for applications to other systems, the state derivatives may be directly measured. For instance, the angular acceleration of an aircraft or robotic systems can be measured with angular accelerometers.

VALVE DYNAMICS

The theoretical INDI control law given by (4.32) is in the form of the accumulation of the control increments calculated in each time step. This requires the assumption of infinitely fast actuator dynamics, which in the hydraulic system applies to the servo-valve dynamics. In practice, the finite actuator bandwidth may cause stability problems

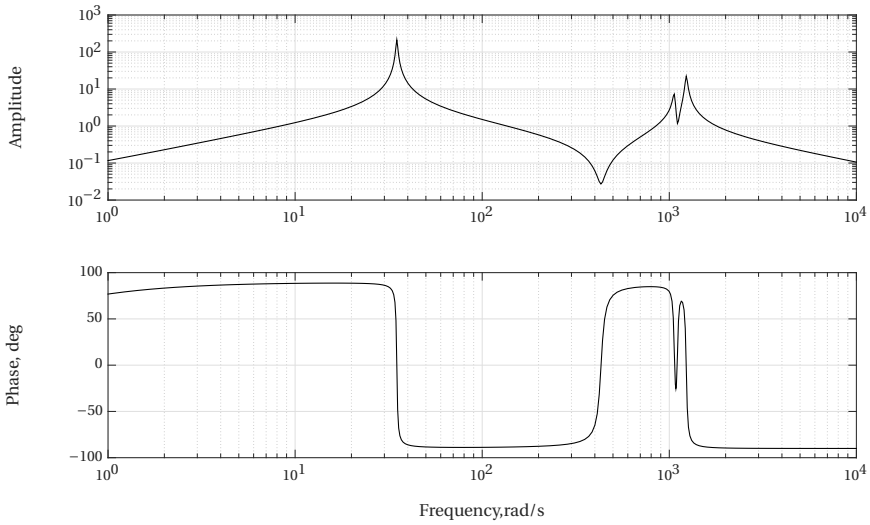


Figure 4.6: Bode plot of hydraulically driven mechanical system model including transmission lines. Input valve displacement x_m , output hydraulic load pressure difference P_L

4

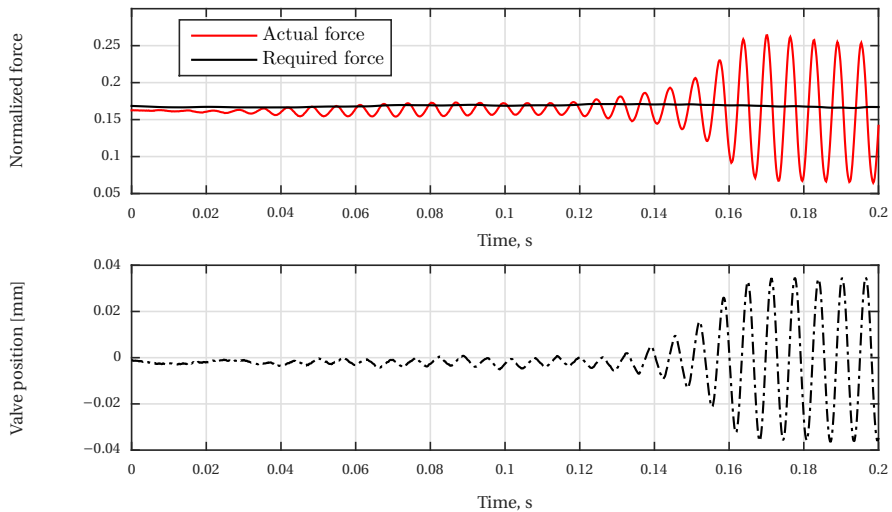


Figure 4.7: High frequency oscillation of load pressure and valve due to the resonance frequencies of transmission lines.

[29], even if it is sufficiently higher than that of the rest of the system. Thus in real-world applications, the real-time measurement of the hydraulic servo-valve spool position is used for u_0 in (4.32) (as shown in Fig. 4.8), instead of the theoretical memory of the accumulated control input. It will be shown in (4.35) that by doing this, with stable servo-valve dynamics, the system stability will not be influenced.

TRANSMISSION LINE DYNAMICS

For hydraulic applications such as flight simulators, the relatively large operational space asks for long-stroke actuators, which inherently introduce high-frequency transmission dynamics of the relatively long oil pipelines between the valve and the actuator, as shown in Fig. 4.2. The modeling of these transmission dynamics was extensively studied in literature [41]. In [42], the so-called "model approximation technique" is adopted to describe the transmission dynamics by an infinite product series of second order models, each of which gives rise to a resonance mode. In the case of the SRS, with the pipelines of around 1.2 meters, a linearized model analysis shows resonance frequencies at 200, 600, 1000 Hz and higher [42]. Given a digital controller at 5000 Hz and valve bandwidth up to about 150 Hz, the first mode is relevant for controller design and analysis.

Fig. 4.6 shows the Bode plots from the input x_m to the output P_L of a hydraulic actuator model including the transmission lines. The eigenfrequencies of the two transmission lines at around 200 Hz combined with the 180° phase lag brought on by the valve dynamics cause stability problems by pressure feedback [39, 42]. In early experiments without consideration of the transmission effects, a heavy self-sustaining oscillation at about 200 Hz occurred for the proposed controller, as shown in Fig. 4.7.

The easiest way to solve this problem is to add a second-order low-pass filter $H_t(z)$ in the pressure feedback loop before the differentiator (see Fig. 4.8), in order to attenuate the resonance peaks and shift the crossover frequency. In practice, a filter with a 35 Hz natural frequency is used for the SRS, with a balance of stability and performance based on trial and error experiments. As discussed before, $H_t(z)$ plays another role in smoothing the P_L measurement, thereby avoiding the amplification of the measurement noise by the numerical differentiation.

As a result, the filtered pressure measurement \dot{P}_{Lf} , instead of the real value \dot{P}_{L0} , is used for feedback. Extra dynamics are thus introduced to the loop and the phase lag introduced by $H_t(z)$ will degrade the control performance [27]. In this study, the technique proposed in literature [29] is adopted, where $H_t(z)$ is also added in the valve spool position measurement loop, as shown in Fig. 4.8. It will be shown in (4.35) that with this compensation, the influence of the additional dynamics is canceled from the system dynamics. We emphasize here that the synchronization of the filters in both loops is an important practical solution for dealing with the phase lag introduced by state derivative estimation.

Taking these issues into consideration, the INDI force controller implemented in reality is illustrated in Fig. 4.8 with a z -domain block diagram representation, where $V(z)$ denotes the valve dynamics and the subscript f denotes the filtered signals. The system dynamics in the dotted line box is based on the incremental form of system dynamics given in (4.30). The controller follows the framework proposed in previous theoretical work [1].

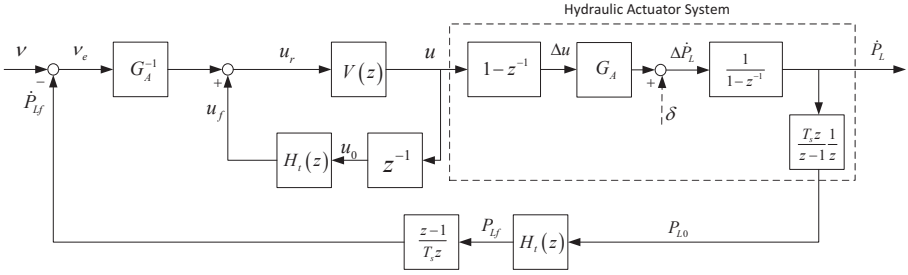


Figure 4.8: Practical INDI control scheme for inner-loop hydraulic actuator force tracking.

The strategies introduced in this section can be easily verified by calculating the closed-loop transfer function from v to \dot{P}_L :

$$\begin{aligned} \frac{\dot{P}_L(z)}{v(z)} &= \frac{V(z)(1 - V(z)H_t(z)z^{-1})^{-1}}{1 + V(z)(1 - V(z)H_t(z)z^{-1})^{-1}H_t(z)z^{-1}} \\ &= \frac{V(z)}{1 - V(z)H_t(z)z^{-1} + V(z)H_t(z)z^{-1}} \\ &= V(z). \end{aligned} \quad (4.35)$$

The valve dynamics $V(z)$ show up in the controlled system transfer function, instead of a single integrator in (4.34). (4.35) suggests that by using the servo-valve output measurement as feedback, system stability is not influenced with the stable servo-valve dynamics. With this measurement, the valve dynamics are considered in the control system, while a precise model is not necessary. It is also verified that the introduction of the filter $H_t(z)$ in the control input memory loop canceled its influence on the measurement feedback loop. With this simple relation, the proportional controller of (4.34) is still sufficient to stabilize the system. The use of input measurement feedback and the compensation filter in that loop to deal with unmodeled dynamics are the main features of the practical INDI technique.

4.4.3. INNER-LOOP NDI BASED FORCE CONTROLLER

NDI is a more traditional nonlinear control strategy as an example of feedback linearization. A direct application can be made to the hydraulic pressure dynamic equation given in (4.5) by simply inverting it as follows:

$$u = G_A^{-1}(P_L, x_m, q)(v - f_A(P_L, q, \dot{q})), \quad (4.36)$$

and the pressure dynamics become $\dot{P}_L = v$, which allows for a simple linear controller for v . This strategy is adopted in various applications [5, 43]. Variants of NDI are also called "cascade ΔP " (CdP) or "cascade" control for some hydraulic control applications [18, 44, 45], which have also been adopted for the SRS [39]. Such NDI-based controllers rely on an accurate model and it will be shown that the performance is significantly degraded when parameter mismatches exist.

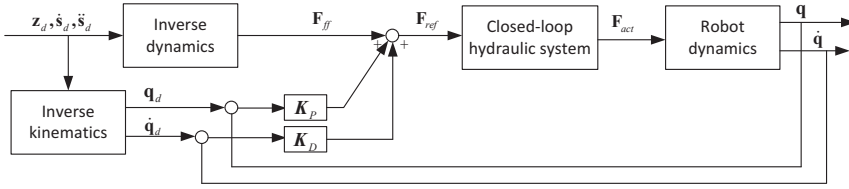


Figure 4.9: Outer-loop feedforward controller with PD feedback for the SRS

4.4.4. OUTER-LOOP MOTION CONTROLLER

As in this study we focus on the novelty of the inner-loop INDI force controller, a widely applied model-based feedforward control approach [8] is used for the outer-loop controller, as illustrated by Fig. 4.9. A feedforward force F_{ff} is calculated by the inverse dynamics of the hexapod and added to the PD feedback terms in the actuation space, before it is sent to the closed-loop hydraulic subsystem. The outer-loop control law is given by:

$$F_{ref} = F_{ff} + K_P (q_d - q) + K_D (\dot{q}_d - \dot{q}). \quad (4.37)$$

4.5. SIMULATION RESULTS

The INDI force controller developed in Section 4.4, as well as the NDI based CdP baseline controller will next be used for motion control of a complete hydraulic hexapod simulation model, cooperating with the aforementioned outer-loop motion controller in a cascaded structure. Performance and robustness of both control schemes are investigated through simulations. A well-validated and fully nonlinear simulation model of a hydraulic hexapod system [32, 42] is used for the simulations. The model is tuned with parameters representative for the SRS. For the simulation model, valve dynamics, hydraulic actuator dynamics and Stewart platform dynamics are modeled by physical laws and connected, with model uncertainties considered such as the valve opening manufacturing error. For details of the model, the readers are referred to [32].

The motion profile of a recent experiment [46] performed on the SRS is chosen as the reference trajectory of the motion system, in which the upper platform periodically move on a circular path in the horizontal plane with a radius of 0.5 meters and a period of five seconds after a brief lead-in period. With this motion profile, most DOFs of the hexapod system and a wide range of hydraulic actuator stroke are used, thus the nonlinear dynamics of both subsystems are well excited. Experiment data for pressure measurements at a stationary neutral position are used to estimate the pressure sensor noise level, which is used to set realistic sensor noise in the pressure feedback loops in the simulation model. As a consequence, a zero mean Gaussian noise ω is applied to the normalized pressure difference \bar{P}_L (P_L normalized by P_s), with a nominal variance of $\delta_{\omega_n}^2 = 1 \times 10^{-7}$.

For all the simulations, the system dynamics are updated at 5000 Hz. The inner-

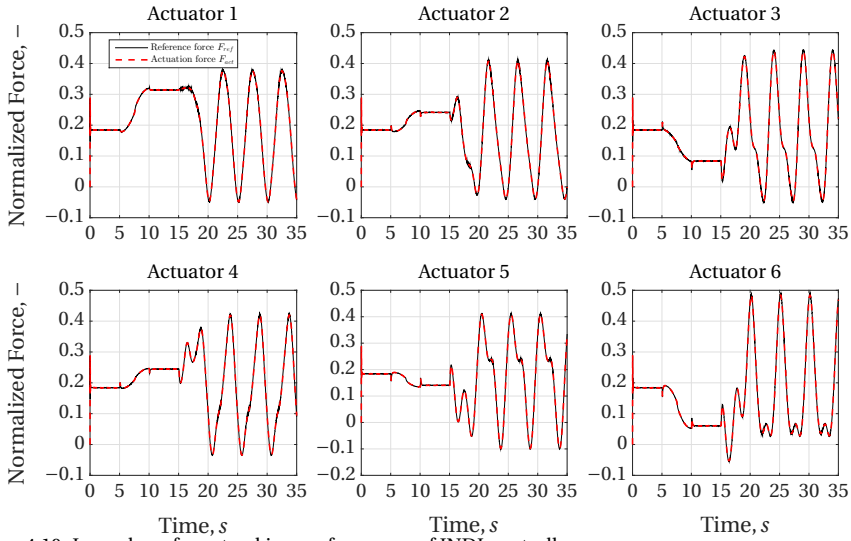


Figure 4.10: Inner-loop force tracking performance of INDI controller

loop controllers are sampled at 5000 Hz (unless otherwise stated) and nominal oil supply pressure is set to 160 bar, which are the same as the SRS. The linear gains of the outer-loop controller are set to be $\mathbf{K}_P = 8 \times 10^5 \mathbf{I}$ and $\mathbf{K}_D = 10^5 \mathbf{I}$. In the real CdP control system of the SRS, the theoretical control law given by Eq. (4.36) is modified. Due to practical limitations, the reference actuator velocity \dot{q}_d is used instead of a true measurement of \dot{q} in order to reduce noise, and the derivative gain is tuned to 3×10^3 .

4

4.5.1. PERFORMANCE UNDER NOMINAL CONDITIONS

The control performance of the INDI approach and the CdP controller under nominal conditions is compared, using the nominal hydraulic model parameters in Eq. (4.5). Fig. 4.10 and Fig. 4.11 present the force/pressure tracking performance of each actuator controlled by the two discussed controllers. The solid lines denote the force references and the dashed lines are the actuation force outputs, both of which are normalized by $A_p P_s$. The maneuver starts from 15 s after a lead-in period, during which the platform moves from the neutral position to the initial position from 5 s to 10 s. A relatively wide range of actuation force is exploited by the maneuver as the pressure differences reach up to half of the maximum supply value.

It is shown that the performance of the INDI is ideal and that the reference pressure difference is perfectly tracked. The influence of noise is reduced by the filters introduced in all feedback loops. As shown in Fig. 4.11, the performance of the CdP controller is satisfactory, while obviously inferior to that of the INDI controller. The average root-mean-squared force tracking error is 0.017, much larger than the 0.0035 of the INDI controller. The relatively high deviation for the CdP controller are caused by the fact that in order to get an expression for the hydraulic pressure dynamics in Eq. (4.5), some small terms are neglected and some assumptions regarding the leakage and valve opening gaps are made compared with the physical model of valve given in Chapter 3, which means that

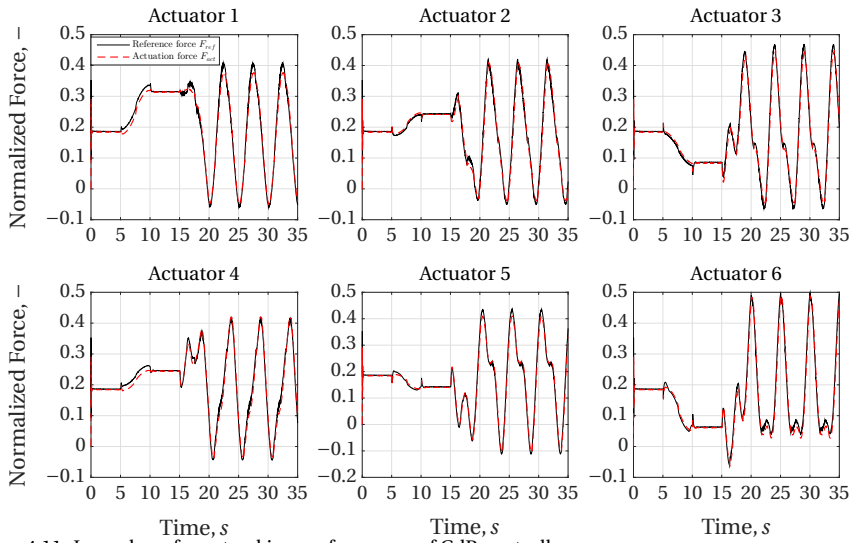


Figure 4.11: Inner-loop force tracking performance of CdP controller

a certain degree of unmodeled dynamics exist in Eq. (4.5). Hence, even when nominal parameters are used, the NDI portion of the CdP controller does not exactly invert the system dynamics and the performance is degraded.

From another point of view, in existence of unmodeled dynamics, the performance of the INDI controller is not affected. Thus, the robustness of the INDI controller to model uncertainties is already illustrated in this nominal condition simulation.

Fig. 4.12 shows the simulated force error and position error for actuator 1 with both controllers. The force tracking error of the CdP controller increases dramatically when the system is in motion, as the nonlinear dynamics are then excited, while the performance attained with the INDI is hardly affected. It can be seen that with exactly the same outer-loop controller, the improved inner-loop force controller greatly contributes to the overall control performance.

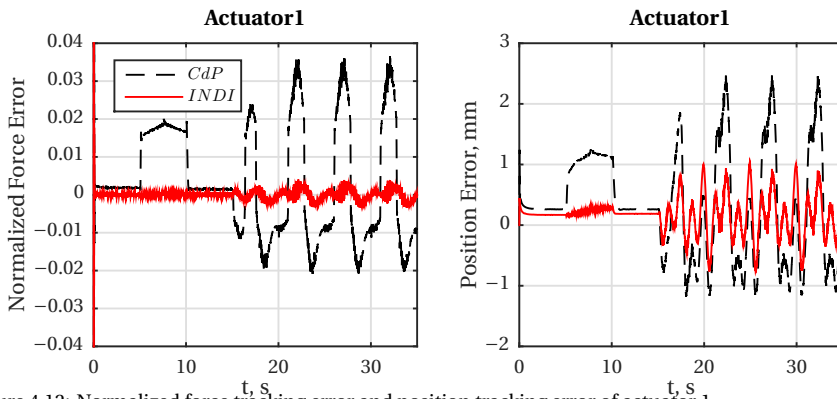


Figure 4.12: Normalized force tracking error and position tracking error of actuator 1

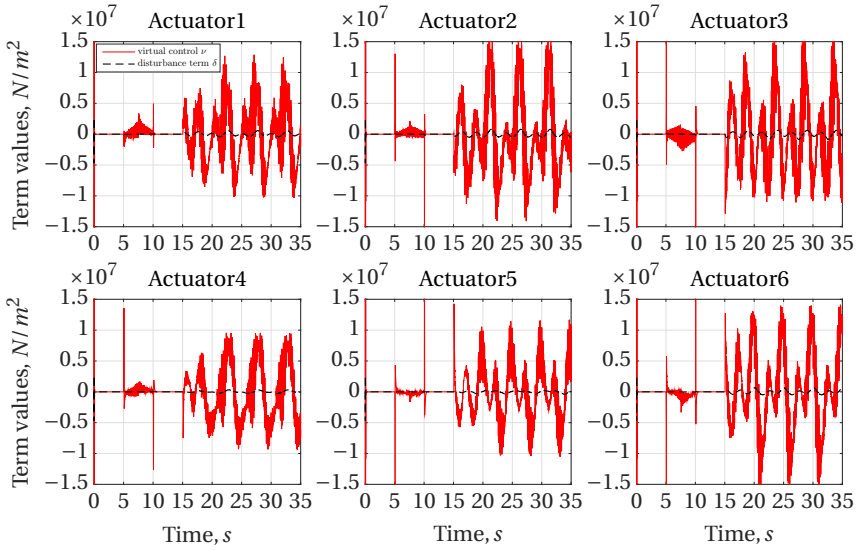


Figure 4.13: Value comparison of virtual control v and disturbance δ terms in Eq. (4.33)

4.5.2. INDI ASSUMPTION VALIDATION

As concluded in Section 4.3, a sufficient sampling rate and reliable sensor measurements are the key assumptions of the INDI controller design. These assumptions are validated in this section.

4

THE SMALLNESS OF THE DEFINED PERTURBATION δ

The assumption of high sampling rate is used multiple times in the INDI controller design, based on which the defined perturbation term δ is bounded by a designed small value in Eq. (4.15). From a practical point of view, the sampling rate of the controller should be chosen fast enough such in Eq. (4.33), the perturbation δ is decreased to be negligible compared with the virtual control v . This guarantees the validity of the linear relation and the robustness of INDI. In this section, the validity of this assumption is studied numerically under a practical controller sampling rate of 5000 Hz. Basically the same simulation as the previous section under the nominal conditions is implemented, during which the terms in (4.33) are calculated and compared. The only difference is in this simulation, without loss of generality, the sensor noise is eliminated in order to make the results readable.

In Fig. 4.13, the values of the virtual control v and disturbance term δ of Eq. (4.33) are compared. The average RMS of the value of v is $1.1 \times 10^7 \text{ N/m}^2$, which is more than one order of magnitude larger than that of the disturbance term d , which is $2.2 \times 10^5 \text{ N/m}^2$. It is hence validated that with the studied sampling rate, the effect of smallness of δ applies and Eq. (4.34) holds. Thus in the next section, the 5000 Hz sampling rate will be used in the real-world experiments. It is noted that despite being inherently rejected by INDI in Eq. (4.33), the effect of δ will be further attenuated by the outer-loop linear controller with properly designed gains.

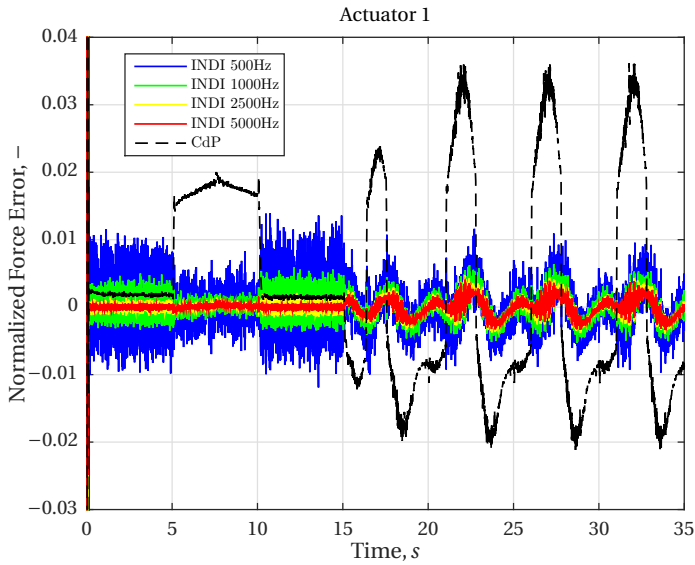


Figure 4.14: Force tracking errors of the CdP the INDI at different sampling rates

LOWER SAMPLING RATE

The previous simulations are executed with a 5000 Hz control sampling rate, which is the same as the actual sampling rate of the CdP controller on the SRS. The motion control computer (MCC) of the SRS featured a 1GHz PowerPC 750GX processor for the motion control. Compared with the CdP control law given in Eq. (4.36), the computational cost of the INDI control law in Eq. (4.12) is even smaller, which makes the discussed 5000 Hz practical for the new controller on the SRS as well as other hydraulic hexapod systems with a decent modern computer. However, it is still of concern how a lower frequency will affect the control performance of the INDI. Simulations with nominal parameters for the INDI at different frequencies are executed and the force tracking error of one of the actuators are presented in Fig. 4.14. As a comparison, the tracking error of the CdP controller is also included. When the sampling rate is reduced to 2500 Hz, the control performance of the INDI is just slightly influenced and is still much better than that of the CdP. When the frequency is reduced to 1000 Hz and 500 Hz, obvious oscillations are observed when the actuator is in the stationary position, however, the tracking performances are just slightly influenced when the actuator is in motion and remain superior to the CdP. It is noted that much more severe oscillation phenomenon is observed when the actuator is controlled to be static than it is in the maneuver. This is explained by the fact that in the model of hydraulic actuator given by Eq. (4.5), based on which the INDI control law is derived, the sign function and square root of valve spool displacement x_m are present. Thus the hydraulic subsystem is highly nonlinear near the zero valve opening situation where the velocity of the actuator is around zero. Thus as an incremental control strategy, the INDI suffers the most when the actuator is stationary. The INDI controller provides decent motion performance even at 500 Hz, however, the

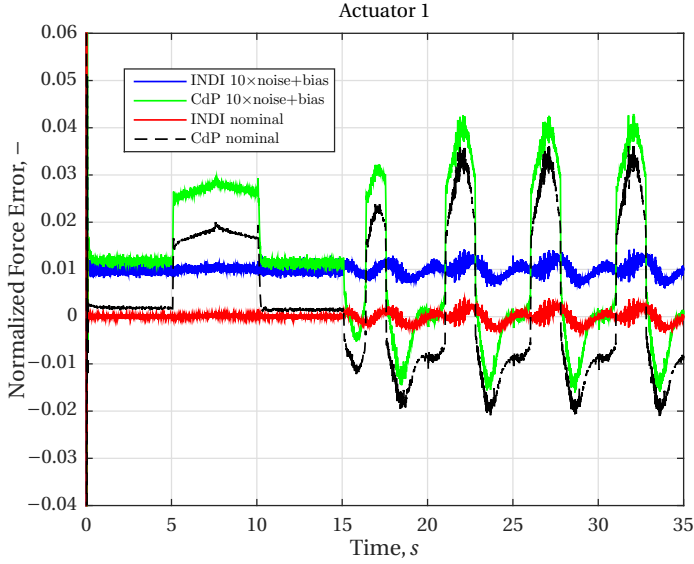


Figure 4.15: Force tracking errors of the CdP the INDI at different pressure sensor measurement noise levels

higher sampling rate is suggested for static position control.

HIGHER NOISE LEVEL

As discussed in Section 4.3, the INDI approach is sensitive to sensor measurement quality, thus the influence of aggressive pressure sensor noise and bias on the control system is of concern. Fig. 4.15 presents the force tracking errors of the INDI and the CdP for actuator 1 with a Gaussian noise of the nominal pressure difference measurement, of which the variance is 10 times of the nominal value $\delta_{\omega_n}^2$ and the constant bias is set to 0.01. The results of the nominal condition are also presented as a comparison. For both controllers, the higher noise level causes more serious oscillation behaviors. The influence of bias on the INDI control error is a linear shift along the vertical axis. This can be easily explained that the bias is equivalent to a constant disturbance in the virtual control term in Eq. (4.34), meanwhile the linearized relation in Eq. (4.34) is verified. A similar phenomenon is observed for the CdP controller, although the error shift during the maneuver is not constant, as the CdP controller does not fully linearize the hydraulic system. Overall the INDI suffers more from sensor noise since numerical differentiation of the measurement is needed, however, with the help of the designed low pass filter, decent force tracking is achieved even when a noise with 10 times variance level over the realistic one is applied.

The control inputs of both controllers to the valve with the same setting are shown in Fig. 4.16. The control input of the INDI controller is significantly more noisy than that of the CdP controller, and is more sensitive to increased noise level. This is reasonable, since INDI directly uses the numerical differentiation of the filtered pressure measurement at 5000 Hz sampling rate. However, as the servo valve itself acts as a low-pass filter,

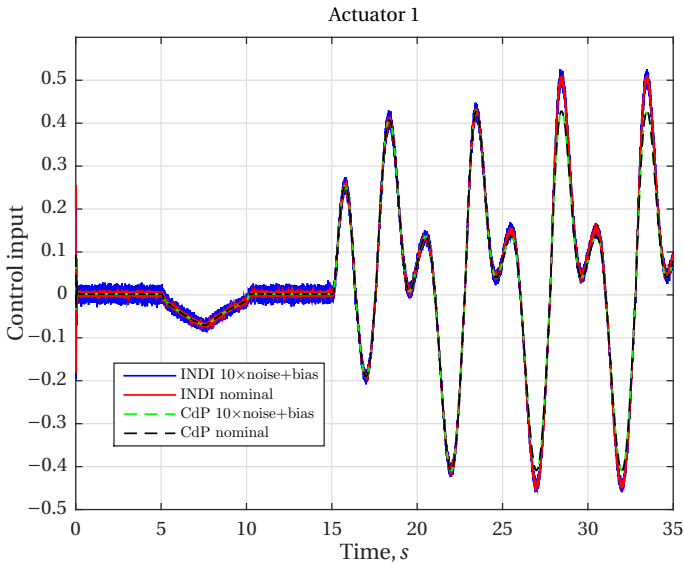


Figure 4.16: Control inputs of the CdP the INDI at different pressure sensor measurement noise levels

the resulting control input is smoothed and the the effects of the noise do not affect the final performance.

4.5.3. ROBUSTNESS TO HYDRAULIC PARAMETER UNCERTAINTIES

The parameter uncertainties of the studied integrated system come from both the hydraulic system and the parallel manipulator. As in this study the proposed INDI control technique is only applied to the inner-loop hydraulic force tracking control, we focus on discussing the robustness of the INDI to hydraulic parameter uncertainties. The robustness performance of the CdP and the INDI control systems are investigated by varying the concerned parameter mismatch level while tracking the same motion profile.

HYDRAULIC VALVE FLOW

One of the most important parameters in Eq. (4.5) is the nominal valve flow Φ_n , for which an accurate value is difficult to estimate due to valve spool gaps, opening overlaps and manufacturing tolerances. Thus the robustness of the force controller against parameter uncertainties is critical. Motion control of the CdP controller and the INDI controller are simulated, with different levels of parameter mismatch in terms of Φ_n added to each actuator, from 50% to 10%. In Fig. 4.17 the force control errors of Actuator 1 are presented. It is clear that the CdP controller is very sensitive to the uncertainty that with a mismatch greater than 30%, the force control error is significant. For reference, the real-world force tracking error of Actuator 1 on the SRS is also shown in Fig. 4.17, which fit in the gap between the simulated CdP control errors with 50% and 30% parameter mismatch. This result indicates that we have a certain degree of overestimation of Φ_n in the real-world implementation and at the same time, our simulation model is validated. Fortunately,

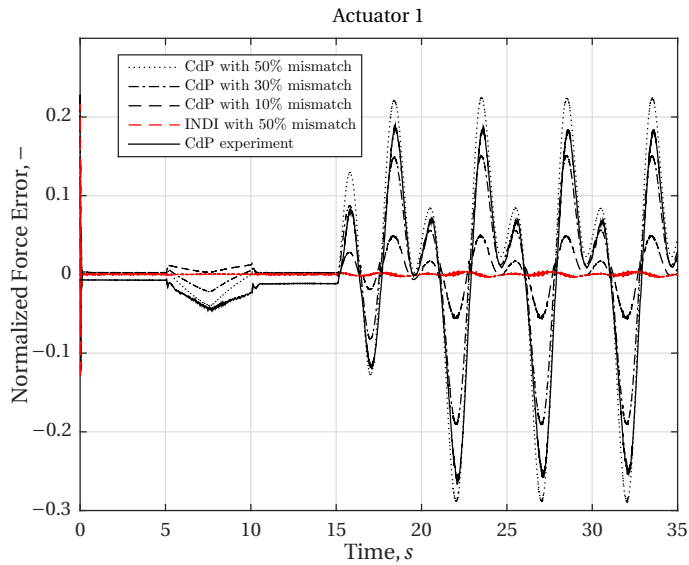


Figure 4.17: Inner-loop force tracking error of two controllers with parameter mismatch

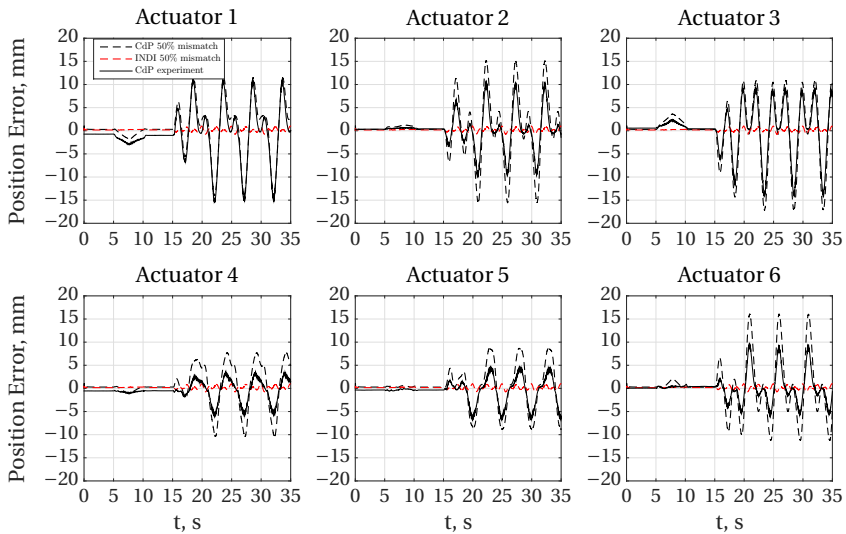


Figure 4.18: Position tracking error of two controllers with 50% parameter mismatch

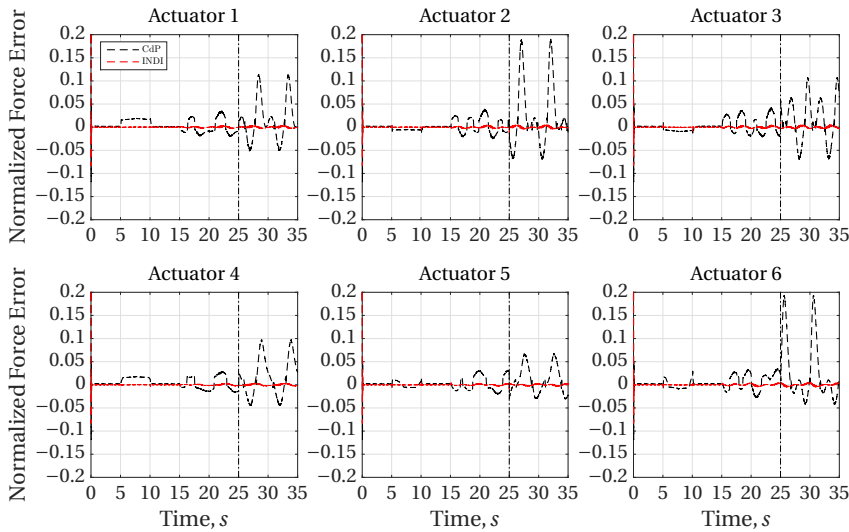


Figure 4.19: Inner-loop force tracking error of two controllers with supply pressure change

with a high-gain outer-loop feedback controller, the overall system is still stable, even in presence of a low performance inner-loop controller.

The performance of the INDI controller is hardly influenced by the mismatch of Φ_n . It is shown in Fig. 4.17 that the performance of the INDI-controlled system is equivalent to the nominal case, while that of the CdP approach is significantly deteriorated. Fig. 4.18 presents the position errors of each leg with 50% parameter mismatch, and similar result is shown, that the overall performance is also insensitive to parameter mismatch for the INDI controller. Again for reference, the position error of the experiment on the SRS of each actuator is also presented, which is equivalent to the simulation case with the CdP controller. Note that when facing uncertainty problems, no gain tuning is necessary, nor possible, for the INDI inner-loop controller, which shows the inherent robustness of INDI controller as analyzed in Section 4.3.

OIL SUPPLY PRESSURE

A second important parameter for the hydraulic system is the oil supply pressure P_s . It is a big perturbation to the system if there is a sudden change of P_s . Thus the robustness of force controller against P_s is of concern. Fig. 4.19 illustrates the normalized force tracking errors of both control schemes when facing a decrease in supply pressure. Both controllers start with a nominal supply pressure $P_s = 160 \text{ bar}$ and after 25 s the supply pressure is suddenly decreased by 20%. It is shown that the CdP controller suffers from the pressure change and the performance is significantly degraded, while the performance of the INDI controller remains intact. Similar results are observed for the position tracking error of each actuator. The robustness of the INDI approach is further verified by this result.

It is also clearly illustrated by the above results that the INDI is inherently insensitive to non-control-effective-related parameters in Eq. (4.5) such as the oil leakage coeffi-

cient L_{lm} , since they do not appear in the control law at all.

4.6. EXPERIMENT RESULTS

After a elaborated simulation verification of the effectiveness and robustness of the proposed INDI controller under the selected sampling rate, it is implemented on a real-life hydraulic parallel robot for experimental validation. This section demonstrates the force control performance of the proposed INDI technique for motion tracking tasks on the hydraulic hexapod motion system of the SRS at TU Delft, for both nominal conditions and cases with significant parameter mismatches. The overall system performance is also demonstrated and compared to a baseline NDI approach, as well as other similar state-of-the-art control schemes.

4.6.1. HARDWARE SETUP

The SRS is a 6-DOF flight simulator with a movable mass of around 4000 kg, capable of carrying two pilots, as shown in Fig. 4.5. The SRS is equipped with a hexapod motion system consisting of six hydraulic cylinders with 1.25 meters total stroke. With a 160 bar working pressure, the actuators are capable of exerting a maximum force of $F_m = 40$ kN, with a 1 m/s maximum actuator velocity. Each actuator is equipped with a Rexroth 4WSE3EE three-stage servo-valve and a PAINE 210-60-090 pressure transducer. Temposonic position sensors are installed on the actuators for position measurement and velocity estimation. The nominal parameters for the actuator model were identified in off-line experiments for the NDI-based controller as a baseline.

The motion control computer (MCC) is equipped with the dSPACE DS1005 system clocked at 1 GHz. The inner-loop controller is sampled at 5000 Hz and the outer-loop controller at 1000 Hz. The filters are designed in the analog plane and discretized using the bilinear transformation.

4.6.2. MOTION PROFILE 1

A set of symmetric motion tracking tasks along the vertical axis are tested first to demonstrate the efficiency of the proposed method with nominal hydraulic parameters. The force tracking error (normalized by $P_s A_p$) of each actuator with the INDI controller and the NDI-based controller in tracking the reference trajectory $z_d = 0.2 \sin 0.4\pi t$ m around the neutral point are shown in Fig. 4.20. The maximum tracking error is consistently around 1% for the INDI controller and 2.5% – 4% for the NDI controller. The performance of the INDI controller is consistently better than that of the NDI controller. The performance of NDI varies significantly for the different actuators, due to the different individual nonlinear dynamics that are not completely canceled. The advantage of INDI is thus already obvious in the nominal case.

The robustness of the INDI controller against parameter uncertainties is demonstrated by intentionally introducing parameter mismatches to the controller in the motion tracking test. In practice, the uncertainty of G_A results from model mismatches of Φ_n , C_m or disturbances of P_s . In this chapter, the value of G_A used for the controller is offset from the nominal case, as would for instance be caused by the proportional mismatches of the maximum oil flow Φ_n , between their estimated and real values. The

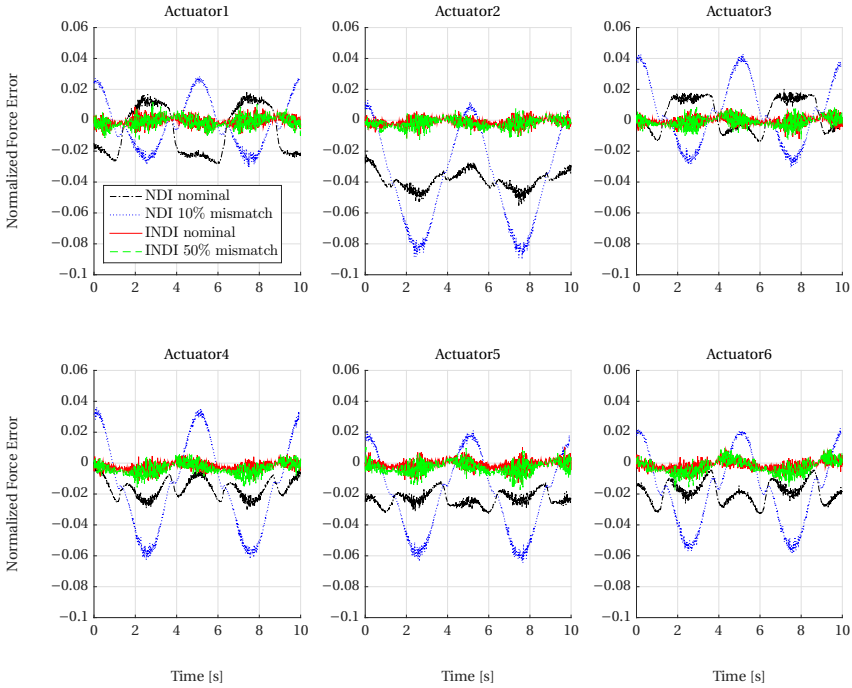


Figure 4.20: Inner-loop force tracking errors for NDI and INDI in nominal and parameter mismatch conditions.

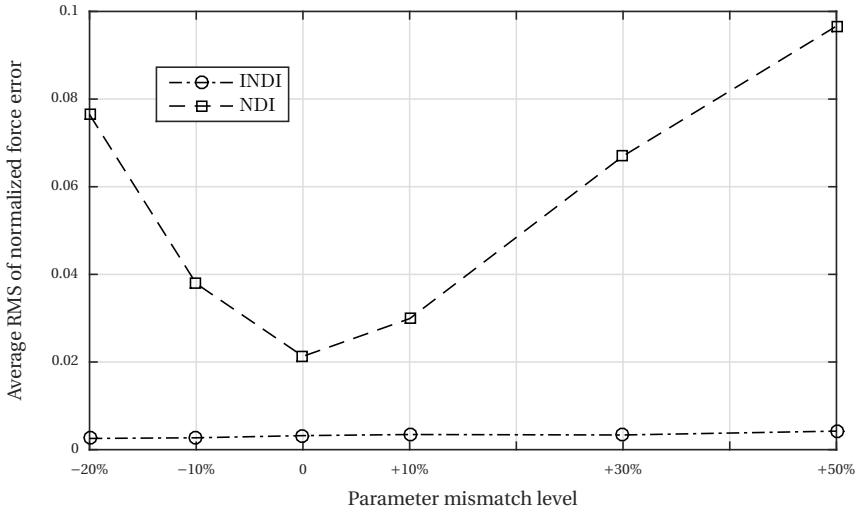


Figure 4.21: Average RMS of normalized force tracking errors of all actuators for the NDI and INDI controllers at different parameter mismatch levels.

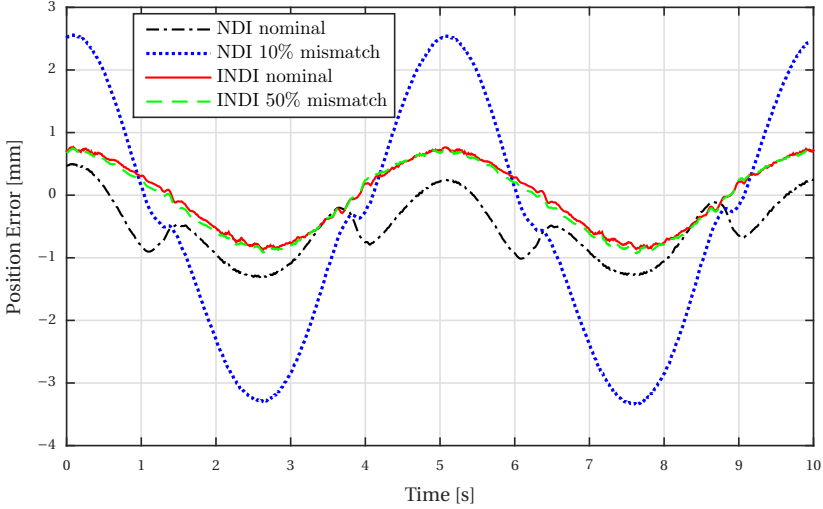


Figure 4.22: Position tracking errors for NDI and INDI in nominal and offset conditions.

Table 4.1: ρ Indicators Compared with State-of-The-Art Studies

Study	ρ [s]	$ e _{\max}$ [mm]	DOF	Type
Koivumaki 2015 [24]	0.0050	5.20	3	serial
Sirouspour 2001 [25]	0.0100	2.60	6	parallel
INDI nominal	0.0035	0.87	6	parallel
INDI 50% mismatch	0.0036	0.91	6	parallel

force tracking errors in mismatch conditions for INDI and NDI are also shown in Fig. 4.20. The performance of the NDI controller is significantly degraded with only +10% mismatch of \hat{G}_A , while that of the INDI controller remains almost intact for up to 50% parameter mismatch. Fig. 4.21 gives the average Root-Mean-Square (RMS) of the normalized force tracking error of all actuators for both controllers, under different levels of parameter mismatch in terms of \hat{G}_A , from -20% to +50%. The INDI shows equivalent performance at each condition, with an RMS of around 0.003, while that of the NDI quickly deteriorates from 0.02 to 0.1 as the mismatch level increases.

This result validates that INDI is resistant to even an unrealistic magnitude of error in parameter estimation for G_A while keeping high-precision performance, as long as the necessary condition $\alpha = \hat{G}_A G_A^{-1} > 0.5$ (see Section 4.3) is fulfilled. Note that INDI is inherently not sensitive to the leakage term $C_l P_L$ and the velocity related term $A_p \dot{q}$ in (4.5), as they are minimized as the perturbation term and do not appear in the control law at all.

Combined with the same outer-loop controller, the overall position tracking errors of both controllers are shown in Fig. 4.22. The maximum position error of the NDI con-

troller is 1.303 mm in nominal condition, and is rapidly increased to 3.3 mm with only +10% mismatch on \hat{G}_A . The performance of INDI is insensitive to the \hat{G}_A mismatch, with a maximum position error of 0.867 mm in nominal condition and a barely larger 0.905 mm maximum error with +50% mismatch. Note that the result for INDI with +10% mismatch is not presented in the graph, as it is not distinguishable from the other settings.

The performance of the proposed controller is evaluated and compared to the state-of-the-art hydraulic robotic manipulator control systems reviewed in a recent survey paper [26], in which the stability guaranteed adaptive nonlinear controllers [24, 25] show the best performance. In [26], a performance indicator ρ is suggested to evaluate the performance by taking into consideration of not only the absolute error, but also the maximum velocity of the trajectory, which is defined as

$$\rho = \frac{\max(|\mathbf{x}_d - \mathbf{x}|)}{\max(|\dot{\mathbf{x}}|)} = \frac{|e|_{\max}}{|\dot{\mathbf{x}}|_{\max}}. \quad (4.38)$$

In Table 4.1, the performance indicators of the proposed INDI control system in nominal and +50% parameter mismatch conditions are compared with the best performance counterparts for parallel hydraulic systems and serial manipulators concluded in the survey [26]. It is clear that the INDI control system gives almost the same performance in both nominal and parameter mismatch conditions, which have also better ρ indicator values listed than other approaches in literature. The advantage of the proposed method is even more obvious by taking the size of the systems into consideration, as the INDI controller applied to the considered SRS system achieves improved position tracking accuracy with a significantly heavier load of over 4000 kg. It can be concluded that the INDI hydraulic control system has one of the best motion control performance of the current hydraulic robotic manipulators.

4.6.3. MOTION PROFILE 2

The more aggressive asymmetrical motion used for the simulation research in Section 4.5 [46] is used to further evaluate the proposed controller, with more excitation of all nonlinear dynamics and kinematics. In this motion, the upper platform traces a 0.5 m radius circular path in the horizontal plane with a period of five seconds. A periodic roll and pitch motion with an amplitude of 10 deg/s and a period of 2.5 s is superimposed on this planar movement. With maximum actuator displacement and velocity of 0.7 m and 0.7 m/s, respectively, this motion exploits up to about 60% of the total safe stroke and 70% of the maximum velocity. The force and position tracking errors of Actuator 2 with different controller settings are shown in Fig. 4.23. The performance of INDI with 50% mismatch is still almost identical to the nominal case, with about 2.5% maximum force error and 2.2 mm maximum position error, while for the NDI controller these are 10% and 6.5 mm for the nominal case and degraded to 20% and 11 mm with only 10% parameter offset. This result indicates that the performance of traditional feedback linearization deteriorates faster than the INDI with more aggressive motions, because more serious nonlinear effects are excited when the system exploits a larger operation space. The trajectory tracking performance in the horizontal plane is illustrated in Fig. 4.24. The maximum error of INDI with 50% parameter mismatch is well below 2 mm, much better than that of the NDI with 4.5 mm in nominal condition and 8 mm with 10% mis-

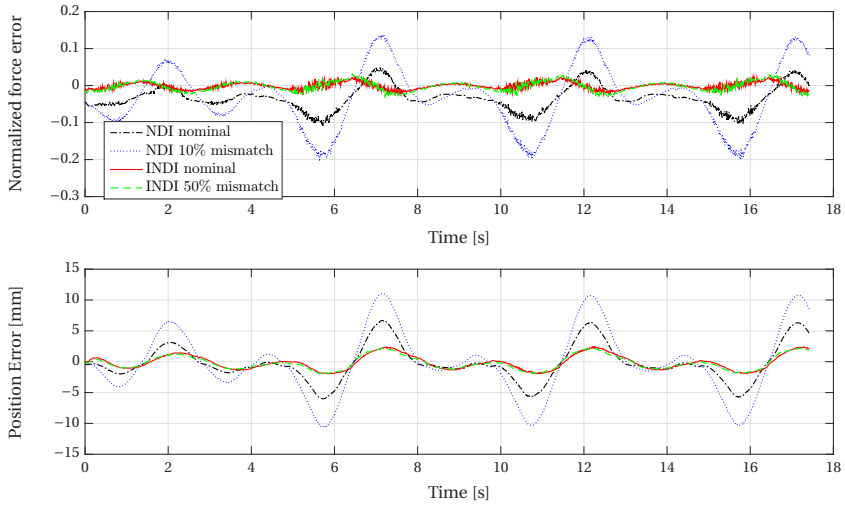


Figure 4.23: Force and position tracking errors for NDI and INDI in nominal and parameter mismatch conditions for actuator 2 with the aggressive manoeuvre of motion profile 2.

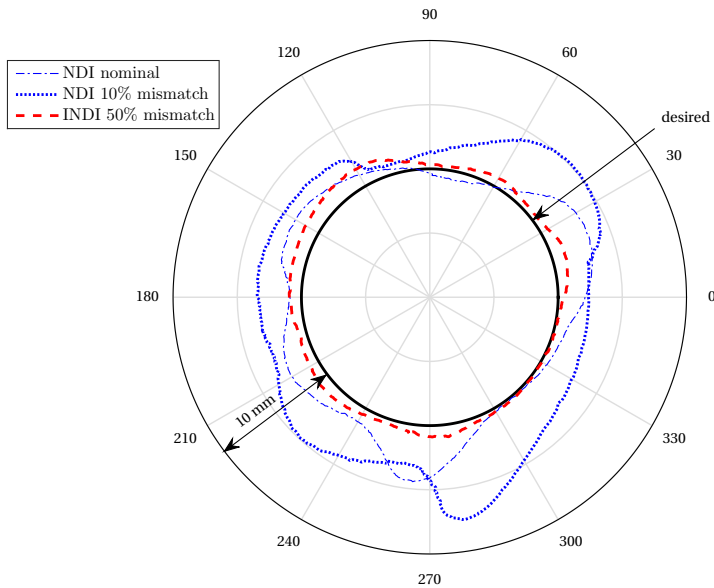


Figure 4.24: Position tracking performance in horizontal plane for NDI and INDI in nominal and parameter mismatch conditions for motion profile 2.

match.

The experiment results show that high-precision hydraulic robot force/motion tracking is achieved with the proposed INDI controller even in existence of significant magnitude of parameter mismatch, without explicit use of computationally heavy adaptive or robust control algorithms. From a practical point of view, the INDI controller design procedure is straightforward and can be easily implemented for other applications.

4.7. CONCLUSION

This chapter presents the development, simulation and implementation of the INDI controller on a full-scale hexapod hydraulic flight simulator motion system. Acting as a hydraulic actuator force tracking controller, the proposed technique is robust against even unrealistic hydraulic parametric uncertainties and disturbances, while providing better tracking performance than a traditional feedback linearization approach. The robustness of INDI against parameter uncertainty and its stability are proven, and an estimation of parameter mismatch tolerance is given as a necessary condition for stability. Combined with a commonly applied force computation outer-loop motion controller, a high-precision motion control system is developed for the hexapod motion system of the SRS. For the implementation on this long-stroke system, solutions to practical problems, such as oil transmission line resonance effect, have been discussed comprehensively, as a guide for other real-world applications. Both simulation and experiment results verify and validate the effectiveness and robustness of the proposed controller with consistent results. We demonstrate a significant improvement of tracking accuracy compared with the state-of-the-art research. The simplicity of the design procedure and the low computation load makes the INDI a potential off-the-shelf control technique for other hydraulic motion systems.

REFERENCES

- [1] Y. Huang, D. M. Pool, O. Stroosma, and Q. P. Chu, "Incremental nonlinear dynamic inversion control for hydraulic hexapod flight simulator motion systems," *IFAC-PapersOnLine*, vol. 50, no. 1, pp. 4294 – 4299, 2017, 20th IFAC World Congress.
- [2] Y. Huang, D. M. Pool, O. Stroosma, and Q. Chu, "Long-stroke hydraulic robot motion control with incremental nonlinear dynamic inversion," *IEEE/ASME Transactions on Mechatronics*, vol. 24, no. 1, pp. 304–314, Feb 2019.
- [3] M. Hutter, P. Leemann, G. Hottiger, R. Figi, S. Tagmann, G. Rey, and G. Small, "Force control for active chassis balancing," *IEEE/ASME Transactions on Mechatronics*, vol. 22, no. 2, pp. 613–622, April 2017.
- [4] C. Semini, V. Barasuol, J. Goldsmith, M. Frigerio, M. Focchi, Y. Gao, and D. G. Caldwell, "Design of the hydraulically actuated, torque-controlled quadruped robot hyq2max," *IEEE/ASME Transactions on Mechatronics*, vol. 22, no. 2, pp. 635–646, April 2017.
- [5] T. Boaventura, J. Buchli, C. Semini, and D. G. Caldwell, "Model-based hydraulic

- impedance control for dynamic robots,” *IEEE Transactions on Robotics*, vol. 31, no. 6, pp. 1324–1336, Dec 2015.
- [6] J. Koivumäki and J. Mattila, “Stability-guaranteed impedance control of hydraulic robotic manipulators,” *IEEE/ASME Transactions on Mechatronics*, vol. 22, no. 2, pp. 601–612, April 2017.
- [7] O. Stroosma, M. M. van Paassen, and M. Mulder, “Using the SIMONA Research Simulator For Human-Machine Interaction Research,” in *AIAA Modeling and Simulation Technologies Conference and Exhibit*, 2003.
- [8] H. Abdellatif and B. Heimann, “Advanced model-based control of a 6-DOF hexapod robot: A case study,” *IEEE/ASME Transactions on Mechatronics*, vol. 15, no. 2, pp. 269–279, April 2010.
- [9] M. Díaz-Rodríguez, A. Valera, V. Mata, and M. Valles, “Model-based control of a 3-DOF parallel robot based on identified relevant parameters,” *IEEE/ASME Transactions on Mechatronics*, vol. 18, no. 6, pp. 1737–1744, Dec 2013.
- [10] L. Ren, J. K. Mills, and D. Sun, “Experimental comparison of control approaches on trajectory tracking control of a 3-DOF parallel robot,” *IEEE Transactions on Control Systems Technology*, vol. 15, no. 5, pp. 982–988, Sept 2007.
- [11] P. H. Chang and J. H. Jung, “A systematic method for gain selection of robust pid control for nonlinear plants of second-order controller canonical form,” *IEEE Transactions on Control Systems Technology*, vol. 17, no. 2, pp. 473–483, March 2009.
- [12] J.-H. Chin, Y.-H. Sun, and Y.-M. Cheng, “Force computation and continuous path tracking for hydraulic parallel manipulators,” *Control Engineering Practice*, vol. 16, no. 6, pp. 697 – 709, 2008, special Section on Large Scale Systems 10th IFAC/IFORS/IMACS/IFIP Symposium on Large Scale Systems: Theory and Applications.
- [13] I. Davliakos and E. Papadopoulos, “Model-based control of a 6-DOF electrohydraulic stewart–gough platform,” *Mechanism and Machine Theory*, vol. 43, no. 11, pp. 1385 – 1400, 2008.
- [14] A. Alleyne and R. Liu, “A simplified approach to force control for electro-hydraulic systems,” *Control Engineering Practice*, vol. 8, no. 12, pp. 1347 – 1356, 2000.
- [15] A. Alleyne, R. Liu, and H. Wright, “On the limitations of force tracking control for hydraulic active suspensions,” in *Proceedings of the 1998 American Control Conference. ACC (IEEE Cat. No.98CH36207)*, vol. 1, Jun 1998, pp. 43–47 vol.1.
- [16] G. Vossoughi and M. Donath, “Dynamic feedback linearization for electrohydraulically actuated control systems,” *ASME. J. Dyn. Sys., Meas., Control.*, vol. 117, no. 4, pp. 468–477, 1995.
- [17] A. Plummer, “Model-based motion control for multi-axis servohydraulic shaking tables,” *Control Engineering Practice*, vol. 53, pp. 109 – 122, 2016.

- [18] J. Heintze and A. van der Weiden, "Inner-loop design and analysis for hydraulic actuators, with an application to impedance control," *Control Engineering Practice*, vol. 3, no. 9, pp. 1323 – 1330, 1995.
- [19] F. Kock and C. Ferrari, "Flatness-based high frequency control of a hydraulic actuator," *Journal of Dynamic Systems, Measurement, and Control*, vol. 134, no. 2, p. 021003, 2012.
- [20] Q. Quan, G. X. Du, and K. Y. Cai, "Proportional-integral stabilizing control of a class of mimo systems subject to nonparametric uncertainties by additive-state-decomposition dynamic inversion design," *IEEE/ASME Transactions on Mechatronics*, vol. 21, no. 2, pp. 1092–1101, April 2016.
- [21] Q. Quan and K. Y. Cai, "Additive-output-decomposition-based dynamic inversion tracking control for a class of uncertain linear time-invariant systems," in *2012 IEEE 51st IEEE Conference on Decision and Control (CDC)*, Dec 2012, pp. 2866–2871.
- [22] B. Yao, F. Bu, J. Reedy, and G. T. C. Chiu, "Adaptive robust motion control of single-rod hydraulic actuators: theory and experiments," *IEEE/ASME Transactions on Mechatronics*, vol. 5, no. 1, pp. 79–91, Mar 2000.
- [23] S. Chen, Z. Chen, B. Yao, X. Zhu, S. Zhu, Q. Wang, and Y. Song, "Adaptive robust cascade force control of 1-DOF hydraulic exoskeleton for human performance augmentation," *IEEE/ASME Transactions on Mechatronics*, vol. 22, no. 2, pp. 589–600, April 2017.
- [24] J. Koivumäki and J. Mattila, "High performance non-linear motion/force controller design for redundant hydraulic construction crane automation," *Automation in construction*, vol. 51, pp. 59–77, 2015.
- [25] M. R. Sirouspour and S. E. Salcudean, "Nonlinear control of hydraulic robots," *IEEE Transactions on Robotics and Automation*, vol. 17, no. 2, pp. 173–182, 2001.
- [26] J. Mattila, J. Koivumäki, and D. G. Caldwell, "A survey on control of hydraulic robotic manipulators with projection to future trends," *IEEE/ASME Transactions on Mechatronics*, vol. 22, no. 2, pp. 669 – 680, 2017.
- [27] S. Sieberling, Q. P. Chu, and J. A. Mulder, "Robust Flight Control Using Incremental Nonlinear Dynamic Inversion and Angular Acceleration Prediction," *Journal of Guidance, Control, and Dynamics*, vol. 33, no. 6, pp. 1732–1742, nov 2010.
- [28] P. Simplício, M. D. Pavel, E. van Kampen, and Q. P. Chu, "An acceleration measurements-based approach for helicopter nonlinear flight control using incremental nonlinear dynamic inversion," *Control Engineering Practice*, vol. 21, no. 8, pp. 1065 – 1077, 2013.
- [29] E. J. J. Smeur, Q. P. Chu, and Guido C. de Croon, "Adaptive incremental nonlinear dynamic inversion for attitude control of micro aerial vehicles," *Journal of Guidance, Control, and Dynamics*, vol. 39, no. 3, pp. 450–461, 2016.

- [30] Y. Huang, D. M. Pool, O. Stroosma, Q. P. Chu, and M. Mulder, "A Review of Control Schemes for Hydraulic Stewart Platform Flight Simulator Motion Systems," in *AIAA Modeling and Simulation Technologies Conference*, January 2016.
- [31] B. Dasgupta and T. Mruthyunjaya, "Closed-form dynamic equations of the general stewart platform through the newton-euler approach," *Mechanism and Machine Theory*, vol. 33, no. 7, pp. 993 – 1012, 1998.
- [32] Y. Huang, D. M. Pool, O. Stroosma, Q. P. Chu, and M. Mulder, "Modeling and Simulation of Hydraulic Hexapod Flight Simulator Motion Systems," in *AIAA Modeling and Simulation Technologies Conference*, January 2016.
- [33] H. E. Merritt, *Hydraulic control systems*. John Wiley & Sons, 1967.
- [34] J.-J. E. Slotine, W. Li *et al.*, *Applied nonlinear control*. Prentice hall Englewood Cliffs, NJ, 1991, vol. 199, no. 1.
- [35] R. Da Costa, Q. Chu, and J. Mulder, "Reentry flight controller design using nonlinear dynamic inversion," *Journal of Spacecraft and Rockets*, vol. 40, no. 1, pp. 64–71, 2003.
- [36] C. H. An, C. G. Atkeson, J. D. Griffiths, and J. M. Hollerbach, "Experimental evaluation of feedforward and computed torque control," *IEEE Transactions on Robotics and Automation*, vol. 5, no. 3, pp. 368–373, Jun 1989.
- [37] H. K. Khalil, *Nonlinear Systems (3rd ed.)*. Prentice Hall, 2002.
- [38] T. C. Hsia and L. S. Gao, "Robot manipulator control using decentralized linear time-invariant time-delayed joint controllers," in *Proceedings., IEEE International Conference on Robotics and Automation*, May 1990, pp. 2070–2075 vol.3.
- [39] S. Koekebakker, "Model based control of a flight simulator motion system," Ph.D. dissertation, Delft University of Technology, 2001.
- [40] Q. Quan and K.-Y. Cai, "Time-domain analysis of the savitzky-golay filters," *Digital Signal Processing*, vol. 22, no. 2, pp. 238 – 245, 2012.
- [41] W. C. Yang and W. E. Tobler, "Dissipative Modal Approximation of Fluid Transmission Lines Using Linear Friction Model," *Journal of Dynamic Systems, Measurement, and Control*, vol. 113, no. 1, pp. 152–162, 1991.
- [42] G. van Schothorst, P. Teerhuis, and A. van der Weiden, "Stability analysis of a hydraulic servo-system including transmission line effects," in *Proceedings of the Third International conference on Automation, Robotics and Computer Vision, Singapore*, 1994, pp. 1919–1923.
- [43] D. Garagic and K. Srinivasan, "Application of nonlinear adaptive control techniques to an electrohydraulic velocity servomechanism," *IEEE Transactions on Control Systems Technology*, vol. 12, no. 2, pp. 303–314, March 2004.

- [44] Y. Pi and X. Wang, "Observer-based cascade control of a 6-DOF parallel hydraulic manipulator in joint space coordinate," *Mechatronics*, vol. 20, no. 6, pp. 648 – 655, 2010.
- [45] H. Guo, Y. Liu, G. Liu, and H. Li, "Cascade control of a hydraulically driven 6-DOF parallel robot manipulator based on a sliding mode," *Control Engineering Practice*, vol. 16, no. 9, pp. 1055 – 1068, 2008.
- [46] I. Miletović, D. Pool, O. Stroosma, M. van Paassen, and Q. Chu, "Improved Stewart platform state estimation using inertial and actuator position measurements," *Control Engineering Practice*, vol. 62, no. Supplement C, pp. 102 – 115, 2017.

5

NON-MODEL-BASED CONTROL OF HYDRAULIC PARALLEL ROBOTS

In the previous chapter, a high performance INDI based force controller is designed for the inner-loop of a hydraulic robot. However, the outer-loop parallel motion control system is still designed with model-based technique. Model uncertainties in the mechanical system, such as the load mass and uncertain frictions, are still degrading the motion tracking performance of the overall system. Therefore, in this chapter, the robust INDI control technique is applied to the outer motion control loop. Combined with the force controller developed in the previous chapter, the complete control system is robust to model uncertainties in both hydraulic subsystem and mechanic subsystem. The developed motion control system is implemented on the SIMONA hydraulic parallel flight simulator motion system. This chapter is organized as follows. After a brief introduction, the highly nonlinear dynamics of the parallel robot are briefly introduced in Section 5.2. Section 5.3 gives the detailed INDI controller design procedure for the parallel robotic systems. The features of the complete controller based on INDI are then discussed in Section 5.4. The performance of the developed controller is tested by experiments on the SIMONA simulator motion system, the results are given in Section 5.5. Main conclusions are drawn in Section 5.6.

This chapter is based on the following articles:

Y. Huang, D. M. Pool, O. Stroosma, and Q. Chu, "Robust incremental nonlinear dynamic inversion controller of hexapod flight simulator motion system," in *Advances in Aerospace Guidance, Navigation and Control*. Cham: Springer International Publishing, 2018, pp. 87–99. [1]

Y. Huang, D. Pool, O. Stroosma, and Q. Chu, "Sensor-based motion control system for parallel hydraulic robots with model uncertainties," *IEEE/ASME Transactions on Mechatronics* (to be submitted)

This chapter presents the design and implementation of the high-precision controller for the parallel robots with model uncertainties based on a novel Incremental Nonlinear Dynamic Inversion technique. Without explicit adaptive or robust control algorithm, the proposed technique is computational efficient and inherently resistant to system dynamic model mismatch, which allows for avoiding the cumbersome identification for a complete parallel robot dynamic model. Combined with a state-of-the-art hydraulic force tracking controller based on the same technique, the proposed motion controller is implemented on a typical 6-DOF parallel hydraulic robot, the SIMONA (Simulation, Motion and Navigation) flight simulator at TU Delft, as a case study. The control performance and resistance against model uncertainties are evaluated with motion tracking experiments on the SIMONA simulator with intentionally introduced rigid body dynamic model mismatch. Significant control performance improvement is demonstrated in existence of model uncertainties, when comparing with the state-of-the-art model-based control strategy.

5.1. INTRODUCTION

Parallel manipulators (PMs) are mechanisms which consist of a moving platform and a stationary base, connected by several independent kinematic chains[2]. As a typical representation of such mechanisms, Stewart-Gough platforms, or hexapods, are 6-DOF PMs with 6 linear actuators, which are wide used in flight simulators and other industrial applications[3]. Compared with serial manipulators, PMs have greater stiffness and rigidity with larger load capability. When manipulating heavy loads, such as in case of flight simulators, it is common that hydraulic actuators are used for the hexapods for their high power ability and robustness[4]. However, such systems meet several control challenges, as the highly nonlinear rigid-body dynamics of PMs intersect with the nonlinear hydraulic fluid dynamics.

In practice, the precision control of parallel manipulators faces unique challenges compared with their serial counterparts[5]. For instance, the control for PMs in work space is not practical since the state measurements are not directly available and the forward kinematics do not have an analytical solution. More importantly, the dynamics of PMs are highly nonlinear and complicated due to their structure with multiple closed chains. Even though different forms of their dynamic models have been very well derived with Lagrangian formulation[6], Newton-Euler formulation[7] or virtual work principle[8], a linear dynamic model with respect to the dynamic parameters is difficult to obtain, and very few publications provide a systematic solution[9, 10]. With the different features in kinematics and dynamics, most recently developed control algorithm are only discussed for serial robots [11, 12], and rarely implemented for parallel robots.

As linear controllers are not suitable when high-performance is required for the PMs with high dynamics, several advanced model-based control systems have been developed[5, 8, 13–16]. The computation of the complete dynamic model plays a central role in most advanced control approaches. In practice-oriented researches, the efforts were mostly focused on model simplification[8, 17] and the corresponding parameter identification for computational efficiency. Compared with the well studied parameter identification methods for serial robots[18, 19], only a few publications discuss that for the PMs[5, 9]. The main reason is that the favorable rigid body dynamic model for parameter identi-

fication, which requires a linear form with respect to the dynamic parameters, is rarely studied and often ill-conditioned due to the structure of a PM[14]. It is concluded in [10] that 88 base inertial parameters need to be identified for a typical 6-DOF parallel manipulator, even with necessary parameter number reduction. Thus model simplification is often necessary by neglecting small inertial terms[8, 20, 21]. It is even reported that the control system based on the reduced model gives better performance than that with the complete dynamic model[14]. In addition to the above difficulties, the tracking performance will degrade for the identified systems when subject to time-varying load, such as the case in a research flight simulator when the installed equipment and number of the pilots can change. In order to further reduce the control error caused by model uncertainties, adaptive control is adopted in a few theoretical researches[15]. However, due to computational issue, their applications for the PMs in reality is limited[5] and few publications give experiment results. It can be concluded that the performance of advanced model-based control systems for parallel robots are still restricted by the fidelity and efficiency of the dynamic model.

An alternative approach is to make the nonlinear control system independent of a precise dynamic model. Incremental Nonlinear Dynamic Inversion (INDI) is a novel nonlinear control technique based on incremental dynamic model and feedback linearization, thus is inherently not sensitive to model uncertainties. By estimating the system derivative by sensor measurements instead of model prediction, INDI can achieve precise input-output linearization without a precise model. Various state-of-the-art applications with INDI have been reported for flight control[22–24] and hydraulic control systems[25], showing high control performance and robustness to model uncertainties. Specifically, the implementation of INDI on highly nonlinear hydraulic force control problem was achieved with significant performance improvement in our previous study[26]. INDI provides attractive advantages for parallel robot control with unique features, including: 1) The inherent robustness against model uncertainties and continuous disturbances allows for the use of rough dynamic models without elaborate parameter identification; 2) The precise linearization of the uncertain nonlinear model allows for high tracking performance; 3) The straightforward design procedure and low computation load allow for easy practical implementation.

In previous work of this study, the theoretical application of INDI to a parallel robot model was discussed in[1]. However, as only simulation results are given and the robot actuator dynamics are neglected from the studied computer model, it did not give enough information for practical applications.

This chapter intends to take a major step forward, by designing and experimental validating the INDI controller on the motion control system of a large-scale 6-DOF parallel robot driven by hydraulic actuators, SIMONA Research Simulator (SRS) at TU Delft. As the developed motion controller asks for ideal force acutators, which is challenging for hydraulic acuaturs [27, 28], our recently developed high-performance INDI-based hydraulic force/pressure controller is used as an inner-loop controller [26]. The resulting combined system proposed in this chapter presents the first fully dual-loop INDI hydraulic parallel robot control system, as will be elaborated in Section 5.4. Featured as a sensor-based approach, the proposed control system depends on the accurate measurements of the hydraulic pressure difference, actuator length and valve displacement,

while being tolerant to significant dynamic model uncertainty. To validate the robustness against parallel robot dynamic mismatch, motion tracking experiments with voluntarily introduced inertial parameter offsets in the rigid body dynamics are performed for the proposed INDI controller, and compared with a baseline model-based feedforward controller with state-of-the-art performance[26]. The main contributions of this chapter are summarized as: 1) The novel INDI controller designed in actuator space is implemented in real-life for parallel robot motion control, for the first time; 2) The stability and robustness analysis of INDI controller is extended to MIMO systems; and 3) The model uncertainty resistance property is validated by motion tracking experiments in existence of significant inertial parameter offsets, with significant tracking performance improvement compared with state-of-the-art studies.

This chapter is organized as follows: Section 5.2 gives a summary of the system dynamic model, including the rigid body and hydraulic dynamics. In Section 5.3, a practical INDI controller is proposed for parallel hydraulic robots subject to model parameter uncertainties, with a proof of its stability and robustness. Section 5.4 discusses the unique properties of the proposed dual-loop INDI control strategy. The motion tracking experiment results on the SRS are presented in Section 5.5 and the main conclusions are drawn in Section 5.6.

5.2. SYSTEM DYNAMIC MODEL

The rigid-body dynamic equations of parallel manipulators are generally easier to be obtained in Cartesian space. As summarized in[5], the dynamic equations can be derived in four formulations with different methods, each of which suitable for different purposes. For simulation or control purpose, Newton-Euler formulation[7] is often adopted as a second-order nonlinear differential equation. For a typical 6-DOF parallel robot, i.e. the hexapod, the dynamics equations are given by[29]:

$$\mathbf{J}_{q,s}^T \mathbf{F} = \mathbf{M}(\mathbf{z}) \ddot{\mathbf{s}} + \boldsymbol{\eta}(\dot{\mathbf{s}}, \mathbf{z}), \quad (5.1)$$

where \mathbf{z} , $\dot{\mathbf{s}}$ and $\ddot{\mathbf{s}}$ are the generalized coordinates, velocities and accelerations defined in the Cartesian space, \mathbf{M} is the positive definite mass matrix, $\boldsymbol{\eta}$ contains the centrifugal, Coriolis and gravity terms, and \mathbf{F} are the actuation forces. $\mathbf{J}_{q,s}$ is the Jacobian matrix between the platform velocities and the actuator velocities, defined by

$$\dot{\mathbf{q}} = \mathbf{J}_{q,s} \dot{\mathbf{s}} = \frac{\partial \dot{\mathbf{q}}}{\partial \dot{\mathbf{s}}} \dot{\mathbf{s}}, \quad (5.2)$$

where \mathbf{q} is the vector of the actuator displacements. A detailed derivation of the model can be found in [29].

Since we are interested in the dynamic properties in actuator space in order to avoid measurement in Cartesian space, (5.1) can be written as a semi-actuator-space form. Taking derivative of (5.2) and substitute it into (5.1) gives

$$\begin{aligned} \ddot{\mathbf{q}} &= \mathbf{J}_{q,s} \mathbf{M}^{-1} \mathbf{J}_{q,s}^T \mathbf{F} - \mathbf{J}_{q,s} \mathbf{M}^{-1} \boldsymbol{\eta} + \dot{\mathbf{J}}_{q,s} \dot{\mathbf{s}} \\ &= \mathbf{G}(\mathbf{z}) \mathbf{F} + \mathbf{f}(\mathbf{z}, \dot{\mathbf{s}}). \end{aligned} \quad (5.3)$$

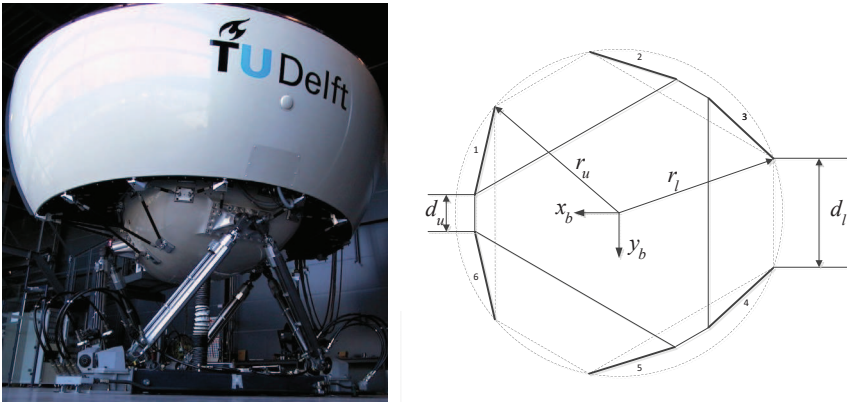


Figure 5.1: A hexapod motion system SRS at TU Delft (left), and its top view drawing (right) [31]

Note that in (5.3), only the acceleration and the forces are described in the actuator space explicitly, which will be shown preferable for the proposed INDI controller. It is also assumed that M and $J_{q,s}$ are invertible in the discussed workspace.

The actuators of the studied hexapod manipulator are hydraulic cylinders, the highly nonlinear dynamics of which are another challenge for the integrated motion system. The hydraulic dynamic model is derived by writing fluid pressure dynamic equation caused by the oil compressibility. Consider a symmetric actuator and ideal valve with matched and symmetrical rectangular orifices, the pressure dynamics can be described by the following equation[30, 31],

$$\begin{aligned} \dot{P}_L &= 2C \left(\frac{C_d \omega x_m}{\sqrt{\rho}} \sqrt{P_s - \frac{x_m}{|x_m|} P_L} - C_l P_L - A_p \dot{q} \right) \\ &= G_A(P_L, x_m, q) x_m + f_A(P_L, q, \dot{q}), \end{aligned} \quad (5.4)$$

where P_L is the load pressure, x_m is the valve displacement, ω , A_p and ρ are the valve orifice width, the cylinder area and oil density, C , C_d and C_l are the hydraulic compliance, the valve discharge coefficient and total leakage coefficient. Assuming negligible friction with good lubrication, the actuation force is equal to $F = A_p P_L$. This fact allows for an actuation force feedback without additional force sensors.

5.3. SENSOR-BASED CONTROLLER DESIGN

Theoretically, feedback linearization is an ideal approach for nonlinear control systems if particular conditions are satisfied[32]. However, in addition to the common problem of model uncertainty, its application on parallel robot is rare because it requires measurements of system states in Cartesian space which are not practical. That is why it is often for advanced model-based control systems to have the feedforward term with motion setpoints in Cartesian space[5, 14], while the feedback loop is designed in actuation space. For such systems, the feedforward loop will introduce big error if the system dynamic model is not properly identified or time varying.

INDI technique is a modified feedback linearization method based on the incremental form of system dynamic model which inherently minimizes most of the model dependent terms as a negligible disturbance. A general discussion on INDI can be found in [26], with stability and robustness analysis for SISO systems. In this chapter, the complete INDI controller for a 6-DOF parallel robot is designed in detail, with its stability and robustness analysis extended to general MIMO systems. It will be shown that the model uncertainty and kinematic problem can be solved simultaneously with proper controller structure, without a compromise in performance.

5.3.1. INDI MOTION CONTROLLER FOR PARALLEL ROBOT

Before preceding, the following assumptions are introduced for the system dynamics (5.1) and (5.3):

Assumption 1: The system actuation forces \mathbf{F} and consequently the system acceleration $\ddot{\mathbf{q}}$ or $\ddot{\mathbf{s}}$ are not necessarily continuous. The system velocity $\dot{\mathbf{s}}$ and position \mathbf{z} are continuous since they are the integration of the acceleration and velocity.

Assumption 2: The nominal inertial matrix $\mathbf{M}(\mathbf{z})$, the combined term $\boldsymbol{\eta}(\dot{\mathbf{s}})$ and the Jacobian $\mathbf{J}_{q,s}$ are differentiable functions of \mathbf{z} and $\dot{\mathbf{s}}$ in the chosen workspace.

Assumption 1 requires that the dynamics of the force generator are much faster than the rigid body dynamics, such that the input to the system can be chosen with sharp changes. Assumption 2 is reasonable since in the derivation of (5.1) with Newton-Euler approach [7, 29], the elements of the discussed matrices or terms are elementary functions of \mathbf{z} and $\dot{\mathbf{s}}$. The continuity can be satisfied by avoiding singular points with the proper choosing of workspace.

Consider the dynamic equation (5.3), taking the first order Taylor expansion of the right side at the beginning of each sample time t_0 gives

$$\begin{aligned} \ddot{\mathbf{q}} = & \ddot{\mathbf{q}}_0 + \mathbf{G}(\mathbf{z}_0)(\mathbf{F} - \mathbf{F}_0) + \left. \frac{\partial [\mathbf{f}(\mathbf{z}, \dot{\mathbf{s}})]}{\partial \dot{\mathbf{s}}} \right|_0 (\dot{\mathbf{s}} - \dot{\mathbf{s}}_0) \\ & + \left. \frac{\partial [\mathbf{G}(\mathbf{z})\mathbf{F} + \mathbf{f}(\mathbf{z}, \dot{\mathbf{s}})]}{\partial \mathbf{z}} \right|_0 (\mathbf{z} - \mathbf{z}_0) \\ & + \mathbf{O}[(\mathbf{z} - \mathbf{z}_0)^2, (\dot{\mathbf{s}} - \dot{\mathbf{s}}_0)^2]. \end{aligned} \quad (5.5)$$

The last three terms on the right hand side of (5.5) represent the contributions of system state changes to the acceleration increment. They are defined as a lumped perturbation term and denoted as $\boldsymbol{\delta}$.

As the system position and velocity vectors are continuous, taking the limits of (5.5) as the time increment T_s goes to 0 results in

$$\begin{aligned} \ddot{\mathbf{q}} = & \lim_{T_s \rightarrow 0} \ddot{\mathbf{q}}_0 + \lim_{T_s \rightarrow 0} \mathbf{G}(\mathbf{z}_0)(\mathbf{F} - \mathbf{F}_0) + \lim_{T_s \rightarrow 0} \boldsymbol{\delta} \\ = & \ddot{\mathbf{q}}_0 + \mathbf{G}(\mathbf{z}_0)(\mathbf{F} - \mathbf{F}_0), \end{aligned} \quad (5.6)$$

in which the increment of the actuator forces is not related to the limit since it is the input command, which can be discontinuous.

(5.6) is the incremental form of system dynamics, which suggests that the perturbation term $\boldsymbol{\delta}$ becomes negligible when the time increment T_s approaches zero. Based

on (5.6), assuming the sample time T_s is very small and the acceleration and actuation forces at t_0 are available through measurement, the INDI control law is designed in every time interval as

$$\begin{aligned} \mathbf{F} &= \mathbf{F}_0 + \mathbf{G}^{-1}(\mathbf{z}_0) (\mathbf{v} - \ddot{\mathbf{q}}_0) \\ &= \mathbf{F}_0 + \left(\mathbf{J}_{q,s}^{-T} \mathbf{M} \mathbf{J}_{q,s}^{-1} \right)_{\mathbf{z}_0} (\mathbf{v} - \ddot{\mathbf{q}}_0), \end{aligned} \quad (5.7)$$

where \mathbf{v} is the pseudo control to be determined. Instead of directly calculating the total control input \mathbf{F} , it is the control increment that is calculated in every sample time and repetitively added to the control input of the last step (\mathbf{F}_0). The resulting system dynamics under the control law (5.7) is

$$\mathbf{v} = \ddot{\mathbf{q}}, \quad (5.8)$$

which is fully linearized as a double integrator. The pseudo control \mathbf{v} can be selected as

$$\mathbf{v} = \ddot{\mathbf{q}}_d + \mathbf{K}_p (\mathbf{q}_d - \mathbf{q}) + \mathbf{K}_d (\dot{\mathbf{q}}_d - \dot{\mathbf{q}}), \quad (5.9)$$

where \mathbf{q}_d are the desired actuator displacements, \mathbf{K}_p and \mathbf{K}_d are gain matrices. Substituting (5.9) into (5.8) gives the error dynamics

$$\ddot{\mathbf{e}} + \mathbf{K}_d \dot{\mathbf{e}} + \mathbf{K}_p \mathbf{e} = 0, \quad (5.10)$$

where the error $\mathbf{e} = \mathbf{q}_d - \mathbf{q}$ is asymptotic stable at zero with the proper choice of \mathbf{K}_p and \mathbf{K}_d .

A full linearization of a nonlinear system in the form of (5.8) asks for a full knowledge of \mathbf{G} . In practice, in the presence of uncertainties, the estimated value, i.e. $\widehat{\mathbf{G}}$, will be used for the INDI controller. It will be shown that in this case, (5.8) will just be disturbed by an equivalent stable transfer function for INDI such that $\ddot{\mathbf{q}}$ will still converge to be equal to \mathbf{v} under a proposed necessary condition, instead of being totally violated for traditional feedback linearization.

5.3.2. ROBUSTNESS ANALYSIS

In the authors' previous study, the robustness of INDI to uncertainties in \mathbf{G} was proved for SISO system and conditionally proved for MIMO systems. In this chapter, the proof will be extended to MIMO case in general.

For the system dynamic equation (5.3), considering the continuity of \mathbf{z} and $\dot{\mathbf{s}}$, $\mathbf{G}(\mathbf{z})$ and $\mathbf{f}(\mathbf{z}, \dot{\mathbf{s}})$ are regarded as constant matrices in a sufficiently small time interval. Thus in every small time interval, the global system model is estimated by a linear local model with a fixed gain \mathbf{G} and a disturbance term \mathbf{f} . This assumption is only valid in a sufficient high sampling rate. Taking Laplace transform of both sides of (5.3) and (5.7) gives

$$s^2 \mathbf{q}(s) = \mathbf{G} \mathbf{F}(s) + \mathbf{f}, \quad (5.11)$$

and

$$\mathbf{F}(s) = e^{-sT_s} \mathbf{F}(s) + \widehat{\mathbf{G}}^{-1} (\mathbf{v}(s) - e^{-sT_s} s^2 \mathbf{q}(s)). \quad (5.12)$$

Note that in (5.12) the estimated $\widehat{\mathbf{G}}$ is used for the control law when model uncertainties are considered.

Substitute (5.11) into (5.12), the controlled system dynamics become

$$\begin{aligned} \widehat{\mathbf{G}}\mathbf{G}^{-1}s^2\mathbf{q}(s) &= \mathbf{v}(s) + (\widehat{\mathbf{G}}\mathbf{G}^{-1} - \mathbf{I})e^{-sT_s}s^2\mathbf{q}(s) \\ &+ \widehat{\mathbf{G}}\mathbf{G}^{-1}\mathbf{f} - \widehat{\mathbf{G}}\mathbf{G}^{-1}e^{-sT_s}\mathbf{f}. \end{aligned} \quad (5.13)$$

Consider the eigenvalue decomposition of the matrix $\widehat{\mathbf{G}}\mathbf{G}^{-1}$

$$\widehat{\mathbf{G}}\mathbf{G}^{-1} = \mathbf{Q}\mathbf{\Lambda}\mathbf{Q}^{-1}, \quad (5.14)$$

with the state and variable transformation

$$\boldsymbol{\theta} = \mathbf{Q}^{-1}\mathbf{q}, \quad \boldsymbol{\mu} = \mathbf{Q}^{-1}\mathbf{v}, \quad \boldsymbol{\eta} = \mathbf{Q}^{-1}\mathbf{f}, \quad (5.15)$$

(5.13) can thus be decoupled as

$$[\mathbf{\Lambda} + (\mathbf{I} - \mathbf{\Lambda})e^{-sT_s}]s^2\boldsymbol{\theta}(s) = \boldsymbol{\mu}(s) + (\mathbf{\Lambda} - \mathbf{\Lambda}e^{-sT_s})\boldsymbol{\eta}(s). \quad (5.16)$$

With (5.16), the controlled system dynamics are decoupled into 6 parallel SISO systems with the same form of transfer functions. The corresponding transfer functions from the transformed pseudo control $\boldsymbol{\mu}$ and disturbance $\boldsymbol{\eta}$ to the acceleration $s^2\boldsymbol{\theta}$ can be written as

$$s^2\boldsymbol{\theta}_i(s) = H_i(s)\boldsymbol{\mu}_i(s) + D_i(s)\boldsymbol{\eta}_i(s), \quad (5.17)$$

where the subscript i denotes the i th element of the according vectors, the transfer functions $H_i(s)$ and $D_i(s)$ can be easily obtained from (5.16) as

$$H_i(s) = \frac{s^2\boldsymbol{\theta}_i(s)}{\boldsymbol{\mu}_i(s)} = \frac{1}{\lambda_i + (1 - \lambda_i)e^{-sT_s}} \quad (5.18)$$

and

$$D_i(s) = \frac{s^2\boldsymbol{\theta}_i(s)}{\boldsymbol{\eta}_i(s)} = \frac{\lambda_i(1 - e^{-sT_s})}{\lambda_i + (1 - \lambda_i)e^{-sT_s}}, \quad (5.19)$$

where λ_i is the i th element of the diagonal matrix $\mathbf{\Lambda}$, i.e. the i th eigenvalue of the matrix $\widehat{\mathbf{G}}\mathbf{G}^{-1}$. Taking the pseudo control (5.9) into account, the complete controlled system dynamics can be described by the equivalent transfer function given in the block diagram in Fig. 5.2. It is clear that with the transformation of the eigenvector matrix \mathbf{Q} , the closed loop MIMO system dynamics are decoupled into 6 parallel channels inside the dashed box, each of which represents the effect of one eigenvalue λ_i .

The stability requirement of (5.18) and (5.19) offers a necessary condition for the stability of the complete system. It is analyzed in [26] that when λ_i are all real numbers, the necessary condition is $\lambda_i > 0.5$. However, as will be elaborated later, all λ_i are real only under specific conditions. In general case when λ_i are complex numbers, (5.18) and (5.19) are transfer functions with complex coefficients. Dynamic systems having transfer functions with complex coefficients are rare, but can be found in recent applications in electrical power system analysis [33] and rotating machinery[34]. Thus the necessary condition for the stability of the INDI controlled MIMO systems is extended and given by the following proposition.

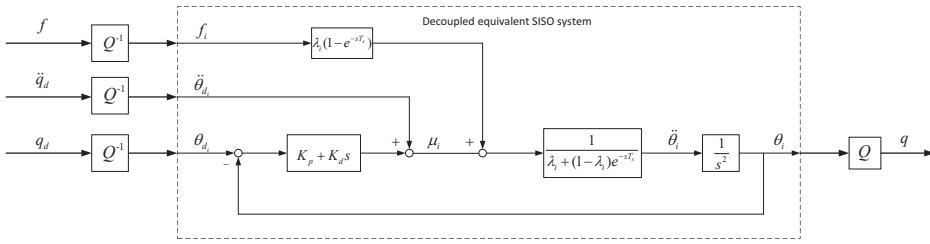


Figure 5.2: Block diagram of the decoupled equivalent SISO system for the INDI-controlled MIMO system

Proposition 1: If the square matrix $\widehat{\mathbf{G}}\mathbf{G}^{-1}$ is diagonalizable and the real part of all its eigenvalues satisfy $Re(\lambda_i) > 0.5$, then the transfer functions $H_i(s)$ and $D_i(s)$ in (5.18) and (5.19) are stable.

proof: The poles of (5.18) and (5.19) are calculated by the equation

$$\lambda + (1 - \lambda)e^{-sT_s} = 0. \quad (5.20)$$

Defining

$$s = \sigma + \omega i, \lambda_i = a + bi, \quad (5.21)$$

the characteristic equation (5.20) becomes

$$e^{-\sigma T_s} e^{-i\omega T_s} = \frac{a + bi}{a - 1 + bi}. \quad (5.22)$$

The absolute values of both sides of (5.22) is

$$\begin{aligned} \left| e^{-\sigma T_s} e^{-i\omega T_s} \right| &= \left| e^{-\sigma T_s} \right| = \left| \frac{a + bi}{a - 1 + bi} \right| \\ &= \frac{\sqrt{(a^2 - a + b^2)^2 + b^2}}{(a - 1)^2 + b^2}. \end{aligned} \quad (5.23)$$

The sufficient and necessary condition for $\sigma < 0$ is that both sides of (5.23) are bigger than 1, which is equivalent to

$$(a^2 - a + b^2)^2 + b^2 > [(a - 1)^2 + b^2]^2. \quad (5.24)$$

Work out (5.24) we have

$$(1 - 2a)[b^2 + (a - 1)^2] < 0, \quad (5.25)$$

which is true if and only if $a > 0.5$.

Thus if and only if $Re(\lambda_i) > 0.5$, the transfer functions (5.18) and (5.19) have poles on the left side of the complex plane, which guarantees their stability. \square

Based on this, the robustness of the INDI can be analyzed with $H_i(s)$ and $D_i(s)$. First, it is easy to explain from (5.19) that the influence of the defined disturbance term $\mathbf{f}(\boldsymbol{\eta})$

in the decoupled system) to the system is inherently rejected by INDI. According to the final value theorem, the step response of $D_i(s)$ approaches 0 over time. The rejection speed will also increase with a smaller sampling time T_s . In fact, when T_s is infinitesimal, $D_i(s)$ approaches 0. This is consistent with the previous analysis in time domain that the incremental perturbation δ approaches 0 with small T_s .

$H_i(s)$ describes the dynamics between the transformed pseudo control and system acceleration. Again, consider the final value theorem, its step response is $\lim_{s \rightarrow 0} H_i(s) = 1$. This means that in spite of the model mismatch in $\hat{\mathbf{G}}$, the acceleration $\ddot{\boldsymbol{\theta}}$ will converge to the $\boldsymbol{\mu}$, as long as the stability condition $Re(\lambda_i) > 0.5$ is fulfilled. Thus the model uncertainties simply add stable dynamics for the linearized system in (5.8) for INDI. Besides, the settling time of the dynamics will decrease as the sampling time T_s decreases. By choosing a sufficiently high sampling rate, the bandwidth of the stable dynamics H_i can be designed to be significantly higher than the frequency of interest. This explains why the INDI is robust to model uncertainties.

The INDI-controlled MIMO system can be analyzed by the equivalent system inside the dashed box in Fig. 5.2. The pseudo control \mathbf{v} is a feedforward control with PD feedback. The stability of the feedward loop and the rejected disturbance channel can be guaranteed by satisfying the condition given in Proposition 1. The stability of the feedback loop needs to be analyzed with Nyquist criterion. For calculation convenience, the transport delay in the transfer function $H_i(s)$ can be replaced by its Padé estimation.

5.3.3. PRACTICAL IMPLEMENTATION

THE FORCE MEASUREMENT

In the INDI control law (5.7), the force increments are calculated in every sample time and added to the actuation forces \mathbf{F}_0 at the previous time sample. In previous preliminary research [1], as the hydraulic actuator dynamics are not considered, \mathbf{F}_0 was simply replaced by the stimulated force command of past history. However, in practice when hydraulic actuator dynamics do exist, the force command and the actual forces are not synchronized. Thus \mathbf{F}_0 needs to be measured. In hydraulic systems, this can be achieved using pressure sensors available at the hydraulic actuators. For systems where the force measurement is not directly available, the actuation forces need to be estimated with the actuator dynamic model.

THE ACCELERATION MEASUREMENT

The use of linear acceleration measurements $\ddot{\mathbf{q}}$ of each hydraulic cylinders is another key feature of (5.7). This is not directly available for most systems. In practice it is reconstructed by numerical differentiation of cylinder displacement measurements. Generally a low-pass filter \mathbf{H}_r is required to deal with the sensor noises and the additional dynamics. However, the phase shift introduced by the low-pass filter will jeopardize the validity of using the Taylor expansion (5.5), as \mathbf{q}_0 and \mathbf{F}_0 should be the values at the same time point t_0 . In order to synchronize these two signals, the filter \mathbf{H}_r is also added in the force measurement loop for INDI controllers in practice. As a result, the filtered measurements \mathbf{q}_f and \mathbf{F}_f are used for the control law (5.7), as illustrated in Fig. 5.3. The effectiveness of this technique have been demonstrated in a number of previous INDI applications [23, 31].

CONTROL LAW SIMPLIFICATION

The calculating of \mathbf{G}^{-1} in (5.7) requires the calculation of the inertial matrix \mathbf{M} and the Jacobian $\mathbf{J}_{q,s}$. The robustness of INDI allows us to use their roughly estimated values for the controller without compromising the performance, as long as the stability condition $Re(\lambda_i) > 0.5$ is satisfied. In practice, this can be easily fulfilled by offline design of $\hat{\mathbf{G}}$. For robot system dynamics, λ_i are always positive real numbers, since the product of two positive definite matrices ($\hat{\mathbf{G}}$ and \mathbf{G}^{-1}) has positive eigenvalues [35]. Thus the stability condition is reduced to $\lambda_i > 0.5$ for robot system dynamics. Calculations based on a high fidelity model of the SRS [29] show that even with a ± 1 m center of gravity (COG) mismatch of the upper platform in $\hat{\mathbf{G}}$, the minimum λ_i is bigger than 0.5, which guarantees the stability. This will be validated in the experiment in Section 5.5.

Also, it is verified that the stability condition leaves a big margin for the mismatch of $\mathbf{J}_{q,s}$. Again, calculations based on the model shows that a constant estimation of $\mathbf{J}_{q,s}$ in neutral position guarantees the condition $\lambda_i > 0.5$ for the entire working space of the SRS. Thus in practice, the reference generalized coordinates \mathbf{z}_d , instead of \mathbf{z} , are used to estimate \mathbf{M} and $\mathbf{J}_{q,s}$. In addition, the inertial matrix calculation can be significantly simplified by using a reduced model, neglecting the hydraulic cylinder dynamics. Experiment results in Section 5.5 validate that this simplification results in sufficiently high performance. In this way, the complicated complete system dynamics and cumbersome feedforward kinematics calculation with system state feedback can be avoided at the same time.

As a result, the practical INDI control law is given by

$$\mathbf{F} = \mathbf{F}_f + \left(\mathbf{J}_{q,s}^{-T} \mathbf{M} \mathbf{J}_{q,s}^{-1} \right)_{\mathbf{z}_d} (\mathbf{v} - \ddot{\mathbf{q}}_f), \quad (5.26)$$

where the subscript f denotes the filtered signals and d denote the reference signals. Though similar in forms, (5.26) has a different physical meaning compared with the theoretical control law (5.7), as will be illustrated in Fig. 5.3.

The control law (5.26) calculates the required actuation forces to be generated by the actuators as the inputs to the robot system. For hydraulic actuators, an inner-loop force tracking controller is necessary, as they are not direct force generators. It will be demonstrated that by combining the proposed controller with a recently reported INDI hydraulic force controller, additional advantages are introduced to the complete system.

5.3.4. INNER-LOOP INDI HYDRAULIC FORCE CONTROLLER

The hydraulic force tracking control itself is challenging due to the high nonlinear hydraulic dynamics, high stiffness and most importantly, large model and parameter uncertainties. In our previous research, the INDI technique was recently implemented for the force control, and significant control performance improvement was achieved [26]. In this chapter, the developed INDI hydraulic force controller is used as the inner-loop controller, in the following way.

Consider the hydraulic dynamics given by (5.4), the dynamic inversion of its incremental form gives the control law as

$$\mathbf{x}_m = \mathbf{x}_{m0} + \mathbf{G}_A^{-1} (\mathbf{v}_i - \dot{\mathbf{P}}_{L0}), \quad (5.27)$$

where v_i is the pseudo control of the inner-loop, x_{m0} and \dot{P}_{L0} are the measurements of valve displacement and load pressure derivative. As the result, the system is turned into a single integrator:

$$\dot{P}_L = v_i. \quad (5.28)$$

By choosing a simple proportional controller for v_i , the hydraulic system is turned into a force generator:

$$\dot{P}_L = v_i = K_{pi} (F_{ref} / A_p - P_L), \quad (5.29)$$

where F_{ref} is the desired force calculated by the outer loop motion controller. Note that practical issues should also be solved with low-pass filters in both measurement loops, the details of which can be found in [26].

So far, the complete hydraulic parallel robot is controller by the INDI based approach. It is proven and validated in [26] that the INDI controlled inner-loop system is resistant against hydraulic model and parameter uncertainties, and the augmentation of INDI to the outer-loop is a big step forward to make the complete control system also robust to uncertainties from the mechanical system. In addition, the combination of the two INDI control loops introduces new advantages to the system, which will be discussed in the next section.

5.4. CONTROL SYSTEM ANALYSIS

The diagram of the proposed dual-loop INDI control design is shown in Fig. 5.3. It is composed of an inner-loop INDI hydraulic force controller, the proposed outer-loop INDI controller for the rigid-body dynamic linearization and an outer-loop linear controller. The detailed discussion for the inner-loop can be found in [26]. The decoupling matrix \mathbf{G}^{-1} for the outer-loop is calculated based on the reference motion in the Cartesian space and a simplified inertial matrix neglecting the inertial of the legs, as proposed in (5.26). As numerical differentiation is used to estimate the actuator accelerations, it is expressed in discrete form in the z domain in the diagram. The same low-pass filter \mathbf{H}_r is placed in both the acceleration and load force measurement loops. Unique features can be concluded for the proposed controller.

5.4.1. RESISTANCE OF PRESSURE MEASUREMENT ERRORS

It can be seen from Fig. 5.3 that the required load force F_{ref} is calculated by adding the filtered load force measurement to the force increment, right before the unfiltered force measurement is subtract from it. This fact makes the control system free from constant force/pressure measurement errors. Denote the constant pressure measurement bias by λ_p , as it will directly go through the low-pass filter, the biased reference force is then

$$\mathbf{F}_b = \mathbf{F}_{ref} + A_p \lambda_p. \quad (5.30)$$

Substituting (5.30) into (5.29) for each actuator yields

$$\begin{aligned} \dot{P}_L = v_i &= K_{pi} [(F_{ref} + A_p \lambda_p) / A_p - (P_L + \lambda_p)] \\ &= K_{pi} (F_{ref} / A_p - P_L), \end{aligned} \quad (5.31)$$

which suggests that the influence of the pressure measurement bias is automatically canceled from the system. This feature is validated by experiments, by intentionally introducing measurement offsets for the pressure sensors.

It should be noted that the added and then subtracted pressure/force measurements can not be avoided, since the low-pass filter H_f needs to be placed in the former loop to synchronize it with the reconstructed leg accelerations.

5.4.2. EASY CALIBRATION

It is discussed that the INDI is resistant to model uncertainties, however, it requires the accuracy of the actuator. For the outer-loop INDI motion controller, suppose the force fault δ_f exists in the actual load force, then (5.7) becomes

$$\mathbf{F} = \mathbf{F}_0 + \mathbf{G}^{-1}(\mathbf{z}_0)(\mathbf{v} - \ddot{\mathbf{q}}_0) + \delta_f, \quad (5.32)$$

which combined with (5.6) and (5.9) gives the error dynamic equation

$$\ddot{\mathbf{e}} + \mathbf{K}_d \dot{\mathbf{e}} + \mathbf{K}_p \mathbf{e} = -\mathbf{G}(\mathbf{z}) \delta_f. \quad (5.33)$$

The force fault mainly comes from force measurement error and inner-loop force control error. As discussed previously, the force measurement errors cancel themselves with the dual-loop INDI control structure. Similar to the outer-loop, the inner-loop force control error comes mainly from its actuator fault, i.e. the valve displacement error δ_v . Similarly, In existence of δ_v , the resulting controller hydraulic pressure dynamics (5.29) becomes

$$\dot{P}_L = K_{pi}(F_{ref}/A_p - P_L) + G_A \delta_v, \quad (5.34)$$

which contribute to stationary force control error.

This suggests that there is a direct relation between the valve displacement error and the position control error, due to the fact that the controlled system is not responding to the pressure/force measurement error.

Thus in practice, the valve displacement measurements is calibrated to eliminate δ_v , as will be discussed in Section 5.5. As no pressure sensor calibration is needed, the calibration of the complete control system is straightforward and simple.

It is noted that although featured as a sensor-based approach, the proposed INDI control system does not require additional sensors besides the commonly equipped ones. The controlled system is even not affected by any constant pressure/force measurement error.

5.5. EXPERIMENTAL RESULTS

The proposed INDI motion control approach is implemented in real-life for the motion tracking tasks of a 6-DOF hydraulic parallel robot, the SRS at TU Delft. Mass offsets are added to both the physical system and the values used for the controller to test the resistance against dynamic model uncertainty. Control performance of the proposed control scheme is evaluated and compared with a baseline control scheme with model-based feedforward outer-loop controller and the same INDI inner-loop force controller, which

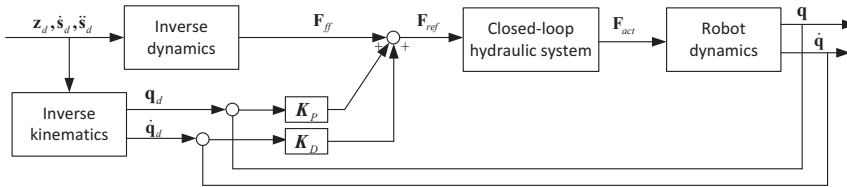


Figure 5.4: Model-based feedforward controller with PD feedback as a comparison[26].

Table 5.1: Geometrical and inertial parameters of the SRS[1]

Parameters	Value
Upper/lower gimbal radius, r_a r_b	1.6, 1.65 m
Upper/lower radius spacing, d_u d_l	0.2, 0.6 m
Piston/cylinder masses, m_2 m_1	120, 150 kg
Piston/cylinder inertia wrt cog, i_2 i_1	20, 36 $kg\ m^2$
Piston/cylinder cog wrt to gimbal, r_2 r_1	0.7, 0.5 m
Platform mass M_p	4000 kg
Platform nonzero inertia I_{xx} I_{yy} I_{zz} I_{xz}	7, 7, 8, $0.5 \times 10^3\ kg\ m^2$

is recently reported with one of the best motion tracking performance with nominal dynamic model parameters[26]. Fig. 5.4 gives a block diagram of the baseline outer-loop model-based controller.

5.5.1. HARDWARE SETUP

As a full scale 6-DOF flight simulator (Fig. 5.1), the SRS is equipped with a movable cockpit of around 4000 kg with 2 pilots capability, and six 1.25 meters stroke hydraulic servo actuators which are connected in parallel at the base frame and the upper platform. Fig. 5.1 gives the SRS motion system kinematic schematic drawing in a top view, and the corresponding geometric and key inertial parameters are given in Table 5.1. The nominal inertial parameters are identified in off-line experiments[36].

The hydraulic actuators work at a 160 bar supply pressure, each of which equipped with a Rexroth 4WSE3EE three-stage servo valve and a PAINE 210-60-090 pressure transducer. The hydraulic actuator displacements are measured by Temposonic position sensors. The motion control computer (MCC) features a dSPACE DS1005 system clocked at 1 GHz. The inner-loop controller is sampled at 5000 Hz and the outer-loop controller at 1000 Hz.

5.5.2. MOTION CONTROLLER SETUP AND CALIBRATION

In the experiments, the feedback gains for the outer-loop INDI controller is chosen as $K_P = 200 \cdot \mathbf{I}_6$ and $K_D = 30 \cdot \mathbf{I}_6$, the inner-loop gain is set to $K_{Pi} = 80$. As the position measurements are numerically differentiated twice, two second-order low-pass filters are connected in series as H_f , the natural frequency is set to 10 Hz. The filters and dif-

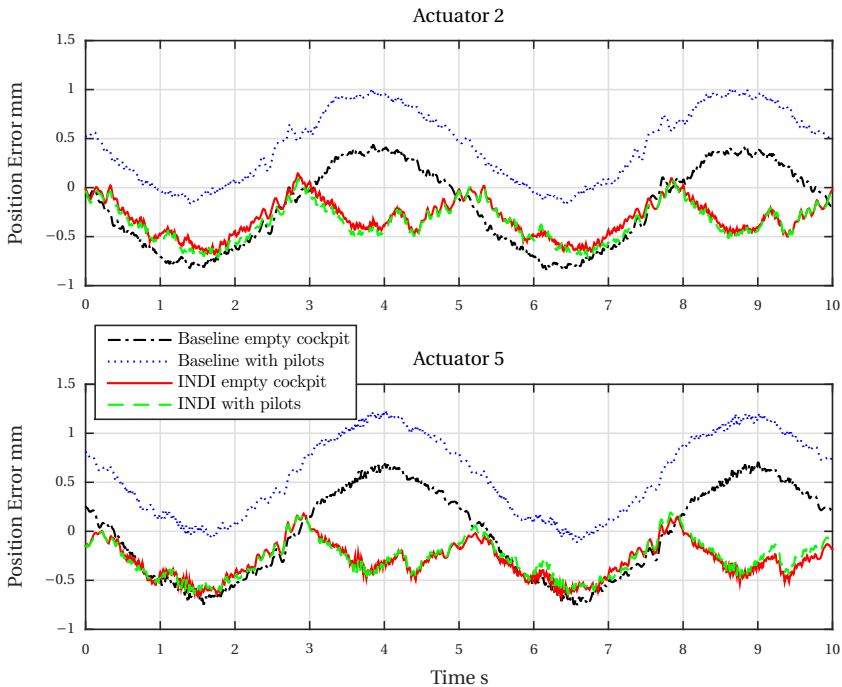


Figure 5.5: Position tracking errors for INDI and model-based feedforward controllers in nominal (empty cockpit) and mass offset (with two pilots for 221.7 kg) conditions for actuator 2 and 5.

ferentialtors are designed in the analog plane and discretized using the bilinear transformation.

5

As discussed in the previous section, the valve displacement is calibrated by adding offsets Δ_v to the valve inputs. When the system is controlled in neutral stationary position, Δ_v is tuned until the difference between the commanded and measured valve displacements coincide, as illustrated in Fig. 5.3. The stationary actuator position tracking errors are immediately minimized to the magnitude of 10^{-5} m when the calibration is finished properly. It is noted that the pressure measurement P_L in Fig. 5.3 is not calibrated at all. Additional random offsets up to 30 % of the measurement values are introduced for it to test its influences, and it turns out that the proposed control system has no response to the pressure measurement bias, as theoretically discussed in Section 5.4.

5.5.3. NOMINAL CONDITION PERFORMANCE

For both baseline and proposed controllers, a set of motion tracking tasks along the vertical axis are tested with the empty cockpit (no pilots), using nominal rigid body dynamic model parameters. The origin of the hexapod upper platform body frame is controlled to track the reference motion $z_d = 0.2 \sin 0.4\pi t$ around the neutral position. The position tracking errors of Actuator 2 and 5 with both controllers are shown in Fig. 5.5, as a rep-

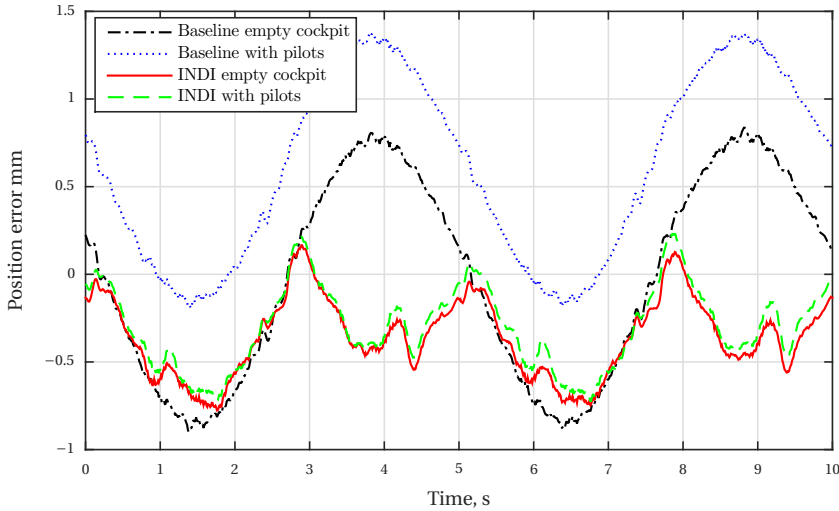


Figure 5.6: Reconstructed Cartesian space position tracking errors for INDI and the baseline model-based feedforward controllers in nominal (empty cockpit) and mass offset (with two pilots for 221.7 kg) conditions.

resentation. To evaluate the tracking performance in the Cartesian space, the values of the generalized coordinates are reconstructed by measured actuator displacements using a numerical forward kinematic algorithm. The position errors of the z axis for both controllers are shown in Fig. 5.6. Despite being different in pattern, the two controllers give similar control accuracy, with a maximum error of 0.88 mm for the computed-force controller and 0.76 mm for the INDI controller. Both controllers give sub-millimeter position accuracy for a 4000 kg hydraulic machine in a relatively large manoeuvre, the effectiveness of the proposed controller is thus validated.

5.5.4. ROBUSTNESS TO MODEL UNCERTAINTY

The motion tracking tests are repeated with two pilots sitting in the cockpit, weighing 221.7 kg in total, which contribute about 5% additional mass to the moving upper platform. The corresponding tracking errors of both controllers in the joint and Cartesian space are shown in Fig. 5.5 and Fig. 5.6, respectively. The load change makes an additional position tracking error of about 0.5 mm to the model-based controller, for which the feedback force has to increase to compensate for the biased feedforward force (see Fig. 5.4). On the other hand, the position tracking performance of the INDI controller remains intact, providing the same position error. For further validation, addition masses (metal bricks) are attached to the cockpit together with the pilots, weighing about 410 kg in total. The resulting motion tracking tests show an over 1 mm additional error for the model-based controller and intact performance for the INDI controller.

The sensitivity of the proposed control in existence of different levels of mass mismatches is then tested with the motion tracking tests. As an additional load heavier than 500 kg is not practical for the simulator and draws safety concern, the mass offsets of the

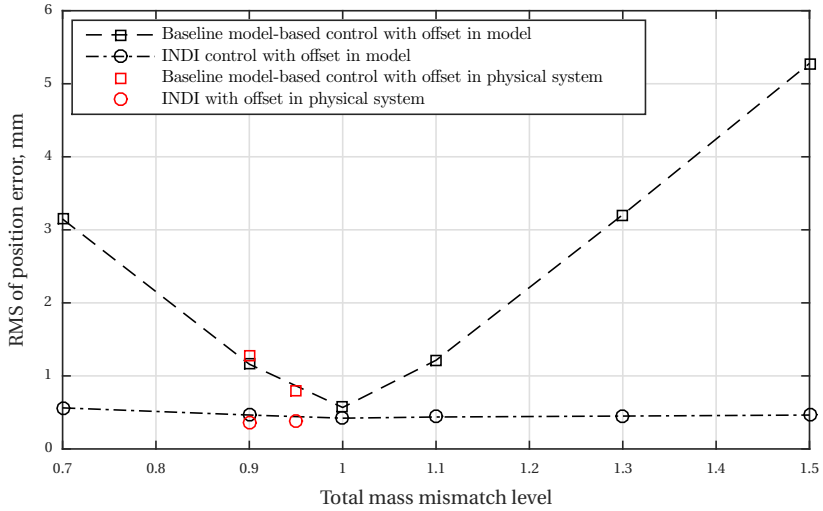


Figure 5.7: RMS of position errors for INDI and the model-based feedforward controllers under different upper-platform mass mismatch levels.

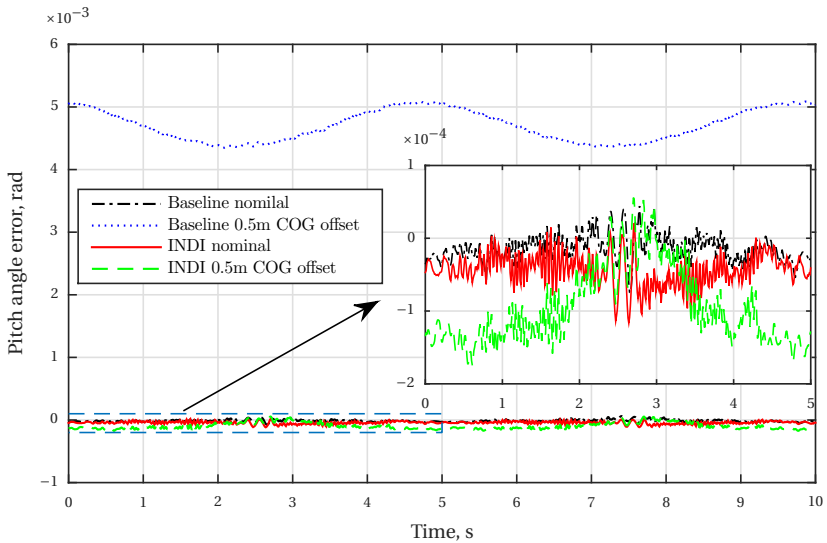


Figure 5.8: Pitch angle errors of INDI and the model-based controllers in nominal and mass COG offset conditions.

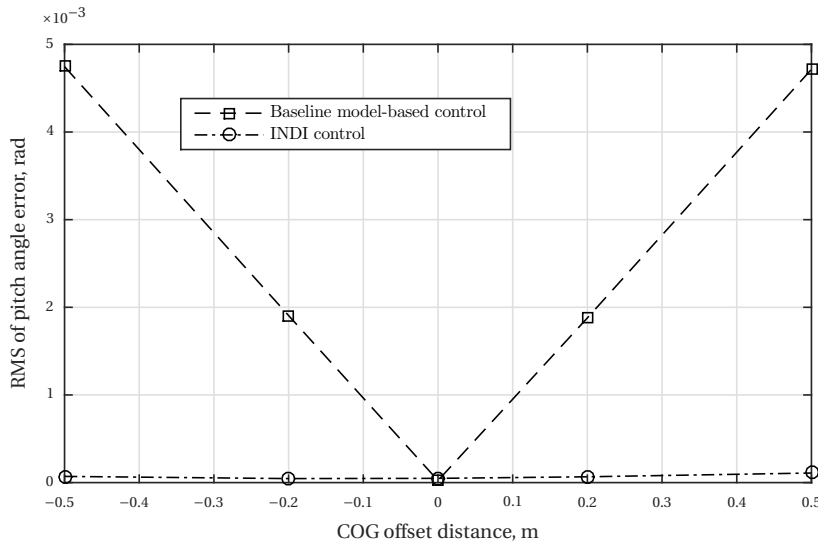


Figure 5.9: RMS of pitch angle errors of INDI and the model-based controllers at different COG offset distances.

upper platform are acted on the models used for the discussed controllers, instead of actually changing the physical system. A large range of mass offsets from -30% to +50% of the upper-platform model (3970 kg) are tested. Fig. 5.7 gives the Root-Mean-Square (RMS) of the z axis position errors for both controllers, under different levels of upper-platform mass offset, from -30% to +50%. Note that the aforementioned tests with pilots and additional masses are also presented as red dots at around -5% and -10% mass offsets (5% and 10% underestimation of the real mass), as a validation. Under the nominal condition, the baseline model-based controller gives state-of-the-art performance [26] with a RMS error of 0.56 mm. However, that quickly degrades to over 5 mm with +50% mass offsets. By contrast, the performance of the INDI controller is barely influenced by large model mismatches, with the RMS errors of 0.56 mm and 0.46 mm with -30% and +50% mass offsets, which are slightly bigger than that of 0.42 mm with nominal mass. The investigated mass offset range introduces three non-unit eigenvalues of $\hat{\mathbf{G}}\mathbf{G}^{-1}$ from about 0.7 to 1.5, for the three Euler equations of the system dynamics[29]. According to Proposition 1 and the robustness analysis in section 5.3, the INDI controller is stable and the disturbance will be inherently rejected. Thus the tracking performance is barely influenced.

In order to introduce a more asymmetrical source of dynamic model mismatch, the center of gravity (COG) of the upper-platform model is shifted away from the nominal location, which will significantly change the inertial property. For both controllers, the COG is set away from the nominal value for ± 0.2 m and ± 0.5 m along the x axis of the body frame, while the same tracking task is repeated. This mismatch setup gives direct influence on the control accuracy of the pitch angle θ . The pitch angle tracking error for both controllers in nominal and offset conditions are shown in Fig. 5.8. In nominal condition, Both controllers give good performance with the maximum pitch angle of the

magnitude of 10^{-5} rad. In the extreme case when there is 0.5 m offset of the COG, the pitch angle error of the baseline controller quickly increase to around 0.005 rad, which gives the robot a visible pitch up angle. On the other hand, the performance of the proposed dual-INDI controller is just slightly degraded, with a maximum pitch angle error of 0.00017 rad. Fig. 5.9 shows the RMS of pitch angle errors of both controllers under each COG offset setup. It is clear that high performance is maintained with the INDI controller under even unrealistic level of model mismatch, while the computed-force controller gives similar performance only with nominal parameter settings.

An estimation based on the SRS dynamic model [29] shows that a ± 1 m COG offset decreases the minimum eigenvalue of $\hat{\mathbf{G}}\mathbf{G}^{-1}$ to be around 0.5. This gives an estimation of the maximum COG offset level for stability with the typical INDI controller. Nevertheless, this limit can be easily relaxed by proportionally increasing $\hat{\mathbf{G}}$, resulting in an increased minimum eigenvalue of $\hat{\mathbf{G}}\mathbf{G}^{-1}$.

It can be summarized that the proposed dual-loop INDI controller gives the same level (slight better) of position control accuracy compared with the state-of-the-art study [26] with correct dynamic model, and significant performance improvement with considerable inertial model mismatches. The effectiveness and resistance of the proposed approach against dynamic model uncertainty is thus validated. In practice, a roughly identified and simplified model is suggested for the INDI controller design, which can avoid the cumbersome complete model identification problem for parallel robots with heavy computation load. Meanwhile, the forward kinematics are avoided by designing the control increment with reference motion profile.

5.6. CONCLUSION

This chapter presents the design and implementation of an INDI motion controller for hydraulic parallel robots. Combined with a previously developed inner-loop INDI hydraulic force controller, which is resistant against hydraulic model uncertainties, the proposed dual-loop INDI control strategy makes a big step forward by introducing INDI for the MIMO mechanical dynamics, with corresponding extended stability and robustness condition. The proposed control strategy is thus also resistant to model uncertainties from the parallel robot rigid-body dynamic models, such as inertial properties, taking advantage of which a highly computationally efficient control structure is designed, avoiding the cumbersome parameter identification and forward kinematic problems for parallel robots. The proposed controller is implemented on a full-scale hexapod flight simulator for motion tracking tests. We demonstrate higher control accuracy compared with a state-of-the-art computed-force controller with nominal dynamic model, and significant performance improvement in existence of model uncertainties, as the performance of the proposed controller is barely degraded even when extreme level of dynamic model offsets are introduced. In addition to the high performance and model uncertainty resistance features validated in this chapter, the simplicity and low computation load of the proposed control strategy makes it highly practical for other parallel robot motion systems.

REFERENCES

- [1] Y. Huang, D. M. Pool, O. Stroosma, and Q. P. Chu, “Robust incremental nonlinear dynamic inversion controller of hexapod flight simulator motion system,” in *Advances in Aerospace Guidance, Navigation and Control*. Cham: Springer International Publishing, 2018, pp. 87–99.
- [2] J.-P. Merlet, *Parallel robots*. Springer Science & Business Media, 2006.
- [3] B. Dasgupta and T. Mruthyunjaya, “The stewart platform manipulator: a review,” *Mechanism and Machine Theory*, vol. 35, no. 1, pp. 15 – 40, 2000.
- [4] J. Mattila, J. Koivumäki, and D. G. Caldwell, “A survey on control of hydraulic robotic manipulators with projection to future trends,” *IEEE/ASME Transactions on Mechatronics*, vol. 22, no. 2, pp. 669 – 680, 2017.
- [5] H. Abdellatif and B. Heimann, “Advanced model-based control of a 6-DOF hexapod robot: A case study,” *IEEE/ASME Transactions on Mechatronics*, vol. 15, no. 2, pp. 269–279, April 2010.
- [6] G. Lebret, K. Liu, and F. L. Lewis, “Dynamic analysis and control of a stewart platform manipulator,” *Journal of Robotic Systems*, vol. 10, no. 5, pp. 629–655.
- [7] B. Dasgupta and T. Mruthyunjaya, “Closed-form dynamic equations of the general stewart platform through the newton–euler approach,” *Mechanism and Machine Theory*, vol. 33, no. 7, pp. 993 – 1012, 1998.
- [8] F. Caccavale, B. Siciliano, and L. Villani, “The tricept robot: dynamics and impedance control,” *IEEE/ASME Transactions on Mechatronics*, vol. 8, no. 2, pp. 263–268, June 2003.
- [9] H. Abdellatif and B. Heimann, “Experimental identification of the dynamics model for 6-DOF parallel manipulators,” *Robotica*, vol. 28, no. 3, p. 359–368, 2010.
- [10] W. Khalil and S. Guegan, “Inverse and direct dynamic modeling of gough-stewart robots,” *IEEE Transactions on Robotics*, vol. 20, no. 4, pp. 754–761, Aug 2004.
- [11] E. Sariyildiz, H. Sekiguchi, T. Nozaki, B. Ugurlu, and K. Ohnishi, “A stability analysis for the acceleration-based robust position control of robot manipulators via disturbance observer,” *IEEE/ASME Transactions on Mechatronics*, pp. 1–1, 2018.
- [12] M. Jin, S. H. Kang, P. H. Chang, and J. Lee, “Robust control of robot manipulators using inclusive and enhanced time delay control,” *IEEE/ASME Transactions on Mechatronics*, vol. 22, no. 5, pp. 2141–2152, Oct 2017.
- [13] M. R. Sirouspour and S. E. Salcudean, “Nonlinear control of hydraulic robots,” *IEEE Transactions on Robotics and Automation*, vol. 17, no. 2, pp. 173–182, 2001.
- [14] M. Díaz-Rodríguez, A. Valera, V. Mata, and M. Valles, “Model-based control of a 3-DOF parallel robot based on identified relevant parameters,” *IEEE/ASME Transactions on Mechatronics*, vol. 18, no. 6, pp. 1737–1744, 2013.

- [15] Q. Meng, T. Zhang, X. Gao, and J. Y. Song, "Adaptive sliding mode fault-tolerant control of the uncertain stewart platform based on offline multibody dynamics," *IEEE/ASME Transactions on Mechatronics*, vol. 19, no. 3, pp. 882–894, June 2014.
- [16] F. Paccot, N. Andreff, and P. Martinet, "A review on the dynamic control of parallel kinematic machines: Theory and experiments," *The International Journal of Robotics Research*, vol. 28, no. 3, pp. 395–416, 2009.
- [17] A. Codourey, "Dynamic modeling of parallel robots for computed-torque control implementation," *The International Journal of Robotics Research*, vol. 17, no. 12, pp. 1325–1336, 1998.
- [18] B. Siciliano, L. Sciacivco, L. Villani, and G. Oriolo, *Robotics: modelling, planning and control*. Springer Science & Business Media, 2010.
- [19] D. Kostic, B. de Jager, M. Steinbuch, and R. Hensen, "Modeling and identification for high-performance robot control: an rrr-robotic arm case study," *IEEE Transactions on Control Systems Technology*, vol. 12, no. 6, pp. 904–919, Nov 2004.
- [20] M. Honegger, R. Brega, and G. Schweiter, "Application of a nonlinear adaptive controller to a 6 DOF parallel manipulator," in *Proceedings 2000 ICRA. Millennium Conference. IEEE International Conference on Robotics and Automation. Symposia Proceedings (Cat. No.00CH37065)*, vol. 2, 2000, pp. 1930–1935 vol.2.
- [21] P. Renaud, A. Vivas, N. Andreff, P. Poignet, P. Martinet, F. Pierrot, and O. Company, "Kinematic and dynamic identification of parallel mechanisms," *Control Engineering Practice*, vol. 14, no. 9, pp. 1099 – 1109, 2006.
- [22] P. Simplício, M. D. Pavel, E. van Kampen, and Q. P. Chu, "An acceleration measurements-based approach for helicopter nonlinear flight control using incremental nonlinear dynamic inversion," *Control Engineering Practice*, vol. 21, no. 8, pp. 1065 – 1077, 2013.
- [23] E. J. J. Smeur, Q. P. Chu, and Guido C. de Croon, "Adaptive incremental nonlinear dynamic inversion for attitude control of micro aerial vehicles," *Journal of Guidance, Control, and Dynamics*, vol. 39, no. 3, pp. 450–461, 2016.
- [24] F. Grondman, G. Looye, R. O. Kuchar, Q. P. Chu, and E.-J. Van Kampen, ser. AIAA SciTech Forum. American Institute of Aeronautics and Astronautics, Jan 2018, ch. Design and Flight Testing of Incremental Nonlinear Dynamic Inversion-based Control Laws for a Passenger Aircraft.
- [25] Y. Huang, D. M. Pool, O. Stroosma, Q. P. Chu, and M. Mulder, "A Review of Control Schemes for Hydraulic Stewart Platform Flight Simulator Motion Systems," in *AIAA Modeling and Simulation Technologies Conference*, January 2016.
- [26] Y. Huang, D. M. Pool, O. Stroosma, and Q. Chu, "Long-stroke hydraulic robot motion control with incremental nonlinear dynamic inversion," *IEEE/ASME Transactions on Mechatronics*, vol. 24, no. 1, pp. 304–314, Feb 2019.

- [27] T. Boaventura, J. Buchli, C. Semini, and D. G. Caldwell, "Model-based hydraulic impedance control for dynamic robots," *IEEE Transactions on Robotics*, vol. 31, no. 6, pp. 1324–1336, Dec 2015.
- [28] J. Koivumäki and J. Mattila, "Stability-guaranteed impedance control of hydraulic robotic manipulators," *IEEE/ASME Transactions on Mechatronics*, vol. 22, no. 2, pp. 601–612, April 2017.
- [29] Y. Huang, D. M. Pool, O. Stroosma, Q. P. Chu, and M. Mulder, "Modeling and Simulation of Hydraulic Hexapod Flight Simulator Motion Systems," in *AIAA Modeling and Simulation Technologies Conference*, January 2016.
- [30] H. E. Merritt, *Hydraulic control systems*. John Wiley & Sons, 1967.
- [31] Y. Huang, D. M. Pool, O. Stroosma, and Q. P. Chu, "Incremental nonlinear dynamic inversion control for hydraulic hexapod flight simulator motion systems," *IFAC-PapersOnLine*, vol. 50, no. 1, pp. 4294 – 4299, 2017, 20th IFAC World Congress.
- [32] J.-J. E. Slotine, W. Li *et al.*, *Applied nonlinear control*. Prentice hall Englewood Cliffs, NJ, 1991, vol. 199, no. 1.
- [33] A. Dòria-Cerezo and M. Bodson, "Design of controllers for electrical power systems using a complex root locus method," *IEEE Transactions on Industrial Electronics*, vol. 63, no. 6, pp. 3706–3716, June 2016.
- [34] Y. Ren, D. Su, and J. Fang, "Whirling modes stability criterion for a magnetically suspended flywheel rotor with significant gyroscopic effects and bending modes," *IEEE Transactions on Power Electronics*, vol. 28, no. 12, pp. 5890–5901, Dec 2013.
- [35] R. A. Horn, R. A. Horn, and C. R. Johnson, *Matrix analysis*. Cambridge university press, 1990.
- [36] S. Koekebakker, "Model based control of a flight simulator motion system," Ph.D. dissertation, Delft University of Technology, 2001.

6

CONCLUSION AND RECOMMENDATIONS

This thesis aims to develop a novel high precision motion control system for hydraulic parallel robots which are generally used for relatively heavy-duty applications, such as vehicle/flight simulators [1, 2], material test devices [3] or offshore stabilization systems [4]. As a case study, the developed controller is implemented on a hydraulic hexapod flight simulator, the SIMONA research simulator (SRS) at TU Delft [2].

Major challenges originate from the two main subsystems of such machines: the hydraulic actuators and the hexapod mechanism. Hydraulic actuators have highly non-linear dynamics, which suffer from serious model uncertainty problems. The hexapod mechanism, which belongs to a wider class of parallel manipulators, shares their common problem of over-complicated (or even ill-conditioned) models for a complete identification [5]. Besides, additional model uncertainties exist, such as the uncertain load mass. This fact stands in the way of further performance improvements with currently existing (mostly model-based) control strategies.

This dissertation aims at overcoming these problems and achieve much improved and robust motion control performance for general hydraulic parallel robots with an innovative sensor-based INDI control method. Hence, the research goal is formulated as

Research Goal

To develop high precision, time efficient motion control algorithms for parallel hydraulic robots, in the presence of considerable model uncertainties in both hydraulic and mechanical subsystems.

In this thesis, a state-of-the-art cascaded control structure is used, dividing the control development into an inner-loop hydraulic *force tracking* problem and an outer-loop parallel manipulator *motion tracking* problem. For this thesis, this leads to two research

questions, each associated with one of the two control loops. In this chapter, first a discussion is given on the how the research questions have been addressed by the proposed methods, then the main findings in light of the theoretical and experimental results are summarized in a final conclusion. Lastly, several recommendations are given for future work.

6.1. DISCUSSION

6.1.1. THE PHILOSOPHY OF CONTROL APPROACHES

Despite the fact that a variety of studies on either hydraulic actuator control [1, 6, 7] or parallel robot motion control [8–11] are seen in literature, only very few directly consider the combined system. For most of these studies, the mechanical dynamics and the actuator dynamics are considered coupled, and the resulting controller is generally only suitable for the specific application. This gives rise to the concern of the versatility of these studies: the developed hydraulic actuator controller should be suitable for different load dynamics, whether these are simple mass damping systems or more complicated 6-DOF manipulators, and the manipulator motion controller should also be general for different actuation methods. Thus a cascaded control system is adopted in this thesis [12, 13], separating the complete control system in two control loops. As a result, the literature survey carried out in Chapter 2 covered control approaches for both loops.

The practical development and improvement of control methods for a physical plant often follows a trend to dive into more model details of the system, from the simple feedback control, to more advanced model-based controllers for performance improvement [8, 14, 15], to adaptive controllers to tackle uncertainties [1, 16–18]. From the survey given in Chapter 2, it can be seen that the state-of-the-art hydraulic and parallel robot controller development also fits this trend. However, model-based controllers are limited in their performance improvement for both subsystems due to the unique features of the model required for this application, which are highly uncertain or highly complex. It is concluded that the effort to consider more complicated models with more elaborated identification or adaptation might not contribute much for a performance improvement for the studied system, without solving the problems like limitation of the computation ability, the ill-conditioned mechanical model and so on.

Considering the model problem of the studied systems, an opposite control philosophy comes to light, i.e., to inherently reduce the sensitivity of the control accuracy to model uncertainties. Inspired by a less-model-sensitive control approach that has been recently developed for flight control systems [19] and which shows great robustness to aircraft model uncertainties [20–22], the Incremental Nonlinear Dynamic Inversion (INDI), a cascaded control framework is proposed in Chapter 2. Designing both inner- and outer-loop controllers within the sensor-based INDI framework allows the use of roughly estimated and highly simplified models for both control loops, without compromising and even improving performance.

6.1.2. THE MODULAR PHYSICAL MODEL: MORE THAN A TEST BED

The requirements for mathematical models of physical systems vary, based on the model's purposes. For controller development, a suitable model generally needs to meet several

(sometimes contradictory) constrains. On the one hand, the model should reflect as much relevant physical details as possible. On the other hand, it is also favorable to be as simple as possible for controller design and parameter identification (or adaptation). Hence, in practical research applications one often sees significant model simplifications for the controller design, with which only the most relevant system characteristics remain.

When developing models for the purpose of numerical simulation, the requirement is more straightforward, as here the resemblance to the physical system is of most importance. Actually, as this dissertation aims at developing a less model dependent controller for the hydraulic parallel robot system, it requires a higher fidelity from the model for simulation, to be able to verify the simplifications made in the designing controller and to validate the robustness to modeling errors. Thus in Chapter 3, a detailed system model based on physical laws is developed for the SRS, which explicitly includes critical nonlinear characteristics of the servo-valves, oil transmission lines, hydraulic actuators and the rigid-body parallel mechanism.

The developed nonlinear model then serves as a test bed for the proposed control system for verification and performance evaluation before the real-world experiments. As particular assumptions should be made for the proposed control strategy, such as fast actuator dynamics and fast state measurement, the physical model also helps to identify which part of the system dynamics may violate those assumptions, such that suitable solutions can be developed. For that purpose, the model is made modular. The complete system is divided into a few subsystems, each of which are modelled as a module. By neglecting or replacing a certain module with simplified linear dynamics, the effects of the corresponding nonlinear phenomena on the response of the controller can then be identified.

The model was validated by comparing the simulation results with available experiment data [23] on the response of the current model-based ‘cascaded ΔP (CdP) controller [12, 24], which acts as a baseline for this thesis. For both the developed inner- and outer-loop INDI controllers, the simulation results successfully predict the motion tracking performance of the later experiments. For instance, the unstable resonance at around 200 Hz for the inner-loop force controller, which is caused by the oil transmission line dynamics, was identified by the model with effective solutions (see Chapter 4). The basic assumptions of the proposed INDI controllers were validated for the studied system with the model, under the designed 5000 Hz inner-loop sampling rate and 1000 Hz outer-loop sampling rate. The practical controller verified by the model was successfully implemented on the SRS, with consistent control performance.

6.1.3. THE INNER-LOOP HYDRAULIC FORCE CONTROLLER

In the proposed framework of a cascaded hydraulic robot control structure, the first step is developing a high precision inner-loop force tracking controller for the hydraulic actuators. As concluded by the survey in Chapter 2, model-based control for hydraulic systems faces serious model uncertainty problems, caused by various nonlinear phenomena such as wear-out and dead zone of the servo-valve, nonlinear frictions and leakages and the possibly time-varying oil bulk modulus, which changes with system temperature variation. Facing these problems, this thesis first aimed at answering the following

research question:

Research Question 1

How to achieve *less model dependent* nonlinear **force/torque tracking control** for the hydraulic actuators with high performance, even when subjected to large hydraulic model uncertainties and disturbances?

This research question is addressed with the theoretical and practical development of a hydraulic force tracking controller based on the sensor-based Incremental Nonlinear Dynamic Inversion (INDI) technique. Instead of depending on a detailed nonlinear system model, like traditional model-based controllers, INDI depends only on the control input related part of the model, replacing the information of the remaining part by the required state measurements, which are generally available for hydraulic actuators with oil pressure feedback.

Chapter 4 gives a detailed description of the typical INDI-based controller design procedure. *In theory*, the robustness of INDI to parameter uncertainties in the control input-related part of the model is proven for the first time, with a necessary condition for stability, which gives requirements on the parameter mismatch level. Practically, the INDI method is adapted for the hydraulic system, solving practical problems such as servo-valve dynamics, state derivative reconstruction, and oil transmission line dynamics. Acting as the actuator of the hydraulic system, the servo-valve output is assumed to be available for measurement, otherwise an identified model of it should be used. As the developed controller needs the derivative of the measured states, practical numerical differentiation is used in this research. The resulting signal noise problem is solved by a practical low-pass filter, which also acts as a way to attenuate the transmission line dynamics.

The proposed controller is first verified by *numerical simulation*, based on the nonlinear model developed in Chapter 3. As a fast sampling rate is a main assumption of INDI, control performances under different sampling frequencies, from 500 Hz to 5000 Hz are investigated with simulated high sensor noise levels. It is verified that all settings give stable tracking results, while a slower sampling rate tends to give more vibrating control performance. Thus the highest practical sampling rate, 5000 Hz, is chosen for the later developed controller for the real-world implementation. The robustness of the controller against parameter uncertainties and external disturbances is also verified by introducing significant levels of parameter offsets and supply pressure disturbances to the simulation model. The simulation results show high control performance under unrealistic levels (i.e., up to 50%) of model mismatch and disturbance, which is one (or more) order(s) of magnitude better than the baseline model-based controller.

With the verification from the simulation results, the developed controller is implemented on a real-world hydraulic robot, the SRS at TU Delft, as the inner-loop hydraulic force controller for motion tracking experiments. A traditional 'feedforward plus PD feedback' controller is used for the outer-loop. Different motion profiles are executed, exploring up to about 70% of the maximum stroke and velocity of the actuators. Compared with a baseline model-based hydraulic force controller, the force tracking accuracy for the proposed controller is improved by 10 times with nominal parameters. Even

under significant levels (up to 50%) of model mismatches, the performance of the proposed inner-loop controller remains intact, while that of the baseline controller quickly degrades by over 10 times. With the high performance inner-loop controller, the resulting overall motion control system achieves world-class performance. For a heavy hydraulic machine weighing about 4000 kg, sub-millimeter position tracking error is achieved in high dynamic manoeuvres. Compared with the best state-of-the-art controllers in literature [25], the control accuracy of the developed control system is about three times better in terms of a standard performance indicator (see Chapter 4).

6.1.4. SENSOR BASED OUTER-LOOP MOTION CONTROLLER

The outer-loop motion control of parallel robots also suffers from modeling problems of the complex multibody dynamics. Unlike their serial counterparts, for parallel manipulators, suitable closed-form models for complete parameter identification are generally not available, due to their complex structure with multiple closed chains. This often leads to significant model simplifications according to the specific manipulator structures (such as negligible masses), which might not be suitable for a general 6-DOF parallel mechanism. This suggests that the effort to increase the model-based control performance with a more accurate parallel manipulator model is inherently not practical, not to mention the effects of a time-varying load mass acting as a disturbance. Facing these difficulties, a non-model-dependent outer-loop motion controller is developed by answering the following research question:

Research Question 2

How to achieve *less model dependent* and high precision **motion control** for general parallel manipulators with large dynamic model offsets and disturbances?

The research question is answered by developing the sensor-based INDI control framework for the general parallel manipulator. Furthermore, it achieved real-world application on the 6-DOF hexapod flight simulator, the SRS. In the mathematical development it is shown that without full knowledge of the model, the proposed INDI controller achieves full input-output linearization like traditional feedback linearization achieves with a precise model. This allows for high performance motion control using a significantly simplified manipulator model and an uncertain load mass.

Chapter 5 proposed an INDI-based motion control system for parallel manipulators in joint space, which is directly combined with the inner-loop hydraulic force controller developed in Chapter 4, as a completion of the proposed cascaded control structure. As an application for MIMO case, the robustness proof of INDI given in Chapter 4 is extended for general MIMO systems, with a refined stability condition. The joint space controller design avoids the state measurement problem in Cartesian space and the forward kinematic problem for parallel manipulators. As a typical INDI controller is dependent on the state derivative measurement, the developed motion controller requires the feedback of the acceleration information of the actuators, which is generally not directly available. This is practically achieved by numerical differentiation of the actuator displacement measurement with low-pass filters.

By directly combining the developed INDI motion controller with the inner-loop

hydraulic INDI controller proposed in Chapter 4, the motion control system is completed with a dual-INDI structure. The complete dual-INDI cascaded control structure is implemented on the SRS for experimental validation after successful simulation verification. The control performance is compared with the traditional feedforward plus PD feedback outer-loop controller used in Chapter 4 (as the baseline), which already achieved state-of-the-art performance with nominal model parameters. Slightly better control accuracy is demonstrated by the proposed INDI controller compared with the baseline controller in nominal conditions, showing sub-millimeter maximum position tracking errors. In model mismatch cases, the dual-INDI controller shows great robustness to inertial offsets, with almost intact performance under 50% upper platform mass offset and 0.5 meter center of gravity (COG) shift. In comparison, the performance of the baseline controller quickly degrades by over 10 times with the same levels of parameter offsets. One additional benefit of the dual-INDI controller is that despite the fact that it is featured as a sensor-based approach, it is even robust to any constant pressure/force measurement error, due to the unique dual-INDI structure, as shown in Chapter 5.

6.2. FINAL CONCLUSIONS

With the two research questions answered, the research goal of the thesis is achieved. With a cascaded control framework, both hydraulic and mechanic subsystems are controlled by sensor-based INDI controllers, with practical issues solved. The resulting inner- and outer-loop controllers are designed individually, thus they are decoupled and modular, which allows for their applications in other control tasks or structure techniques. A direct combination of both results in the dual-INDI motion control system for hydraulic parallel robots, developed in Chapter 5 of this thesis. The resulting controller uses little model information from both subsystems, and is inherently robust to the existing model uncertainties.

The finally developed dual-INDI control system achieves significantly better control performance than the (mostly model-based) state-of-the-art control techniques described in literature, for both force tracking and position tracking tests on the SRS. The experiment results show a great agreement with the simulation results, validating the high fidelity of the developed nonlinear model.

The robustness of the INDI control technique for general MIMO nonlinear systems is proven in theory, with accompanying stability conditions limited by the parameter mismatch level. In practice, extreme levels (up to 50%) of model parameter mismatch for the hydraulic fluid features and manipulator inertial characteristics are introduced in simulation and real-world experiments for robustness validation, together with existence of unmodeled nonlinear features such as nonlinear leakages and frictions. The performance of the developed INDI control system remains virtually intact, i.e., showing extreme robustness to model uncertainties.

For the practitioners, the proposed controller is also computationally time efficient. Thanks to the avoidance of using a full system model, the computational load of INDI is similar to that of a PID controller. The controller design and tuning procedures are also straightforward and simple. Besides, this thesis gives a comprehensive guideline with solutions for practical issues, such as sampling rate requirements, state derivative estimation, actuator dynamics, and even unmodeled dynamics in the measurement loop.

Thanks to the cascaded structure, the developed techniques can be applied to more general applications, such as serial manipulators or robots driven by electrical actuators.

6.3. RECOMMENDATIONS AND FUTURE WORK

The research discussed in this thesis addresses several control limitations due to the physical characteristics of the implemented hardware, while also giving rise to new research directions. In light of the scope and the further opportunities revealed by this thesis, some recommendations for the future work on advanced hydraulic robot control are given in this section.

For the inner-loop force controller, the modelling, analysis, controller design and implementation are based on the symmetric hydraulic actuators, which are equipped on the SRS. For more general applications such as asymmetric single-rod hydraulic actuators [26], the proposed controller needs to be modified. As the areas of the two hydraulic chambers are different, the actuation force is no longer proportional to the pressure difference. In this case, as the force measurement plays an essential role for the proposed controller, pressure measurements of both chambers are necessary. Besides, the controller needs to include the resulting more complex pressure dynamic equations.

In the proposed practical INDI-based controllers, the required system state derivatives are estimated by numerical differentiation, together with second order low-pass filters to attenuate effects of sensor noise. The relatively low bandwidth of the filters influences the frequency characters of the closed loop system. In future work, the possible use of more advanced state derivative estimation techniques, such as Kalman filters, should be considered. Besides, with the development of advanced sensors, it is recommended to use direct measurements of the state derivatives. For instance, the use of angular accelerometers which directly provide angular acceleration measurements of the applied system.

The proposed and implemented cascaded control system has a complex multiple-loop structure. Both the inner-loop and outer-loop controller have additional linear control loops outside the INDI linearization loops. Thus, even though the INDI control loop itself requires minimum gain tuning efforts, the gain combination for the multiple control loops was still designed by heuristic tuning. In order to achieve the optimal frequency response of the complete system, a systematic multi-loop gain optimization for the proposed cascade control system is recommended for future work.

Despite that it is featured as a sensor-based controller, which is not dependent on the precise model, the proposed dual-INDI control system in Chapter 5 is even free from constant pressure sensor errors, which largely simplified the calibration workload. However, the controller is still sensitive to servo-valve opening errors, which requires careful calibration for its measurement, as otherwise a constant control error will remain. This is caused by the inherent feature of INDI, that is, being sensitive to the actuator error. This problem should be resolved in theory and practice, since actuator errors exist in every real-world application. A possible solution is to use the dynamic model of the actuator for its output feedback, which makes the controller less sensitive to the output measurement.

In this thesis, the control system is only designed for free motion applications, as the studied flight simulator system works in free space. However, for more advanced appli-

cations where the robot needs to interact with the environment, such as legged robots, force control is necessary for the resulting constrained motion cases [27]. This gives new opportunities for extending the proposed INDI controller to force control tasks, possibly bringing its inherent advantages, such as high precision and good disturbance rejection properties.

In addition, further relevant applications for the developed INDI controllers should be studied, such as motion systems of offshore stabilizing platforms. In this thesis, as the studied case is an indoor machine, only inherent parameter offsets are considered for the robustness test. For possible future applications on outdoor machines, the robustness against external disturbances (such as wind disturbance for offshore machines) for the INDI control system should also be investigated.

REFERENCES

- [1] M. R. Sirouspour and S. E. Salcudean, "Nonlinear control of hydraulic robots," *IEEE Transactions on Robotics and Automation*, vol. 17, no. 2, pp. 173–182, 2001.
- [2] O. Stroosma, M. M. van Paassen, and M. Mulder, "Using the SIMONA Research Simulator For Human-Machine Interaction Research," in *AIAA Modeling and Simulation Technologies Conference and Exhibit*, 2003.
- [3] TU Delft, "TU Delft ready to unleash the beast," <https://www.tudelft.nl/en/3me/research/check-out-our-science/tu-delft-ready-to-unleash-the-beast/>, accessed: 2018-07-10.
- [4] Ampelmann, "Safe and efficient people transfer," <https://www.ampelmann.nl/systems/a-type>, accessed: 2018-07-10.
- [5] M. Díaz-Rodríguez, A. Valera, V. Mata, and M. Valles, "Model-based control of a 3-dof parallel robot based on identified relevant parameters," *IEEE/ASME Transactions on Mechatronics*, vol. 18, no. 6, pp. 1737–1744, Dec 2013.
- [6] T. Boaventura, J. Buchli, C. Semini, and D. G. Caldwell, "Model-based hydraulic impedance control for dynamic robots," *IEEE Transactions on Robotics*, vol. 31, no. 6, pp. 1324–1336, Dec 2015.
- [7] J. Koivumäki and J. Mattila, "High performance nonlinear motion/force controller design for redundant hydraulic construction crane automation," *Automation in Construction*, vol. 51, pp. 59 – 77, 2015. [Online]. Available: <http://www.sciencedirect.com/science/article/pii/S0926580514002581>
- [8] H. Abdellatif and B. Heimann, "Advanced model-based control of a 6-dof hexapod robot: A case study," *IEEE/ASME Transactions on Mechatronics*, vol. 15, no. 2, pp. 269–279, April 2010.
- [9] M. Díaz-Rodríguez, A. Valera, V. Mata, and M. Valles, "Model-based control of a 3-dof parallel robot based on identified relevant parameters," *IEEE/ASME Transactions on Mechatronics*, vol. 18, no. 6, pp. 1737–1744, Dec 2013.

- [10] L. Ren, J. K. Mills, and D. Sun, "Experimental comparison of control approaches on trajectory tracking control of a 3-dof parallel robot," *IEEE Transactions on Control Systems Technology*, vol. 15, no. 5, pp. 982–988, Sept 2007.
- [11] P. H. Chang and J. H. Jung, "A systematic method for gain selection of robust pid control for nonlinear plants of second-order controller canonical form," *IEEE Transactions on Control Systems Technology*, vol. 17, no. 2, pp. 473–483, March 2009.
- [12] J. Heintze and A. van der Weiden, "Inner-loop design and analysis for hydraulic actuators, with an application to impedance control," *Control Engineering Practice*, vol. 3, no. 9, pp. 1323 – 1330, 1995.
- [13] S. Koekebakker, "Model based control of a flight simulator motion system," Ph.D. dissertation, Delft University of Technology, 2001.
- [14] G. Vossoughi and M. Donath, "Dynamic feedback linearization for electrohydraulically actuated control systems," *ASME. J. Dyn. Sys., Meas., Control.*, vol. 117, no. 4, pp. 468–477, 1995.
- [15] F. Kock and C. Ferrari, "Flatness-based high frequency control of a hydraulic actuator," *Journal of Dynamic Systems, Measurement, and Control*, vol. 134, no. 2, p. 021003, 2012.
- [16] J. Koivumäki and J. Mattila, "High performance non-linear motion/force controller design for redundant hydraulic construction crane automation," *Automation in construction*, vol. 51, pp. 59–77, 2015.
- [17] M. Namvar and F. Aghili, "A combined scheme for identification and robust torque control of hydraulic actuators," *Journal of Dynamic Systems, Measurement, and Control*, vol. 125, no. 4, pp. 595–606, Jan 2004. [Online]. Available: <http://dx.doi.org/10.1115/1.1636777>
- [18] M. Honegger, A. Codourey, and E. Burdet, "Adaptive control of the hexaglide, a 6 dof parallel manipulator," in *Proceedings of International Conference on Robotics and Automation*, vol. 1, April 1997, pp. 543–548 vol.1.
- [19] S. Sieberling, Q. P. Chu, and J. A. Mulder, "Robust Flight Control Using Incremental Nonlinear Dynamic Inversion and Angular Acceleration Prediction," *Journal of Guidance, Control, and Dynamics*, vol. 33, no. 6, pp. 1732–1742, nov 2010.
- [20] P. Simplicio, M. D. Pavel, E. van Kampen, and Q. P. Chu, "An acceleration measurements-based approach for helicopter nonlinear flight control using incremental nonlinear dynamic inversion," *Control Engineering Practice*, vol. 21, no. 8, pp. 1065 – 1077, 2013.
- [21] E. J. J. Smeur, Q. P. Chu, and de Croon, Guido C., "Adaptive Incremental Nonlinear Dynamic Inversion for Attitude Control of Micro Aerial Vehicles," *Journal of Guidance, Control, and Dynamics*, vol. 39, no. 3, pp. 450–461, 2016.

- [22] F. Grondman, G. Looye, R. O. Kuchar, Q. P. Chu, and E.-J. Van Kampen, ser. AIAA SciTech Forum. American Institute of Aeronautics and Astronautics, Jan 2018, ch. Design and Flight Testing of Incremental Nonlinear Dynamic Inversion-based Control Laws for a Passenger Aircraft.
- [23] I. Miletović, D. Pool, O. Stroosma, M. van Paassen, and Q. Chu, “Improved Stewart platform state estimation using inertial and actuator position measurements,” *Control Engineering Practice*, vol. 62, no. Supplement C, pp. 102 – 115, 2017.
- [24] G. van Schothorst, P. Teerhuis, and A. van der Weiden, “Stability analysis of a hydraulic servo-system including transmission line effects,” in *Proceedings of the Third International conference on Automation, Robotics and Computer Vision, Singapore*, 1994, pp. 1919–1923.
- [25] J. Mattila, J. Koivumäki, and D. G. Caldwell, “A survey on control of hydraulic robotic manipulators with projection to future trends,” *IEEE/ASME Transactions on Mechatronics*, vol. 22, no. 2, pp. 669 – 680, 2017.
- [26] F. Bu and B. Yao, “Observer based coordinated adaptive robust control of robot manipulators driven by single-rod hydraulic actuators,” in *Proceedings 2000 ICRA. Millennium Conference. IEEE International Conference on Robotics and Automation. Symposia Proceedings (Cat. No.00CH37065)*, vol. 3, 2000, pp. 3034–3039 vol.3.
- [27] B. Siciliano, L. Sciavicco, L. Villani, and G. Oriolo, *Robotics: modelling, planning and control*. Springer Science & Business Media, 2010.

A

INCREMENTAL NONLINEAR DYNAMIC INVERSION

This appendix presents a general derivation and discussion of Incremental Nonlinear Dynamic Inversion (INDI) control technique for a general control affine nonlinear system.

INDI is inherently a variant of the input-output Linearization (or input-output decoupling) approach, which can reduce the sensitivity to parameter uncertainties compared to traditional input-output Linearization.

Consider a nonlinear control inputs affine system given by

$$\begin{aligned}\dot{\mathbf{x}} &= \mathbf{f}(\mathbf{x}) + \mathbf{G}(\mathbf{x}) \mathbf{u} \\ \mathbf{y} &= \mathbf{h}(\mathbf{x}),\end{aligned}\tag{A.1}$$

where, $\mathbf{x} \in \mathbb{R}^n$, $\mathbf{u} \in \mathbb{R}^m$, $\mathbf{y} \in \mathbb{R}^m$, $\mathbf{f}: \mathbb{R}^n \rightarrow \mathbb{R}^n$, $\mathbf{h}: \mathbb{R}^n \rightarrow \mathbb{R}^m$, $\mathbf{G}: \mathbb{R}^n \rightarrow \mathbb{R}^{n \times m}$. $\mathbf{f}(\mathbf{x})$, $\mathbf{G}(\mathbf{x})$ and $\mathbf{h}(\mathbf{x})$ are assumed to be \mathcal{C}^∞ functions of \mathbf{x} and all degrees of differentiation are bounded. The j th column of \mathbf{G} is denoted by \mathbf{g}_j and the i th row of \mathbf{h} is denoted by \mathbf{h}_i .

For a typical input-output linearization, we take the derivative of \mathbf{y}_i , until at least one of the control inputs \mathbf{u}_i explicitly appears. If ρ_i is the minimal integer such that the following satisfies

$$\begin{aligned}\mathcal{L}_{\mathbf{g}_j} \left(\mathcal{L}_{\mathbf{f}}^k (\mathbf{h}_i(\mathbf{x})) \right) &= 0, & \forall \mathbf{x} \in \mathbb{R}^n, k = 0, 1, \dots, \rho_i - 2, \\ \mathcal{L}_{\mathbf{g}_j} \left(\mathcal{L}_{\mathbf{f}}^{\rho_i - 1} (\mathbf{h}_i(\mathbf{x})) \right) &\neq 0, & \forall \mathbf{x} \in \mathbb{R}^n.\end{aligned}\tag{A.2}$$

then the ρ_i -th time derivative of \mathbf{y}_i is

$$\mathbf{y}_i^{\rho_i} = \mathcal{L}_{\mathbf{f}}^{\rho_i} (\mathbf{h}_i(\mathbf{x})) + \sum_{j=1}^m \mathcal{L}_{\mathbf{g}_j} \left(\mathcal{L}_{\mathbf{f}}^{\rho_i - 1} (\mathbf{h}_i(\mathbf{x})) \right) \mathbf{u}_j.\tag{A.3}$$

where $\mathcal{L}_{\mathbf{f}}(*)$ and $\mathcal{L}_{\mathbf{g}_j}(*)$ are the Lie derivatives of the vector along $\mathbf{f}(\mathbf{x})$ and \mathbf{g}_j , respectively.

Defining the vector $\boldsymbol{\rho} = [\rho_1, \dots, \rho_m]$ as the relative degree vector of the system, the total relative degree of the system is equal to $r = \sum_{j=1}^m \rho_j$. Eq. (A.3) can be written in matrix form

$$\mathbf{y}^{\boldsymbol{\rho}} = \mathbf{a}(\mathbf{x}) + \mathbf{B}(\mathbf{x}) \mathbf{u},\tag{A.4}$$

where

$$\mathbf{a}(\mathbf{x}) = \left[\mathcal{L}_{\mathbf{f}}^{\rho_1} (\mathbf{h}_1(\mathbf{x})), \dots, \mathcal{L}_{\mathbf{f}}^{\rho_m} (\mathbf{h}_m(\mathbf{x})) \right]^T,\tag{A.5}$$

and

$$\mathbf{B}(\mathbf{x}) = \begin{bmatrix} \mathcal{L}_{\mathbf{g}_1} \left(\mathcal{L}_{\mathbf{f}}^{\rho_1 - 1} (\mathbf{h}_1(\mathbf{x})) \right) & \dots & \mathcal{L}_{\mathbf{g}_m} \left(\mathcal{L}_{\mathbf{f}}^{\rho_1 - 1} (\mathbf{h}_1(\mathbf{x})) \right) \\ \vdots & & \vdots \\ \mathcal{L}_{\mathbf{g}_1} \left(\mathcal{L}_{\mathbf{f}}^{\rho_m - 1} (\mathbf{h}_m(\mathbf{x})) \right) & \dots & \mathcal{L}_{\mathbf{g}_m} \left(\mathcal{L}_{\mathbf{f}}^{\rho_m - 1} (\mathbf{h}_m(\mathbf{x})) \right) \end{bmatrix}\tag{A.6}$$

Until here, INDI is identical to the input-output linearization technique, the difference comes as follows. Typical input-output linearization uses an inverse of Eq. (A.4) as

$$\mathbf{u} = \mathbf{B}^{-1}(\mathbf{x}) [\mathbf{v} - \mathbf{a}(\mathbf{x})],\tag{A.7}$$

which requires that the $m \times m$ matrix $\mathbf{B}(\mathbf{x})$ is not singular. Thus the system can be linearized to be $\mathbf{y}^{\boldsymbol{\rho}} = \mathbf{v}$. This requires a full knowledge of $\mathbf{a}(\mathbf{x})$ and $\mathbf{B}(\mathbf{x})$ and thus the input-output linearization is very sensitive to parameter uncertainties. The INDI approach is

proposed to reduce the sensitivity of system parameter uncertainty. The basic idea is to replace the model of the right side of Eq. (A.4) by the sensor measurement of its left side, with the assumption of a sufficiently accurate measurement.

This is achieved by writing Eq. (A.4) in a Taylor expansion around the beginning instant of **every** control sampling period (denoted by subscript 0):

$$\mathbf{y}^\rho = \mathbf{y}_0^\rho + \mathbf{B}(\mathbf{x}_0)(\mathbf{u} - \mathbf{u}_0) + \left. \frac{\partial[\mathbf{a}(\mathbf{x}) + \mathbf{B}(\mathbf{x})\mathbf{u}]}{\partial \mathbf{x}} \right|_0 (\mathbf{x} - \mathbf{x}_0) + \mathbf{O}((\mathbf{x} - \mathbf{x}_0)^2). \quad (\text{A.8})$$

Note that the subscript 0 does not denote a particular fixed equilibrium point. Now assume that \mathbf{y}_0^ρ can be measured or estimated, and define the last two terms of Eq. (A.8) as a disturbance term $\boldsymbol{\delta}$:

$$\boldsymbol{\delta}(\Delta \mathbf{x}) = \left. \frac{\partial[\mathbf{a}(\mathbf{x}) + \mathbf{B}(\mathbf{x})\mathbf{u}]}{\partial \mathbf{x}} \right|_0 (\mathbf{x} - \mathbf{x}_0) + \mathbf{O}((\mathbf{x} - \mathbf{x}_0)^2), \quad (\text{A.9})$$

where $\Delta \mathbf{x} = \mathbf{x} - \mathbf{x}_0$. Thus Eq. (A.8) becomes

$$\mathbf{y}^\rho = \mathbf{y}_0^\rho + \mathbf{B}(\mathbf{x}_0)(\mathbf{u} - \mathbf{u}_0) + \boldsymbol{\delta}(\Delta \mathbf{x}). \quad (\text{A.10})$$

As $\dot{\mathbf{x}}$ exists everywhere and \mathbf{x} is continuous, $\boldsymbol{\delta}$ approaches zero as the time interval between \mathbf{x} and \mathbf{x}_0 , defined by T_s , approaches zero, because

$$\lim_{T_s \rightarrow 0} \boldsymbol{\delta}(\Delta \mathbf{x}) = \lim_{T_s \rightarrow 0} \left. \frac{\partial[\mathbf{a}(\mathbf{x}) + \mathbf{B}(\mathbf{x})\mathbf{u}]}{\partial \mathbf{x}} \right|_0 (\mathbf{x} - \mathbf{x}_0) + \lim_{T_s \rightarrow 0} \mathbf{O}((\mathbf{x} - \mathbf{x}_0)^2) = 0 \quad (\text{A.11})$$

Based on Eq. (A.10) and (A.11), the INDI control law is designed in an **incremental** form as

$$\mathbf{u} = \mathbf{u}_0 + \mathbf{B}^{-1}(\mathbf{x}_0)(\mathbf{v} - \mathbf{y}_0^\rho) \quad (\text{A.12})$$

which means that, at every next control sampling interval, \mathbf{u} is updated by adding the calculated control increment $\Delta \mathbf{u} = \mathbf{B}^{-1}(\mathbf{x}_0)(\mathbf{v} - \mathbf{y}_0^\rho)$ to \mathbf{u}_0 , its value at the beginning instance of the period. The update frequency is chosen with a designed small control sample period T_s . Note here that the measurement of \mathbf{y}_0^ρ is assumed available, and no explicit use of $\mathbf{a}(\mathbf{x})$ appears, because most of its information is already contained in \mathbf{y}_0^ρ . **Thus, INDI uses the inverse of the $m \times m$ matrix $\mathbf{B}(\mathbf{x}_0)$, which is required to be non-singular.** For a discrete control system, Eq. (A.12) can be written in a more explicit and iterative form:

$$\mathbf{u}_k = \mathbf{u}_{k-1} + \mathbf{B}^{-1}(\mathbf{x}_{k-1})(\mathbf{v}_k - \mathbf{y}_{k-1}^\rho) \quad (\text{A.13})$$

Substituting Eq. (A.12) into (A.10) we obtain

$$\mathbf{y}^\rho = \mathbf{v} + \boldsymbol{\delta}(\Delta \mathbf{x}) \quad (\text{A.14})$$

in which, according to Eq. (A.11), the defined disturbance term $\boldsymbol{\delta}(\Delta \mathbf{x})$ approaches 0 when choosing a sufficiently small control sampling period T_s .

By choosing each row of the virtual control \mathbf{v} in Eq. (A.14) to be

$$v_i = y_{d_i}^{\rho_i} + k_{1_i} \left(y_{d_i}^{\rho_i-1} - \mathcal{L}_f^{\rho_i-1} h_i(\mathbf{x}) \right) + \dots + k_{\rho_i} (y_{d_i} - h_i(\mathbf{x})), \quad (\text{A.15})$$

the controlled system error dynamics become

$$e_i^{\rho_i} + k_{1i}e_i^{\rho_i-1} + \dots + k_{\rho_i}e_i = \delta_i(\Delta\mathbf{x}). \quad (\text{A.16})$$

where e_i is the error between the desired trajectory y_{d_i} and the i th output, i.e. $e_i = y_i - y_{d_i}$.

For an ideal infinitely fast control sampling frequency, $\delta_i(\Delta\mathbf{x}) \rightarrow 0$ as $T_s \rightarrow 0$, thus by choosing the parameters $k_{1i}, \dots, k_{\rho_i}$ to be Hurwitz, the controlled error dynamics Eq. (A.16) are asymptotically stable and e_i goes to zero.

For a practical small $T_s > 0$, Eq. (A.11) suggest that $\forall \varepsilon > 0, \exists T_s > 0$, s.t. $\|\delta(\Delta\mathbf{x})\|_2 \leq \varepsilon$. Thus again by choosing the parameters $k_{1i}, \dots, k_{\rho_i}$ to be Hurwitz, the error e_i will be globally ultimately bounded by εc for some $c > 0$. The ultimate bound can be decreased with a high sampling rate, instead of high gains of traditional feedback controllers.

Besides, $\delta_i(\Delta\mathbf{x})$ is bounded by a small value (decided by T_s) during tracking behavior when the system is in motion. When the system is stabilized at a particular point, $\delta_i(\Delta\mathbf{x}) = 0$, so the error truly goes to zero. This is why for the simulation and experiment results when the system is stationary, the controlled system shows a similar behaviour of asymptotic stability, and the error only shows up when the system is in motion.

From this respect, the INDI approach removes the reliance of traditional input-output linearization on model information of $\mathbf{a}(\mathbf{x})$ in Eq. (A.7), as no such model is explicitly used in the INDI control law, Eq. (A.12). Instead, the required information about the system is included through the measurement \mathbf{y}_0^ρ .

Note that the INDI control law in Eq. (A.12) thus does not neglect $\mathbf{a}(\mathbf{x})$ with a high gain. Even if it does not explicitly show up in the INDI control law, most of its contribution is included in the measurement of \mathbf{y}_0^ρ . A more explicit explanation is as follows:

The Taylor expansion expression in Eq. (A.8) can be written as

$$\mathbf{y}^\rho = \underbrace{\mathbf{B}(\mathbf{x}_0)\mathbf{u}_0 + \mathbf{a}(\mathbf{x}_0)}_{\mathbf{y}_0^\rho} + \underbrace{\frac{\partial \mathbf{a}(\mathbf{x})}{\partial \mathbf{x}} \Big|_0 \Delta\mathbf{x} + \mathbf{O}(\Delta\mathbf{x}^2)}_{\delta(\Delta\mathbf{x})} + \frac{\partial \mathbf{B}(\mathbf{x})}{\partial \mathbf{x}} \Big|_0 \Delta\mathbf{x} + \mathbf{B}(\mathbf{x}_0)(\mathbf{u} - \mathbf{u}_0) \quad (\text{A.17})$$

in which the contribution of $\mathbf{a}(\mathbf{x})$ is split into $\mathbf{a}(\mathbf{x}_0)$, its value at time point 0, and the increments, included in \mathbf{y}_0^ρ and $\delta(\Delta\mathbf{x})$ respectively. As the chosen sampling period $T_s \rightarrow 0$, $\delta(\Delta\mathbf{x}) \rightarrow 0$ and so does the increment of $\mathbf{a}(\mathbf{x})$, thus its contribution to system dynamics is mostly included in \mathbf{y}_0^ρ , which can be directly measured or estimated from sensor information, thereby avoiding the explicit use of the model of $\mathbf{a}(\mathbf{x})$. The use of the measurement of \mathbf{y}_0^ρ is one main feature, and assumption, of the INDI control method.

Note that the above discussion requires that the system relative degree $r = \sum_{j=1}^m \rho_j$ to be equal to n . Otherwise the $r - n$ degrees of internal dynamics need to be stable.

ACKNOWLEDGEMENTS

This thesis is the result of four and a half years work in the Control and Simulation (C&S) department at Delft University of Technology. During these unforgettable years, I have not only received highly rewarding scientific training, experienced rich Dutch culture, but also gained life-long memory of all the lovely people I met for providing guidance, friendship and help. It is my honor to express my thanks to everyone studying and working at C&S.

My highest respect and gratitude first goes to my promotor, Prof. Max Mulder. You provided me the chance to pursue my PhD in TU Delft, and have been invariably supportive ever since. You provide profound and insightful guidance for my work, from which I consistently gain motivation and inspiration. Your profession feedback and remarks have improved this thesis to a higher level. You are also the most efficient and enthusiastic people I have ever met, and have been always available and approachable in spite of your busy agenda. I am truly grateful for your consistent trust and support over the years, especially when I experienced the utmost difficulties in my life.

To my second promotor, Dr. QiPing Chu, goes my deepest gratitude. Thank you for guiding me throughout the entire thesis with your profound and insightful scientific knowledge, for giving me precious suggestions and encouragement on my research, while providing unconditional support for my life in Delft like a family member. Beyond our age gap and your role as a supervisor, I regard you as my true friend, to whom I do feel free to talk about both my joy and sadness.

I would like also to express my profound appreciation to my co-promotor, Dr. Daan M. Pool. Daan, Thank you for your patient guidance and efficient supervision. Not only were you always available for our countless inspiring meetings and conversations, but you were also supportive after your office hours when I need help, even after midnight before deadlines. I miss your signature red comments for paper drafts, which invariably brought significant improvements with better scientific insight. I would never forget your unconditional support and cheerful encouragement.

It is also my pleasure to express my deep gratitude to my daily supervisor, Ir. Olaf Stroosma. Thank you not only for your teaching and constructive suggestions, but more importantly for your trust and support for every risky experiments we did together, in countless Friday afternoons with your hand prepared for the emergency button. This study won't have succeeded without your significant contribution. In addition, My special thanks for helping translate the summary of this thesis.

Also my special thanks to Alwin Damman, Erik-Jan van Kampen and Daniel Friesen, for helping and participating my motion control experiments. Special thanks to Bertine, for always being supportive and patient. Many thanks to other members of C&S: Prof. Bob Mulder, Prof. Jacco Hoekstra, René van Paassen, Coen de Visser, Clark Borst, Joost Ellerbroek, Guido de Croon, Marilena Pavel, Alexander in't Veld, Hans Mulder, Bertine

Markus, Ferdinand Postema, Andries Muis, Harold Thung, Alwin Damman, and many others, thank you for making C&S such a nice group to study in.

I would also like to express my deep gratitude to all the friends I met in Delft. To my roommate in 0.10, Kasper, Daniel and Tao, thank you for making the little room full of fun and inspiration; To my dear Chinese PhD colleagues and friends, Ye Zhou and Hann Woei Ho, Ligu Sun, Peng Lu and Xiang Li, Wei Fu and Gehua Wen, Junzi Sun and your family, Xuerui Wang and Sihao Sun, Shuo Li, Shushuai Li and Mel, Lei Yang, Bo Sun, Ying Yu, Yingfu Xu, thank you for all the amazing trips, lovely Chinese cooking showing-off, fabulous Chinese new year parties, and all the silly jokes, inspiring conversations and helping hands you offered. I enjoyed every moment spent with you. To my dear PhD (and Postdoc) fellows, Sophie Armanini, Ivan Miletović, Dirk Van Baelen, Isabel Metz, Kirk Scheper, Jaime Junell, Henry Tol, Ewoud Smeur, João Caetano, Emmanuel Sunil, Dyah Jatiningrum, Yazdi Jenie, Tommaso Mannucci, Rolf Klomp, Kimberley McGuire, Diana Olejnik, Matěj Karásek, Jelmer Reitsma, Mario Coppola, Jerom Maas, Julia Rudnyk, Sarah Baarendswaard, Tom van Dijk, Annemarie Landmann, Federico Paredes Vallés, thank you for all the conversations, silly jokes, laughs, drinks, sailing trips, C&S barbecues, and other events we had together. I particularly enjoy the trips we made together, to the US, the Paris air show, Dirk's wedding and Henry's beautiful home in Volendam. Your positive attitudes, lovely personalities and always available helping hands have made my little journey in Delft wonderful.

My deepest gratitude to my parents, who had raised me and largely shaped me with your unconditional love and support. Even in my mother language I do not find enough words to express how grateful I am. Just as an old Chinese poem says: Who says the tiny inch-tall blade of grass, can ever repay the warm sunshine of spring? My gratitude also extends to Ye's parents, for your persistent trust, support and encouragement.

Finally, my greatest and heartfelt appreciation to my wife, Ye Zhang. You have not only provided persistent love and support, demonstrated optimism and faith on me, but also have given my strengths to overcome the darkest period of time in my life. Thank you for being part of my life.

CURRICULUM VITÆ

Yingzhi HUANG

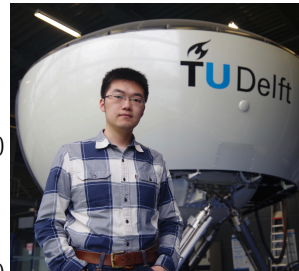
29-08-1990 Born in Yueyang, Hunan, China.

EDUCATION

2008–2012 BSc, School of Astronautics
Northwestern Polytechnical University (NPU)
China

2012–2014 MSc, School of Astronautics
Northwestern Polytechnical University (NPU)
China

2014-2019 PhD., Faculty of Aerospace Engineering
Delft University of Technology (TU Delft), the Netherlands
Thesis: Incremental Nonlinear Control of Hydraulic Parallel
Robots - a Case Study on the Simona Research Simulator
Promotors: Prof. dr. ir. M. Mulder and dr. Q. P. Chu



AWARDS

2012 Distinguished Bachelor student (in NPU)

2012 Distinguished Bachelor degree dissertation (in NPU)

2014 Distinguished Master student (in NPU)

LIST OF PUBLICATIONS

6. **Y. Huang**, D. Pool, O. Stroosma, and Q. Chu, *Sensor-based motion control system for parallel hydraulic robots with model uncertainties*, IEEE/ASME Transactions on Mechatronics (to be submitted)
5. **Y. Huang**, D. Pool, O. Stroosma, and Q. Chu, *Long-stroke hydraulic robot motion control with incremental nonlinear dynamic inversion*, IEEE/ASME Transactions on Mechatronics, vol. 24, no. 1, pp. 304-314, Feb 2019.
4. **Y. Huang**, D. Pool, O. Stroosma, and Q. Chu, *Robust incremental nonlinear dynamic inversion controller of hexapod flight simulator motion system*, In *Advances in Aerospace Guidance, Navigation and Control*, pp. 87-99. Springer, Cham, 2018..
3. **Y. Huang**, D. Pool, O. Stroosma, and Q. Chu, *Incremental nonlinear dynamic inversion control for hydraulic hexapod flight simulator motion systems*, IFAC-PapersOnLine, vol. 50, no. 1, pp. 4294 – 4299, 2017, 20th IFAC World Congress..
2. **Y. Huang**, D. Pool, O. Stroosma, and Q. Chu, *Modeling and Simulation of Hydraulic Hexapod Flight Simulator Motion Systems*, AIAA Modeling and Simulation Technologies Conference, AIAA SciTech Forum (San Diego, California, USA, 2016), (AIAA 2016-1437).
1. **Y. Huang**, D. Pool, O. Stroosma, and Q. Chu, *A review of control schemes for hydraulic Stewart platform flight simulator motion systems*, AIAA Modeling and Simulation Technologies Conference, AIAA SciTech Forum (San Diego, California, USA, 2016), (AIAA 2016-1436).